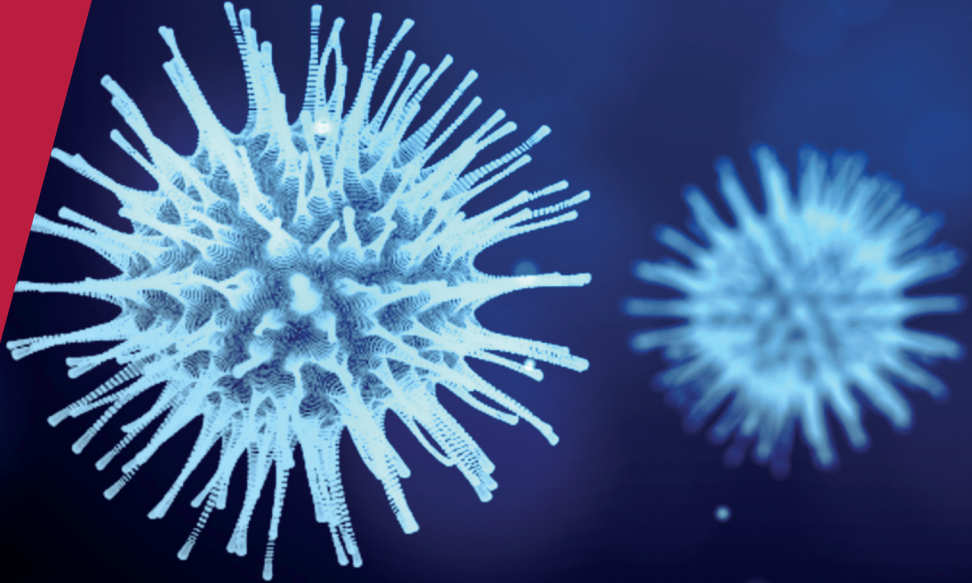


**CENTRE FOR  
ECONOMIC  
POLICY  
RESEARCH**

**CEPR PRESS**



**COVID ECONOMICS  
VETTED AND REAL-TIME PAPERS**

**ISSUE 69  
18 FEBRUARY 2021**

**FLIGHT FROM METROPOLITAN  
CENTERS**

Arpit Gupta, Vrinda Mittal, Jonas Peeters  
and Stijn Van Nieuwerburgh

**LOCATIONAL SPILLOVERS**

Gabriele Guaitoli and Todor Tochev

**INSOLVENCY AND DEBT  
OVERHANG**

Lilas Demmou, Sara Calligaris,  
Guido Franco, Dennis Dlugosch,  
Müge Adalet McGowan and Sahra Sakha

**MEASURING PREVALENCE**

Sotiris Georganas, Alina Velias  
and Sotiris Vadoros

**INTERSECTORAL SPILLOVERS**

Mikhail Anufriev, Andrea Giovannetti  
and Valentyn Panchenko

**SCHOOL-CLOSING**

Coen N. Teulings

---

# Covid Economics

## Vetted and Real-Time Papers

*Covid Economics, Vetted and Real-Time Papers*, from CEPR, brings together formal investigations on the economic issues emanating from the Covid outbreak, based on explicit theory and/or empirical evidence, to improve the knowledge base.

**Founder:** Beatrice Weder di Mauro, President of CEPR

**Editor:** Charles Wyplosz, Graduate Institute Geneva and CEPR

**Contact:** Submissions should be made at <https://portal.cepr.org/call-papers-covid-economics>. Other queries should be sent to [covidecon@cepr.org](mailto:covidecon@cepr.org).

Copyright for the papers appearing in this issue of *Covid Economics: Vetted and Real-Time Papers* is held by the individual authors.

### **The Centre for Economic Policy Research (CEPR)**

The Centre for Economic Policy Research (CEPR) is a network of over 1,500 research economists based mostly in European universities. The Centre's goal is twofold: to promote world-class research, and to get the policy-relevant results into the hands of key decision-makers. CEPR's guiding principle is 'Research excellence with policy relevance'. A registered charity since it was founded in 1983, CEPR is independent of all public and private interest groups. It takes no institutional stand on economic policy matters and its core funding comes from its Institutional Members and sales of publications. Because it draws on such a large network of researchers, its output reflects a broad spectrum of individual viewpoints as well as perspectives drawn from civil society. CEPR research may include views on policy, but the Trustees of the Centre do not give prior review to its publications. The opinions expressed in this report are those of the authors and not those of CEPR.

Chair of the Board

Sir Charlie Bean

Founder and Honorary President

Richard Portes

President

Beatrice Weder di Mauro

Vice Presidents

Maristella Botticini

Ugo Panizza

Philippe Martin

Hélène Rey

Chief Executive Officer

Tessa Ogden

---

# Editorial Board

**Beatrice Weder di Mauro**, CEPR

**Charles Wyplosz**, Graduate Institute Geneva and CEPR

**Viral V. Acharya**, Stern School of Business, NYU and CEPR

**Guido Alfani**, Bocconi University and CEPR

**Franklin Allen**, Imperial College Business School and CEPR

**Michele Belot**, Cornell University and CEPR

**David Bloom**, Harvard T.H. Chan School of Public Health

**Tito Boeri**, Bocconi University and CEPR

**Alison Booth**, University of Essex and CEPR

**Markus K Brunnermeier**, Princeton University and CEPR

**Michael C Burda**, Humboldt Universitaet zu Berlin and CEPR

**Luis Cabral**, New York University and CEPR

**Paola Conconi**, ECARES, Universite Libre de Bruxelles and CEPR

**Giancarlo Corsetti**, University of Cambridge and CEPR

**Fiorella De Fiore**, Bank for International Settlements and CEPR

**Mathias Dewatripont**, ECARES, Universite Libre de Bruxelles and CEPR

**Jonathan Dingel**, University of Chicago Booth School and CEPR

**Barry Eichengreen**, University of California, Berkeley and CEPR

**Simon J Evenett**, University of St Gallen and CEPR

**Maryam Farboodi**, MIT and CEPR

**Antonio Fatás**, INSEAD Singapore and CEPR

**Pierre-Yves Geoffard**, Paris School of Economics and CEPR

**Francesco Giavazzi**, Bocconi University and CEPR

**Christian Gollier**, Toulouse School of Economics and CEPR

**Timothy J. Hatton**, University of Essex and CEPR

**Ethan Ilzetzki**, London School of Economics and CEPR

**Beata Javorcik**, EBRD and CEPR

**Simon Johnson**, MIT and CEPR

**Sebnem Kalemli-Ozcan**, University of Maryland and CEPR Rik Frehen

**Tom Kompas**, University of Melbourne and CEBRA

**Miklós Koren**, Central European University and CEPR

**Anton Korinek**, University of Virginia and CEPR

**Michael Kuhn**, International Institute for Applied Systems Analysis and Wittgenstein Centre

**Maarten Lindeboom**, Vrije Universiteit Amsterdam

**Philippe Martin**, Sciences Po and CEPR

**Warwick McKibbin**, ANU College of Asia and the Pacific

**Kevin Hjortshøj O'Rourke**, NYU Abu Dhabi and CEPR

**Evi Pappa**, European University Institute and CEPR

**Barbara Petrongolo**, Queen Mary University, London, LSE and CEPR

**Richard Portes**, London Business School and CEPR

**Carol Propper**, Imperial College London and CEPR

**Lucrezia Reichlin**, London Business School and CEPR

**Ricardo Reis**, London School of Economics and CEPR

**Hélène Rey**, London Business School and CEPR

**Dominic Rohner**, University of Lausanne and CEPR

**Paola Sapienza**, Northwestern University and CEPR

**Moritz Schularick**, University of Bonn and CEPR

**Paul Seabright**, Toulouse School of Economics and CEPR

**Flavio Toxvaerd**, University of Cambridge

**Christoph Trebesch**, Christian-Albrechts-Universitaet zu Kiel and CEPR

**Karen-Helene Ulltveit-Moe**, University of Oslo and CEPR

**Jan C. van Ours**, Erasmus University Rotterdam and CEPR

**Thierry Verdier**, Paris School of Economics and CEPR

---

# Ethics

*Covid Economics* will feature high quality analyses of economic aspects of the health crisis. However, the pandemic also raises a number of complex ethical issues. Economists tend to think about trade-offs, in this case lives vs. costs, patient selection at a time of scarcity, and more. In the spirit of academic freedom, neither the Editors of *Covid Economics* nor CEPR take a stand on these issues and therefore do not bear any responsibility for views expressed in the articles.

## Submission to professional journals

The following journals have indicated that they will accept submissions of papers featured in *Covid Economics* because they are working papers. Most expect revised versions. This list will be updated regularly.

<i>American Economic Journal, Applied Economics</i>	<i>Journal of Economic Theory</i>
<i>American Economic Journal, Economic Policy</i>	<i>Journal of the European Economic Association*</i>
<i>American Economic Journal, Macroeconomics</i>	<i>Journal of Finance</i>
<i>American Economic Journal, Microeconomics</i>	<i>Journal of Financial Economics</i>
<i>American Economic Review</i>	<i>Journal of Health Economics</i>
<i>American Economic Review, Insights</i>	<i>Journal of International Economics</i>
<i>American Journal of Health Economics</i>	<i>Journal of Labor Economics*</i>
<i>Canadian Journal of Economics</i>	<i>Journal of Monetary Economics</i>
<i>Econometrica*</i>	<i>Journal of Public Economics</i>
<i>Economic Journal</i>	<i>Journal of Public Finance and Public Choice</i>
<i>Economics of Disasters and Climate Change</i>	<i>Journal of Political Economy</i>
<i>International Economic Review</i>	<i>Journal of Population Economics</i>
<i>Journal of Development Economics</i>	<i>Quarterly Journal of Economics</i>
<i>Journal of Econometrics*</i>	<i>Review of Corporate Finance Studies*</i>
<i>Journal of Economic Growth</i>	<i>Review of Economics and Statistics</i>
	<i>Review of Economic Studies*</i>
	<i>Review of Financial Studies</i>

(\*) Must be a significantly revised and extended version of the paper featured in *Covid Economics*.



---

# Covid Economics

## Vetted and Real-Time Papers

Issue 69, 18 February 2021

### Contents

Flattening the curve: Pandemic-induced revaluation of urban real estate <i>Arpit Gupta, Vrinda Mittal, Jonas Peeters and Stijn Van Nieuwerburgh</i>	1
Do localised lockdowns cause labour market externalities? <i>Gabriele Guaitoli and Todor Tochev</i>	46
Insolvency and debt overhang following the COVID-19 outbreak: Assessment of risks and policy responses <i>Lilas Demmou, Sara Calligaris, Guido Franco, Dennis Dlugosch, Müge Adalet McGowan and Sahra Sakha</i>	87
On the measurement of disease prevalence <i>Sotiris Georganas, Alina Velias and Sotiris Vandoros</i>	109
Social distancing policies and intersectoral spillovers: The case of Australia <i>Mikhail Anufriev, Andrea Giovannetti and Valentyn Panchenko</i>	140
School-closure is counterproductive and self-defeating <i>Coen N. Teulings</i>	166

# Flattening the curve: Pandemic-induced revaluation of urban real estate<sup>1</sup>

Arpit Gupta,<sup>2</sup> Vrinda Mittal,<sup>3</sup> Jonas Peeters<sup>4</sup> and  
Stijn Van Nieuwerburgh<sup>5</sup>

Date submitted: 10 February 2021; Date accepted: 12 February 2021

*We show that the COVID-19 pandemic brought house price and rent declines in city centers, and price and rent increases away from the center, thereby flattening the bid-rent curve in most U.S. metropolitan areas. Across MSAs, the flattening of the bid-rent curve is larger when working from home is more prevalent, housing markets are more regulated, and supply is less elastic. Housing markets predict that urban rent growth will exceed suburban rent growth for the foreseeable future.*

- 1 The authors would like to thank Zillow for providing data. The authors have no conflicts of interest to declare.
- 2 Assistant Professor of Finance, Department of Finance, Stern School of Business, New York University.
- 3 Ph.D. Candidate in Finance and Economics, Department of Finance, Columbia Business School.
- 4 New York University Center for Data Science.
- 5 Earle W. Kazis and Benjamin Schore Professor of Real Estate and Professor of Finance, Department of Finance, Columbia Business School; CEPR Research Fellow.

Copyright: Arpit Gupta, Vrinda Mittal, Jonas Peeters and Stijn Van Nieuwerburgh

## I Introduction

Cities have historically been a major source of growth, development, and knowledge spillovers (Glaeser, 2011). In developing and developed countries alike, rising urbanization rates (United Nations, 2019) have led to increased demand for real estate in city centers and contributed to problems of housing affordability (Favilukis, Mabilie, and Van Nieuwerburgh, 2019), especially in superstar cities (Gyourko, Mayer, and Sinai, 2013). The inelasticity of housing supply in urban centers means that a large fraction of economic growth in the last few decades has accrued to property owners, rather than improving the disposable income of local workers (Hornbeck and Moretti, 2018; Hsieh and Moretti, 2019).

This long-standing pattern reversed in 2020 as the COVID-19 pandemic led many residents to flee city centers in search for safer ground away from urban density. This urban flight was greatly facilitated by the ability, indeed the necessity, to work from home. Office use in downtown areas was still below 25% in most large office markets at the end of 2020, with New York City at around 10%, and San Francisco lower still, turning many temporary suburbanites into permanent ones.<sup>1</sup> We document that this migration had a large impact on the demand for suburban relative to urban real estate, and differential price impact in different locations within metropolitan areas.

An important question is whether real estate markets will return to their pre-pandemic state or be changed forever. There is much uncertainty circling around this question. Existing survey evidence indicates increasing willingness by employers to let employees work from home, and increasing desire to do so from employees, but without much evidence on lost productivity.<sup>2</sup> In this paper, we argue that by comparing the changes in

---

<sup>1</sup>According to JLL, U.S. office occupancy declined by a record 84 million square feet in 2020, propelling the vacancy rate to 17.1% at year-end. In addition, the sublease market grew by 50% in 2020, an increase of 47.6 million square feet (Jones Lang LaSalle, 2020).

<sup>2</sup>A survey of company leaders by Gartner found that 80% plan to allow employees to work remotely at least part of the time after the pandemic, and 47% will allow employees to work from home full-time. A PwC survey of 669 CEOs shows that 78% agree that remote collaboration is here to stay for the long-term. In a recent FlexJobs survey, 96% of respondents desire some form of remote work; 65% of respondents

house prices—which are forward looking—versus rents in city centers versus suburbs, we can glance an early answer to this difficult question.

We begin by documenting how urban agglomeration trends have shifted in the wake of the COVID-19 pandemic. The central object of interest is the bid-rent function, or the land price gradient, which relates house prices and rents to the distance from the city center. Prices and rents in the city center tend to be higher than in the suburbs, with the premium reflecting the scarcity of land available for development (including due to regulatory barriers), closer proximity to work, urban amenities, and agglomeration effects. Bid-rent functions are downward sloping. However, since COVID-19 struck, we document striking changes in the slope of this relationship. House prices far from the city center have risen faster than house prices in the center between December 2019 and December 2020. Likewise, rents in the suburbs grew much faster than rents in the center over this period. The negative slope of the bid-rent function has become less negative. In other words, the pandemic has flattened the bid-rent curve.

Figure 1 illustrates this changing slope. Each observation is the slope of the bid-rent function for a particular month. House prices are on the left, rents are on the right. The graph is estimated by pooling all ZIP codes for the largest 30 metropolitan areas in the U.S., and estimating the relationship between log prices or log rents and  $\log(1+\text{distance})$  in a pooled regression with CBSA fixed effects and ZIP-level control variables. Distance from city hall is expressed in kilometers. The elasticity of price to distance changes from -0.125 pre-pandemic to -0.115 in December 2020. For rents, the change in slope is much larger: from -0.04 to -0.005. The change in slope for price means that house prices 50kms from the city center grew by 5.7 percentage points more than house prices in the center. The slope change for rents corresponds to suburban rents appreciating by 9.9 percentage

report wanting to be full-time remote employees post-pandemic, and 31% want a hybrid remote work environment. Bloom (2020) finds that 42% of the U.S. workforce was working remotely as of May 2020, and Barrero, Bloom, and Davis (2020) estimates that the number of working days spent remote will increase four-fold in future years to 22%.

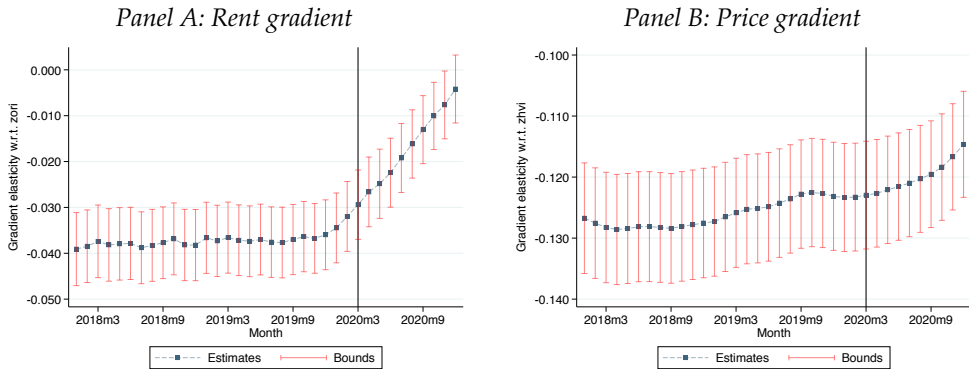


Figure 1. Rent and Price Gradients across top 30 MSAs

This plot shows coefficients from a repeated cross-sectional regression at the ZIP Code level as in equation 1 for the top 30 MSAs. We regress the distance from the city center (measured as the log of  $1 + \log$  distance to City Hall in kms) against log rent (left) and log price (right). We include additional controls (log of annual gross income in 2017, median age of the head of household, proportion of Black households in 2019, and proportion of individuals who make over 150k in 2019), as well as MSA fixed effects, and run the specification separately each month. Price and rent data are drawn from Zillow.

points more than in the core.<sup>3</sup>

We also find large changes in housing quantities. A measure of the housing inventory, active listings, displays large increases in the urban center and large decreases in the suburbs. A measure of housing liquidity shows that days-on-the-market rises in the urban core and falls sharply in the suburbs. There is a strong negative cross-sectional relationship between the house price change in a ZIP code on the one hand and the change in inventory and days-on-the-market on the other hand. Since housing supply elasticity tends to be substantially higher in suburbs than in the urban core, quantities do some of the adjustment. While the quantity adjustments are arguably limited over the nine months since the pandemic took hold, we expect them to be larger in the medium run. Shifting population to areas with higher supply elasticity will have important implications for housing affordability.

We use a simple present-value model in the tradition of [Campbell and Shiller \(1989\)](#) to study what the relative changes in urban versus suburban house prices and rents teach

<sup>3</sup>The main results, which use Zillow quality-adjusted house price data, are corroborated by using an alternative data source, Realtor, on asking prices.

us about the market's expectations on future rent growth in urban versus suburban locations. By studying differences between suburban and urban locations, we difference out common drivers of house prices such as low interest rates. Simply put, the much larger decline in rents than in prices in urban zip codes and the equally large increase in prices and rents in the suburbs, implies that the price-rent ratio became more steeply downward sloping. If housing markets expect a gradual return to the pre-pandemic state, then the increase in the urban-minus-suburban price-rent ratio implies higher expected rent growth in the urban core than in the suburbs for the next several years. If urban minus suburban risk premia did not change (increased by 1% point) that differential rent change is 7.5% points (15% points) in the average MSA. If housing markets instead expect the pandemic to have brought permanent changes to housing markets, then the change in price-rent ratios implies that urban rents will expand by 0.5% points faster than suburban rents going forward, assuming that risk premia did not change (changed by 1% point). The truth is somewhere in between the fully transitory and fully permanent cases. But in either case, the model predicts strong urban rent growth going forward.

We zoom in on New York, San Francisco, and Boston which were hit particularly hard by this pandemic-induced migration. More generally, we study the cross-MSA variation in the change in slope of the bid-rent function. We find that the changes are larger in MSAs that have higher presence of jobs that can be done from home (using a measure developed by [Dingel and Neiman, 2020](#)), and have lower housing supply elasticity or higher physical or regulatory barriers to development. Pre-pandemic price levels (rent levels) in the MSA are a good summary predictor of the price (rent) gradient changes.

**Related Literature** Our research connects to a long literature examining the role of urban land gradients in the context of agglomeration effects. [Albouy, Ehrlich, and Shin \(2018\)](#) estimates bid-rent functions across metropolitan areas in the United States. [Albouy \(2016\)](#) interprets the urban land premium in the context of local productivity, rents,



and amenity values, building on the influential spatial equilibrium approach of [Rosen \(1979\)](#) and [Roback \(1982\)](#). [Moretti \(2013\)](#) argues that skilled workers have increasingly sorted into expensive urban areas, lowering the real skilled wage premium. A key finding from this literature is that productive spillovers and amenity values of cities account for a steep relationship between real estate prices and distance, the importance of which has been growing over time—particularly for skilled workers. We find strong and striking reversals of this trend in the post-COVID-19 period, especially for metros with the highest proportions of skilled workers, who can most often work remotely.

A large and growing literature studies the effect of COVID-19 broadly. One strand of this literature has examined the spatial implications of the pandemic on within-city changes in consumption resulting from migration, changing commutes, and changing risk attitudes, such as [Althoff, Eckert, Ganapati, and Walsh \(2020\)](#) and [De Fraja, Matheson, and Rockey \(2020\)](#). A number of recent contributions have also begun to think about the impact of COVID-19 on real estate markets. [Delventhal, Kwon, and Parkhomenko \(2021\)](#) proposes a spatial equilibrium model with many locations. Households can choose where to locate. [Davis, Ghent, and Gregory \(2021\)](#) likewise study the effect of working from home on real estate prices. [Liu and Su \(2021\)](#) examines changes in real estate valuation as a function of density—we differ by focusing on the urban bid-rent curve and what the conjunction of prices and rents tell us about the persistence of the shock. [Ling, Wang, and Zhou \(2020\)](#) studies the impact of the pandemic on asset-level commercial real estate across different categories. Our focus is on residential real estate and changes in rents and prices resulting from household migration.

The literature has begun to use high-frequency location data from cell phone pings ([Gupta, Van Nieuwerburgh, and Kontokosta, 2020](#)). [Coven, Gupta, and Yao \(2020\)](#) shows that the pandemic led to large-scale migration. This migration is facilitated by increased work-from-home policies and shutdowns of city amenities—both of which raised the premium for housing characteristics found in suburbs and outlying areas such as increased

space.

We also connect to a finance literature that exploits risky equity claims of various maturities (Van Binsbergen, Brandt, and Koijen, 2012; Van Binsbergen, Hueskes, Koijen, and Vrugt, 2013) have examined decompositions of stock price movements into transitory and long run shocks. Gormsen and Koijen (2020) finds that stock markets priced in the risk of a severe and persistent economic contraction in March 2020 before revising that view later in 2020.

The rest of the paper is organized as follows. Section II describes our data sources. Section III describes our results on the price and rent gradient and how it has evolved from its pre-pandemic to its pandemic state. Section IV uses a present-value model to extract from the relative changes in price and rent gradients market expectations about the future expected rent changes. Section V studies cross-sectional variation in the price gradient and rent gradient to get at the mechanism. The last section concludes.

## II Data

We focus on the largest 30 MSAs by population. The list is presented in Table A.I in Appendix A. Our house price and rent data are at the ZIP code level derived from Zillow.<sup>4</sup> We use the Zillow House Value Index (ZHVI), which adjusts for house characteristics using machine learning techniques as well as the Zillow Observed Rental Index (ZORI), which is also a constant-quality rental price index capturing asking rents. Housing units include both single-family and multi-family units for both the price and the rent series.

We also use data from listing agent Realtor. We obtain ZIP code-level variables at the monthly level for all the ZIP codes in the U.S. Particularly, we use median listing price, median listing price per square foot, active listing counts, and median days a property is on the market.

---

<sup>4</sup>The data are publicly available from <https://www.zillow.com/research/data/>.

Additionally, we obtain ZIP-code level variables, such as the proportion of households with yearly income higher than 150 thousand dollars, the proportion of Black residents, and median household income from the Census Bureau. These variables will serve as control variables in our analysis. The list of variables is shown in Table A.II in the appendix.

Finally, we draw on a rich set of MSA-level variables from prior research to investigate the MSA-level factors that drive the changes in urban land gradients. We use the [Dingel and Neiman \(2020\)](#) measure of the fraction of local jobs which can potentially be done remotely. From Facebook data on social connectivity ([Bailey, Cao, Kuchler, Stroebel, and Wong, 2018](#)), we compute the fraction of connections (friends) who live within 100 miles relative to all connections for the residents in each MSA. A high share of local friends suggests more connectivity between the urban and suburban parts of the MSA and lower connectivity to other MSAs. We measure constraints on local housing development through several measures commonly used in the literature. The Wharton regulatory index ([Gyourko, Saiz, and Summers, 2008](#)) captures constraints on urban construction. We also measure physical constraints on housing using the [Lutz and Sand \(2019\)](#) measure of land unavailability, which is an extension of the [Saiz \(2010\)](#) measure. These physical constraints allow us to measure the elasticity of the local housing stock.

### III Results

We begin by showing descriptive evidence of price and rent changes across ZIP codes in various large MSAs.

#### III.A Raw Price and Rent Growth

Figure 2 plots maps of the New York (left column) and San Francisco MSAs (right columns). The top two rows report price growth between December 2019 and December

2020; the last row shows rent growth over the same period. The bottom two rows zoom in on the city center. Darker green colors indicate larger increases, while darker red colors indicate larger decreases. We see rent decreases in the urban core (Manhattan, centered around Grand Central Terminal) and rent increases in the suburbs, with particularly high values in the Hamptons on the far east of the map. The pattern for price changes is similar, but less extreme. For San Francisco, we also see dramatic decreases in rents and prices in the downtown zip codes, and increases in more distant regions such as Oakland.

### III.B Bid-Rent Function

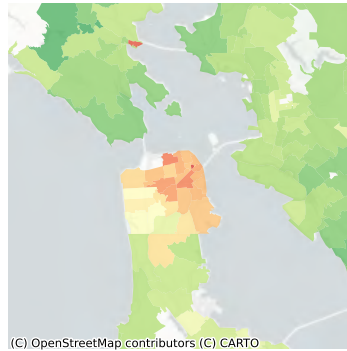
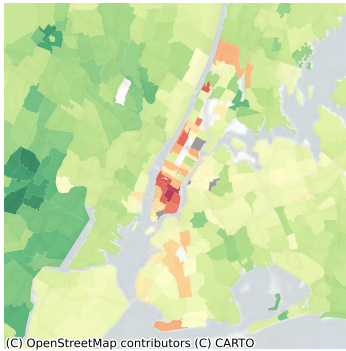
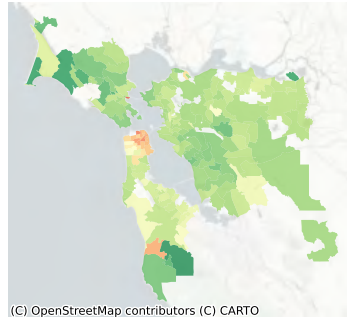
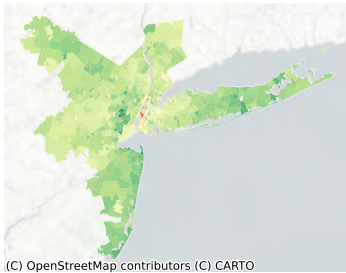
Figure 3 shows the cross-sectional relationship in the New York metropolitan area between log rent and  $\log(1+\text{distance})$  in the left panel and log price and  $\log(1+\text{distance})$  in the right panel. Lighter points indicate ZIP codes. Green dots are measurements as of December 2019, while red dots are for December 2020. The darker points indicate averages by 5% distance bins (binscatter). The figure also includes the best-fitting linear relationship. It is apparent that the bid-rent function is much flatter at the end of 2020 than at the end of 2019, particularly for rents.

Figure 4, shows similar changes in San Francisco, Boston, and Chicago. Figure 5 shows that Los Angeles displays a more complex picture with rents falling in the center, but an upward-sloping bid-rent function both pre- and post-pandemic. LA has a weaker monocentric structure and both very expensive and cheap areas and roughly similar distance.

A flattening bid-rent function implies that rent or price changes are higher in the suburbs than in the center. Another way to present the changing rent and price gradients is then to plot the percentage change in rents or prices between December 2019 and December 2020 on the vertical axis. Figure 6 shows percentage change in rents in New York and San Francisco metropolitan areas in panel A, while the second panel shows the percentage change in prices.

Figure 7 shows the change in rents plotted against the pre-pandemic level of rents

Price Changes



Rent Changes

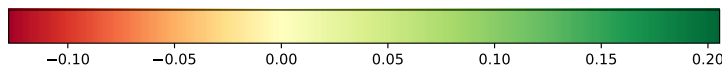
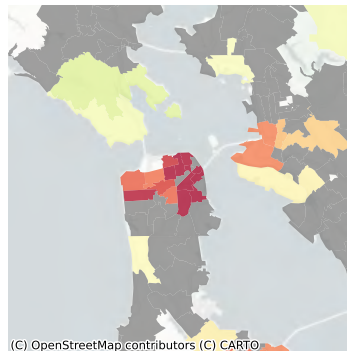
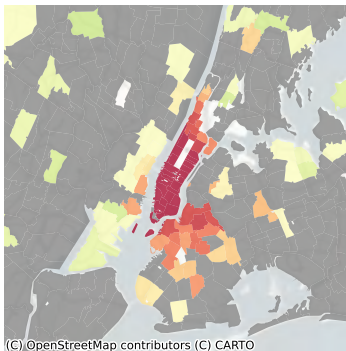


Figure 2. Price and Rent Growth, NYC and SF

This map shows year-over-year changes in prices (top four panels) and rents (bottom two panels) for the New York City and San Francisco MSAs at the ZIP code level over the period Dec 2019 – Dec 2020.

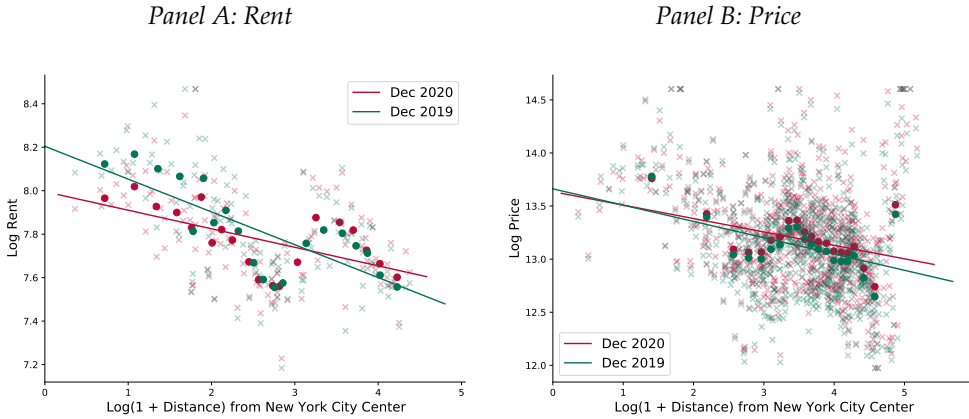


Figure 3. Bid-rent function for New York City

This plot shows the bid-rent function for the New York-Newark-Jersey City MSA. Panel A on the left shows the relationship between distance from the city center (the log of 1 + the distance in kilometers from Grand Central Station) and the log of rents measured at the ZIP code level. Panel B on the right repeats the exercise for prices. Both plots show this relationship prior to the pandemic (Dec 2019, in green) as well as afterwards (Dec 2020, in red).

in the top row. The bottom row of the figure plots changes in house prices against pre-pandemic house price levels. Both panels show very strong reversals of value in the most expensive ZIP Codes, measured using either rents or prices.

### III.C Estimating the Bid-Rent Function

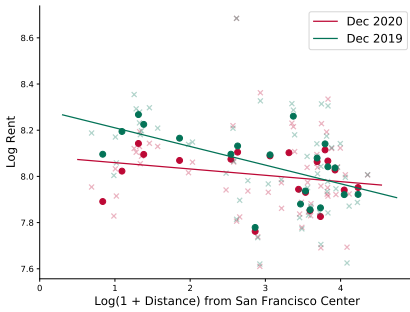
Next, we turn to formal estimation of the slope of the bid-rent function using the following empirical specification:

$$\ln p_{ijt} = \alpha_{jt} + \delta_{jt} [\ln(1 + D(\mathbf{z}_{ij}^z, \mathbf{z}_j^m))] + \beta X_{ij} + e_{ijt}, \quad e_{ijt} \sim \text{i.i.d.}\mathcal{N}(0, \sigma_e^2) \quad (1)$$

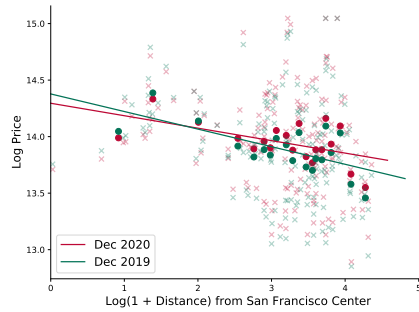
The unit of observation is a ZIP code-month. Here  $p_{ijt}$  refers to the price or rent in zip code  $i$  of MSA  $j$  at time  $t$ , and  $D(\mathbf{z}_{ij}^z, \mathbf{z}_j^m)$  is the distance in kilometers between the centroid of zip code  $i$  and centroid of MSA  $j$ , where  $i \in j$ . We control for MSA fixed effects, time fixed effects, and ZIP code level control variables ( $X_{ij}$ ). The ZIP Code controls are: log of annual gross income in 2017, median age of the head of household, proportion of Black



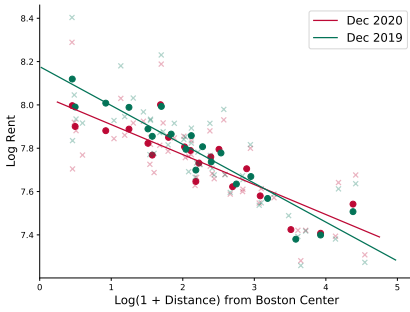
Panel A: San Francisco — Rent



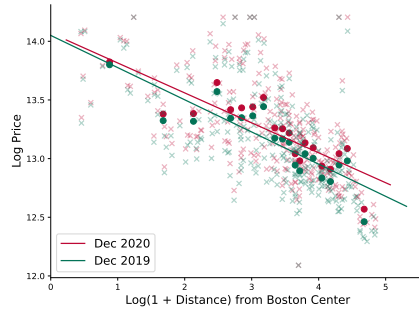
Panel B: San Francisco — Price



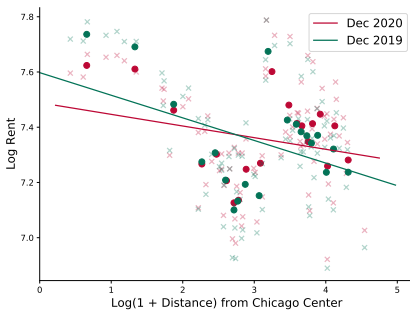
Panel C: Boston — Rent



Panel D: Boston — Price



Panel E: Chicago — Rent



Panel F: Chicago — Price

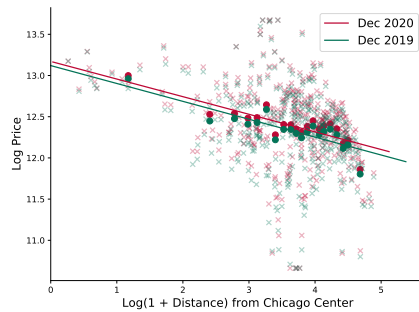


Figure 4. Bid-rent Functions for Other Cities

This plot shows the bid-rent function for the San Francisco-Oakland-Berkeley CA, Boston-Cambridge-Newton-MA-NH, and Chicago-Naperville-Elgin-IL-IN-WI MSAs. Panels on the left show the relationship between distance from the city center (the log of 1 + the distance in kilometers from City Hall) and the log of rents measured at the ZIP code level. Panels on the right repeats the exercise for prices. Both plots show this relationship prior to the pandemic (Dec 2019, in green) as well as afterwards (Dec 2020, in red).

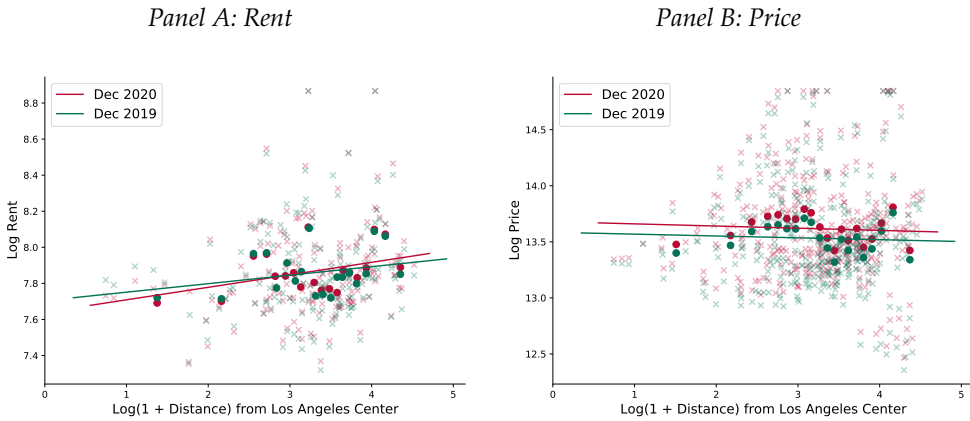


Figure 5. Bid-rent Functions for LA

This plot shows the bid-rent function for the Los Angeles-Long Beach-Anaheim MSA. Panel A on the left shows the relationship between distance from the city center (the log of 1 + the distance in kilometers from City Hall) and the log of rents measured at the ZIP code level. Panel B on the right repeats the exercise for prices. Both plots show this relationship prior to the pandemic (Dec 2019, in green) as well as afterwards (Dec 2020, in red).

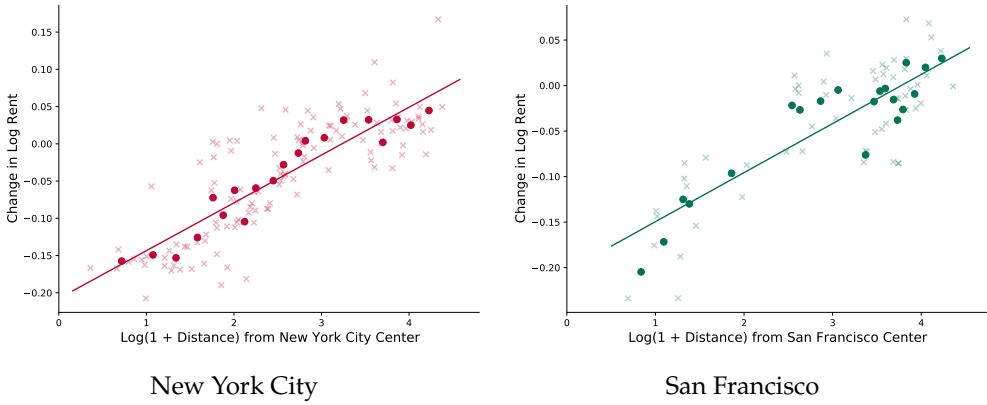
households in 2019, and proportion of individuals who make over 150k in 2019. The controls are all measured pre-pandemic (based on the latest available data) and do not vary over time during our estimation window.

The coefficient of interest is  $\delta_{jt}$  which measures the elasticity of prices or rents to distance between the zip code and the center of the MSA. We refer to it as the price or rent gradient. Historically,  $\delta_{jt}$  is negative, as prices and rents decrease as we move away from the city center. Our main statistic of interest is  $\delta_{jt+1} - \delta_{jt}$ , shown in Figure 1. Properties away from the city center have become more valuable over the course of 2020, *flattening the bid-rent curve*, and resulting in a positive estimate for  $\delta_{jt+1} - \delta_{jt}$ . Figure 8 shows the change in price and rent gradient over the US.

### III.D Listing Prices

As an alternative to Zillow prices and to explore homeowners' listing behavior, we also study list prices from Realtor. Figure 9 shows the changes in log of median listing

Panel A: Rent



Panel B: Price

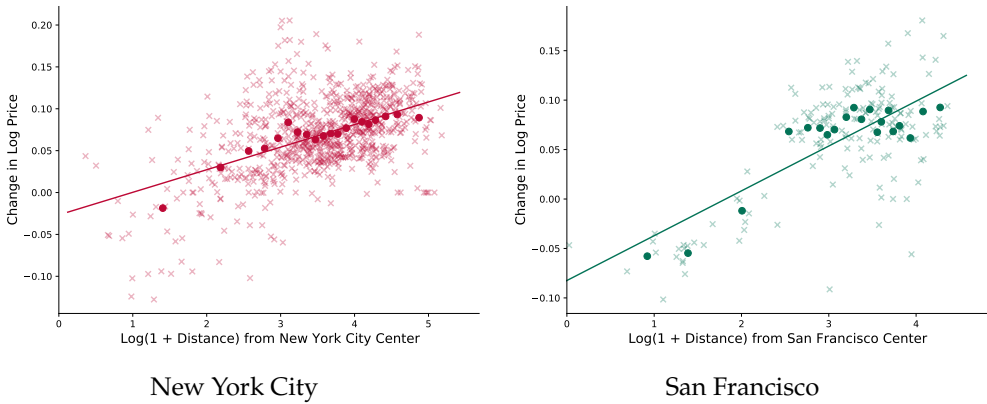
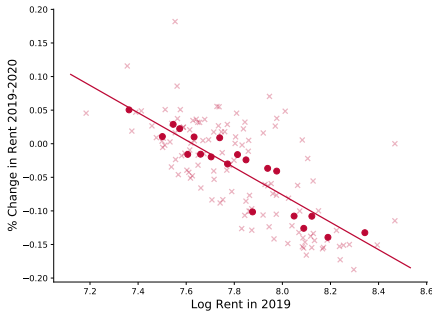


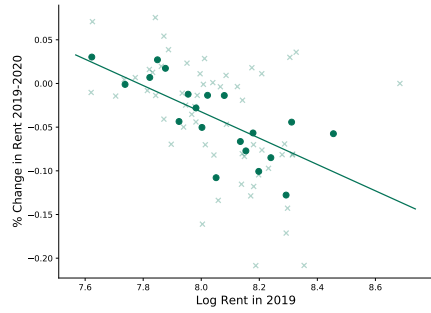
Figure 6. Change in the Bid-rent function

These plots show the change in the bid-rent functions for New York City (left) and San Francisco (right). Each observation corresponds to the changes in either rents (Panel A) or prices (Panel B) between Dec 2019 and Dec 2020 within each city, plotted against the distance to the center of the city.

Panel A: Rent

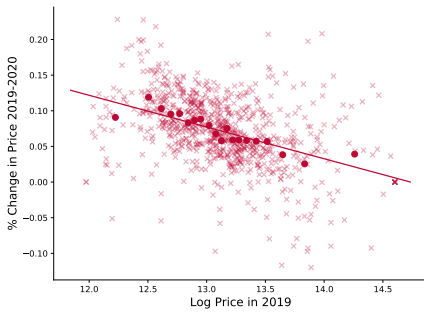


New York City

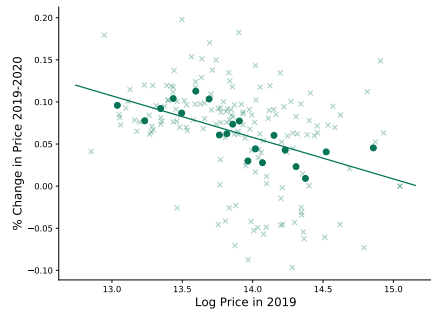


San Francisco

Panel B: Price



New York City



San Francisco

Figure 7. Changes in Rents and Prices Against Pre-Pandemic Levels

These plots show the changes in rents (Panel A) and prices (Panel B) against pre-pandemic levels of rents and prices for New York City (left) and San Francisco (right). Each observation corresponds to the changes in either rents (Panel A) or prices (Panel B) between Dec 2019 and Dec 2020 within each city, plotted against the Dec 2019 log level of rents or prices.

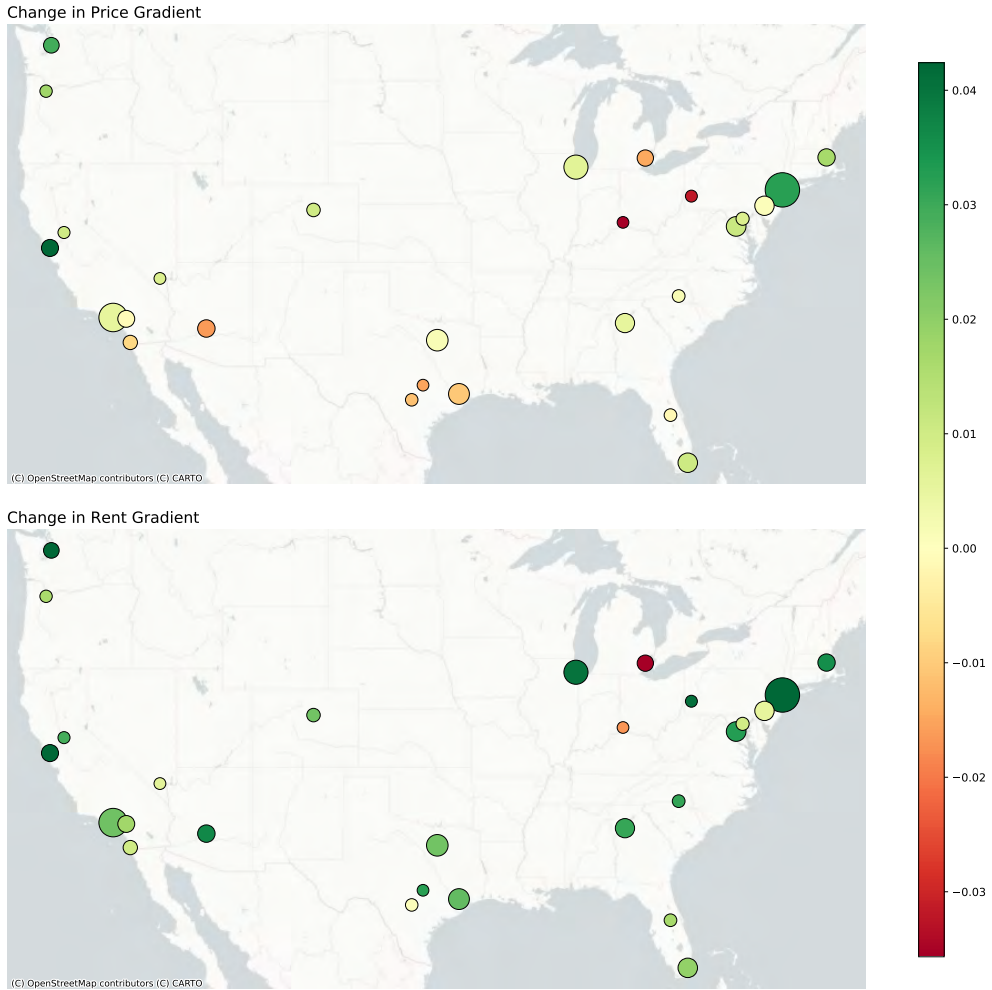


Figure 8. MSA level Changes in Price and Rent Gradients

This map plots the change in price and rent gradients across the U.S. over the period Dec 2019 – Dec 2020. For each MSA, we estimate the price and rent gradient as in equation 1, and plot the resulting change at the MSA-level. Higher values correspond to a flatter bid-rent curve. The size of the circle corresponds to the magnitude of the change.

price for New York and San Francisco metropolitan areas in Panel A, and changes in log of median listing price per square foot in Panel B. They confirm larger increases in listing prices in the suburbs than in the urban core.

### III.E Quantity Adjustments

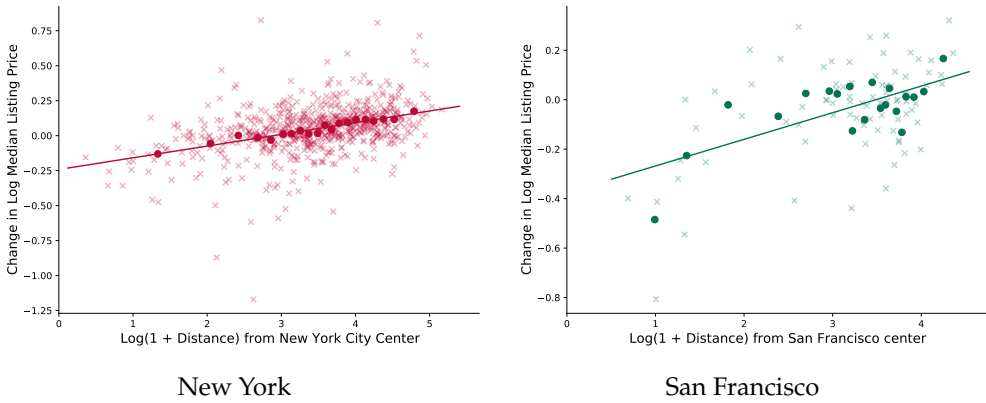
Next we turn to two measures of housing quantities, which are often interpreted as measures of liquidity. Active listings measures the number of housing units that are currently for sale. The top panel of Figure 10 shows large increases in the housing inventory in the urban core of New York and San Francisco metros between December 2019 and December 2020. It shows large declines in inventory in the suburbs. Buyers depleted large fractions of the available housing inventory in the suburbs during the pandemic, even after taking into account that a strong sellers' market may have prompted additional suburban homeowners to put their house up for sale over the course of 2020.

The second measure we study is median days-on-the-market (DOM), a common metric used in the housing search literature (Han and Strange, 2015) to quantify how long it takes to sell a house. Panel B of Figure 10 shows that DOM rose in the urban cores of New York and San Francisco and fell in the suburbs. Housing liquidity improved dramatically in the suburbs and deteriorated meaningfully in the center. We find similar results for the other 28 metro areas.

Figure 11 plots the changes in house prices on the vertical axis against changes in active listings in the left panel, and against changes in median DOM in the right panel. It includes all ZIP codes of the top-30 metropolitan areas in the U.S. There is a strongly negative cross-sectional relationship between price and quantity changes. ZIP codes in the suburbs are in the top left corner of this graph while ZIP codes in the urban core are in the bottom right corner.



Panel A: Median listing price



Panel B: Median listing price per sq. ft.

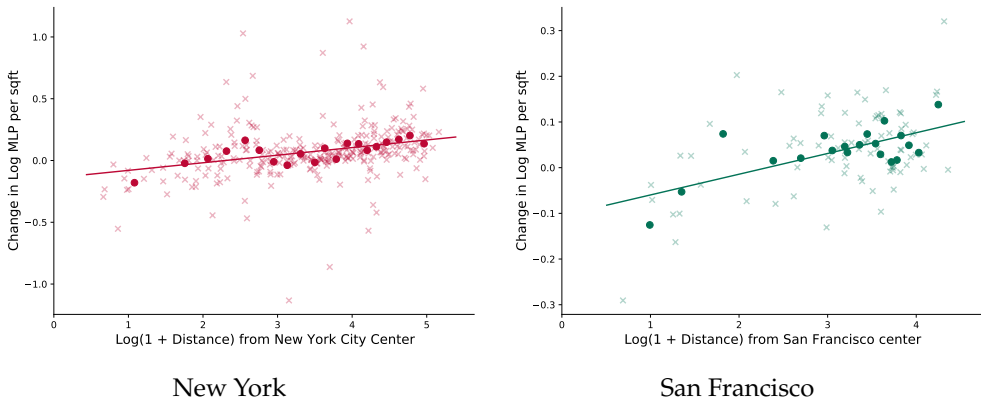
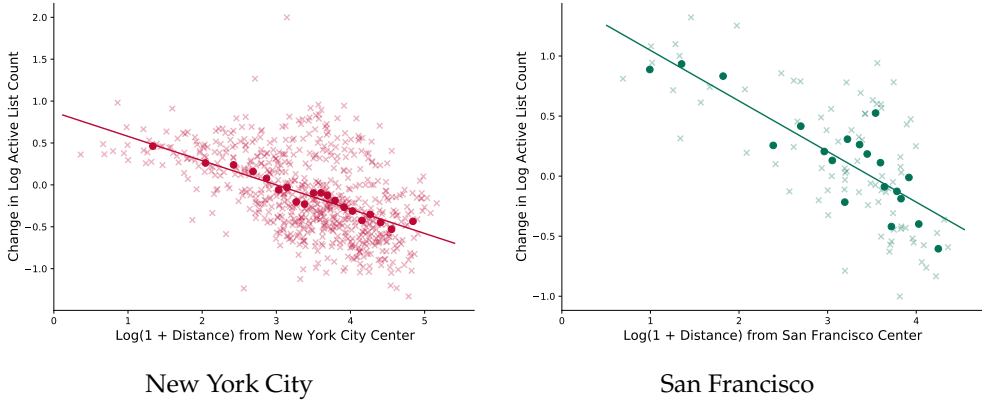


Figure 9. Changes in Listing Prices

These plots show the relationship between changes listing prices, measured as either the median listing price (Panel A) or the median listing price per sq. ft. (Panel B) with respect to distance. Each observation is at the ZIP code level, and measures the change in the the listing price variable from 2019 - Dec 2020, plotted against distance from the center of city for the New York MSA (left) as well as San Francisco (right).

Panel A: Active listings



Panel B: Median Days on Market

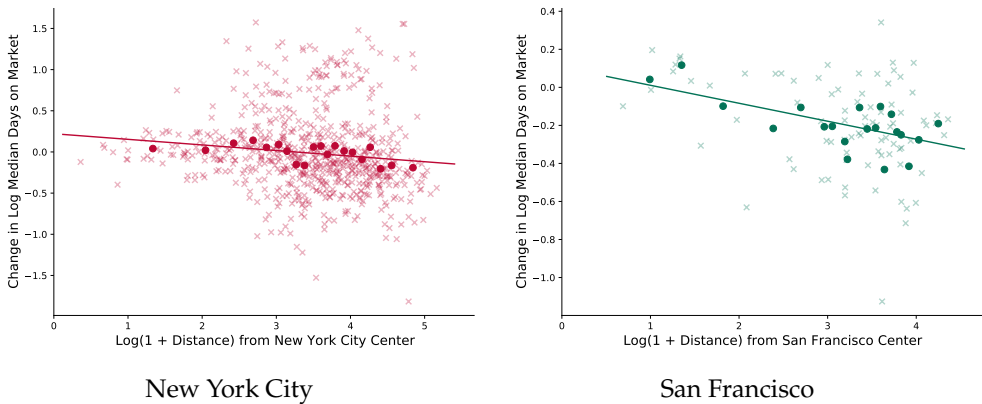
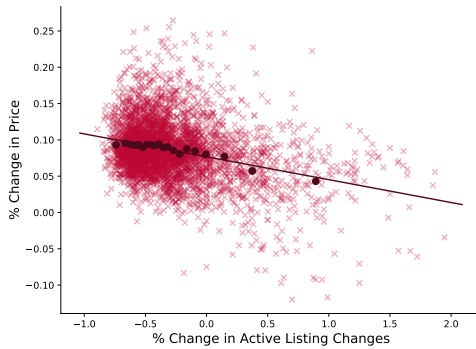


Figure 10. Changes in Market Inventory

This plot measures changes in two measures of market inventory, active listings (Panel A) and median days on market (Panel B) against distance from the center of the city for New York (left) and San Francisco (right). Each observation is a ZIP Code and represents the change in the market inventory measure from Dec 2019 to Dec 2020.

*Panel A: Price change against active listing changes*



*Panel B: Price and median days on market changes*

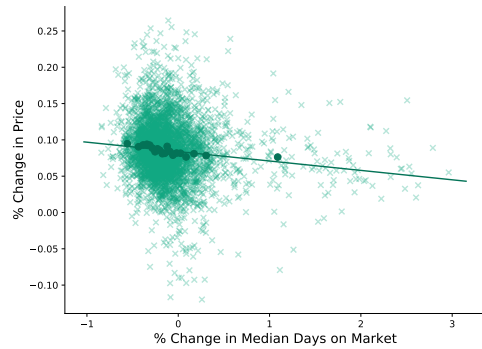


**Figure 11. Price change against Changes in Inventory**

This plot measures changes in prices against changes in two measures of inventories. Panel A plots the relationship between the percentage change in house prices from Dec 2019 – Dec 2020 against the percentage change in active listings over this period. Panel B plots the same change in house prices against the percentage change in days on market over the same period.

### III.F Migration

### III.G Price-Rent Ratios

For the analysis that follows, it is useful to work with price-rent ratios. Since the Zillow data are quality-adjusted, it is reasonable to interpret the price-rent ratio in a ZIP code as pertaining to the same typical property that is either for rent or for sale. For our purposes, we need a much weaker condition to hold. It is enough that the change over time in the price-rent ratio is comparable across ZIP codes within an MSA.

Figure 14 plots the pre-pandemic price-rent ratio for the New York metro as a function of distance from the center. It is constructed by first calculating the price-rent ratio for each ZIP-month over the period January 2014 (when the rent data starts) until December 2019. We then average over these 72 months. We think of this average as a good proxy for the long-run equilibrium price-rent ratio before the pandemic. As the figure shows, not only are prices high in the city center, price-rent ratios are high. The price-rent ratio

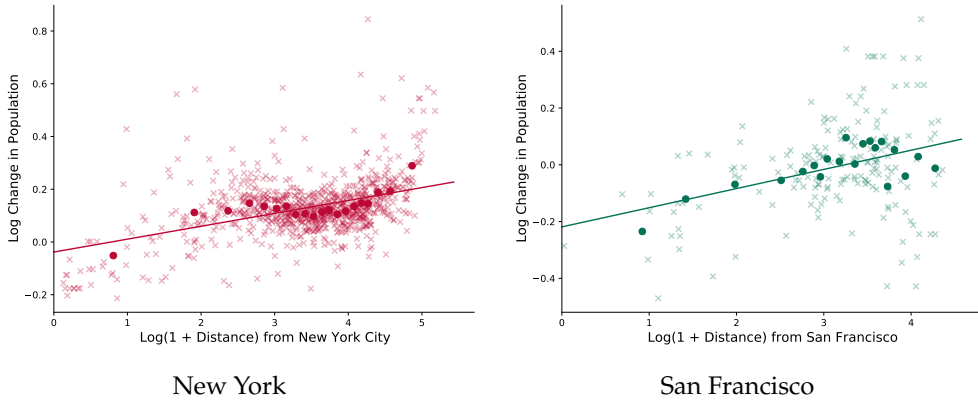


Figure 12. Changes in Population

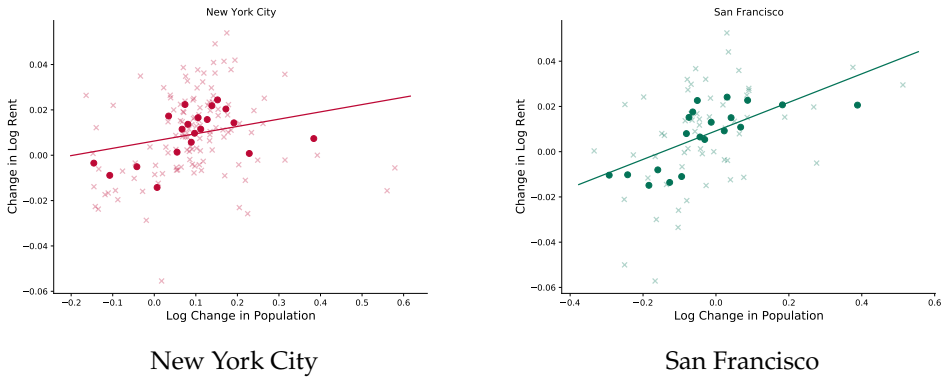
Description

decreases from 25 in the urban core to 17 in the suburbs.

The graph also shows the price-rent ratio in the fourth quarter of 2020, averaging the price-rent ratios of October, November, and December 2020.<sup>5</sup> In the suburbs, rents and prices rise by about the same amount, leaving the price-rent ratio unchanged. In the urban core, rents fall much more than prices, resulting in a large increase in the price-rent ratio. That is to say, the price-rent ratio curve has become steeper during the pandemic. It has become cheaper to rent than to own in the core and relatively more expensive to rent in the suburbs. Figure 15 plots average 12-month rent growth over the January 2014 to December 2019 as a function of distance from the center in New York City. Rental growth is modestly higher in the core than in the suburbs in normal times. These trends change dramatically post-pandemic, as both prices and rents grow more slowly in core areas.

<sup>5</sup>As long as the price-rent ratio in one of the months is available, the ZIP code is included in the analysis.

Panel A: Rent



Panel B: Price

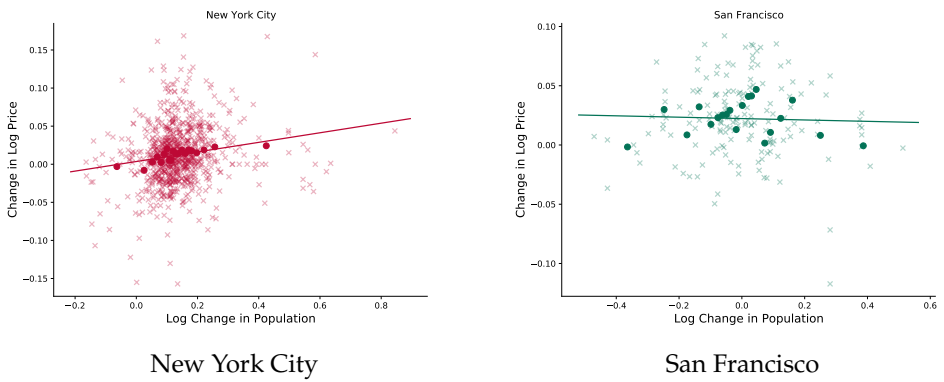


Figure 13. Changes in Rents and Prices Against Migration

Description

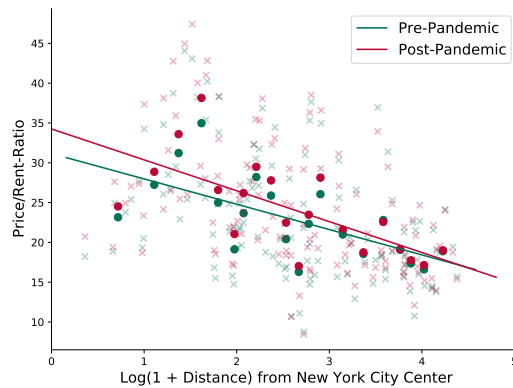


Figure 14. Price-Rent Ratio against Distance for New York City

This plot shows the relationship between the price-to-rent ratio before the pandemic (2019Q4, in gray) and after the pandemic (2020Q4, in red) across distance, measured as log of 1 + distance to Grand Central in kilometers.

## IV Beliefs About Rent Growth

In this section, we investigate what housing markets tell us about future rent growth expectations following the COVID-19 shock. To do so, we combine the observed changes in the price and rent gradient to back out expectations about the relative rent growth rate in suburbs versus the urban core over the next several years.

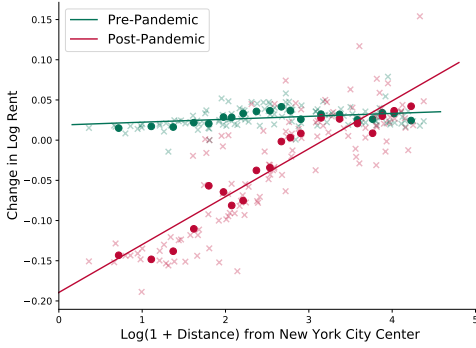
### IV.A Present-Value Model

We briefly review the the present-value model of [Campbell and Shiller \(1989\)](#), a standard tool in asset pricing. [Campbell, Davis, Gallin, and Martin \(2009\)](#) were the first to apply the present value model to real estate. They studied a variance decomposition of the aggregate residential house price-rent ratio in the U.S. [Van Nieuwerburgh \(2019\)](#) applied the model to REITs, publicly traded vehicles owning (mostly commercial) real estate.

Let  $P_t$  be the price of a risky asset, in our case the house,  $D_{t+1}$  its (stochastic) cash-flow,



Panel A: Rent Growth



Panel B: Price Growth

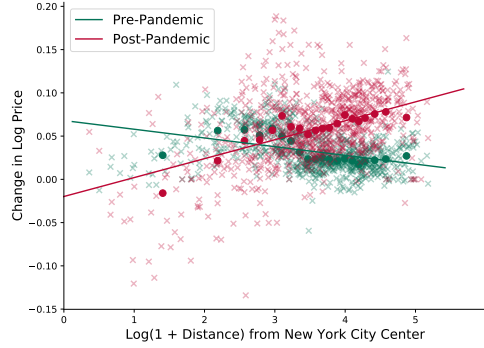


Figure 15. Changes in Rent and Price Growth Rates

This plot shows the changes in rental growth rates (Panel A) and price growth rates (Panel B) over the pre-pandemic period (Jan 2014–Dec 2019) compared with the post-pandemic period (Jan 2020–Dec 2020) across distance from the center of New York (log of 1 + distance to Grand Central in kilometers).

in our case the rent, and  $R_{t+1}$  the cum-dividend return:

$$R_{t+1} = \frac{P_{t+1} + D_{t+1}}{P_t}.$$

We can log-linearize the definition of the cum-dividend return to obtain:

$$r_{t+1} = k + \Delta d_{t+1} + \rho pd_{t+1} - pd_t,$$

where all lowercase letters denote natural logarithms and  $pd_t = p_t - d_t = -dp_t$ . The constants  $k$  and  $\rho$  are functions of the long-term average log price-rent ratio. Specifically,

$$\rho = \frac{\exp(\overline{pd})}{1 + \exp(\overline{pd})}, \quad k = \log(1 + \exp(\overline{pd})) - \rho \overline{pd}. \tag{2}$$

By iterating forward on the return equation, adding an expectation operator on each side, and imposing a transversality condition (i.e., ruling out rational bubbles), we obtain the

present-value model of [Campbell and Shiller \(1989\)](#):

$$pd_t = \frac{k}{1 - \rho} + E_t \left[ \sum_{j=1}^{+\infty} \rho^{j-1} \Delta d_{t+j} \right] - E_t \left[ \sum_{j=1}^{+\infty} \rho^{j-1} r_{t+j} \right]. \tag{3}$$

A high price-rent ratio must reflect either the market’s expectation of higher future rent growth, or lower future returns on housing (i.e., future price declines), or a combination of the two.

This equation also holds unconditionally:

$$\overline{pd} = \frac{k}{1 - \rho} + \frac{\bar{g}}{1 - \rho} - \frac{\bar{x}}{1 - \rho}, \tag{4}$$

where  $\bar{g} = E[\Delta d_t]$  and  $\bar{x} = E[r_t]$  are the unconditional expected rent growth and expected return, respectively. Equation (4) can be rewritten to deliver the well-known Gordon Growth model (in logs) by plugging in for  $k$ :

$$\log \left( 1 + \exp \overline{pd} \right) - \overline{pd} = \bar{x} - \bar{g}. \tag{5}$$

The left-hand side variable is approximately equal to the long-run rental yield  $\overline{D/P}$ .

Subtracting equation (4) from (3), we obtain:

$$pd_t - \overline{pd} = E_t \left[ \sum_{j=1}^{+\infty} \rho^{j-1} (\Delta d_{t+j} - \bar{g}) \right] - E_t \left[ \sum_{j=1}^{+\infty} \rho^{j-1} (r_{t+j} - \bar{x}) \right]. \tag{6}$$

Price-rent ratios exceed their long-run average, or equivalently rental yields are below their long-run average, when rent growth expectations are above their long-run average or expected returns are below the long-run expected return.

**Expected Rent Growth** In what follows, we assume that expected rent growth follows an autoregressive process. Denote expected rent growth by  $g_t$ :

$$g_t \equiv E_t[\Delta d_{t+1}]$$

and assume an AR(1) for  $g_t$ :

$$g_t = (1 - \rho_g)\bar{g} + \rho_g g_{t-1} + \varepsilon_t^g \quad (7)$$

Under this assumption, the rent growth term in equation (6) can be written as a function of the current period's expected rent growth in excess of the long-run mean:

$$E_t \left[ \sum_{j=1}^{+\infty} \rho^{j-1} (\Delta d_{t+j} - \bar{g}) \right] = \frac{1}{1 - \rho \rho_g} (g_t - \bar{g}). \quad (8)$$

**Expected Returns** Similarly, define expected returns by  $x_t$

$$x_t \equiv E_t[r_{t+1}]$$

and assume an AR(1) for  $x_t$  following [Lettau and Van Nieuwerburgh \(2008\)](#); [Binsbergen and Kojien \(2010\)](#); [Kojien and van Nieuwerburgh \(2011\)](#):

$$x_t = (1 - \rho_x)\bar{x} + \rho_x x_{t-1} + \varepsilon_t^x \quad (9)$$

Under this assumption, the return term in equation (6) can be written as a function of the current period's expected return in excess of the long-run mean:

$$E_t \left[ \sum_{j=1}^{+\infty} \rho^{j-1} (r_{t+j} - \bar{x}) \right] = \frac{1}{1 - \rho \rho_x} (x_t - \bar{x}). \quad (10)$$

**Implied Dividend Growth Expectations** With equations (8) and (10) in hand, we can restate equation (6)

$$pd_t - \overline{pd} = A(g_t - \overline{g}) - B(x_t - \overline{x}). \quad (11)$$

where  $A = \frac{1}{1-\rho\rho_g}$  and  $B = \frac{1}{1-\rho\rho_x}$ .

From (11), we can back out the current-period expectations about future rent growth:

$$g_t = \overline{g} + (1 - \rho\rho_g) \left( pd_t - \overline{pd} \right) + \frac{1 - \rho\rho_g}{1 - \rho\rho_x} (x_t - \overline{x}). \quad (12)$$

Current beliefs about rent growth depend on long-run expected rent growth (first term), the deviation of the price-rent ratio from its long-run mean (second term), and the deviation of expected returns from their long-run mean (third term). Long-run expected dividend growth  $\overline{g}$  is obtained from (4) given  $\overline{pd}$  and  $\overline{x}$ .

#### IV.B Pandemic is Transitory

We assume that zip codes were at their long-run averages  $(\overline{x}^{ij}, \overline{g}^{ij})$  prior to covid, in December 2019. They imply  $\overline{pd}^{ij}$  per equation (5). In a first set of calculations, we assume that following the covid-19 shock, expected rent growth and expected returns (and hence the mean pd ratio) will gradually return to those pre-pandemic averages. Under those assumptions, we can ask what the observed changes in the price-rent ratios between December 2019 and December 2020 imply about the market's expectations about rent growth in urban relative to suburban zip codes over the next several years.

If  $pd_t$  is measured as of December 2020, then equation (11) measures the percentage change in the price-rent ratio post versus pre-pandemic. Let  $i = u$  denote a ZIP code in the urban core. Let  $i = s$  denote a ZIP code in the suburbs, then the difference-in-difference between post- and pre-pandemic and between suburban and urban ZIP codes

in the same MSA is given by:

$$\begin{aligned} \Delta pd^j &= \left[ A^{uj} \left( g_t^{uj} - \bar{g}^{uj} \right) - A^{sj} \left( g_t^{sj} - \bar{g}^{sj} \right) \right] - \left[ B^{uj} \left( x_t^{uj} - \bar{x}^{uj} \right) - B^{sj} \left( x_t^{sj} - \bar{x}^{sj} \right) \right] \quad (13) \\ \Delta pd^j &\equiv \left( pd_t^{uj} - \bar{pd}^{uj} \right) - \left( pd_t^{sj} - \bar{pd}^{sj} \right) \end{aligned}$$

where the second line defines  $\Delta pd^j$  for an MSA  $j$ .

We observe the left-hand side of the first equation, but there are two unknowns on the right-hand side. Hence, there is a fundamental identification problem which is well understood in the asset pricing literature. One either needs additional data on return expectations or on expected cash flow growth, for example from survey data, or one needs to make an identifying assumption. We follow the second route.

**Assumption 1.** Expected returns and expected rent growth have the same persistence across geographies:  $\rho_x^{ij} = \rho_x$  and  $\rho_g^{ij} = \rho_g$ . We also assume that  $\rho^{ij} = \rho^j$ .

This assumption implies that  $A^{ij}$  and  $B^{ij}$  only depend on the MSA  $j$ .<sup>6</sup>

Under Assumption 1, we can use the present-value relationship to back out the market's expectation about expected rent growth in urban minus suburban zip codes:

$$g_t^{uj} - g_t^{sj} = \bar{g}^{uj} - \bar{g}^{sj} + (1 - \rho^j \rho_g) \Delta pd^j + \frac{1 - \rho^j \rho_g}{1 - \rho^j \rho_x} \Delta x^j. \quad (14)$$

where

$$\Delta x^j \equiv \left( x_t^{uj} - \bar{x}^{uj} \right) - \left( x_t^{sj} - \bar{x}^{sj} \right)$$

Equation gives the expected rent growth differential over the next twelve month, measured as of December 2020, i.e., between December 2020 and December 2021. But since expected rent growth follows an AR(1), there will be further changes in 2022, 2023, etc.

<sup>6</sup>This is an approximation. The mean log price-rent ratio,  $\bar{pd}^{ij}$ , and hence  $\rho^{ij}$  depends on  $(i, j)$  because of heterogeneity in  $(\bar{x}^{ij}, \bar{g}^{ij})$ . We construct the population-weighted mean of  $\bar{pd}^{ij}$  across all zip codes in the MSA, call it  $\bar{pd}^j$ , and then form  $\rho^j$  from  $\bar{pd}^j$  using (2).

Those expected cumulative rent changes over all future years are given by:

$$\frac{g_t^{uj} - g_t^{sj}}{1 - \rho^j \rho_g} = \frac{\bar{g}^{uj} - \bar{g}^{sj}}{1 - \rho^j \rho_g} + \Delta p d^j + \frac{\Delta x^j}{1 - \rho^j \rho_x}. \quad (15)$$

$\Delta x^j$  measures how much the pandemic changed the risk premium on urban versus suburban housing. Estimating time-varying risk premia is hard, even in liquid markets with long-time series of data. It is neigh impossible for illiquid assets like homes over short periods of time like the 12-month period we are interested in. Hence, all we can do is make assumptions and understand their impact. We consider three alternative assumptions on  $\Delta x^j$  below.

**Assumption 2.** Expected returns did not change differentially in urban and suburban areas in the same MSA in the pandemic:  $\Delta x^j = 0$ .

This assumption allows for expected returns to be different in urban and suburban ZIP codes and for expected returns to change in the pandemic. It precludes that this change was different for suburban and urban areas. Expected returns can be written as the interest rate plus a risk premium. Since the dynamics of interest rates (and mortgage rates more generally) are common across space, this assumption is one on the dynamics of urban-suburban risk premia.

Expected returns in suburban areas are typically higher than in urban areas pre-pandemic. An alternative assumption on the expected returns is that the gap between suburban and urban expected returns shrinks by a fraction  $\kappa$  of the pre-pandemic difference:

**Assumption 3.** Urban minus suburban risk premia in the pandemic are:  $x_t^{sj} - x_t^{uj} = (1 - \kappa)(\bar{x}^{sj} - \bar{x}^{uj})$ . This implies:  $\Delta x^j = \kappa(\bar{x}^{sj} - \bar{x}^{uj}) > 0$ .

Note that our previous assumption 2 is a special case of assumption 3 for  $\kappa = 0$ . Another special case is  $\kappa = 1$ , where the pandemic wipes away the entire difference in suburban-urban risk premia. We use a value of  $\kappa = 0.5$ , which we consider to be quite a strong reversal of relative risk premia.

The third assumption we make is simply a constant change in urban minus suburban risk premia in each MSA:

**Assumption 4.**  $\Delta x^j = .01, \forall j$ .

#### IV.C Pandemic is Permanent

The opposite extreme from assuming that everything will go back to the December 2019 state is to assume that the situation as of December 2020 is the new permanent state.

In that case, we can use equation (5) to back out what the market expects the new long-term expected urban minus suburban rent growth to be, denoting the new post-pandemic steady state by hatted variables:

$$\widehat{g}^{uj} - \widehat{g}^{sj} = \left( \widehat{pd}^{uj} - \widehat{pd}^{sj} \right) - \left( \log \left( 1 + \exp \widehat{pd}^{uj} \right) - \log \left( 1 + \exp \widehat{pd}^{sj} \right) \right) + \widehat{x}^{uj} - \widehat{x}^{sj}. \quad (16)$$

The first two terms can be computed directly from the observed price-rent ratios in December 2020. The last term requires a further assumption.

We consider two different assumptions on post-pandemic urban minus suburban expected returns (or equivalently risk premia, since interest rates are common for urban and suburban areas). The first one is that urban minus suburban risk premia differences remain unchanged pre- versus post-pandemic.

**Assumption 5.**  $\widehat{x}^{uj} - \widehat{x}^{sj} = \bar{x}^{uj} - \bar{x}^{sj}, \forall j$ . We refer to this as  $\Delta \bar{x}^j = 0$ .

Alternatively, we assume that urban risk premia rise relative to suburban risk premia by a constant amount.

**Assumption 6.**  $\widehat{x}^{uj} - \widehat{x}^{sj} = \bar{x}^{uj} - \bar{x}^{sj} + 0.01, \forall j$ . We refer to this as  $\Delta \bar{x}^j = 0.01$ .

## IV.D Results

For each of the 30 largest MSAs which have rent data available for at least some of the suburban areas, Table I reports the results.

We define the urban core to be the ZIP codes less than 10 kilometers from the MSA centroid (city hall), and the suburbs to be the zip codes more than 40 kilometers from the MSA centroid. For each zip code, we compute the price-rent ratio in each month from January 2014 (the start of ZORI data) and December 2019. We compute the time-series mean of the price-rent ratio. Similarly, we compute the time-series mean of the average annual rental growth rate for each zip code over the 2014–2019 period. We then compute population-weighted averages among the urban and among the suburban zip codes. This delivers the first four columns of Table I. For presentation purposes, the mean price-rent ratio is reported in levels (rather than logs) and average rent growth is multiplied by 100 (expressed in percentage points). We use equation (5) to compute the expected annual returns in columns (5) and (6). These expected returns are also multiplied by 100 in the table (annual percentage points). Expected returns are between 5% and 14%. Typically, though not always, expected returns are higher in the suburbs.

Columns (7) and (8) report the price-rent ratio (in levels) for the pandemic. We report the mean computed over October, November, and December of 2020 (or over as many of these three months as are available in the data).

Column (9) reports  $\Delta pd$ , the change in the urban-minus-suburban price-rent ratio in the pandemic versus before the pandemic. It is expressed in levels. Most of its values are positive, implying that price-rent ratios went up in urban relative to suburban areas. What this implies depends on the model in question.

### IV.D.1 Pandemic is Transitory

In the model in which the pandemic is purely transitory, the positive  $\Delta pd$  implies that urban rent growth is expected to exceed suburban rent growth:  $g_t^u - g_t^s > 0$ . After



the steep decline in urban rents, urban rent growth is expected to rebound to restore the price-rent ratio to its pre-pandemic level. The large increase in suburban rents also mean reverts, leading to slower expected rent growth in the suburbs. Column (10)-(12) report the urban minus suburban cumulative rent differential, computed from equation (15) under assumptions 2, 3, and 4, respectively.

To implement equation (15), we need values for  $(\rho_g, \rho_x, \rho^j)$ . We set  $\rho_g = 0.747$ . This is the estimated 12-month persistence of annual rent growth rates in the U.S. between 1982 and 2020. It implies a half-life of expected rent shocks of approximately 2.5 years. Note that the AR(1) assumption on expected rents means that a 1% point change in current period expected rent translates into a  $(1 - \rho^j \rho_g)^{-1} \approx 3.5\%$  point cumulative change in rents over the current and all future periods (assuming a typical value for  $\rho^j$ ).

We set  $\rho_x = 0.917$  based on the observed persistence of aggregate annual price-dividend ratios.<sup>7</sup>

We compute  $\rho^j$  from equation (2), using the population-weighted mean price-rent ratio for all zip codes in the MSA pre-pandemic.

---

<sup>7</sup>We compute the log price-rent ratio for the United States from January 1987 until December 2020 as the log of the Case-Shiller Core Logic National House Price Index minus the log of the CPI Rent of Primary Residence series. We then take the 12-month autocorrelation.

Table I. Backing Out Expected Rents

#	MSA	(1)	(2)	(3)	(4)	(5)	(6)	(7)	(8)	(9)	(10)	(11)	(12)	(13)	(14)
		Pre-pandemic						Pandemic		$\Delta pd^j$	Transitory Change			Permanent Change	
		$\overline{PD}^{uj}$	$\overline{PD}^j$	$\overline{g}^{uj}$	$\overline{g}^j$	$\overline{x}^{uj}$	$\overline{x}^j$	$PD_t^{uj}$	$PD_t^j$			$(g_t^{uj} - g_t^j) / (1 - \rho^j \rho_g)$	$\kappa = 0.5$	$\Delta x^j = 0.01$	$\Delta \overline{x}^j = 0$
1	New York-Newark-Jersey City, NY-NJ-PA	24.85	17.47	2.50	2.91	6.44	8.47	27.06	17.93	5.99	4.56	12.75	12.64	-0.23	0.77
2	Los Angeles-Long Beach-Anaheim, CA	29.55	24.48	5.76	4.12	9.09	8.13	34.95	25.47	12.82	18.65	14.53	27.25	1.99	2.99
3	Chicago-Naperville-Elgin, IL-IN-WI	17.40	11.34	2.88	2.79	8.47	11.24	18.73	11.94	2.18	2.48	12.21	9.51	0.07	1.07
4	Dallas-Fort Worth-Arlington, TX	15.18	12.62	4.27	4.02	10.65	11.65	17.51	13.76	5.55	6.37	9.74	13.12	0.46	1.46
5	Houston-The Woodlands-Sugar Land, TX	20.52	14.05	0.99	1.83	5.74	8.71	22.18	14.46	4.87	2.10	12.16	8.89	-0.69	0.31
6	Washington-Arlington-Alexandria, DC-VA-MD-WV	23.91	17.74	2.94	1.99	7.04	7.47	26.71	18.75	5.59	8.88	10.60	16.78	1.09	2.09
7	Miami-Fort Lauderdale-Pompano Beach, FL	16.26	11.93	2.79	4.00	8.75	12.05	18.08	12.96	2.29	-1.66	9.38	5.04	-1.25	-0.25
8	Philadelphia-Camden-Wilmington, PA-NJ-DE-MD	10.60	14.85	3.11	2.43	12.12	8.95	12.88	15.75	13.61	15.82	5.01	22.63	1.85	2.85
9	Atlanta-Sandy Springs-Alpharetta, GA	16.26	13.66	6.21	4.58	12.18	11.64	18.40	14.39	7.13	12.49	10.65	19.31	1.96	2.96
10	Phoenix-Mesa-Chandler, AZ	14.98	15.84	7.31	6.26	13.78	12.38	16.82	16.34	8.47	12.03	6.91	19.37	1.56	2.56
11	Boston-Cambridge-Newton, MA-NH	21.30	17.08	3.88	4.64	8.47	10.33	24.40	18.65	4.83	2.19	9.60	10.15	-0.65	0.35
12	San Francisco-Oakland-Berkeley, CA	33.56	26.38	4.02	4.68	6.95	8.40	39.07	28.94	5.92	3.55	9.90	12.33	-0.58	0.42
15	Seattle-Tacoma-Bellevue, WA	30.71	16.04	5.59	6.46	8.79	12.51	36.29	18.67	1.50	-1.56	13.62	6.60	-1.22	-0.22
17	San Diego-Chula Vista-Carlsbad, CA	21.46	22.13	5.56	4.95	10.11	9.37	23.72	23.66	3.36	5.51	2.44	13.73	0.76	1.76
18	Tampa-St Petersburg-Clearwater, FL	11.51	9.46	5.03	4.89	13.36	14.95	14.39	11.26	4.82	5.27	10.37	11.71	0.20	1.20
19	Denver-Aurora-Lakewood, CO	21.68	18.58	5.68	5.03	10.18	10.27	24.34	19.72	5.63	7.87	8.20	15.65	0.84	1.84
20	St Louis, MO-IL	13.77	12.93	3.11	2.67	10.12	10.12	14.70	14.01	-1.44	-0.02	-0.05	6.26	0.32	1.32
21	Baltimore-Columbia-Towson, MD	8.84	14.93	1.43	1.57	12.15	8.05	9.47	15.74	1.64	1.21	-12.30	7.80	0.23	1.23
22	Charlotte-Concord-Gastonia, NC-SC	15.06	13.25	6.07	3.14	12.50	10.42	18.36	14.06	13.91	23.55	16.38	30.46	3.65	4.65
23	Orlando-Kissimmee-Sanford, FL	12.99	11.85	5.45	4.31	12.87	12.41	15.01	12.98	5.34	9.08	7.54	15.84	1.43	2.43
24	San Antonio-New Braunfels, TX	11.63	13.94	3.99	2.46	12.24	9.39	13.27	15.13	5.09	10.05	0.64	16.63	1.99	2.99
26	Sacramento-Roseville-Folsom, CA	17.91	22.18	7.09	7.99	12.53	12.40	19.32	19.97	18.08	14.96	14.49	22.80	-0.04	0.96
29	Austin-Round Rock-Georgetown, TX	21.07	14.47	4.16	3.11	8.80	9.80	25.30	16.32	6.26	9.82	13.54	17.28	1.07	2.07
	MSA Population Weighted Average									6.45	7.47	10.02	14.96	0.54	1.54

Covid Economics 69, 18 February 2021: 1-45

When there is no differential change in urban versus suburban risk premia (column 10), urban rent growth will exceed suburban rent growth by 4.5% points in New York over the next several years cumulatively. However, if the urban risk premium temporarily rises by 1% point relative to the suburban risk premium (which is the case for New York under both assumptions 2 and 3), and that difference then slowly reverts back to 0, then urban rent growth will exceed suburban rent growth by 12.7%.

Los Angeles is expected to see much larger cumulative urban-suburban rent growth, between 14.5% and 27.3% depending on the assumption on risk premia. This is because the change in the urban minus suburban price-rent ratio is much larger in LA (12.8%). Restoring the pre-pandemic urban-suburban price-rent multiples requires large catch-up growth in urban rents.

Miami, St Louis, and Baltimore are at the other end of the spectrum with low urban-suburban rent growth expectations under the assumption of no risk premium changes (column 10). Baltimore is unusual in that it has higher price-rent ratios, lower rent growth, and much higher risk premia in the urban core than in the suburbs pre-pandemic. If the risk premium differential becomes smaller by 2% points (column 11), this implies that the urban risk premium falls, requiring a smaller change in rents. Indeed, urban rent growth is now 12.3% below that in the suburbs. If instead the suburban risk premium falls relative to the urban one by 1% point (column 12), urban rent growth must exceed suburban growth by 7.8% to restore the old price-rent ratios.

#### IV.D.2 Pandemic is Permanent

In the model where the pandemic is permanent, the interpretation of the price-rent ratio change  $\Delta p d^j$  is quite different. Columns (13) and (14) report the expected urban minus suburban rent growth, as given by equation (16) under assumptions 4 and 5, respectively. These columns report an annual growth rate differential (not a cumulative change), which is now expected to be permanent.

If risk premia did not change (column 13), New York's price-rent ratio in December 2020 implies permanently lower annual rent growth of -0.23% in urban than in suburban zip codes. However, if the urban-suburban risk premium rose permanently by 1% point (thereby shrinking it from -2% pre-pandemic to -1% post-pandemic), urban rent growth is expected to exceed suburban growth by 0.77% annually. Naturally, the numbers in columns (13) and (14) differ by exactly 1% point, the assumed difference in urban-suburban risk premia between the two columns. Column (14) can be compared to column (12), after dividing column (12) by about 3.5 (more precisely, multiplying it by  $1 - \rho^j \rho_g$ ). Both numbers then express an annual expected rent growth under the assumption that risk premia in urban areas go up by 1% point relative to suburban areas. For New York, the temporary model implies 3.65% higher rent growth in urban zip codes while the permanent model implies 0.77% higher growth. Of course, in the temporary model, both the expected rent growth and the expected return will revert to pre-pandemic levels while in the permanent model they will not. However, both models suggest that the market expects the rent in urban zip codes in New York to grow more strongly than in the suburbs in the future.

In Los Angeles, the permanent model implies urban rent growth that will exceed suburban growth by 2% (column 13) or 3% (column 14). We find similar rent growth differences for Atlanta, and even stronger rent growth differences for Charlotte.

Miami, Seattle, and San Diego see the lowest urban growth differentials.

## V Mechanisms

This section explores potential drivers of the changing price and rent gradient, exploiting variation across MSAs.

Table II regresses the change in price gradient for each of the top-30 MSAs on several MSA-level characteristics, while Table III does the same for the change in rent gradient.

Column (1) shows that the MSAs with the highest price or rent levels before the pandemic saw the largest change in price or rent gradient. This one variable alone explains 45.6% of variation in price gradient changes and 23.6% of variation in rent gradient changes. The next columns try to unpack why price or rent levels are such strong cross-sectional predictors.

Table II. Explaining the Variation in Price Gradient Changes

	(1)	(2)	(3)	(4)	(5)	(6)	(7)
Log Price 2018	0.0228*** (0.00470)						
Saiz supply elasticity		-0.00929* (0.00386)					-0.00945 (0.00502)
Land unavailable percent			0.0290 (0.0290)				-0.0296 (0.0352)
Wharton Regulatory Index				0.0123* (0.00469)			0.00406 (0.00606)
Dingel Neiman WFH					0.219* (0.0818)		0.173 (0.0943)
Share of local friends						-0.0170 (0.357)	0.204 (0.335)
Constant	-0.286*** (0.0596)	0.0176* (0.00665)	-0.00297 (0.00678)	-0.00101 (0.00320)	-0.0778* (0.0303)	0.0197 (0.348)	-0.241 (0.329)
Observations	30	30	30	30	30	30	30
R <sup>2</sup>	0.456	0.171	0.034	0.196	0.204	0.000	0.365
Adjusted R <sup>2</sup>	0.437	0.142	-0.000	0.168	0.176	-0.036	0.232
F	23.47	5.793	1.000	6.848	7.190	0.00227	2.756

Standard errors in parentheses

\*  $p < 0.05$ , \*\*  $p < 0.01$ , \*\*\*  $p < 0.001$

Columns (2)–(4) find evidence that metros with more inelastic supply experience, as measured by the housing supply elasticity measure of [Saiz \(2010\)](#), the land unavailability of [Lutz and Sand \(2019\)](#), or the Wharton regulatory and land use restrictions index ([Gyourko, Saiz, and Summers, 2008](#)) experience stronger reversals in their price gradients. This suggests that some of the most inelastic regions are experiencing a reversal in urban concentration, and residents migrate to suburban areas and other metros that have higher land elasticity.

Column (5) finds strong evidence that cities with a greater fraction of jobs which can be done from home (Dingel and Neiman, 2020) see a larger increase in their price gradient — suggesting that the greater adoption of remote work practices has led to a spatial flattening of real estate prices. The DN measure varies between 29% and 45% for the MSAs in our sample. A 10% increase in the fraction of jobs that can be done from home results in a change in slope of 0.02, which is larger than the entire nationwide average change in the price gradient and nearly half of the average change in rent gradient. Variation in remote work across MSAs explains 20.4% of the variation in price gradients and 25.4% of the variation in rent gradients.

Column (6) examines social connectivity using Facebook data (Bailey, Cao, Kuchler, Stroebel, and Wong, 2018). We find that areas that have a higher share of local friends (as opposed to connections in other MSAs) see smaller increases in their price and rent gradients, which is the opposite sign to the one we expected to find. This relationship is not significant, however.

All independent variables combined explain 37% of the variation in price gradients and 29% of the variation in rent gradients, as indicated in column (7). This is nearly as much (more than) as the effect of price (or rent) in column (1), which capitalize (summarize) all supply elasticity, amenity, and commuting effects.

Prior research has indicated that as much as half of the national increase in rents over 2000–2018 have come from individuals sorting to inelastic areas (Howard and Liebersohn, 2020). If individuals continue migrating to areas which are both cheaper and more elastic in their housing supply, future housing cost increases will moderate compared to the recent past. Our results point to dynamic aggregate gains for renters if Covid-associated sorting continues.

Table III. Explaining the Variation in Rent Gradient Changes

	(1)	(2)	(3)	(4)	(5)	(6)	(7)
Log Rent 2018	0.0401** (0.0137)						
Saiz supply elasticity		-0.00394 (0.00527)					0.00197 (0.00667)
Land unavailable percent			0.0392 (0.0364)				0.0417 (0.0468)
Wharton Regulatory Index				0.0121 (0.00616)			0.00193 (0.00806)
Dingel Neiman WFH					0.307** (0.0995)		0.276* (0.125)
Share of local friends						-0.254 (0.446)	-0.201 (0.446)
Constant	-0.275* (0.101)	0.0283** (0.00909)	0.0140 (0.00850)	0.0182*** (0.00421)	-0.0912* (0.0369)	0.270 (0.435)	0.104 (0.437)
Observations	30	30	30	30	30	30	30
R <sup>2</sup>	0.236	0.020	0.040	0.121	0.254	0.011	0.289
Adjusted R <sup>2</sup>	0.209	-0.015	0.006	0.090	0.228	-0.024	0.141
F	8.641	0.558	1.164	3.861	9.542	0.324	1.955

Standard errors in parentheses

\*  $p < 0.05$ , \*\*  $p < 0.01$ , \*\*\*  $p < 0.001$ 

## VI Conclusion

A central paradox of the internet age has been that digital tools enable greater collaboration at further distances, yet have led to even more concentrated economic activity into a handful of dense urban areas. We document that the COVID-19 pandemic has partially reversed this trend. The spatial dispersal in activity is particularly strong for rents but also present in prices. Housing markets paint an optimistic picture of urban revival, indicating higher rent growth in urban versus suburban areas for the foreseeable future. These shifts in economic activity appear to be related to practices around working from home, suggesting that they may also persist to the extent that employers allow remote working practices.

A key benefit to workers of this changing economic geography is being able to access

the larger and more elastic housing stock at the periphery of cities, thereby alleviating rent burden at least temporarily. However, our results also point to potential problems for local government finances in the wake of the pandemic. Urban centers may confront dwindling populations and lower tax revenue from property and sales in the short and medium run. More dispersed economic activity may offer greater opportunities for areas which have been previously left behind, but potentially at the cost of agglomeration economies built in urban areas. Overall our results suggest important challenges and opportunities in the context of a radically reshaped urban landscape.



## References

- Albouy, David, 2016, What are cities worth? Land rents, local productivity, and the total value of amenities, *Review of Economics and Statistics* 98, 477–487.
- Albouy, David, Gabriel Ehrlich, and Minchul Shin, 2018, Metropolitan Land Values, *The Review of Economics and Statistics* 100, 454–466.
- Althoff, Lukas, Fabian Eckert, Sharat Ganapati, and Conor Walsh, 2020, The City Paradox: Skilled Services and Remote Work, *CESifo Working Paper No. 8734*.
- Bailey, Michael, Rachel Cao, Theresa Kuchler, Johannes Stroebel, and Arlene Wong, 2018, Social Connectedness: Measurement, Determinants, and Effects, *Journal of Economic Perspectives* 32, 259–80.
- Barrero, Jose Maria, Nicholas Bloom, and Steven J. Davis, 2020, Why Working From Home Will Stick, *Working Paper*.
- Binsbergen, Jules van, and Ralph Koijen, 2010, Predictive Regressions: A Present-Value Approach, *Journal of Finance* 65 (4).
- Bloom, Nicholas, 2020, How Working from Home Works Out, Working paper Institute for Economic Policy Research (SIEPR).
- Campbell, John Y, and Robert J Shiller, 1989, The Dividend-Price Ratio and Expectations of Future Dividends and Discount Factors, *Review of Financial Studies* 1, 195–228.
- Campbell, Sean D., Morris A. Davis, Joshua Gallin, and Robert F. Martin, 2009, What Moves Housing Markets: A Variance Decomposition of the Rent-Price Ratio, *Journal of Urban Economics* 66.
- Coven, Joshua, Arpit Gupta, and Iris Yao, 2020, Urban Flight Seeded the COVID-19 Pandemic Across the United States, *Covid Economics* 54.

- Davis, Morris A., Andra C. Ghent, and Jesse Gregory, 2021, The Work-at-Home Technology Boon and its Consequences, *Working Paper*.
- De Fraja, Gianni, Jesse Matheson, and James Charles Rockey, 2020, Zoomshock: The Geography and Local Labour Market Consequences of Working from Home, *Covid Economics* 64.
- Delventhal, Matt, Eunjee Kwon, and Andrii Parkhomenko, 2021, How Do Cities Change When We Work from Home?, *Working Paper*.
- Dingel, Jonathan I, and Brent Neiman, 2020, How many jobs can be done at home?, *Journal of Public Economics* 189, 104235.
- Favilukis, Jack, Pierre Mabilie, and Stijn Van Nieuwerburgh, 2019, Affordable Housing and City Welfare, Working Paper 25906 National Bureau of Economic Research.
- Glaeser, Edward L., 2011, *Triumph of the City: How Our Greatest Invention Makes Us Richer, Smarter, Greener, Healthier, and Happier*. (Penguin Press New York).
- Gormsen, Niels Joachim, and Ralph SJ Koijen, 2020, Coronavirus: Impact on stock prices and growth expectations, *The Review of Asset Pricing Studies* 10, 574–597.
- Gupta, Arpit, Stijn Van Nieuwerburgh, and Constantine Kontokosta, 2020, Take the Q Train: Value Capture of Public Infrastructure Projects, Working Paper 26789 National Bureau of Economic Research.
- Gyourko, Joseph, Christopher Mayer, and Todd Sinai, 2013, Superstar Cities, *American Economic Journal: Economic Policy* 5, 167–99.
- Gyourko, Joseph, Albert Saiz, and Anita Summers, 2008, A new measure of the local regulatory environment for housing markets: The Wharton Residential Land Use Regulatory Index, *Urban Studies* 45, 693–729.

- Han, Lu, and William C Strange, 2015, The Microstructure of Housing Markets, *Handbook of Regional and Urban Economics* 5, 813–886.
- Hornbeck, Richard, and Enrico Moretti, 2018, Who Benefits From Productivity Growth? Direct and Indirect Effects of Local TFP Growth on Wages, Rents, and Inequality, Working Paper 24661 National Bureau of Economic Research.
- Howard, Greg, and Jack Liebersohn, 2020, Why is the Rent So Darn High?, *Working Paper*.
- Hsieh, Chang-Tai, and Enrico Moretti, 2019, Housing Constraints and Spatial Misallocation, *American Economic Journal: Macroeconomics* 11, 1–39.
- Jones Lang LaSalle, 2020, United States Office Outlook — Q4 2020, Technical report.
- Koijen, Ralph, and Stijn van Nieuwerburgh, 2011, Predictability of Stock Returns and Cash Flows, *Annual Review of Financial Economics* 3, 467–491.
- Lettau, Martin, and Stijn Van Nieuwerburgh, 2008, Reconciling the Return Predictability Evidence: In-Sample Forecasts, Out-of-Sample Forecasts, and Parameter Instability, *Review of Financial Studies* 21, 1607–1652.
- Ling, David C, Chongyu Wang, and Tingyu Zhou, 2020, A first look at the impact of COVID-19 on commercial real estate prices: Asset-level evidence, *The Review of Asset Pricing Studies* 10, 669–704.
- Liu, Sitian, and Yichen Su, 2021, The Impact of the COVID-19 Pandemic on the Demand for Density: Evidence from the U.S. Housing Market, Working paper.
- Lutz, Chandler, and Ben Sand, 2019, Highly Disaggregated Land Unavailability, *Working Paper*.
- Moretti, Enrico, 2013, Real wage inequality, *American Economic Journal: Applied Economics* 5, 65–103.

- Roback, Jennifer, 1982, Wages, rents, and the quality of life, *Journal of political Economy* 90, 1257–1278.
- Rosen, Sherwin, 1979, Wage-based indexes of urban quality of life, *Current issues in urban economics* pp. 74–104.
- Saiz, Albert, 2010, The geographic determinants of housing supply, *The Quarterly Journal of Economics* 125, 1253–1296.
- United Nations, Population Division, 2019, World Urbanization Prospects: The 2018 Revision, Working paper, United Nations.
- Van Binsbergen, Jules, Michael Brandt, and Ralph Kojen, 2012, On the Timing and Pricing of Dividends, *American Economic Review* 102, 1596–1618.
- Van Binsbergen, Jules, Wouter Hueskes, Ralph Kojen, and Evert Vrugt, 2013, Equity Yields, *Journal of Financial Economics* 110, 503–519.
- Van Nieuwerburgh, Stijn, 2019, Why Are REITs Currently So Expensive?, *Real Estate Economics* 47, 18–65.

## A Data Appendix

Table A.I shows the MSAs included in our sample

Table A.I. Top-30 MSAs

#	MSA	Population (Millions)	Pre-pandemic Price Gradient	Pre-pandemic Rent Gradient	Change in Price Gradient	Change in Rent Gradient
1	New York-Newark-Jersey City, NY-NJ-PA	19.22	-0.241	-0.133	0.032	0.056
2	Los Angeles-Long Beach-Anaheim, CA	13.21	-0.227	-0.056	0.005	0.024
3	Chicago-Naperville-Elgin, IL-IN-WI	9.46	-0.170	-0.052	0.006	0.040
4	Dallas-Fort Worth-Arlington, TX	7.57	-0.092	0.006	0.001	0.024
5	Houston-The Woodlands-Sugar Land, TX	7.07	-0.089	-0.051	-0.011	0.026
6	Washington-Arlington-Alexandria, DC-VA-MD-WV	6.28	-0.162	-0.064	0.011	0.033
7	Miami-Fort Lauderdale-Pompano Beach, FL	6.17	-0.131	-0.006	0.010	0.019
8	Philadelphia-Camden-Wilmington, PA-NJ-DE-MD	6.10	-0.011	-0.042	0.001	0.005
9	Atlanta-Sandy Springs-Alpharetta, GA	6.02	-0.212	-0.040	0.005	0.031
10	Phoenix-Mesa-Chandler, AZ	4.95	-0.063	0.103	-0.016	0.037
11	Boston-Cambridge-Newton, MA-NH	4.87	-0.239	-0.132	0.017	0.036
12	San Francisco-Oakland-Berkeley, CA	4.73	-0.159	-0.081	0.042	0.052
13	Riverside-San Bernardino-Ontario, CA	4.65	-0.166	-0.019	-0.001	0.017
14	Detroit-Warren-Dearborn, MI	4.32	0.033	0.295	-0.015	-0.049
15	Seattle-Tacoma-Bellevue, WA	3.98	-0.151	-0.031	0.029	0.055
16	Minneapolis-St Paul-Bloomington, MN-WI	3.64	-0.116	-0.025	0.005	0.034
17	San Diego-Chula Vista-Carlsbad, CA	3.34	-0.071	0.043	-0.008	0.010
18	Tampa-St Petersburg-Clearwater, FL	3.19	-0.079	-0.029	0.007	0.014
19	Denver-Aurora-Lakewood, CO	2.97	-0.092	0.060	0.010	0.024
20	St Louis, MO-IL	2.80	0.004	0.043	0.010	0.014
21	Baltimore-Columbia-Towson, MD	2.80	0.069	0.025	0.008	0.010
22	Charlotte-Concord-Gastonia, NC-SC	2.64	-0.223	-0.003	0.002	0.031
23	Orlando-Kissimmee-Sanford, FL	2.61	-0.044	0.023	-0.002	0.017
24	San Antonio-New Braunfels, TX	2.55	-0.040	0.130	-0.012	0.001
25	Portland-Vancouver-Hillsboro, OR-WA	2.49	-0.101	0.168	0.018	0.016
26	Sacramento-Roseville-Folsom, CA	2.36	-0.083	0.032	0.010	0.029
27	Pittsburgh, PA	2.32	0.028	-0.350	-0.032	0.041
28	Las Vegas-Henderson-Paradise, NV	2.27	0.015	0.074	0.008	0.006
29	Austin-Round Rock-Georgetown, TX	2.23	-0.329	-0.124	-0.015	0.032
30	Cincinnati, OH-KY-IN	2.22	0.009	0.204	-0.036	-0.017

Table A.II. List of variables used at the ZIP code level

Variable Name	Source	Description
Zillow Home Value Index (ZHVI)	Zillow	All Homes (SFR, Condo/Co-op) Time Series, Smoothed, Seasonally Adjusted (\$)
Zillow Observed Rent Index (ZORI)	Zillow	All Homes Plus Multifamily Time Series, Smoothed, Seasonally Adjusted (\$)
Median List Price	Realtor	The median listing price within the specified geography during the specified month (\$)
Median List Price Per Sqft	Realtor	The median listing price per square foot within the specified geography during the specified month (\$)
Active Listing Count	Realtor	The active listing count tracks the number of for sale properties on the market, excluding pending listings where a pending status is available. This is a snapshot measure of how many active listings can be expected on any given day of the specified month.
Median Days on Market	Realtor	The median number of days property listings spend on the market between the initial listing of a property and either its closing date or the date it is taken off the market.
Median Household Income	Census Bureau	Median income of a household (2017).
Proportion of Rich Households	Census Bureau	Proportion of households with yearly income higher than 150 thousand dollars (2016).
Proportion of Black Residents	Census Bureau	Proportion of black residents (2016).

# Do localised lockdowns cause labour market externalities?<sup>1</sup>

Gabriele Guitoli<sup>2</sup> and Todor Tochev<sup>3</sup>

Date submitted: 10 February 2021; Date accepted: 14 February 2021

*The business restrictions introduced during the Covid-19 pandemic greatly affected the labour market. However, quantifying their costs is not trivial as local policies affect neighbouring areas through spillovers. Exploiting the U.S. local variation in restrictions and commuting, we estimate the causal direct and spillover impacts of lockdowns. Spillovers alone account for 10-15% of U.S. job losses. We corroborate these results with causal evidence for a consumption-based mechanism: shops whose consumers reside in neighbouring areas under lockdown experience larger employment losses, even if no local restriction is in place. Accounting for spillovers implies larger lockdowns' total effects, but smaller direct ones.*

1 We would like to thank Roland Rathelot, Roberto Pancrazi, Clement Imbert, Manuel Bagues, Thijs van Rens, Marta Santamaria, Velichka Dimitrova, Riccardo Degasperi, Song Yuan, Simon Hong, Ashish Aggarwal, and Teodora Tsankova for valuable comments, suggestions and discussions. All remaining errors are our own. Both authors gratefully acknowledge support from the ESRC.

2 University of Warwick, Department of Economics.

3 PhD Student, Department of Economics, University of Warwick.

Copyright: Gabriele Guitoli and Todor Tochev

# 1 Introduction

Following the diffusion of Covid-19 since December 2019, economic activity around the globe has experienced an unprecedented disruption. Given the lack of effective treatments or vaccines, public health authorities were forced to rely on non-pharmaceutical interventions to curb the virus's spread, often restricting non-essential economic activity.

In the United States, no such policy was implemented at the federal level, as the decision was left to local officials. These enacted policies based on their own judgement, public health conditions and local institutional constraints, creating a significant variation in the size of restrictions across time and space: while the first stay-at-home orders were implemented as early as 15th March 2020, the latest one was introduced almost three weeks later in South Carolina.

However, local measures are unlikely to have local consequences only. The interconnectedness of geographically distant locales is one of the defining features of modern economies, with a quarter of all U.S. workers crossing county, state or even country borders on their way to work. Similarly, consumers look for goods and services outside their immediate neighbourhood (Davis et al., 2019). Consequently, policies restricting local economic activity are likely to generate negative spillover effects in neighbouring jurisdictions.

In this paper, we quantify these spillovers. First, we show that an unbiased estimate of the effects of lockdowns on labour market outcomes requires to account for the spatial dimension of economic activity. Then, we exploit exogenous variations in local areas' exposure to neighbours' policies to provide a causal estimate of lockdown effects. We provide results for both residence-based unemployment and establishment-based employment, capturing different aspects of the spillovers. Finally, we provide novel causal evidence for a mechanism behind employment spillovers: we show that measures restricting consumers' mobility affect employment at the individual shop/branch level. Shops whose consumers base is highly exposed to measures implemented by neighbouring counties experience large falls in employment, even if no local restriction is in place.



We find that the impact of spillovers is substantial, accounting for approximately 15-20% of the total change in residence-based unemployment between February and April 2020, or a third of the estimated total effect of lockdowns. Moreover, spillovers explain 10-15% of the fall in establishment-based employment, showing that lockdown orders affected not only local jobs but also businesses in neighbouring counties. Summing direct and spillover effects, the total impact is at least equal, if not larger, than previous estimates which did not account for externalities. With respect to these, we estimate a different spatial distribution of the impact of lockdowns. On the one hand, suburban areas and border regions of states that followed different lockdown policies experienced unemployment increases due to their neighbours' policies. On the other, cities and suburban "commercial" areas were the most affected by consumers' behaviour restrictions.

These results are relevant for policy-makers, as lockdowns cause large economic effects extending beyond the jurisdiction in which they are enacted. While this does not preclude localised lockdowns from being optimal<sup>1</sup>, our results empirically show that the spillovers are non-negligible and should be accounted for. Policies such as grants schemes for businesses affected by mandatory closures should be designed taking into account the spatial externalities affecting neighbouring regions. For example, this was not the case for the UK's *Local Restrictions Support Grants* scheme, which only supports businesses *within* the geographical areas directly affected by the lockdown tier system.

### Related Literature

Our paper is related to a rapidly developing literature on the economic effects of the Covid-19 pandemic. [Coibion, Gorodnichenko, and Weber \(2020\)](#) find that almost 20 million jobs were lost by April 2020. [Baek et al. \(2020\)](#) find that an additional week of exposure to a stay-at-home (SAH) order increased state unemployment claims by around 1.9% of a state's employment level. We contribute by i) providing an estimate of lockdowns' effects on labour market outcomes which approximates an ideal agnostic decomposition and ii) establishing the causal effect of spillovers originating from neighbours' orders.

---

<sup>1</sup>All state-wide orders generate potentially large spillovers too, both within the state in which they were enacted and in bordering counties.

On the consumption side, [Goolsbee and Syverson \(2020\)](#) find that SAH orders explain only 7% of the total fall in foot-fall traffic of local POIs. Extending the analysis, we estimate the effects of a broader range of non-pharmaceutical intervention and account for spatial externalities. Moreover, we address the question of the impact on labour markets more directly through a proxy for shop-level employment. Our results provide causal evidence for facts similar to those observed in [Althoff et al. \(2020\)](#) regarding the effect of restrictions on employment in areas whose economy relies on commuters and consumers' mobility.

[Fajgelbaum et al. \(2020\)](#) design an optimal lockdown policy when considerable commuting flows within large urban areas are present, taking into account both epidemiological and economic aspects. Human interaction linkages across space have been found to be relevant drivers of the pandemic spread, as in [Antràs, Redding, and Rossi-Hansberg \(2020\)](#) and, using granular data, [Chang et al. \(2020\)](#). These facts have relevant implications when studying the economic impact of the Covid-19 epidemic with SIR-economic models as in [Birge, Candogan, and Feng \(2020\)](#) and [Giannone, Paixão, and Pang \(2020\)](#). With respect to the existing literature, we provide causal evidence for the determinants the spatial distribution of changes in economic activity during the pandemic, as well as evidence *matching* employment and exposure to neighbours' policies at the Point-Of-Interests (POIs) level, providing direct empirical evidence for a mechanism at work in both our empirical and their theoretical model.

Finally, we differentiate between the extensive (how long) and intensive (how many workers are affected) margins of spatial restrictions. Contributions such as [Borri et al. \(2020\)](#) and [Barrot, Grassi, and Sauvagnat \(2020\)](#) use similar distinctions to estimate the restrictions' economic costs and social benefits. Using granular mobility data and commuting flows, we further decompose these costs between those arising due to "own" and "neighbours" restrictions.

## Sections and Notation

Throughout the following pages, we will use "lockdown" as a shortcut to mean any order mandating the closure of some businesses, unless otherwise specified. These include SAH orders, but also less strict orders such as mall closures and capacity restrictions (or closures) of bars, restaurants, and other entertainment venues.

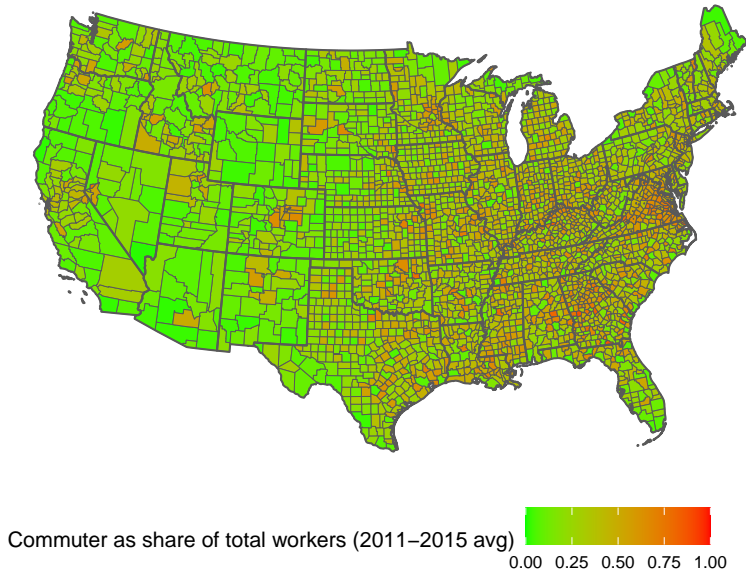
In Section 2 we present relevant facts about the U.S. labour market during the Covid-19 pandemic. In Section 3 we set how to reason about the spatial effects of lockdowns and provide a parsimonious framework. Section 4 presents the data, with the empirical application results in Section 5. We provide evidence for a mechanism behind these macro-level estimates in Section 6. We discuss further robustness checks and results in Section 7. Section 8 closes the paper.

## 2 Labour market facts during the pandemic

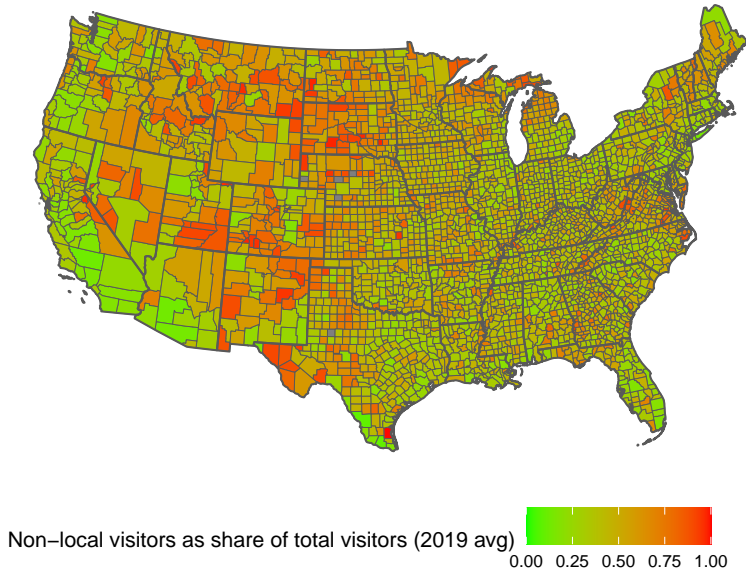
In this section, we provide evidence supporting the relevance of spatial spillovers arising from lockdown policies. First, we examine the county-level labour market outcomes during the first phase of the Covid-19 pandemic in the United States. Then, we demonstrate the existence of a correlation between these outcomes and counties' exposure to their neighbours' lockdown measures.

Figure 2.1a illustrates the share of each county's working-age population which commutes to other counties. Figure 2.2a maps the changes in unemployment divided by working-population between February 2020 and May 2020. Comparing the two maps shows how counties in the commuting area of large cities with more prolonged or severe closures have experienced larger unemployment increases than other counties within the same state. The same holds for counties bordering states in lockdowns. Figure 2.3a confirms this correlation. We plot the residual of the unemployment to working-age population ratio (with respect to a regression on local lockdown intensity, time FE and county by month FE) against our measure of neighbours' lockdown intensity weighted by the strength

Figure 2.1: Mobility flows in the United States



(a) Work Commuting Intensity (outflows)



(b) Consumption Commuting Intensity (inflows)

Note: share of visits to Points Of Interest of local county in the leisure sector incoming from other counties, out of total visits. Data by SafeGraph Inc.

of commuting relationships<sup>2</sup> and find a positive relationship. Note that these are the residuals that would be the ones obtained by a "naive" empirical strategy omitting the spillovers, providing further evidence for omitted variable bias.

Figure 2.2b shows similar facts for establishment-based employment. Larger falls appear connected to large cities, suburban areas and counties bordering states in lockdown. We find a negative relationship between employment residuals and spillovers in Figure 2.3b.

We will show that these facts are not only due to local sectors' closures or pre-determined factors such as the exposure to pandemic-sensitive sectors. Instead, provide robust evidence for a causal relationship between local labour market outcomes and commuting/consumption flows toward or from areas in lockdown. In the next section, we lay out the framework within which we model the relationship between labour market outcomes and lockdown policies.

### 3 Estimation Framework

We now describe the framework within which we estimate the main and spillover effects of localised lockdowns.

Consider a set of locations  $c \in C = \{1, 2, \dots, N\}$ . Each of these locations has "neighbours", locations with which it has some kind of economic relationship.

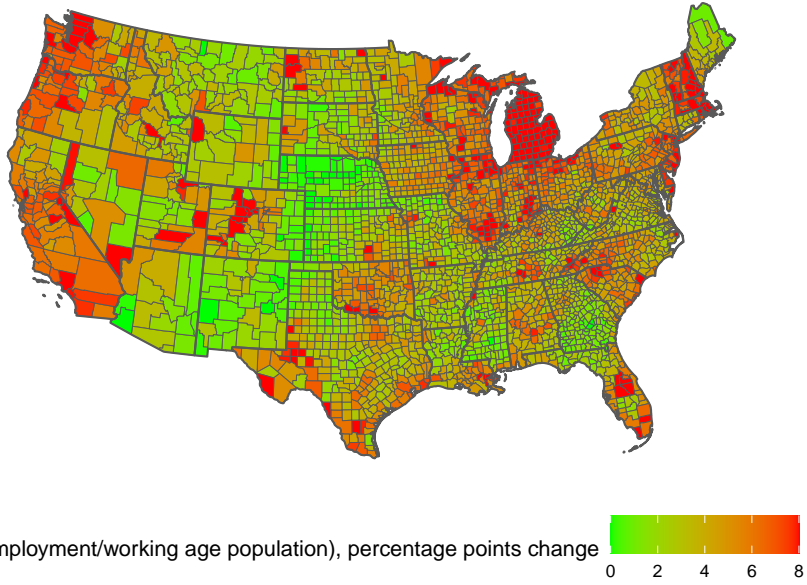
Define  $E_{ct}$  as the residents of county  $c$  employed at time  $t$ . Residents can work in other locations than  $c$ , so that total employment is the sum the individual flows toward each neighbour, including  $c$  itself. Define  $E_{cit}$  as the time- $t$  number of workers living in  $c$  and working in  $i$  (commuters). The following identity holds:

$$E_{ct} \equiv \sum_{i \in C} E_{cit} \quad (1)$$

One can think about  $E_{cit}$  as a function of the current local business conditions and pre-

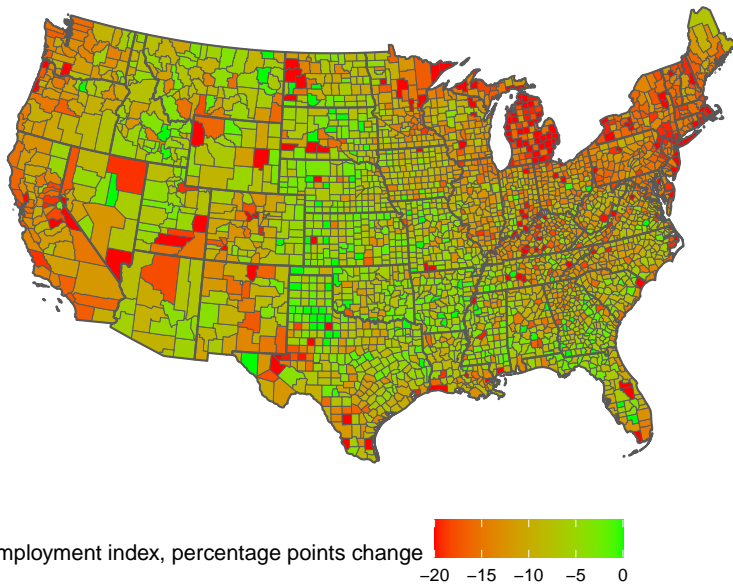
<sup>2</sup>We define this weighted lockdown intensity spillover in Section 4.2.

Figure 2.2: Labour market dynamics during the pandemic



Note: adjusted by the average February-May change between 2015 and 2019. Data from BLS's LAU estimates.

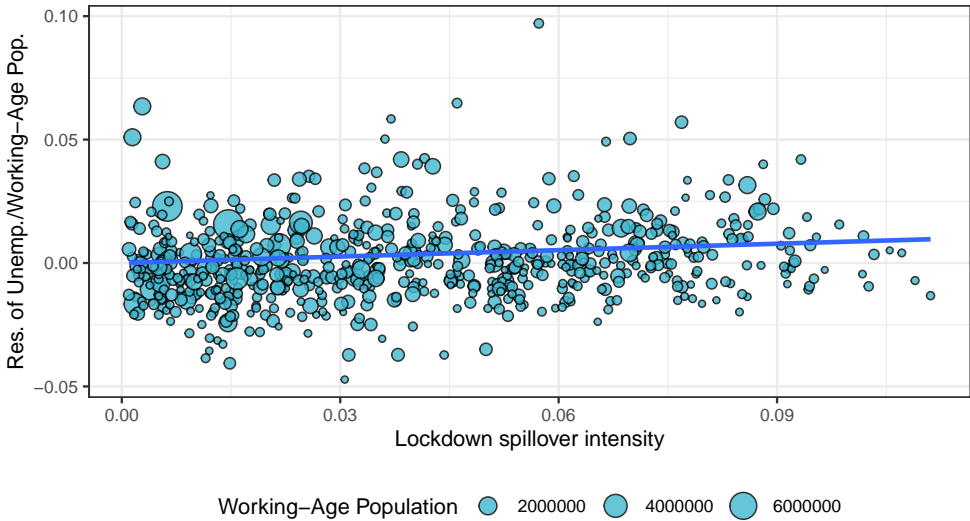
(a) Change in unemployment/working age population, May 2020.



Note: adjusted by the average February-May change between 2017 and 2019. Data from BLS's QCEW local area files.

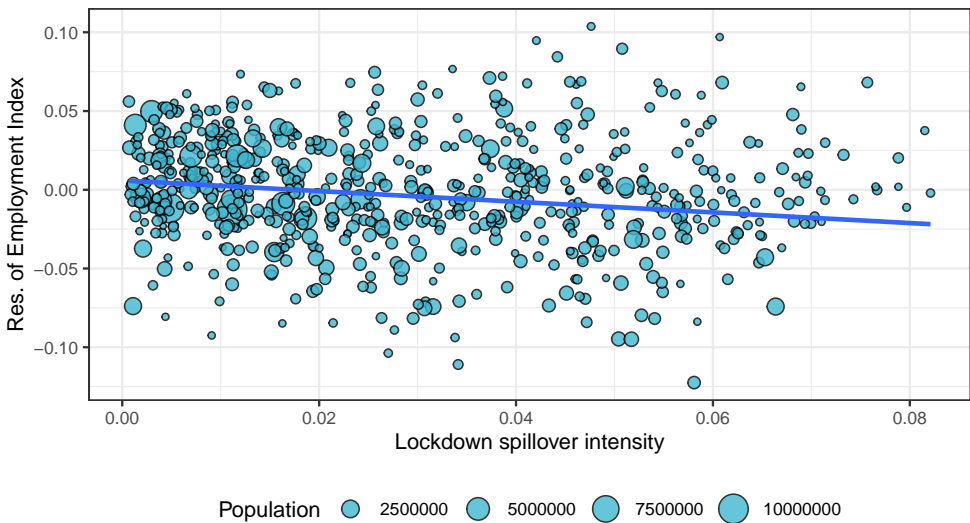
(b) Change in employment index (1=2019 average), May 2020

Figure 2.3: County-level labour market dynamics and neighbours' lockdown intensity



Note: residual of unemployment/working age population, April and May 2020, after controlling for time and countyXmonth fixed effects and the intensity of own lockdown; against lockdown intensity spillover. Only counties with an higher working age population than 150'000 are represented on the graph to enhance readability of the figure. The linear fit is weighted by the working-age population of each observation.

(a) Unemployment and spillover intensity



Note: Residual of change in employment/population, April and May 2020, after controlling for time and countyXmonth fixed effects and the intensity of own lockdown; against lockdown intensity spillover. Only counties with an higher working age population than 150'000 are represented on the graph to enhance readability of the figure. The linear fit is weighted by the population of each observation.

(b) Employment Index and spillover intensity

Covid Economics 69, 18 February 2021: 46-86

determined (at business cycle frequencies) parameters such as geography, infrastructure or the local pool of skills, capital and labour supply. At very short frequencies, we can consider prices as pre-determined too. In other words - given all predetermined factors -  $E_{cit}$  will depend on the demand for goods and services experienced by county  $i$  and  $c$ , and the consequent demand for labour. That is:  $E_{cit} = E_{cit}(D_{it}, D_{ct}, \cdot)$  with  $D_{xt}$  being the demand for labour in county  $x$  at time  $t$ .

To understand how  $E_{cit}$  responded to the pandemic and the related policies, it is important to highlight why  $D_i$  can be affected by lockdowns. Lockdowns directly affect the demand for labour in county  $i$  by restricting economic activities. Moreover, they may indirectly affect labour demand through changes in consumption patterns: if consumers cannot or do not need to reach a shop in a different county (think about commuters from Newark to Manhattan who start working from home), also demand for labour generated by such businesses may temporarily fall. To this, several higher-order effects can be added. In this sense,  $D_i$ ,  $D_c$  and thus  $E_{cit}$  may be contemporaneously affected by policies taken in *all* other counties. To provide a tractable framework and pin down the most relevant facts and effects of lockdowns, we need to discipline our analysis.

We focus on four main channels through which lockdown policies are likely to affect employment in county  $c$  consistently:

1. The direct effects of county  $c$ 's policies affecting residents working in  $c$  itself ( $E_{cc}$ ) as local businesses face restrictions to their activity;
2. The direct effect of county  $i$ 's policies on local workers, a share of which may reside (and thus turn up as unemployed) in  $c$ ;
3. The second-order effects in county  $c$  due to its residents losing jobs in county  $i$ ;
4. The spillovers arising from changes in the patterns of consumers' mobility from  $i$  to  $c$ , and vice versa (i.e. consumers residing in  $i$  stop spending in county  $c$ ).

Our analysis of unemployment changes will focus on channels (1) and (2): we show how unemployment increases in counties whose residents are likely to have been laid off from



jobs in neighbouring counties. Our analysis of employment will focus on channels (1), (3) and (4), exploring more directly how lockdowns cause the loss of additional jobs in neighbouring counties. We will provide causal, high-frequency evidence for the mechanism behind channel (4) using shop-level data.

### Decomposition of lockdown effects

Given the channels/mechanisms we focus on, we show how we empirically estimate the effects of lockdowns and why their estimate is likely to be biased if it does not account for spillovers. Define a set of lockdown-independent determinants  $X_t$ , a vector of lockdown intensities across all locations  $L_t = \{L_1, L_2, \dots, L_N\}$  and lockdown-dependent determinants  $X'_i(L_t)$  (possibly a vector) and assume we can write  $E_{cit} = E_{ci}(L_t, X_{ci}, X'_i(L_t))$ . Taking a first-order Taylor approximation around  $E_{c0}$ , we can decompose total employment in county  $c$  at time  $t$  into a lockdown-related and a lockdown-independent term:

$$E_{ct} \approx E_{c0} + \sum_{i' \in C} \sum_{i \in C} \left( \frac{\partial E_{ci}}{\partial L_{i't}} + (\nabla_{X'_{i'}(L)} E_{ci})' (\nabla_{L_{i't}} X'_{i'}(L)) \right) \Delta L_{i't} + \sum_{i \in C} \frac{\partial E_{ci}}{\partial X_{ci}} \Delta X_{cit} \quad (2)$$

Under the main assumption of limiting our attention to first-order effects across all  $c$  and  $i$  for which  $E_{ci} > 0$  or  $X'_{ci} > 0$  and assuming that the effects are linear in the weights of the adjacency matrix (for a complete treatment of the assumptions required and derivation see Appendix A.1), we can write this first-order approximation as a parsimonious specification of linear terms:

$$E_{ct} = E_{c0} + \frac{\partial E_c}{\partial L} \left( \sum_{i \in C} E_{ci} \Delta L_{it} \right) + \frac{\partial E_c}{\partial X'_c} \frac{\partial X'_c}{\partial L'} \left( \sum_{i \in C} X'_{ci} \Delta L_{it} \right) + \frac{\partial E_c}{\partial X} \Delta X_{tc} \quad (3)$$

Notice how this is a linear equation in a constant term  $E_{c0}$ , a control term depending on county-specific characteristics  $X$  and two lockdown-related terms regarding the direct effects  $\frac{\partial E_c}{\partial L}$  and the indirect effects  $\frac{\partial E_c}{\partial X'} \frac{\partial X'}{\partial L}$  arising from the effect of lockdowns on relevant variables (such as consumption flows). The direct term is the derivative of employment

with respect to the lockdown intensity  $L$ , defined as the commuting-flows weighted average of county-specific lockdown intensities  $L_i$ . Similarly, the indirect term includes a weighted average (through  $X'$  ex-ante relationships) of lockdown terms.

Both terms can be decomposed into "own" lockdown effects (the terms depending on  $\Delta L_{ct}$ ) and "spillover" (neighbours') lockdown effects (the sum of all those where  $i \neq c$ ). Throughout the paper, we will use this distinction when talking about "own" and "spillover" effects of either direct or indirect effects of lockdowns.

While Equation 3 is sufficient to illustrate our framework, in Appendix A.1 we show alternative results derived under more relaxed assumptions. We allow for different effects of own and neighbours' lockdowns and derive parsimonious specifications taking into account the heterogeneity of lockdown orders, which can close smaller or larger shares of the economy.

## 4 Data

The decomposition in the previous section shows how, in order to estimate the effects of lockdowns on the labour market, we need data on i) local labour market dynamics, ii) pre-pandemic commuting and iii) the size of the treatment across different areas and sectors.

We build a monthly and a weekly dataset which contains all the aforementioned elements. Both cover 3108 counties from the continental U.S. (except Alaska). The monthly dataset covers the period from January 2017 to July 2020 included, while the weekly one covers January 2019 to June 2020. The unit of observation of the monthly dataset is the county, whereas the unit of observation of the weekly dataset is the individual business (e.g. shop, branch or venue). In the Safegraph dataset, these are referred to as Places of Interest (POIs).

The monthly dataset contains data on county-level employment and unemployment. Employment is establishment-based (employees are accounted for in the county where they

work), from BLS's Quarterly Census of Employment and Wages (QCEW). Unemployment is residence-based (unemployed are accounted for in the county where they live), from Local Area Unemployment Statistics by BLS. We use the American Community Survey's 2011-2015 estimates cross-county commuting flows, SafeGraph Point-Of-Interests' (POIs) mobility data for consumers' mobility flows. Data on Covid-19 deaths and cases was obtained from the New York Times GitHub repository (Mitch Smith et al., 2020). Data pm population is from Census Current Population estimates.

Local Area Unemployment (LAU) Statistics by BLS uses mixed sources to estimate the number of unemployed persons at the county level. These estimates are mainly based on detailed county-level unemployment claims<sup>3</sup>. Relative county-level estimates are then matched to the official estimates of the state unemployment level published by BLS, based on CPS data.

The county-level commuting flows are from the 2011-2015 ACS commuting files. These represent physical commuting flows: the place of work is the county where the workers physically carry out their job.

We hand collect a dataset of county-level orders, differentiating between stay-at-home orders, retail closures, restaurant closures and bar closures. While we cross-check our data with Goolsbee et al. (2020), we consider the possibility of multiple spells of orders, extend it until July 2020 and make further differentiations circa the type of business closures.

The weekly POI-level dataset uses the same lockdown orders data as the monthly one and includes location data from SafeGraph<sup>4</sup>, a data company that aggregates anonymised location data from numerous applications in order to provide insights about physical places, via the Placekey<sup>5</sup> Community. To enhance privacy, SafeGraph excludes census block group information if fewer than five devices visited an establishment in a month from a given census block group. The panel includes data from 45 million mobile phone

---

<sup>3</sup>See the related technical documentation <https://www.bls.gov/opub/hom/lau/calculation.htm>

<sup>4</sup><https://www.safegraph.com/>

<sup>5</sup><https://www.placekey.io/>

devices in the US (or approximately 14% of the population). We observe the weekly number of visitors by census block group of origin for each business, which we aggregate to the county level to match the level of detail of our orders' dataset. For a subset of businesses - those classified as non-essential and whose sector has suitable visits patterns - we take the number of visitors as a proxy for the number of consumers who visited the business and the total number of visits longer than four hours as a proxy for the number of workers/shifts.

For more information on data collection and cleaning, see Appendix [A.2](#).

#### 4.1 Flow-weighted lockdown intensity index

In the rest of this section, we describe our measures of own lockdown and exposure to spillovers. The goal is to construct treatment variables that can be used as estimates of all variational components in our decomposition of lockdown effects. In this way, we can empirically estimate their impact by OLS or IV.

To define notation, we consider a set of counties indexed by  $c \in C$ . Each of these counties has a given number of employed residents  $E_c^R$  and employed workers  $E_c^w$ . The difference between these is that  $E_c^R$  considers all employed residents - regardless of where they work - while  $E_c^w$  considers workers employed at establishments situated within the county's borders, regardless of where they live.

One can decompose the county's employment into flows of commuting workers. Define  $\text{flow}_{cr}$  the number of workers living in county  $c \in C$  which commute to county  $r \in C$ . By definition, we have that

$$E_c^R \equiv \sum_{r \in C} \text{flow}_{cr}, \quad E_c^w \equiv \sum_{r \in C} \text{flow}_{rc}$$

We say that a county is "under lockdown of type  $Z$  on a given day", where  $Z$  is one of the lockdown types previously described, if there is a  $Z$ -type lockdown order put in place by some authority (state, county or others) affecting county  $c$ . For a given month  $t$ , we

define the lockdown status of county  $c$  as

$$L_{tc}^Z = \frac{\text{Days in lockdown of type } Z}{\text{Days in month } t}$$

Finally, we define two lockdown intensity indexes for a county’s residents: one taking into account ”own” lockdown decisions only and one taking into account ”neighbours” decisions only. Consistently with the decomposition from Section 3, we define the intensity of own lockdown as

$$\kappa_{Ztc}^{\text{own}} = \frac{L_{tc}^Z \cdot \text{flow}_{cc}}{(\text{Working-Age Population})_c} \tag{4}$$

where we define the working-age population as all individuals between 16 and 65 years old. We measure how much a county is exposed to neighbours’ decisions by weighting other counties’ decisions by the commuting flows toward ( $\kappa_{Ztc}^{\text{outflow}}$ ) or from ( $\kappa_{Ztc}^{\text{inflow}}$ ) those counties:

$$\begin{aligned} \kappa_{Ztc}^{\text{outflow}} &= \frac{\sum_{r \in C: r \neq c} L_{tr}^Z * \text{flow}_{cr}}{(\text{Working-Age Population})_c} \\ \kappa_{Ztc}^{\text{inflow}} &= \frac{\sum_{r \in C: r \neq c} L_{tr}^Z * \text{flow}_{rc}}{(\text{Working-Age Population})_c} \end{aligned} \tag{5}$$

These indicators weight the overall exposure of county  $c$  to own and neighbours’ lockdown orders by the pre-pandemic flows. Notice that two counties  $c$  and  $c'$  with different flows can have their population/workforce equally treated even if county  $c$  is in lockdown but its neighbours are not, and vice versa for county  $c'$ . In fact, it is straightforward to notice that

$$\kappa_{Ztc}^{\text{own}} + \kappa_{Ztc}^{\text{outflow}} \in [0, 1]$$

With  $= 1$  strictly only if  $L_{tr}^Z = 1 \ \forall r \in \bar{C}_c = \{r \in C : \text{flow}_{cr} > 0\}$  and  $\sum_{r \in C} \text{flow}_{cr} = (\text{Working-Age Population})_c$ . The same holds for the analogous inflow-based measure.

It is now clear why all the variables here presented are rescaled by working-age population. First, this ensures that  $\kappa_{Ztc}^{own} + \kappa_{Ztc}^{outflow} \in [0, 1]$  since  $E_c^w < \text{Working-age population}$ . Second, this allows us to use the same normalising factor of the LHS. In fact, we do not use the unemployment rate as it may respond differently across counties due to heterogeneous changes or ex-ante differences in the denominator.

## 4.2 Sector- and flow-weighted lockdown intensity index

The formulation of treatment measures in the previous section relies on assuming that equally strong lockdown orders have the same direct and spillover effect across all counties, regardless of local employment composition. However, an area with large manufacturing employment is unlikely to be affected by restrictions to the accommodation sector as much as a tourism-focused county.

We can address this problem while maintaining a parsimonious specification through an alternative assumption. We assume all lockdowns affect local economies in a linear proportion to the employment share of the affected sectors (for a detailed explanation of the assumptions needed to justify this step in Equation 3, see Assumption 5 in the Appendix). Under this assumption, we can limit our attention to a pair of sector-weighted lockdown indices. The first to capture direct effects. The second to capture spillover effects. We build the sector-weighted lockdown index for spillovers by weighting each order type  $s \in S$  by the share of the economy in county  $r$  it affects ( $\mu_{rs}$ )<sup>6</sup>:

$$\hat{\kappa}_{Ztc}^{outflow} = \frac{\sum_{r \in C: r \neq c} \left( \sum_{s \in S} L_{tr}^Z \times \mu_{rs} \right) \times \text{flow}_{cr}}{(\text{Working-Age Population})_c} \tag{6}$$

where the term  $\sum_{s \in S} L_{tr}^Z \mu_{rs}$  is the share of the economy in  $r$  which is closed due to the orders in place in  $r$ . We compute in a similar fashion the one for own lockdown. To calculate  $\mu_{rs}$  we use establishment-level employment data from the 2019 QCEW and match the

<sup>6</sup>We assume that the industrial composition of a commuting flow is the same as that of the destination county due to data availability.

NAICS to the businesses which are not defined as "essential" by the lockdown orders<sup>7</sup>. Such indices are subject to variation through i) the intensive margin (the share of the economy ordered to close) and ii) the extensive margin (the length of the closures, the share of neighbours with some closures) of lockdowns.

### 4.3 Descriptive statistics

Table 1 summarises a few facts about the interconnections within the U.S. economy, showing the average share of commuters among all working residents of a given county, of all inbound workers (people whose workplace is in the county) and of consumption for the Leisure sector. The share of pre-pandemic employment in the Leisure sector at the LMA level is a control we will use in most estimations. Panel B shows descriptive statistics about the treatment (lockdown orders).

Table 1: Summary statistics for the monthly dataset: commuting

Panel A: Commuting					
	N	Mean	Std.Dev	Min	Max
Commuting workers share of working residents, 2010 - 2015	3108	0.28	0.18	0.02	0.92
Commuting (inbound) workers share of total workers, 2010 - 2015	3108	0.26	0.13	0.00	0.92
Consumption inflow of total consumption (NAICS 71,72)	3108	0.33	0.12	0.09	1.00
Exposure to Leisure Sector (LMA level)	3108	0.12	0.03	0.00	0.57
Panel B: Treatment					
	N	Mean	Std.Dev	Min	Max
Average monthly exposure to neighbours orders (March-July 2020)	3108	0.10	0.06	0	0.37
Average monthly exposure to neighbours retail orders (March-July 2020)	3108	0.05	0.04	0	0.26
Average monthly exposure to neighbours SAH orders (March-July 2020)	3108	0.04	0.03	0	0.26
Average monthly exposure to own orders (March-July 2020)	3108	0.19	0.11	0	0.61
Average monthly exposure to own retail orders (March-July 2020)	3108	0.08	0.05	0	0.47
Average monthly exposure to own SAH orders (March-July 2020)	3108	0.07	0.06	0	0.47
Mean months under any order (March-July 2020)	3108	2.96	1.35	0	5.52
Mean months under retail order (March-July 2020)	3108	1.34	0.68	0	5.29
Mean months under SAH order (March-July 2020)	3108	1.13	0.84	0	5.29

### Lockdown intensity over time

Figure 4.1 shows the *own* and *spillover* average lockdown (i.e. treatment) intensity by type of order and the sector-weighted index. We can observe a clear precedence of

<sup>7</sup>Due to data availability, we proxy the weight of non-essential manufacturing closures by the county-level weight of the manufacturing and construction sectors, times the state-level share of non-essential employment in the corresponding sectors.

lockdown orders, with entertainment closures being in place in more counties than retail closures and stay-at-home orders. Spillover intensities are generally smaller than own lockdown ones as the proportion of cross-county commuters to local workers is  $\approx 1:2$  in the USA. Figure A.1 in the Appendix presents the share of counties under lockdown by month and type of order.

## 5 Empirical Analysis

### 5.1 Methodology

Our goal is to provide an estimation of the labour market effects of lockdown policies, with a focus on the role of spillovers. To do so, we implement the decomposition of Section 3 through OLS, using the exposure indicators we presented. We estimate the reduced form model

$$y_{tc} = \beta_0 + \beta_1 X_{tc} + I_c + I_t + \Theta_{tc} + \varepsilon_{tc} \quad (7)$$

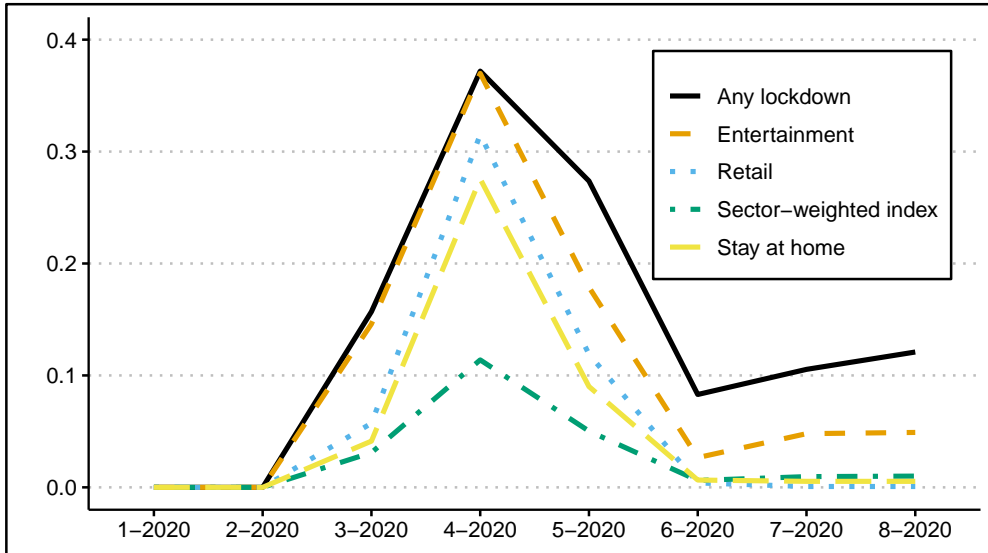
where:  $y_{tc}$  is the county-level dependent variable of choice (unemployment-to-population ratio or employment index);  $X_{tc}$  is a vector of county-level controls (such as industry exposure to Covid-19 and a third-degree polynomial of days since first Covid-19 deaths);  $I_c$  and  $I_t$  are county by calendar month and time fixed-effects; and  $\Theta_{tc}$  is the term measuring the effects of own and neighbours' lockdown orders. The estimation of the components of  $\Theta_{tc}$  is the main focus of our analysis. In our baseline specification, we define  $\Theta_{tc}$  as the sum of own and spillover effects of lockdowns

$$\Theta_{\text{outflow}} = \gamma_1 \kappa_{tc}^{\text{own}} + \gamma_2 \kappa_{tc}^{\text{outflow}}$$

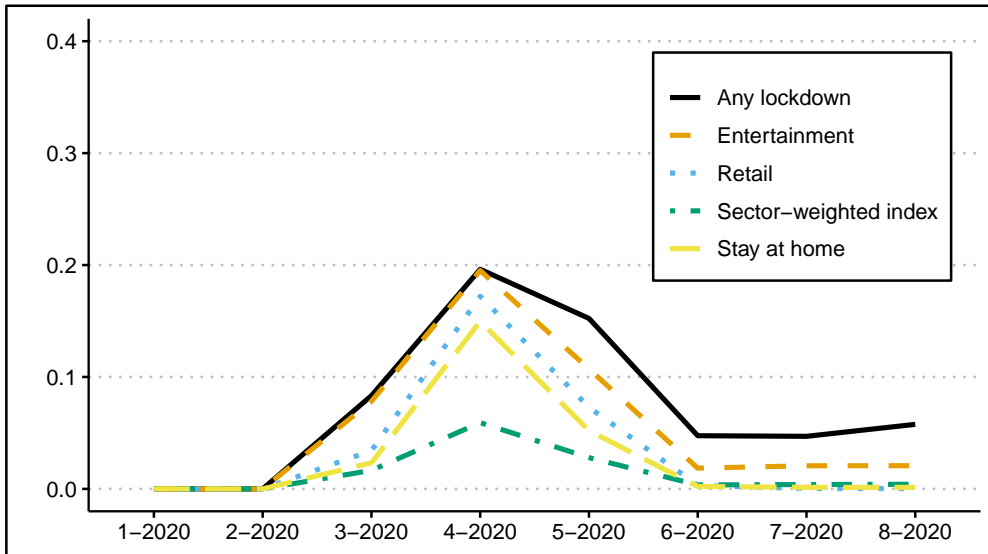
where  $\gamma_1$  measures the effect of own lockdown and  $\gamma_2$  measures the spillover effects due to neighbouring authorities' lockdown status, weighted by outbound commuting (outflows). We also run additional specifications including lags, county-specific interaction terms, and consumption-mediated effects of lockdowns.



Figure 4.1: Own and spillover lockdown intensity over time, by type of order



(a) Average own lockdown intensity ( $\kappa^{\text{own}}$ )



(b) Average lockdown spillover spillover ( $\kappa^{\text{outflow}}$ )

In the following sections, we show our baseline OLS estimations and discuss potential endogeneity concerns. We then turn to an IV approach to provide a causal identification of the effects of lockdown orders and their commuting-related externalities.

In all OLS specifications using unemployment, we construct both the dependent variable and the lockdown intensities  $\kappa$  using working-age population as a normalising factor<sup>8</sup>. Establishment-based employment data are indexed to their 2019 average, and lockdown intensities are normalised by population. Baseline estimates are run on 3108 counties. We drop all observations for which we do not have data on local employment exposure to what we define Covid-sensitive sectors (NAICS 71, 72) in their *whole* Labour Market Area when we use it as control. For the sector-weighted indicators, we drop all counties for which we do not observe detailed enough data on employment composition (see A.2 for more details). All errors are clustered by county. Unless otherwise specified, all following regressions include (county) X (calendar month) FE and time FE to account for common shocks and seasonality.

The labelling convention for our indicators is as follows. We use the term "any lockdown" to refer to situations where at least one order, of any type, is in place. Given the observed hierarchy between lockdown orders, this corresponds to at least having a capacity restriction on bars. The subsequent generally observed sequence of orders is bar closures, restaurants to retail to manufacturing closures or stay at home orders.

## 5.2 Unemployment - OLS

Table 2 shows estimates from an OLS specification where we regress the unemployment to working-age population ratio on *outflow*-based measures of lockdown intensity. For this specification, we aggregate all lockdown orders under a single indicator.

Column 1 corresponds to a reference model without spillovers, similar to what was previously estimated in the literature. In this specification, the unemployment to working-age population ratio is regressed on the monthly share a county has spent under at least

<sup>8</sup>That is all individuals between 15 and 65 years old from the specific year's Census Current Population estimates. For the year 2020, we use 2019 estimates.

one lockdown order. A full month under any lockdown order is associated with an approximately 1.9 percentage points increase in the dependent variable. For reference, the unemployment-to-working-population ratio was 2.5% in February 2020 and reached a maximum of 9% in April.

Column 2 shows another specification without spillovers, but using the flow-weighted own lockdown variable. While this is not the specification a more naive analysis would consider, it is useful to illustrate how adding the spillover terms affect the estimated coefficients.

Table 2: OLS estimates, outflows

	Unemployment/(working age population)					
	(1) No Spillovers	(2) No Spillovers Alt.	(3) Baseline	(4) Lags	(5) Exposure	(6) Exposure+Lags
Share of Month in Any Lockdown	0.0187*** (0.00281)					
Own Any lockdown		0.0417*** (0.00850)	0.0326*** (0.00470)	0.0228*** (0.00490)	-0.0249* (0.0115)	-0.0292** (0.0108)
Any lockdown spillover			0.0204* (0.00961)	-0.00929 (0.00944)	0.0288*** (0.00784)	-0.00278 (0.00808)
L.Own Any lockdown				0.0430*** (0.00473)		0.0306* (0.0123)
L.Any lockdown spillover				0.0661*** (0.0120)		0.0713*** (0.0117)
Own Any lockdown × Exposure					0.460*** (0.0925)	0.408*** (0.0857)
L.Own Any lockdown × L.Exposure						0.128 (0.106)
Constant	0.0299*** (0.000210)	0.0300*** (0.000269)	0.0300*** (0.000835)	0.0286*** (0.000719)	0.0302*** (0.000865)	0.0287*** (0.000757)
Observations	133644	133644	133644	130536	129759	126741
R <sup>2</sup>	0.876	0.878	0.884	0.891	0.890	0.899
Unemployment mean 02-2020	.025	.025	.025	.025	.025	.025
County and Month FEs	Yes	Yes	Yes	Yes	Yes	Yes
Covid controls	Yes	Yes	Yes	Yes	Yes	Yes
Industry Exposure	No	No	No	No	Yes	Yes

Note: Standard errors in parentheses. Errors clustered by county. Significance levels: \* = 0.05; \*\* = 0.01; \*\*\* = 0.001. This table presents estimates from a model regressing the unemployment to working population ratio on measures of the own county lockdown intensity and spillover intensity coming from neighbour's lockdown orders. The lockdown intensity measures are proportional to the time spent under any lockdown order, where we define "any lockdown order" as any order that is equally or more stringent than mandated bar closures. The own lockdown intensity is proportional to the own-county commuting flow as described in the main text, whereas spillover measures are proportional to the commuting outflow between the observed county and its neighbours. All commuting flows are 2011-2015 averages. Controls include month and county x calendar month fixed effects, together with a third-degree polynomial of days since the first Covid-19 case was registered in the county. In columns 5 and 6, we also include a measure of the labour market area's industrial exposure to the effects of Covid-19.

Column 3 - our baseline specification - adds the spillover term to the specification in column 2. Own county lockdowns increase the unemployment-to-working-age-population ratio by approximately 3.3 percentage points if  $\kappa_{tc}^{own\ flow} = 1$ , that is, if the entire working-

age population is employed and works in their home county, and the home county is under lockdown for the entire month. Spillovers have significant effects: the dependent variable increases by around 2 percentage points if  $\kappa_{tc}^{\text{outflow}}$  changes from 0 to 1 (that is, in the case of a county whose entire working-age population commutes to neighbouring counties, all of which go into lockdown for a full month). Given an average own lockdown exposure of 0.37, and average spillover exposure of 0.2 in April 2020, at the peak of the restrictions the direct effects added approximately 1.4 percentage points to the unemployment-to-working-population ratio, with spillovers adding a further 0.3 pp.

We next consider several alternative specifications. First, lockdowns are likely to affect unemployment also in subsequent periods, so in column 4 we introduce lags. While the own county lockdown appears to increase unemployment both contemporaneously and with a lag, for spillover only the lagged effects are significant. In column 5, we add a control for the degree to which the county industrial composition is exposed to pandemic shocks (see Appendix A.2 for details on how we calculate this index). While the estimated coefficient of own lockdown is negative, note that the effect of own lockdown is the sum of this coefficient and the large positive effect of the interaction coefficient between lockdown and exposure. Column 6 combines the lagged and exposure specifications, showing similar results.

In Table 2 we limited our exploration to the extensive lockdown margin. Motivated by the decomposition in section A.1, we will now look at the intensive margin, i.e., whether lockdown effects vary by the set of affected industries. The main finding (Table A8 in the Appendix) is that harsher orders are associated with larger spillover effects. The fitted effect of spillovers from retail closures is more than twice the one estimated in the generic (any order) specifications.

Similarly, Table 4, Panel B, shows in columns 1-3 the OLS estimates employing sector-weighted lockdown indices. The results in column 2 suggest that for each 10 own county jobs affected by a lockdown order and held by local residents, 1.9 residents will become unemployed due to the effects of the own lockdown. In addition, for every 10 jobs held

by residents in neighbouring counties and affected by neighbouring counties' lockdown orders, 1.5 own county residents will become unemployed. To interpret these coefficients in light of the average commuting flows, an additional 10% closure of the own economy increases the dependent variable by 0.8 percentage points in the average county. On the other hand, for each 10% of the neighbours' economy being closed, the unemployment ratio increases by 0.2 percentage points. Fitting the coefficients to April 2020 data shows that spillovers were associated with a 0.9 pp. increase in the U.S. unemployment/working-age-population ratio, compared to 2 pp. due to own lockdowns.

Overall, we find that spillovers arising from neighbours' closures are quantitatively relevant and statistically significant across all OLS estimates. Harsher orders are estimated to cause both more spillovers and direct effects than milder ones.

### 5.3 IV strategy

Lockdown policies are chosen by local (state, county or city) authorities, which may directly or indirectly include the state of the economy among key indicators to determine their policies. When counties' economic activity becomes a relevant variable to decide their lockdown status - or when some counties have a relevant weight in determining the state's average - we can run into an endogeneity problem. In this section, we formalise our concerns and propose a solution.

#### Lockdown implementation process

First, we formalise how to think about the decision process that leads a county and its neighbours to be under lockdown. We say that a county is under a lockdown closing sector  $Z$  at time  $t$  ( $L_{tc}^Z$  according to the previously introduced notation) if there is at least one order coming from a relevant authority that affects that county. These orders can be at the state, county or city level or county/city-specific orders imposed by the state. Call these orders  $O_{ta(c)}^Z$ , for  $a(c)$  being the local authority imposing the order on county  $c$ . Then,  $c$ 's lockdown status is  $L_{tc}^Z = \max\{O_{ta_1(c)}^Z, O_{ta_2(c)}^Z, \dots\}$ . In principle, lockdowns can affect the unobservables that determine local economic outcomes  $y_{tc}$ , which in turn can affect

the likelihood of imposing lockdown orders. This can create an endogeneity problem: if neighbouring counties are subject to the same authority  $a$  which determines the lockdown in county  $c$  (e.g. a state, or a city spanning over multiple counties), then county  $c$ 's spillover indicators  $\kappa_{tc}^{\text{outflow}}$  may be endogenous to  $c$ 's outcomes  $y_{tc}$  if a common authority of a neighbour  $r$  ( $a(r) = a(c)$ ) takes  $y_{tc}$  into account when determining  $O_{ta(r)}^Z$ . That is, we are concerned that neighbours' orders are a function of  $y_{tc}$ :  $O_{ta(r)} = O_{ta(r)}(y_{tc}, \cdot)$ . Formally,

$$O_{ta(r)} = O_{ta(r)}(y_{tc}, \cdot) \implies \kappa_{tc}^{\text{outflow}}(L, \text{flows}) = \kappa_{tc}^{\text{outflow}}(L(y_{tc}, \cdot), \text{flows}) \quad (8)$$

which implies that estimates of the effect of  $\kappa^{\text{outflow}}$  will be biased due to reverse causality between own county outcomes and neighbours' lockdown status.

For example, consider a state-wide order affecting all counties within that state. Suppose the state implements a reopening based on health and economic indicators correlated to the local county's outcomes  $y_{tc}$  (due to size or preferences which make  $c$  pivotal in the lockdown decision process). In that case, the error term  $\varepsilon = y - \beta X$  will be correlated with the regressors  $\kappa^{\text{outflow}}$  if innovations to  $y_{tc}$  cause changes in the neighbouring counties' orders too (i.e. if a state reopens a "block" of neighbouring counties at once, based on outcomes from  $c$ ). Thus  $\kappa^{\text{outflow}}$  is now possibly endogenous to  $y_{tc}$ , biasing OLS estimates.

To address this issue, we propose an instrument based on neighbouring states' orders. These are unlikely to be endogenous to the outcome  $y_{tc}$  of an individual county located in a different state<sup>9</sup>. While some groups of states agreed on what pandemic-related factors to base the reopening on (Caspani and Resnick-Ault, 2020; Klayman, 2020), these coalitions explicitly mentioned that they did not coordinate the reopening dates, consistent with what we observe in the data. These agreements are not in conflict with the assumption that neighbouring states' lockdown orders are - after controlling for pandemic-related indicators - exogenous to neighbouring states' counties' employment outcome. Hence, we

<sup>9</sup>One could consider using county-level orders from neighbouring states instead. However, counties in close proximity may individually coordinate even across state lines. While potentially less efficient, we consider that our approach is more likely to provide a valid instrument.

claim that this instrument satisfies the exclusion restriction. Furthermore, the proposed instrument is relevant as it is correlated with the spillover intensity measure  $\kappa^{outflow}$ , which directly enters into its computation.

**Instrument Computation**

We build instruments for county  $c$ 's neighbours' lockdown intensity by i) dropping all same-state counties and ii) proxying neighbour  $r$ 's lockdown indicator by its state-level order. The variation we use to identify the effects of lockdowns comes exclusively from the direct exposure (through commuting relationships) of county  $c$  to state-wide lockdown orders enacted by neighbouring states (but not  $c$ 's own state) which affect  $c$ 's out-of-state neighbours.

To see how this relates to our treatment variable, consider the following decomposition of the lockdown spillover intensity measure:

$$\kappa_{stc}^{outflow} = \underbrace{\frac{\sum_{r \in C: r \neq c, s(r) \neq s(c)} L_{tr}^s * flow_{cr}}{\text{Working-age population}}}_{\text{Contribution from out-of-state counties}} + \underbrace{\frac{\sum_{r \in C: r \neq c, s(r) = s(c)} L_{tr}^s * flow_{cr}}{\text{Working-age population}}}_{\text{Contribution from same-state counties}} \tag{9}$$

Where  $s(\cdot)$  is the state of a county. The variation in the first term comes from counties in different states. Under the assumption that neighbouring states' orders are exogenous to own-county outcomes, we can use  $O_{ts(r)}^Z$  (the state-wide order affecting  $r$ ) as an exogenous proxy for their lockdown status  $L_{tr}^Z$ . The instrument is then calculated as:

$$\kappa_{IV,Ztc}^{outflow} = \frac{\sum_{r \in C: r \neq c, s(r) \neq s(c)} O_{ts(r)}^Z * flow_{cr}}{(\text{Working-age population})_{tc}} \tag{10}$$

We call this instrument the *non-rescaled instrument*, which is highly dependent on how much a county is exposed to commuting toward other states than its own. However, notice that this instrument is implicitly imposing that the best prediction of the  $y_c$ -exogenous variation in  $L_{tr}^Z$  for all counties located in the same state as  $c$  is zero. In other words, the variation coming from the second component in Equation 9 is ignored. This does not need

Covid Economics 69, 18 February 2021: 46-86

to be the case. An improvement can be to proxy the same-state counties' lockdown state by the conditional commuting-weighted average of the neighbouring states' lockdowns. In this way, we can define an equally valid but stronger instrument. After some algebra, this is equivalent to Equation 11: the conditional flow-weighted average of neighbouring states' closures (first term), scaled by the overall share of commuting working-age individuals in the county (second term). For proof of this, see Appendix A.3.

$$F_{IV,Ztc}^{outflow} = \frac{\sum_{r \in C:r \neq c, s(r) \neq s(c)} O_{ts(r)}^Z * flow_{cr}}{\sum_{r \in C:s(r) \neq s(c)} flow_{cr}} \times \frac{\sum_{r \in C:r \neq c} flow_{cr}}{(Working-age population)_{tc}} \quad (11)$$

This *rescaled instrument* exploits the variation of neighbouring states even for counties with weak exposure to out-of-state orders.

Given the way we have defined both instruments, an IV specification will estimate the Local Average Treatment Effect (LATE) for counties whose spillover intensity has increased due to closures in neighbours who are in a different state.

**First Stage**

Panel A in Table 3 reports the results for the first stage of all the specifications. The rescaled instrument is strong, with the first stage coefficient of lockdown intensity being close to 1 for the simpler specifications and ≈ 0.8 for richer ones. It is always strongly significant, with a large F-statistic (reported with the second stage results). For the non-rescaled instrument, the variation is coming mostly from counties close to the state border.

**Results**

Table 3, Panel B, shows the results when instrumenting spillovers from any lockdown order with the rescaled instrument. Table 4 provides results for the sector-weighted index in columns 4-6 of Panel B. We find a pattern of results broadly similar to the OLS ones. The coefficients on spillovers are all statistically significant, confirming the causal

Covid Economics 69, 18 February 2021: 46-86



Table 3: Single instrument estimation for Any lockdown spillover

Panel A: First Stage

	Baseline		Lags		Exposure		Exposure + Lag	
	(1)	(2)	(3)	(4)	(5)	(6)	(6)	(6)
	Any lockdown spillover	Any lockdown spillover	L.Any lockdown spillover	Any lockdown spillover	Any lockdown spillover	L.Any lockdown spillover	L.Any lockdown spillover	L.Any lockdown spillover
Any Lockdown Spillover IV (rescaled)	0.983*** (0.0156)	0.831*** (0.0191)	-0.00530 (0.0118)	0.976*** (0.0157)	0.823*** (0.0196)	-0.00519 (0.0121)		
Own Any lockdown	0.165*** (0.00961)	0.180*** (0.0110)	0.00813 (0.00494)	0.246*** (0.0174)	0.280*** (0.0191)	0.0164 (0.00876)		
L.Any Lockdown Spillover IV (rescaled)		0.193*** (0.0345)	1.032*** (0.0171)		0.195*** (0.0345)	1.029*** (0.0171)		
L.Own Any lockdown		-0.0486* (0.0189)	0.128*** (0.0103)		-0.0930*** (0.0242)	0.153*** (0.0145)		
Own Any lockdown × Exposure				-0.832*** (0.109)	-0.832*** (0.109)	-0.0728 (0.0581)		
L.Own Any lockdown × L.Exposure					0.342** (0.107)	-0.223*** (0.0620)		
Observations	133644	130536	130536	129759	126741	126741		

Note: Standard errors in parentheses. Errors clustered by county. Significance levels: \* = 0.05; \*\* = 0.01; \*\*\* = 0.001. This table presents estimates from the first stage of a model regressing the unemployment to working population ratio on measures of the own county lockdown intensity and spillover intensity coming from neighbour's lockdown orders, where we instrument spillover intensity with the rescaled instrument outlined in section 5.3.

Panel B: Results

	Unemployment/(working age population)					
	(1)	(2)	(3)	(4)	(5)	(6)
	No Spillovers	No Spillovers Alt.	Baseline	Lags	Exposure	Exposure+Lags
Share of Month in Any Lockdown	0.0187*** (0.00281)					
Own Any lockdown		0.0417*** (0.00850)	0.0327*** (0.00470)	0.0220*** (0.00445)	-0.0276* (0.0112)	-0.0316** (0.0104)
Any lockdown spillover			0.0405** (0.0126)	0.00356 (0.00887)	0.0499*** (0.0109)	0.00867 (0.00774)
L.Any lockdown spillover				0.0721*** (0.00942)		0.0804*** (0.00909)
L.Own Any lockdown				0.0466*** (0.00526)		0.0337** (0.0125)
Own Any lockdown × Exposure					0.484*** (0.0919)	0.423*** (0.0866)
L.Own Any lockdown × L.Exposure						0.134 (0.106)
Observations	133644	133644	133644	130536	129759	126741
R <sup>2</sup>	0.876	0.878	0.107	0.168	0.154	0.226
Kleinberg-Paap F-stat			3944.17	1389.93	3884.22	1319.95
Unemployment mean 02-2020	.025	.025	.025	.025	.025	.025
County and Month FEs	Yes	Yes	Yes	Yes	Yes	Yes
Covid controls	Yes	Yes	Yes	Yes	Yes	Yes
Industry Exposure	No	No	No	No	Yes	Yes

Note: Standard errors in parentheses. Errors clustered by county. Significance levels: \* = 0.05; \*\* = 0.01; \*\*\* = 0.001. This table presents estimates from a model regressing the unemployment to working population ratio on measures of the own county lockdown intensity and spillover intensity coming from neighbour's lockdown orders, where we instrument spillover intensity with the rescaled instrument outlined in section 5.3. The instrument exploits variation in neighbouring states' lockdown orders, which we argue are exogenous to unobservables that may also determine the own county outcomes. The lockdown intensity measures are proportional to the time spent under the corresponding lockdown order. We define being under any lockdown order as restrictions equally or more stringent than mandated bar closures. The own lockdown intensity is proportional to the own-county commuting flow, whereas spillover measures are proportional to the commuting outflow between the observed county and its neighbours. All commuting flows are 2011-2015 averages. Controls include month and county × calendar month fixed effects, together with a third-degree polynomial of days since the first Covid-19 case was registered in the county. In columns 5 and 6, we also include a measure of the local market area's industrial exposure to the effects of Covid-19.

interpretation of our findings.

Table 4: NAICS-Weighted lockdown impact indicator (Unemployment)

Panel A: First Stage

	IV (neighbours)		IV (neighbours 2)		IV (lags)	
	(1)	(2)	(3)	(4)	(3)	(4)
	Lockdown spillover	Lockdown spillover	Lockdown spillover	L.Lockdown spillover	Lockdown spillover	L.Lockdown spillover
Lockdown Spillover IV (rescaled)	0.968*** (0.0168)		0.883*** (0.0146)	0.0127* (0.00611)		
Own lockdown	0.101*** (0.00923)	-0.0200 (0.0145)	0.106*** (0.00917)	-0.00897 (0.00507)		
Lockdown Spillover IV (not rescaled)		0.894*** (0.0790)				
L.Lockdown Spillover IV (rescaled)			0.127*** (0.0191)	0.963*** (0.0179)		
L.Own lockdown			-0.0275*** (0.00776)	0.0989*** (0.00927)		
Observations	126549	126549	123606	123606		

Note: Standard errors in parentheses. Errors clustered by county. Significance levels: \* = 0.05; \*\* = 0.01; \*\*\* = 0.001. This table presents estimates from the first stage of a model regressing the unemployment to working population ratio on measures of the own county lockdown intensity and spillover intensity coming from neighbour's lockdown orders, where we instrument spillover intensity with the instruments outlined in section 5.3.

Panel B: Results

	Unemployment/(working age population)					
	(1)	(2)	(3)	(4)	(5)	(6)
	No Spillovers	Baseline	Lags	IV (rescaled)	IV (non-rescaled)	IV (Lags, res)
Own lockdown	0.184*** (0.0202)	0.188*** (0.0198)	0.135*** (0.0183)	0.191*** (0.0200)	0.190*** (0.0195)	0.135*** (0.0177)
Lockdown spillover		0.149*** (0.0322)	0.0536* (0.0263)	0.252*** (0.0343)	0.189* (0.0923)	0.103*** (0.0238)
L.Own lockdown			0.171*** (0.0162)			0.183*** (0.0169)
L.Lockdown spillover			0.252*** (0.0350)			0.346*** (0.0412)
Constant	0.0293*** (0.000959)	0.0285*** (0.000919)	0.0273*** (0.000852)			
Observations	126549	126549	123606	126549	126549	123606
R <sup>2</sup>	0.892	0.894	0.904	0.178	0.184	0.252
Kleinberg-Paap F-stat				3334.49	127.84	1498.06
Unemployment mean 02-2020	.025	.025	.025	.025	.025	.025
CountyxMonth and Time FEs	Yes	Yes	Yes	Yes	Yes	Yes
Covid controls	Yes	Yes	Yes	Yes	Yes	Yes
Industry Exposure	Yes	Yes	Yes	Yes	Yes	Yes

Note: Standard errors in parentheses. Errors clustered by county. Significance levels: \* = 0.05; \*\* = 0.01; \*\*\* = 0.001. This table presents estimates from a model regressing the unemployment to working population ratio on measures of the own county lockdown intensity and spillover intensity coming from neighbour's lockdown orders. In columns 4, 5 and 6 we instrument spillover intensity with the instruments outlined in section 5.3. The instruments exploit variation in neighbouring states' lockdown orders, which we argue are exogenous to unobservables that may also determine the own county outcomes. The lockdown intensity measure is proportional to the time spent under the corresponding lockdown order. The intensities are calculated in proportion to the share of sectors affected by lockdown orders in either the own county or the neighbouring counties (see section 4.2). The own lockdown intensity is proportional to the own-county commuting flow, whereas spillover measures are proportional to the commuting outflow between the observed county and its neighbours. All commuting flows are 2011-2015 averages. Controls include month and county x calendar month fixed effects, together with a third-degree polynomial of days since the first Covid-19 case was registered in the county. All specifications include a measure of the local market area's industrial exposure to the effects of Covid-19.

## 5.4 Establishment-Based Employment

Up to now, we have restricted our attention to residence-based labour market data. These data are mechanically related to commuting flows as they report the unemployed in the county where they live and inform us that the number of unemployed in local communities increased due to neighbouring authorities' orders. However, is there any further externality on the local economies? This section addresses this question by providing estimates of the effect of lockdown spillovers on establishment-based employment.

We depart from the previous specifications by i) creating an index of employment based on the 2019 average and ii) employing an own-lockdown intensity measure based on the average share of the economy closed during a month. For  $\tau$  days in a given month  $t$ , this is calculated as:

$$\hat{F}_{tc}^{\text{own, employment}} = \frac{\sum_{\tau \in t} \sum_{z \in Z} L_{\tau c}^z \times \mu_{cz}}{(\text{Days in month } t)} \quad (12)$$

where we do not take into account the own commuting flow nor normalise by population because we now look at all jobs located in the own county, irrespective of whether they are held by residents or not. Since our dependent variable is an index equal to 1 when employment corresponds to the 2019 mean, there is no need to normalise by population. Similarly, the effect on this index will come from the actual closures, regardless of the local population. However, we normalise the spillovers terms by total population instead of working-age population. This is because we believe that spillovers may arise as the local spending capacity is affected. Furthermore, normalising the spillovers by population provides a better comparison of the effect of laying off a person on local spending behaviour in two counties of different size, as also the elderly consume but are not counted as part of the working-age population.

The results from columns 1 through 3 in Panel B of Table 5 show that one full month of total closure of the local economy<sup>10</sup> decreases establishment-based employment by 23%.

<sup>10</sup>This can be the case only if there are no lockdown-exempt essential activities carried out in the county.

Table 5: NAICS-Weighted lockdown impact indicator (Employment)

Panel A: First Stage

	IV (neighbours)	IV (neighbours 2)	IV (lags)	
	(1)	(2)	(3)	(4)
	Lockdown spillover	Lockdown spillover	Lockdown spillover	L.Lockdown spillover
Lockdown Spillover IV (rescaled)	0.883*** (0.0190)		0.804*** (0.0163)	0.0345*** (0.00638)
Own lockdown intensity	0.0578*** (0.00422)	0.0830*** (0.00566)	0.0571*** (0.00368)	0.00205 (0.00209)
Lockdown Spillover IV (not rescaled)		0.892*** (0.0755)		
L.Lockdown Spillover IV (rescaled)			0.130*** (0.0174)	0.850*** (0.0189)
L.Own lockdown intensity			-0.00263 (0.00253)	0.0567*** (0.00395)
Observations	123606	123606	120663	120663

Panel B: Results

	Establishment-based Employment index (1 = 2019 employment)					
	(1)	(2)	(3)	(4)	(5)	(6)
	No Spillovers	Baseline	Lags	IV (rescaled)	IV (non-rescaled)	IV (Lags, res)
Own lockdown intensity	-0.253*** (0.0189)	-0.229*** (0.0214)	-0.178*** (0.0185)	-0.213*** (0.0219)	-0.129*** (0.0319)	-0.164*** (0.0190)
Lockdown spillover		-0.285* (0.127)	-0.274** (0.102)	-0.473** (0.146)	-1.476*** (0.285)	-0.409*** (0.115)
L.Own lockdown intensity			-0.138*** (0.0193)			-0.131*** (0.0189)
L.Lockdown spillover			-0.0651 (0.0827)			-0.155 (0.0935)
Constant	0.983*** (0.000881)	0.984*** (0.00105)	0.985*** (0.00114)			
Observations	123606	123606	120663	123606	123606	120663
R <sup>2</sup>	0.815	0.816	0.824	0.078	0.027	0.104
Kleinberg-Paap F-stat				2163.09	139.61	900.63
Unemployment mean 02-2020	.025	.025	.025	.025	.025	.025
CountyxMonth and Time FEs	Yes	Yes	Yes	Yes	Yes	Yes
Covid controls	Yes	Yes	Yes	Yes	Yes	Yes
Industry Exposure	Yes	Yes	Yes	Yes	Yes	Yes

Note: Standard errors in parentheses. Errors clustered by county. Significance levels: \* = 0.05; \*\* = 0.01; \*\*\* = 0.001. This table presents estimates from a model regressing the establishment-based index (with 2019 average = 1) on measures of the own county lockdown intensity and spillover intensity coming from neighbour's lockdown orders. In columns 4, 5 and 6 we instrument spillover intensity with the instruments outlined in section 5.3. The instruments exploit variation in neighbouring states' lockdown orders, which we argue are exogenous to unobservables that may also determine the own county outcomes. The lockdown intensity measure is proportional to the time spent under the corresponding lockdown order. The intensities are calculated in proportion to the share of sectors affected by lockdown orders in either the own county or the neighbouring counties (see section 4.2). The own lockdown intensity is proportional to the share of month under lockdown, whereas spillover measures are proportional to the commuting outflow between the observed county and its neighbours over population. All commuting flows are 2011-2015 averages. Controls include month and county x calendar month fixed effects, together with a third-degree polynomial of days since the first Covid-19 case was registered in the county. All specifications include a measure of the local market area's industrial exposure to the effects of Covid-19.

Lagged specifications show a contemporaneous effect of 18%, and a lagged effect of 14%. An additional 1% of local population commuting to neighbours who have fully closed their economy decreases local employment by 0.29 percentage points. Considering that only 48% of the U.S. population is employed, for every 7 commuters whose jobs were affected by lockdown orders, 1 additional job was lost in their residence county. Taking into account the magnitude of the treatment variables at the average county, an additional 10% of the neighbours' economy being closed caused a fall of 0.4 pp. in local employment according to the model. The IV specifications reported in columns 4 through 6 show that the effects are causal. These findings imply that lockdown spillovers are not merely due to an automatic reporting effect from unemployment claims due to individuals working in neighbouring counties, but also have broader effects.

When we allow for spillovers to run also through consumption mobility (Table 6) we find that these seem to be a relevant driver of local job losses. We measure the consumption spillover intensity as:

$$K_{tc}^{\text{consumption inflow}} = \frac{L_{tr} * \text{visits}_{rc}}{(\text{total visits})_c} * (\mu_{\text{non-essential retail}} + \mu_{\text{leisure}}) \quad (13)$$

where  $\text{visits}_{rc}$  are visits from neighbouring counties to non-essential retail and leisure POIs,  $L_{tr}$  is the share of the month spent under an entertainment lockdown order,  $(\text{total visits})_c$  are total visits (to non-essential retail and leisure POIs), and  $\mu_x$  is the share of employment in county  $c$  in sector  $x$ . This captures the extent to which visits from neighbours are important for the local economy. The coefficients in column 2 imply that for each 10% of own county consumption coming from neighbours which are under an entertainment lockdown, the own county employment in non-essential retail and leisure will decrease by 3.5 percentage points (for the average county, this corresponds to a 0.4 pp. fall in the total employment index). However, if the own county is also under lockdown, the effect will be attenuated, as part of those jobs would have been lost regardless. These consumption spillovers need to be added to the commuting ones, implying large overall spillovers effects.

Table 6: NAICS-Weighted lockdown, consumption indicators (Employment)

	Establishment-based Employment index (1 = 2019 employment)				
	(1) No Spillovers	(2) Baseline	(3) Lags	(4) IV (rescaled)	(5) IV (non-rescaled)
Own lockdown intensity	-0.253*** (0.0189)	-0.226*** (0.0238)	-0.163*** (0.0194)	-0.222*** (0.0244)	-0.151*** (0.0339)
Lockdown spillover		-0.230 (0.139)	-0.284** (0.102)	-0.433** (0.152)	-1.526*** (0.316)
Entertainment Lockdown Consumption Spillover		-0.358*** (0.0846)	-0.0231 (0.109)	-0.393*** (0.115)	-0.315* (0.129)
Ent. Lockdown Cons. Spillover × share month in ent. order		0.246* (0.114)	-0.0569 (0.139)	0.332* (0.131)	0.369* (0.150)
L.Own lockdown intensity			-0.115*** (0.0203)		
L.Lockdown spillover			0.0193 (0.0855)		
L.Entertainment Lockdown Consumption Spillover			0.0966 (0.111)		
L.Ent. Lockdown Cons. Spillover × L.share month in ent. order			-0.218 (0.116)		
Constant	0.983*** (0.000881)	0.984*** (0.00105)	0.985*** (0.00105)		
Observations	123606	123606	120663	123606	123606
R <sup>2</sup>	0.815	0.817	0.824	0.081	0.024
Kleinberg-Paap F-stat				869.96	41.2
Unemployment mean 02-2020	.025	.025	.025	.025	.025
CountyxMonth and Time FEs	Yes	Yes	Yes	Yes	Yes
Covid controls	Yes	Yes	Yes	Yes	Yes
Industry Exposure	Yes	Yes	Yes	Yes	Yes

Note: Standard errors in parentheses. Errors clustered by county. Significance levels: \* = 0.05; \*\* = 0.01; \*\*\* = 0.001. This table presents estimates from a model regressing the establishment-based index (with 2019 average = 1) on measures of the own county lockdown intensity and spillover intensity coming from neighbour's lockdown orders. In columns 4, 5 and 6 we instrument spillover intensity with the instruments outlined in section 5.3. The instruments exploit variation in neighbouring states' lockdown orders, which we argue are exogenous to unobservables that may also determine the own county outcomes. The lockdown intensity measure is proportional to the time spent under the corresponding lockdown order. The intensities are calculated in proportion to the share of sectors affected by lockdown orders in either the own county or the neighbouring counties (see section 4.2). The own lockdown intensity is proportional to the share of month under lockdown, whereas spillover measures are proportional to the commuting outflow between the observed county and its neighbours over population.

### 5.5 Spatial Distribution of Impacts

We find that large shares of the increase in local unemployment originated from jobs lost due to neighbours' lockdown status. Using establishment-based data, we find additional job losses in areas affected by spillovers. Since we find both significant and sizeable effects of the spillover terms, specifications ignoring them are likely to give biased results. This is both a *quantitative* and *spatial* bias since the relative intensity of spillovers varies across time as well as space.

To interpret the coefficients presented in the previous section, consider that the mean share of commuting workers is 27.6%. Moreover, 60% of the U.S. working-age population is employed, and at most 34% of total U.S. employment has been contemporaneously affected by some order. Based on these numbers, Figure 5.1a shows the fitted total effects

of lockdown orders on unemployment from our specification with exposure<sup>11</sup>, while Figure 5.1b includes lags. The spillovers account for approximately 15% of the total change in unemployment between March and June 2020. However, this average proportion is heterogeneously distributed across counties, with spillover effects larger in counties with above-median commuting levels, as shown in Figures 5.1c and 5.1d. The solid orange line in each graph plots the effect estimated using our same data and a specification without spillover terms. When spillovers are omitted, the average effect of lockdowns is always smaller than our main estimates.

The spatial heterogeneity in the importance of spillovers is presented graphically in Figure 5.3a. We map the difference (in percentage points) in the total predicted increase in May's unemployment due to lockdowns between our sector-weighted OLS specification and the alternative without spillovers. A few patterns can be observed. First, state-wide measures generate spillovers across all counties within the same state: a lockdown imposed over multiple counties always implies commuting-related spillovers. This is one reason why local restrictions can be an optimal policy, as they always cause less spatial spillovers than state-wide ones. Second, the spillover model predicts large effects around cities which have been under lengthier or more stringent measures, highlighting how urban areas can generate large externalities.

Figure 5.2 compares predictions for employment from our model with spillover and the one with no spillovers. We find that approximately 10% of the total change in employment is due to spillovers. A model not accounting for consumption-related spillovers strongly underestimates the fall in employment observed in both in suburban areas and certain rural areas highly exposed to consumption inflows (Figure 5.3b). Interestingly, our model does not estimate larger spillover effects for cities. This is because most large cities are less exposed to commuting (Fig. 2.1a) and partially to consumption (Fig. 2.1b) flows from neighbours than their suburban areas. Moreover, not many of their neighbours implemented local restrictions after the end of the state-wide orders and cities were scarcely affected by spillovers.

---

<sup>11</sup>We use the specification from Section 4.2 with neighbouring states' OLS

Figure 5.1: Effects of lockdown on unemployment/working-age population

Note: "No lags" specification corresponds to Baseline in Table 4. "Lags" specification refers to a specification with two lags of each covariate of the "no lags" specification.

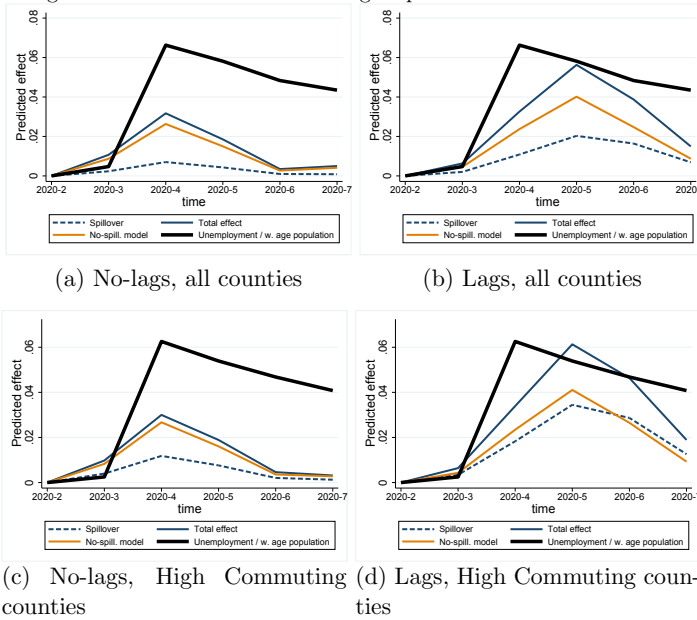


Figure 5.2: Effects of lockdown on establishment-based employment index

Note: "No lags" specification corresponds to Baseline in Table 6. "Lags" specification refers to a specification with two lags of each covariate of the "no lags" specification.

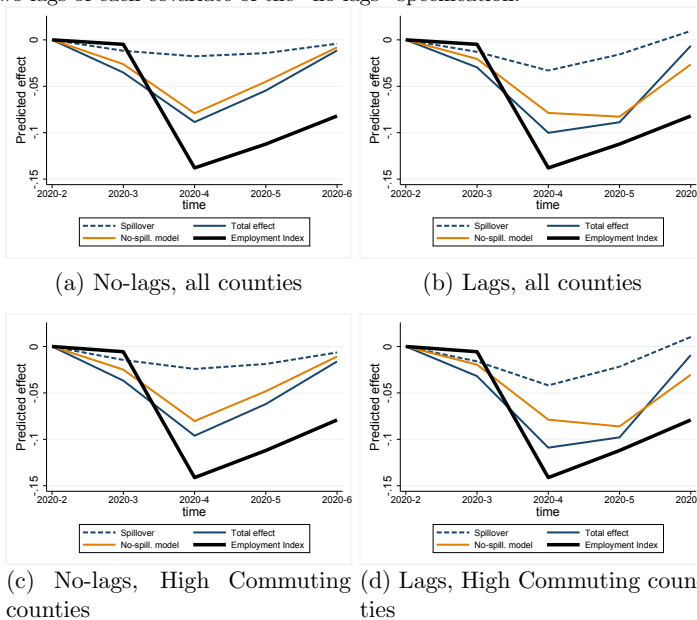
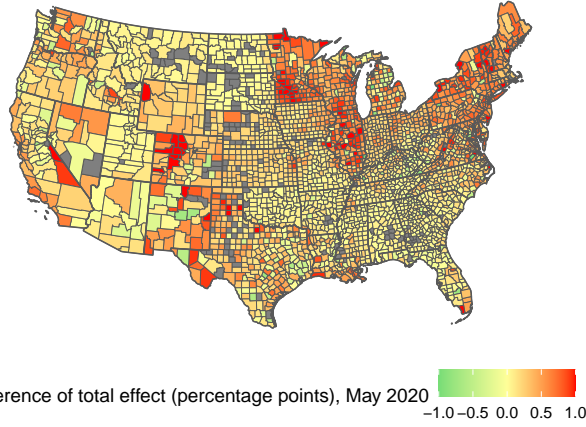
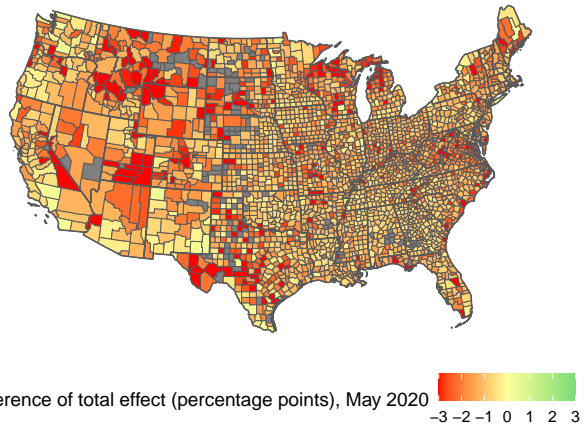




Figure 5.3: Differences in predicted effects: spillover models vs no-spillover model



(a) Unemployment-to-working-population ratio, LAU data



(b) Employment Index (2019 county average = 1), QCEW data

## 6 P.O.I. Employment and Mobility Spillovers

A simple explanation of why local unemployment increases when a neighbour issues a lockdown order is that, whenever a sector is ordered to close down, workers employed in occupations which cannot be carried out remotely are likely to lose their jobs. To this, several secondary effects can be added: unemployed people may cut their expenditure, reducing demand for labour; they may look for jobs in neighbouring counties, reducing

local job finding rates; orders in neighbouring counties may prevent or dissuade consumers from moving across borders for shopping, reducing demand for retail jobs.

While we have already found evidence that consumption-driven spillovers seem relevant to explain changes in local employment, here we provide further evidence for a micro-level mechanism behind those results. We estimate a linear POI-level model of a foot-fall proxy for employment. After focusing our analysis on the sectors where customers are unlikely to spend long times in the venue<sup>12</sup>, we argue that long visits ( $\geq 4$  hours) indexed to the 2019 POI's average can be used as a proxy of employment at the shop level<sup>13</sup>. We validate the aggregate trends and the county-level correlation between our employment proxy for restaurants (NAICS 7225) and the corresponding QCEW data, finding a consistent cross-sectional correlation of approximately 0.76 for the period between January and June 2020<sup>14</sup>.

As a novelty with respect to the literature, we estimate how the employment of individual POIs more exposed to out-of-county visits (POIs whose 2019 visitors came from outside of the county) are more affected by neighbours' orders. This level of analysis is achieved thanks to the high granularity and the panel dimension of our data.

While we provide both OLS and IV estimates, we are less concerned about endogeneity for these POI-level models. We justified the need for IV at the county level by arguing that some counties may be large or pivotal. However, for estimates at the POI level, the assumption of atomicity of each granular unit is more likely to be valid.

---

<sup>12</sup>For example, hotels' costumers are almost certainly spending "long visits" at the premises.

<sup>13</sup>For details on the data processing, see [A.2](#).

<sup>14</sup>Notice that QCEW registers all workers who worked any time during the month, while our proxy registers weekly employment/jobs, so we do not expect the two to be correlated 1:1. In particular, we expect QCEW data to overestimate average employment, which is the dimension captured by our proxy. On the other hand, our proxy does not account for back-end employees who are not working in the "shops" themselves (think about marketing, higher-level management, HR divisions or logistics incorporated in large brands' companies).

Table 7: OLS estimates of lockdown effects on Restaurants' and Non-Essential Retail's footfall-based employment index (1 = POI's 2019 average)

	Long visits index, Restaurants			Long visits index, Non-Essential Retail		
	(1)	(2)	(3)	(4)	(5)	(6)
	Baseline	SAH	Neigh. SAH	Baseline	SAH	Neigh. SAH
Closed Sector	-0.144*** (0.0157)	-0.137*** (0.0154)	-0.149*** (0.0152)	-0.126*** (0.0163)	-0.0990*** (0.0168)	-0.120*** (0.0182)
Neighbours' restaurants closures	-0.446*** (0.103)	-0.523*** (0.107)	-0.499*** (0.107)			
Closed Sector × Neighbours' rest. closures	0.0361 (0.108)	0.125 (0.105)	0.177 (0.103)			
Own SAH order		-0.0926*** (0.0127)	-0.0716*** (0.0162)		-0.0402*** (0.0105)	-0.0174 (0.0120)
Neighbours' SAH closures			-0.118*** (0.0343)			-0.111** (0.0371)
Neighbours' retail closures				-0.375*** (0.0499)	-0.388*** (0.0511)	-0.316*** (0.0606)
Closed Sector × Neighbours' retail closures				0.159** (0.0530)	0.176*** (0.0523)	0.201*** (0.0535)
Constant	0.976*** (0.00586)	0.983*** (0.00501)	0.983*** (0.00497)	0.975*** (0.00642)	0.975*** (0.00634)	0.975*** (0.00634)
Observations	27064950	27064950	27064950	22352175	22352175	22352175
R <sup>2</sup>	0.113	0.114	0.114	0.104	0.104	0.104
POI FE	Yes	Yes	Yes	Yes	Yes	Yes
Time FE	Yes	Yes	Yes	Yes	Yes	Yes
Covid controls	Yes	Yes	Yes	Yes	Yes	Yes

Note: Standard errors in parentheses. Errors clustered by county. Significance levels: \* = 0.05; \*\* = 0.01; \*\*\* = 0.001. This table presents estimates from a model regressing the long-visits index of individual POIs in NAICS 7225 and 7223 - for columns 1-3 labelled "Restaurants" - and in the non-essential retail sector - for columns 4-6 labelled "Non-Essential Retail" - (with each POI's 2019 average = 1) on measures of the own county lockdown intensity and spillover intensity coming from neighbour's lockdown orders. The intensities are calculated in proportion to the share of sectors affected by lockdown orders in either the own county or the neighbouring counties (see section 4.2). The own lockdown intensity is proportional to the share of month under lockdown, whereas spillover measures are proportional to the consumption inflows between the observed county and its neighbours over population. All consumption inflows are 2019 averages from SafeGraph data. "Closed Sector" regressor refers to the specific order which closed the subset of POIs considered in the specification, equivalent to an "entertainment" (restaurants) order or "retail" order as defined in the main text. Controls include month and county X calendar month fixed effects, together with a third-degree polynomial of days since the first Covid-19 case was registered in the county, death/population ratio and cases/population ratio.

Columns 1 through 3 of Table 7 report the weekly OLS estimates for restaurants and catering (NAICS 7225 and 7223). In this specification, we define the *closed sector* regressor as the weekly share in which a sector of interest has been closed. All regressors taking into account neighbours' closures are weighted by consumption inflows in a similar fashion to what described in the previous sections. In column 1, we estimate that own county restaurant closures reduce employment by 14.4%. Column 2 shows that stay-at-home orders - which heavily restricted mobility - are associated with a further 9.3% drop in the long visits index (given a month-long order). In both columns 1 and 2, the spillovers arising from neighbours' restaurant closures are large and significant, with a coefficient

of -0.45 implying that they can explain a further 15 percentage points fall in the average restaurant employment (as the mean inflow of visits from other counties is approximately 33% of the total). The specification in column 3, where we account simultaneously for restaurant and stay at home closures, shows that the impact of neighbours' closures is reduced by 6 percentage points ( $\beta = 0.18$ ) on average, as some of the employment was lost already when either local or neighbours' closures were first enforced. Neighbours' Stay-At-Home orders - which prevent mobility for non-essential reasons - imply a 4 percentage point ( $\beta = 0.12$ ) loss in restaurants' employment in the U.S.

We find similar evidence for non-essential retail (columns 4-6). Our IV specifications (in Appendix A) confirm the causal interpretation of these findings.

## 7 Additional Results

We perform a few further robustness checks. In Appendix A.4 we address possible concerns about consumers' or firms' anticipation of lockdown orders, which could invalidate our instrumental variables strategy. Using Google Trends data, we find some evidence that own-state lockdowns were slightly anticipated in compliers. However, we find no evidence of anticipation of neighbouring states' orders.

Using data from Chetty et al. (2020), we also examine the effect on small businesses' revenues. We find that these are strongly negatively affected by both own and neighbouring counties' orders, consistent with the fall in visits and workers we observe at the POI-level. IV estimates imply a causal relationship.

All additional tables and figures not present in the text are in the [Online Appendix](#).

## 8 Conclusions

The high degree of economic interconnection across counties and states is a characteristic of the U.S. economy. For this reason, the business closures implemented to stop the spread of Covid-19 have generated negative spillovers across geographically close locales.

These spillovers have affected both employment and consumption.

The size of the spillovers is large: we estimate that lockdown spillovers accounted for a further 1.5-3 p.p. fall in employment (out of a total fall of 14 points between February and April 2020) and a 1-1.5 p.p. further increase in the share of working-age population being unemployed (out of a 6.5 p.p. increase). In counties highly exposed to commuting (mainly suburban areas), spillovers accounted for twice these figures. Empirically, accounting for spillovers implies larger estimates of the overall negative impact of lockdowns on the labour market. Our analysis contributes to explain not only aggregate effects, but also the observed spatial distribution of labour market outcomes during the pandemic. Using POI-level data, we provide causal evidence for one of the mechanisms at work behind these aggregate estimates: shops highly reliant on customers from neighbouring counties suffered more job losses as customers' visits fell more sharply.

These findings have relevant policy implications. First, the presence of spillovers poses a problem for a "national" planner: local officials with the power to impose restrictions on local economic activities may not have incentives to internalise the externalities of lockdowns. It is unclear *whose* welfare would be maximised under such an institutional framework, but we leave this question to future research.

Second, policy-makers should account for spillovers when designing policies, as we find them to be quantitatively relevant. According to our results, job-retention schemes, loans or grants focused only on businesses in closed areas (or even just "directly affected" ones) are unlikely to target all the economic actors affected by lockdown externalities. This is the case - among many - of England's Local Restriction Support Grants, which supported only businesses *within* the geographical areas affected by the restrictions, but not those which experienced losses in revenues due to the additional spillovers.

## References

- Althoff, Lukas, Fabian Eckert, Sharat Ganapati, and Conor Walsh (2020). *The City Paradox: Skilled Services and Remote Work*. CESifo Working Paper Series 8734.
- Antràs, Pol, Stephen J Redding, and Esteban Rossi-Hansberg (Sept. 2020). “Globalization and pandemics”. In: *Covid Economics* 49.
- Baek, ChaeWon, Peter B McCrory, Todd Messer, and Preston Mui (2020). “Unemployment effects of stay-at-home orders: Evidence from high frequency claims data”. In: *Review of Economics and Statistics*, pp. 1–72.
- Barrot, Jean-Noël, Basile Grassi, and Julien Sauvagnat (May 2020). “Estimating the costs and benefits of mandated business closures in a pandemic”. en. In: *CEPR Discussion Papers* 14757. URL: <https://ideas.repec.org/p/cpr/ceprdp/14757.html> (visited on 02/16/2021).
- Birge, John R, Ozan Candogan, and Yiding Feng (2020). “Controlling Epidemic Spread: Reducing Economic Losses with Targeted Closures”. In: *University of Chicago, Becker Friedman Institute for Economics Working Paper* 2020-57.
- Borri, Nicola, Francesco Drago, Chiara Santantonio, and Francesco Sobbrío (2020). *The “Great Lockdown” Inactive Workers and Mortality by Covid-19*. CESifo Working Paper Series 8584. CESifo. URL: [https://ideas.repec.org/p/ces/ceswps/\\_8584.html](https://ideas.repec.org/p/ces/ceswps/_8584.html).
- Caspani, Maria and Jessica Resnick-Ault (2020). “New York, California and other states plan for reopening as coronavirus crisis eases”. In: *Reuters*. URL: [www.reuters.com/article/us-health-coronavirus-usa-idUSKCN21V185](http://www.reuters.com/article/us-health-coronavirus-usa-idUSKCN21V185).
- Chang, Serina, Emma Pierson, Pang Wei Koh, Jaline Gerardin, Beth Redbird, David Grusky, and Jure Leskovec (2020). “Mobility network models of COVID-19 explain inequities and inform reopening”. In: *Nature*, pp. 1–8.
- Chetty, Raj, John N Friedman, Nathaniel Hendren, Michael Stepner, and The Opportunity Insights Team (2020). *The economic impacts of COVID-19: Evidence from a new public database built using private sector data*. w27431. National Bureau of Economic Research.

Coibion, Olivier, Yuriy Gorodnichenko, and Michael Weber (May 2020). “Labor markets during the Covid-19 crisis: A preliminary view”. In: *Covid Economics* 21.

Davis, Donald R, Jonathan I Dingel, Joan Monras, and Eduardo Morales (2019). “How segregated is urban consumption?” In: *Journal of Political Economy* 127.4, pp. 1684–1738.

Fajgelbaum, Pablo, Amit Khandelwal, Wookun Kim, Cristiano Mantovani, and Edouard Schaal (2020). *Optimal Lockdown in a Commuting Network*. Working Paper 27441. National Bureau of Economic Research.

Giannone, Elisa, Nuno Paixão, and Xinle Pang (2020). “The geography of pandemic containment1”. In: *Covid Economics*, p. 68.

Goolsbee, Austan, Nicole Bei Luo, Roxanne Nesbitt, and Chad Syverson (2020). “COVID-19 Lockdown Policies at the State and Local Level”. In: *University of Chicago, Becker Friedman Institute for Economics Working Paper* 2020-116.

Goolsbee, Austan and Chad Syverson (2020). “Fear, lockdown, and diversion: Comparing drivers of pandemic economic decline 2020”. In: *Journal of Public Economics* 193, p. 104311.

Klayman, Ben (2020). “U.S. Midwest governors to coordinate reopening economies battered by coronavirus”. In: *Reuters*. URL: [www.reuters.com/article/us-health-coronavirus-midwest-economy-idUSKBN21Y2ZB](http://www.reuters.com/article/us-health-coronavirus-midwest-economy-idUSKBN21Y2ZB).

Mitch Smith, Karen Yourish, Sarah Almkhatar, Keith Collins, Danielle Ivory, and Amy Harmon (2020). *nytimes/covid-19-data*. original-date: 2020-03-24. URL: <https://github.com/nytimes/covid-19-data> (visited on 09/07/2020).

# Insolvency and debt overhang following the COVID-19 outbreak: Assessment of risks and policy responses<sup>1</sup>

Lilas Demmou,<sup>2</sup> Sara Calligaris,<sup>3</sup> Guido Franco,<sup>2</sup>  
Dennis Dlugosch,<sup>2</sup> Müge Adalet McGowan<sup>2</sup> and Sahra Sakha<sup>2</sup>

Date submitted: 2 February 2021; Date accepted: 3 February 2021

*This paper investigates the likelihood of corporate insolvency and the potential implications of debt overhang of non-financial corporations induced by economic shock associated with the outbreak of COVID-19. Based on simple accounting models, it evaluates the extent to which firms deplete their equity buffers and increase their leverage ratios in the course of the COVID-19 crisis. Next, relying on regression analysis and looking at the historical relationship between firms' leverage and investment, it examines the potential impact of higher debt levels on investment during the recovery. Against this background, the discussion outlines a number of policy options to flatten the curve of crisis-related insolvencies, which could potentially affect otherwise viable firms, and to lessen the risk of debt-overhang, which could slow down the speed of recovery.*

1 The authors are grateful to Giuseppe Nicoletti (OECD Economics Department) for insightful suggestions and discussions. The authors would also like to thank for helpful comments Laurence Boone, Sarah Box, Aida Caldera Sánchez, Chiara Criscuolo, Luiz de Mello, Alain de Serres, Filippo Gori, Dirk Pilat, Andrew Wyckoff, and many colleagues from the OECD Economics Department, the OECD Directorate for Science, Technology and Innovation, the OECD Directorate for Employment, Labour and Social Affairs and the OECD Directorate for Financial and Enterprise Affairs, as well as delegates to OECD Working Parties and participants to the conference "Rencontres Economiques de Bercy". The views and opinions expressed in the paper do not reflect the official view of the OECD.

2 OECD Economics Department.

3 OECD Directorate for Science, Technology and Innovation

Copyright: Lilas Demmou, Sara Calligaris, Guido Franco, Dennis Dlugosch,  
Müge Adalet McGowan and Sahra Sakha



## 1. Introduction

A swift and decisive response of policy makers across OECD countries has helped businesses to bridge the short-term liquidity shortfalls induced by the economic shock following the COVID-19 outbreak, avoiding immediate and widespread insolvency crises. Countries are now in the second phase of the pandemic and the shock is likely to translate into an enduring risk of a wave of corporate insolvencies, as well as in a significant increase in leverage, thereby depressing investment and job creation for long.

Building on previous work on corporate liquidity shortfalls during the pandemic (Demmou et al., 2021), this paper assesses two key types of risks in the medium and long-term:

- *Widespread distress and increase in leveraging.* The number of non-financial corporations in distress, i.e. firms that are anticipated to have a negative book value of equity and therefore a high risk of insolvency, is increasing worldwide. At least two channels are at work. First the economic shock following the COVID-19 crisis diminished actual and expected sales and profits, thereby putting downward pressure on the value of firms' assets. Second, the injection of liquidity provided in the form of loan guarantees and new lines of credit increased firms' leverage ratios and hence their default risk.<sup>1</sup> To shed light on these challenges, we perform an accounting exercise in the spirit of Carletti et al. (2020) and Guerini et al. (2020). Based on a sample of almost one million firms located in 14 European countries and in comparison to a business-as-usual counterfactual, we calculate the decline of net profit over a one year period, the associated decline in equity and the increase in leverage ratios.
- *The negative effect of debt overhang on investment.* Higher levels of corporate debt require businesses to reduce investment in the aftermath of economic crises (Kalemli-Ozcan et al., 2019; Barbiero et al., 2020). This can slow down the speed of the recovery. Relying on regression analysis and looking at the historical relationship between investment and the financial leverage ratio at the firm level, we find that higher financial leverage tends to be associated with lower investment and that this negative relationship has been particularly pronounced during and after the global financial crisis (GFC). We then calculate the potential implications of this projected increase in leveraging as compared to normal times for investment ratios in the recovery period following the COVID-19 crisis.

Against these risks, the paper discusses options for policy makers to prevent widespread insolvencies and how to support firms' investment without further increasing debt and leverage across firms. An additional layer of complexity concerns identifying the prevalence of non-viable firms, which could further undermine the strength of the recovery by locking-in resources in less productive firms (Adalet McGowan et al., 2017). The exceptional magnitude of the crisis and the high levels of uncertainty firms are still facing are likely to make the distinction between viable and non-viable firms more difficult. The risk of supporting potentially non-viable firms needs to be balanced against the risk of forcing viable and productive firms into premature liquidation. This is because insolvency frameworks tend to become less efficient in time of crisis, especially when courts are congested, potentially leading to liquidation of a higher number of viable firms than desirable, with adverse effects on growth (Iverson, 2018). To get around the necessity to identify non-viable firms at an early stage, it is critical to organise policy support under the premise of preserving optionality, i.e., helping firms weather the COVID crisis but regularly re-assessing their viability (e.g. stage-financing approach as suggested by Hanson et al., 2020).

<sup>1</sup> Through a second round effect, the deterioration of assets value could reduce firms' solvency even more, a channel not investigated in this paper.

More broadly, one potential strategy for governments would be to adopt a multidimensional cascading approach. At first, policy makers could aim at “flattening the curve of insolvencies” by providing additional resources and restoring equity of distressed firms. Next, if those additional resources are not sufficient, they could encourage timely debt restructuring to allow distressed firms to continue operating smoothly. These two first steps are expected to reduce the number of viable firms that would be otherwise liquidated. Finally, to deal with firms that would still be non-viable despite public support and debt restructuring, governments could improve the efficiency of liquidation procedures to unlock potentially productive resources. Indeed, looking forward, policy makers will acquire new information on how the “post-pandemic” normal will look like and policy may need to facilitate the “necessary” reallocations implied by COVID-19.

The remainder of the paper is organized as follows. In Section 2, we discuss the methods to assess the potential impact of the COVID-19 outbreak on firms’ financial conditions and present the main related findings. Section 3 describes the empirical framework to investigate the relationship between leverage and investment both in normal and crisis time, and discusses the outcome of the regression analysis. In Section 4, we discuss a wide range of policy options that could simultaneously help the recovery and strengthen the resilience of the corporate sector.

## 2. An empirical assessment of firms financial conditions following the COVID-19 outbreak

Using a simple accounting exercise in the spirit of Carletti et al. (2020), we evaluate quantitatively the impact of the pandemic on firms’ long-term viability. In particular, the economic shock is modelled as a change in firms’ operating profits, resulting from the sharp reversal in sales and from firms’ limited ability to fully adjust their operating expenses. After calculating the decline in profits, also taking into consideration governments’ job support schemes implemented following the outbreak of the crisis, the paper sheds light on two different but related issues. First, it assesses the share of distressed firms (i.e. firms whose net equity is predicted to be negative), which are at high risk of being insolvent, and the share of firms not able to cover interest expenses) one year after the implementation of confinement measures. This exercise informs about the amount of equity that would be needed to restore firms’ pre-crisis financial structure. Second, the paper assesses the increase in firms’ leverage ratios caused by the crisis.

### 2.1. Size and dynamics of the shock

The magnitude of the sales shock during confinement months is based on the first-round demand and supply shocks computed at a detailed sectoral level by del Rio-Chanona et al. (2020).<sup>2</sup> To quantify the supply shock, they classified industries as either essential or non-essential and constructed a Remote Labour Index, which measures the ability of different occupations to work from home: the supply shock is not binding for essential industries, while inversely proportional to the capacity to telework for non-essential ones. To quantify the demand shock, del Rio-Chanona et al. drew on a study of the potential impact of a severe influenza epidemic developed by the US Congressional Budget Office. In this paper, we identify the resulting sector-specific – but country invariant – shock as the largest between the supply and the demand shock.<sup>3</sup>

<sup>2</sup> The full dataset on the confinement shock provided by del Rio-Chanona et al. (2020) can be found [here](#).

<sup>3</sup> To see why this is the case, consider the following example. Due to confinement measures, a firm is able to produce 50% of its normal time output (e.g. supply shock). If the demand shock, due to changes in consumers’ preferences, implies a 60% reduction in demand for the products of the firm, the firm will produce only what it is able to sell – 40% of its normal time output – and the demand shock is binding. On the contrary, if the reduction in consumers’ demand is expected to be lower (e.g. 20%), the firm will still produce at its maximum capacity during confinement and the supply shock is binding.

The model presents two alternative scenarios with respect to the duration of the shock in 2020 (Table 1):

- An upside scenario, which foresees a sharp drop in activity lasting two months (the confinement period), followed by progressive but not complete recovery in the remaining part of the year. The recovery path is dependent on the initial shock, so that the most severely hit sectors face a larger absolute decline in revenues also after confinement, but the speed of the recovery is assumed, for simplicity, to be the same across sectors.
- A downside scenario, which overlaps with the upside scenario for the first seven months, but then embeds a second, relatively smaller, outbreak from the eighth month onwards, accompanied by more limited lockdowns.<sup>4</sup>

**Table 1. Detailed dynamic of the two alternative revenues shock scenarios**

Month		Mar-20	Apr-20	May-20	Jun-20	Jul-20	Aug-20	Sep-20	Oct-20	Nov-20	Dec-20	Jan-21	Feb-21
Size of the shock	Upside scenario	S	S	S*0.75	S*0.4	S*0.4	S*0.4	S*0.2	S*0.2	S*0.1	S*0.1	S*0.05	S*0.05
	Downside scenario	S	S	S*0.75	S*0.4	S*0.4	S*0.4	S*0.2	S*0.75	S*0.4	S*0.2	S*0.05	S*0.05

Note: The tables shows the detailed dynamic underpinning each of the alternative scenarios. The revenues shock (S) is sector specific and calculated each month with respect to normal time revenues.

Source: OECD calculations.

## 2.2. Data

The analysis relies on the 2018 financial statements of non-financial corporations from the latest vintage of the Orbis database. After applying standard data cleaning procedures (Gal, 2013), the final sample consists of 872 648 unique firms with at least 3 employees, operating in both manufacturing and business non-financial services industries, for 14 relatively well-covered European countries: Belgium, Denmark, Finland, France, Germany, Hungary, Ireland, Italy, Poland, Portugal, Romania, Spain, Sweden and the United Kingdom.<sup>5,6</sup> Table A.1 reports descriptive statistics of the main variables used.

Importantly, as the objective of the exercise is to investigate the extent to which solvent firms may turn distressed due to the COVID-19 shock, we exclude from the sample firms that would have been distressed (e.g. firms with negative book value of equity at the end of 2018) and would have experienced negative profits even in normal times. It follows that the findings show an *incremental* – rather than total – effect following the COVID-19 shock. Moreover, firms in Orbis are on average disproportionately larger, older and more productive than in the population, even within each size class (Bajgar et al., 2020). As these

<sup>4</sup> The sectoral implications of the second outbreak characterizing the “double-hit” scenario are assumed to be smaller than those of the initial confinement period (e.g. 75% of the size of the initial confinement shock), taking into consideration for example the increased hospital capacity and implementation of better targeted distancing measures.

<sup>5</sup> More specifically, the analysis covers all economic sectors except the followings (Nace Rev.2 classification): agriculture (VA), mining (VB), financial (VK), public administration (VO), education (VP), human health (VQ) and activities of households and organizations (VT and VU).

<sup>6</sup> At present, Orbis is the largest cross-country firm-level dataset available and accessible for economic and financial research. However, it does not cover the universe of firms, and the extent of the coverage varies considerably across countries. Indeed, in our sample, Italian and Spanish firms add up to half of the observations, while French, Hungarian, Portuguese, Romanian and Swedish firms account, each separately, for 5% to 11% of the observations; all other countries display lower shares. To deal with those limitations, the analysis purposely avoids in depth cross-country comparisons, as well as the provision of absolute numbers on the aggregate level of the shortfall.

firms are on average healthier than their smaller, younger and often less productive counterparts, the results from this analysis should be interpreted as a lower bound for the impact of the COVID-19 outbreak on firms' solvency and leveraging.

### 2.3. A stylised accounting framework

Operationally, taking as reference year the last available data for each firm (end of 2018) with respect to its revenues, operating expenses, tax payments and the book value of equity, firms' profits during the COVID-19 outbreak are calculated as follows:

$$CovidProfits_i = \sum_{t=1}^{12} [(1 - s_{st}) * Revenues_i - (1 - c * s_{st}) * Intermediates_i - (1 - w * s_{st}) WageBill_i - (1 - s_{st}) * Taxes_i] \quad (1)$$

where  $s_{st}$ ,  $c$ ,  $w$  refer, respectively, to the size of the shock in sector  $s$  and month  $t$ , the sales elasticity of intermediate costs, and the sales elasticity of the wage bill. Firms' sales, intermediate costs, wage bill, and taxes are annual values divided by 12. Consistent with Demmou et al. (2021), the elasticity of intermediate costs to sales is set to 0.8, in order to allow for short-run lower adjustment capacity, especially with respect to the partially fixed share of these costs. The elasticity of the wage bill to sales is also set to 0.8, taking into consideration the widespread job support schemes that reduced staff costs for firms during the pandemic. In line with several wage support programmes, such an elasticity implies that workers are compensated by the government at the constant rate of 80% of the usual wage for any hour not worked, while employers are assumed to bear the full costs of any hours worked and only 20% of the costs of hours not worked.

Building on the relationship between profits and equity (i.e. "reference year" equity is the outcome of "reference year" profits), the hypothetical new value of equity is obtained as:

$$PostCovidEquity_i = Equity_i - (Profits_i - CovidProfits_i) \quad (2)$$

This calculation allows us to classify firms as distressed if their pre-crisis equity buffer is not enough to cover the decline in profits, and thus if their "Post-COVID Equity" is negative.

Next, we assume that the reduction in equity relative to the reference year that follows the decline in profits translates directly into increases in firms' leverage ratios (i.e. liabilities to total assets ratio). Under this assumption, the post-COVID equity can be directly related to the post-COVID leverage according to the following accounting relationship:

$$PostCovidLiabilities_i = PostCovidAssets_i - PostCovidEquity_i \quad (3)$$

In principle, and abstracting from an injection of equity capital by the owners, an increase in the leverage ratio can follow either from an increase in liabilities (for instance benefitting from the widespread liquidity support offered by Governments in the form of new loans or guarantees) or from a decline or sale of assets (for instance depleting their cash reserves) that firms implement to weather the crisis and re-pay their current commitments. In practice, since the two channels cannot be distinguished in the context of our exercise, we assume that firms need to find financing resources equivalent to the decline in profits in order to cover all their financial commitments, such as repaying the principal of debt (i.e. the value of assets is

anchored to normal time and the adjustment occurs on the liabilities side of the balance sheet).<sup>7</sup> Importantly, by calculating the leverage ratio using a reference year, we might overestimate the post-COVID leverage if firms have the opportunity to reduce their financial commitments in some areas compared to this year. At the same time, results may be conservative if firms have taken loans for precautionary savings due to favourable credit conditions and uncertainty on a double hit (OECD, 2020a).

## 2.4. Simulation results

The estimated decline in profits is sizeable, on average between 40% and 50% of normal time profits (depending on the scenario considered).<sup>8</sup> Following this sharp reduction, 7.3% (9.1%) of otherwise viable companies would become distressed in the upside (downside) scenario (Figure 1, top left panel) and, accordingly, 6.2% (7.7%) of previously “safe jobs” are endangered. The highlighted incremental effect following the COVID-19 shock implies that the total number of distressed firms would double compare to “normal times”, as we estimate approximately 8% of firms being endangered in a No-COVID scenario.

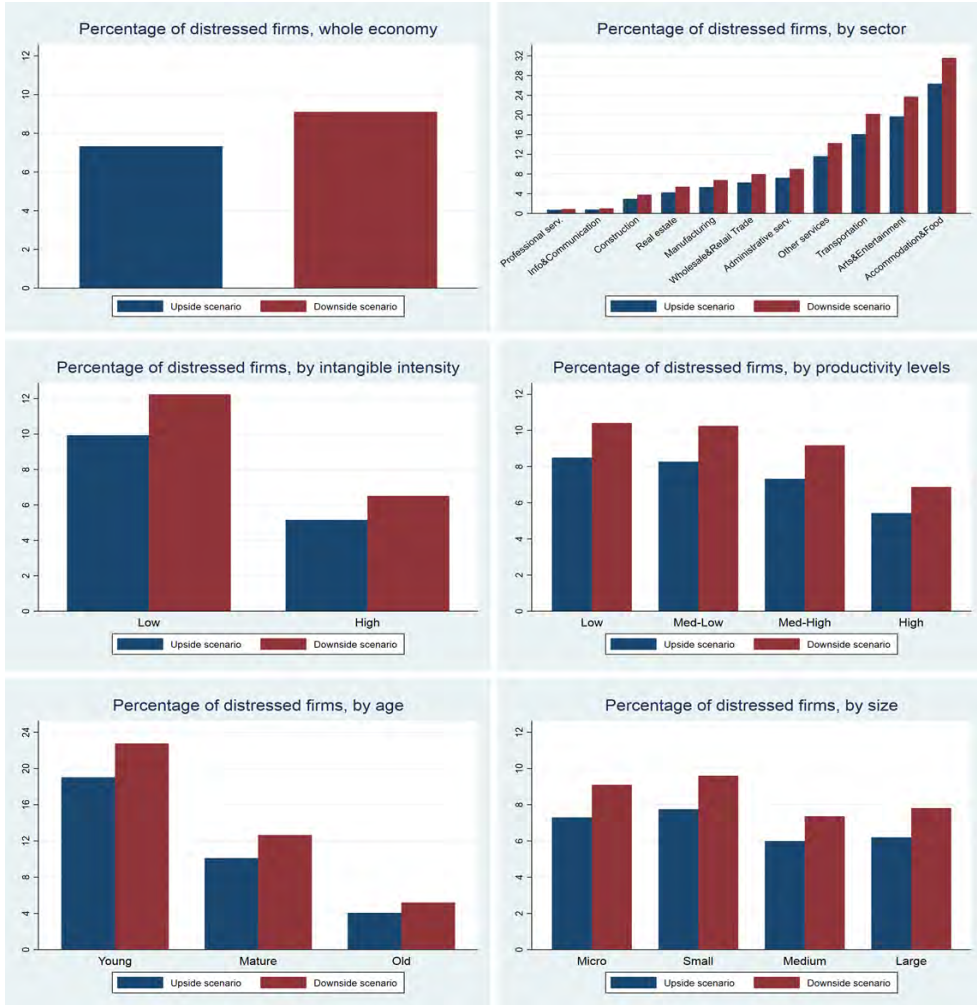
The results are quite heterogeneous across sectors and type of firms. The percentage of otherwise viable companies becoming distressed reaches 26% (32%) in the “Accommodation and food service activities” sector, while it is almost null in the “Information and communication” and “Professional services” ones (Figure 1, top right panel). The “Transports”, “Wholesale and retail trade”, as well as “Arts, entertainment and recreation” and “Other services activities” sectors are also severely hit by the crisis. The percentage of distressed firms in manufacturing is instead below average.<sup>9</sup> More broadly, and consistent with the diverse ability to rely on innovative technologies and teleworking arrangements, tangible-intensive sectors are relatively more affected than intangible-intensive ones (Figure 1, middle left panel). Similarly, more productive companies are relatively less impacted than low-productivity firms; yet, the estimated percentage of firms in the top quartile of the productivity distribution becoming distressed is not negligible (5.4% and 6.8% in the upside and the downside scenarios, respectively; middle right panel). In addition, old and large firms are better positioned to face the shock compared to their younger and smaller counterparts (Figure 1, bottom panels).

<sup>7</sup> Results are qualitatively unchanged under alternative assumptions with respect to the choice of the adjustment variables -- for instance, if we assume that firms deplete their assets to cover losses and increase their liabilities to cover the remaining portion of the decline in profits. Furthermore, they are robust to the computation of an alternative accounting framework, outlined in Annex B.

<sup>8</sup> Consistently, between 23% and 29% of previously profitable companies are expected to face losses due to the COVID-19 outbreak.

<sup>9</sup> Accordingly, the percentage of jobs at risk reaches 20% (24%) in the “Accommodation and food service activities” sector in the upside (downside) scenario; it is around 16% (20%) for “Transports” and “Arts, entertainment and recreation”, and negligible in least impacted sectors.

Figure 1. A substantial portion of otherwise viable firms is predicted to become distressed

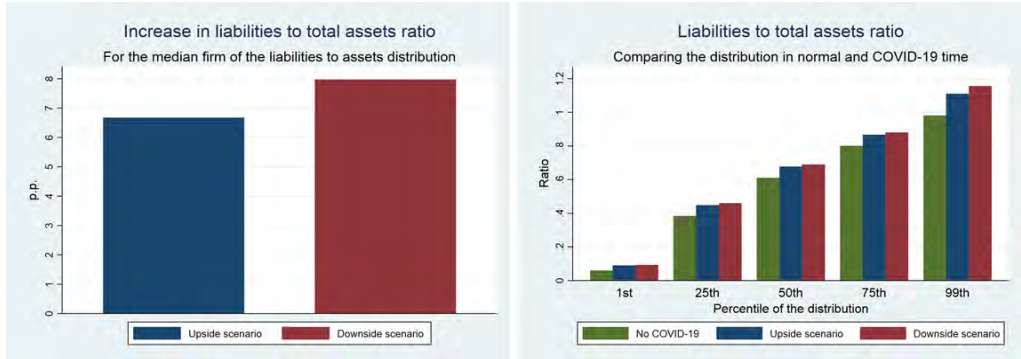


Source: OECD calculations based on Orbis® data. Intangible intensity is obtained from Demmou et al. (2019).

The reduction in equity relative to a business-as-usual scenario has immediate consequences on firms' leverage ratios: the ratio of total liabilities to total assets would increase by 6.7 percentage points in the upside scenario and 8 percentage points in the downside scenario for the median firm in the sample (Figure 2, left panel). Importantly, while leverage ratios are estimated to substantially increase due to the COVID-19 shock over the whole range of the pre-crisis distribution of leverage, the new distribution of firms according to their leverage ratio shows a larger portion of firms with very high leverage ratios, underlying the likelihood of large-scale over-indebtedness (Figure 2, right panel).



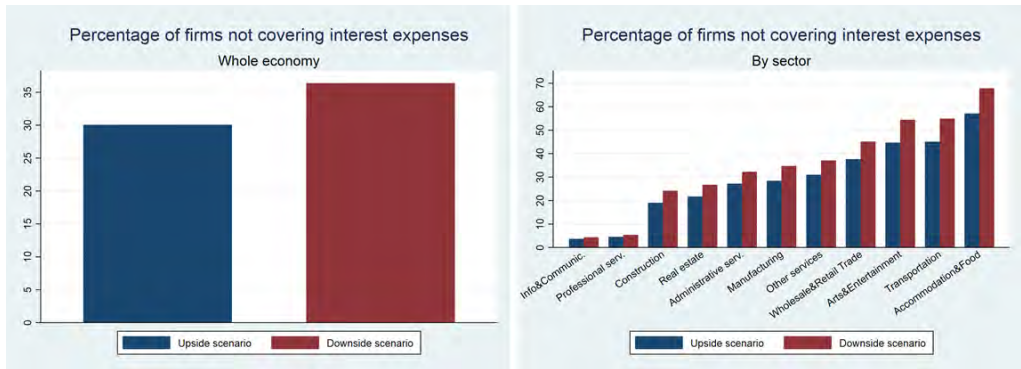
**Figure 2. Firms' leverage is expected to increase in the aftermath of the crisis**



Source: OECD calculations based on Orbis® data.

Similarly, the sizeable decline in profits relative to business-as-usual may impair firms' ability to service their debt. The left panel of Figure 3 shows that, despite assuming no increase in interest payments compared to normal times, 30% (36%) of the companies are not profitable enough to cover their interest expenses in the upside scenario (downside scenario) – i.e., they have an interest coverage ratio lower than unity. In line with this, the interest coverage ratio is estimated to be approximately halved due the COVID-19 outbreak for the median firm in the sample. The right panel of Figure 3 disaggregates results at the sector level, showing once again large heterogeneity across sectors and pointing out that a consistent portion of firms in the “Accommodation and food service activities”, “Arts, entertainment and recreation” and “Transport” sectors will find it difficult to service their debt. Unsurprisingly, young, small and less productive companies are predicted to be hit more severely by the crisis also according to this metric.

**Figure 3. A large portion of otherwise viable firms will find it hard to service their debt**



Source: OECD calculations based on Orbis® data.

Covid Economics 69, 18 February 2021: 87-108

The above findings relate to an expanding literature on the impact of the COVID-19 pandemic on business liquidity shortages and failures across the population of SMEs. The main messages are qualitatively homogeneous across studies, while there are some differences with respect to the quantification of firms' distress. A large portion of these differences could be accounted for by the heterogeneous assumptions underlying the simulations, which all rely on historical data to predict firms' position during the COVID-19 outbreak. Two main empirical approaches emerged so far. On the one hand, Gourinchas et al. (2020) – and IMF (2020), who use the same framework – rely on a structural partial-equilibrium model of the firms' short-run cost-minimization problem. On the other hand, Carletti et al. (2020) and Schivardi and Romano (2020) rely on an ad-hoc accounting model similar to ours.<sup>10</sup> A notable exception, Guerini et al. (2020) combine the structural approach with a partial adjustment mechanism. Given the elevated uncertainty over the future course of the pandemic and the different points throughout 2020 the analyses have been undertaken, the literature also differs in the size of the initial economic shock and, importantly, also on the dynamic of the shock. While Schivardi and Romano (2020) assume a V-shape recovery in 2020, our paper builds simulations around a more pessimistic scenario, where firms do not get back to their pre-crisis level of activity. The size and evolution of the shock in Gourinchas et al. (2020) and Guerini et al. (2020) appear to lie in between.

### 3. An empirical assessment of the leverage-investment relationship and the potential debt-overhang following the COVID-19 outbreak

The increase in the level of indebtedness and risk of default can push firms towards the so-called “debt overhang” risk. When a firm has a high outstanding debt on which the likelihood of default is significant, the return from any investment tends to disproportionately benefit senior debt-holders compared to shareholders (Myers, 1977).<sup>11</sup> Therefore, the expected return from an investment project needs to be high enough to cover the value of outstanding debt held by senior creditors and to offer an additional return to new investors and equity holders. This implies that debt overhang raises the threshold that determines whether an investment is profitable. As a result, businesses may only realise investment projects with a relatively high expected rate of return as opposed to all projects with a positive net present value (Chatterjee, 2013).

With less options to finance working capital, highly leveraged firms may need to cut costs or downsize to be able to shoulder interest payments in order to avoid a corporate default. Firms that built up significant debt in boom times are particularly exposed to sudden changes in economic conditions and may need to embark in a painful deleveraging process (Dell’Ariccia et al., 2016). Similarly, firms with elevated debt at short durations which find it difficult to roll-over debt in times of crisis, but also large listed firms that intend to avoid insolvency and therefore devote more resources to debt repayments than investment are prone to debt overhang and the subsequent deleveraging (Acharya et al., 2011; Brunnermeier and Krishnamurthy, 2020). Since a large share of firms with high levels of debt can significantly increase the share of non-performing loans and thus undermine the ability of banks to extend lending to healthy firms, debt overhang can also impact the ability to obtain credit by healthy firms (Caballero et al., 2008; Becker and Ivashina, 2014). The deleveraging process could hence slow down the recovery from the current crisis.

<sup>10</sup> Further, the ultimate outcome variable defining the risk of insolvency varies across studies. Gourinchas et al. (2020) define business failure if corporate cash balances and operating cashflow cannot cover financial expenses any more. Carletti et al. (2020), IMF (2020) and Guerini et al. (2020) are closer to our approach and classify firms as distressed if their net equity is predicted to be negative. Also, relevant differences relate to the underlying sample of firms, as the coverage of Orbis data varies significantly across countries, potentially impacting the comparability of the findings.

<sup>11</sup> For example, if the assets of the firm are liquidated, the payment accrues first to senior creditors, next to junior creditors and only lastly to equity holders.



Recent financial indicators corroborate that the combination of negative pressure on sales, high uncertainty about future sales and profits, and growing debt burdens has increased the risk of default, putting particular downward pressure on corporate credit ratings.<sup>12</sup>

A large stream of the literature have examined the impact of debt overhang on investment. For instance, Hennessy et al. (2007) find that a 1 percent increase in leverage for a corporation with a median level of leverage leads to a 1 percent decline in investment. Kalemli-Ozcan et al. (2019) find that debt overhang for European firms contributed to almost half of the decline in the investment-to-capital ratio during the financial crisis. Barbiero et al. (2020) find that on average, higher debt is associated with lower capital investment. The problem of low investment is mitigated if the firm is facing growth opportunities, however only if leverage is not too high.

### 3.1. Empirical approach

In order to more formally assess how the rising tide of debt associated with the COVID-19 outbreak would affect investment and to size the potential magnitude of the effect, we investigate empirically the historical relationship between indebtedness and investment, as well as the specific features characterising the relation during the global financial crisis.<sup>13</sup>

The analysis relies again on latest vintage of the Orbis database and covers both manufacturing and business non-financial services industries in the same 14 countries. Differently from previous exercise, we exploit the panel nature of the data tracking firms back in time up to 1995 and, given that some regression specifications exploit exclusively within firm variation, the dataset is restricted to firms reporting for at least three consecutive years.

We test the historical relationship between firms' financial leverage and investment by estimating the following panel fixed effects reduced-form model over the 1995-2018 period:

$$\begin{aligned} \text{InvestmentRatio}_{ics,t} & & (4) \\ &= \beta_0 + \beta_1 \text{FinLeverageRatio}_{ics,t-1} \\ &+ \beta_2 \text{InterestCoverage}_{ics,t-1} + \beta_3 X_{ics,t-1} + \delta_i + \tau_{cst} + \varepsilon_{icst} \end{aligned}$$

where subscripts  $i$ ,  $c$ ,  $s$ ,  $t$  stand for firm, country, sector and time, respectively; the dependent variable  $\text{InvestmentRatio}_{ics,t}$  is the ratio between investments (either total, tangible or intangible) at time  $t$  and total capital (respectively, total, tangible or intangible) at  $t-1$ ;  $\text{FinLeverageRatio}$  is the ratio between financial debt and total assets of firm  $i$  in  $t-1$ ;  $\text{InterestCoverage}$  is the ratio between total profits and interest expenses of firm  $i$  in  $t-1$ ; the vector  $X$  includes a set of firm level controls - namely, the log of age, log of size, cash holdings over total assets and ROA at  $t-1$ , and sales growth at time  $t$ ;  $\delta_i$  indicates firm fixed effects and  $\tau_{cst}$  country by sector by time dummies.

The model is closely related to the approaches adopted by Kalemli-Ozcan et al. (2019) and Barbiero et al. (2020). It is estimated by OLS, clustering standard errors at the firm level. The main parameters of interest are the estimates of  $\beta_1$  and  $\beta_2$ , which we expect to be respectively negative and positive. To diminish concerns of endogeneity resulting from the relationship between investment and financial leverage, we use a rich fixed effects structure: firm fixed effects absorb the unobserved firm-specific heterogeneity that might simultaneously affect both variables; the triple interacted country-sector-year fixed effects control for

<sup>12</sup> In line with this, there is large evidence that investment collapsed in the aftermath of the global financial crisis and experienced sluggish growth in the following years (OECD, 2020g).

<sup>13</sup> While this analysis sheds light on the investment-leverage relationship in crisis time, it is worth stressing that the GFC and the COVID-19 shock display very different features (e.g. ranging from the underlying causes to government responses) and thus that results could be interpreted in the light of the current situation only to a limited extent.

the effects of all time-varying shocks at the country-sector level. Moreover, we lag all firm level regressors to further reduce the simultaneity bias, and use a large set of firm-level controls to control for the potential omitted variable bias arising from firm time-varying characteristics. Nonetheless, the simple nature of the model calls for a careful interpretation of the findings in terms of causality.

Next, we check whether the relationship presents different features during sharp downturns by estimating the following cross-sectional model, as in Kalemli-Ozcan et al. (2019):

$$\begin{aligned} \Delta InvestmentRatio_{ics} & & (5) \\ &= \beta_0 + \beta_1 \Delta FinLeverageRatio_{ics} \\ &+ \beta_2 \Delta InterestCoverage_{ics} + \beta_3 \Delta X_{ics} + \tau_{cs} + \varepsilon_{ics} \end{aligned}$$

where notations are consistent with equation 4 and all variables are expressed as first differences between the average levels in the post-GFC period (2008-2013) and the average pre-GFC (2002-2007) levels. Again, we expect  $\beta_1$  and  $\beta_2$  to be respectively negative and positive, hinting that an increase in the financial leverage (interest coverage) ratio reduces (increases) investment during the crisis. The specification in differences implicitly absorbs firm fixed effects with respect to the levels variables, and country by sector dummies ( $\tau_{cs}$ ) control notably for demand effects.

Moreover, Equation 5 is further extended to investigate whether the impact of an increase in financial leverage has heterogeneous effects depending on firms' financial leverage levels when entering the GFC. This is done by including as an extra term in equation (5) the interaction between the pre-crisis leverage levels and the change in the leverage ratio. This is of particular interest in the current COVID-19 crisis characterized by both high indebtedness levels and low growth rates.

### 3.2. Empirical results

Consistent with previous studies (e.g. Kalemli-Ozcan et al., 2019; Barbiero et al., 2020), the results from the panel model confirms the existence of a negative and statistically significant relationship between financial leverage and investment (see Table A.2). The magnitude of the effect is not negligible. A 19 percentage points (43 percentage points) increase (decrease) in the debt to assets ratio (interest coverage ratio) – e.g. approximately equivalent to a one-standard deviation in our sample – is correlated to a decrease in the investment ratio of 6 percentage points (1 percentage point). In other words, such a change in financial leverage (the interest coverage ratio) would explain 15% (3%) of the observed variation in investment over the period, if interpreted as causal. Results are confirmed when focusing exclusively on tangible or intangible investments, and are consistent with respect to a wide range of robustness checks.<sup>14</sup>

The left panel of Figure 4 further explores the implied magnitude of the estimated relationship between investment and financial leverage ratios by assuming an increase in the debt to total assets ratio comparable to that predicted by our accounting model in the post-COVID period.<sup>15</sup> Specifically, it illustrates the inferred decrease in investment to fixed assets under the hypothetical increase in financial leverage as shown in Figure 2 (left panel) for the median firm in the sample. Investments to fixed assets would decrease by 2 percentage points in the upside scenario and 2.3 in the downside one.

The outcome of the cross-sectional model strengthens these findings and shows that the relationship holds in the presence of a large shock such as the GFC (see Table A.3). An increase in firms' financial leverage

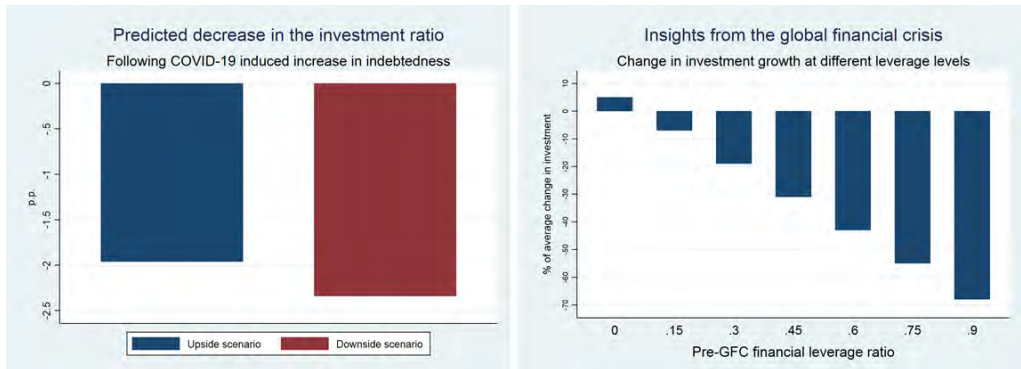
<sup>14</sup> For instance, looking separately at the pre- and post-GFC periods or using quartiles of the financial leverage ratio variable, rather than its continuous value, to capture firms' indebtedness levels. Moreover, results are qualitatively unchanged if using the liabilities to total assets ratio rather than financial leverage as the main explanatory variable.

<sup>15</sup> In other words, we assume that the increase in the liabilities to total assets ratio is fully driven by an increase in financial debt, as the simple accounting model presented in section 2 and data limitations do not allow to calculate the development of the different components of liabilities following the COVID-19 outbreak.

has on average a significant and negative correlation with the growth of investment in the aftermath of the crisis. Similarly, the positive coefficient for the interest coverage ratio implies that a decrease in the ability to service debt is also associated with lower investment growth. However, the effect of a change in debt on investment is heterogeneous across firms and is increasing with initial leverage levels (Figure 4, right panel): firms that entered the GFC with a higher financial leverage ratio experienced a sharper decline in investment; on the contrary, the relation can turn positive, and thus an increase in debt could be positive related to investment, for firms with very low initial indebtedness levels. The effect is economically considerable. For instance, a 15 percentage points increase in the change in financial leverage – approximately equivalent to a one-standard deviation – implies a decrease in the investment rate equivalent to 18% of its average change for firms with a financial leverage ratio around 0.3, while it implies a 5% increase for firms with no previous debt.

Overall, these results suggest that, if we interpret them causally, debt-overhang could hamper investment and impede a fast recovery following the COVID-19 outbreak, given the record-high debt levels at the beginning of 2020 and the ongoing and expected rise in corporate debt to face the economic consequences of the pandemic. Moreover, the analysis hints that looking exclusively at average effects may convey policy makers only a partial picture, and that a further increase in debt may not be the appropriate answer for highly indebted firms, both from a viability and an investment perspective.

**Figure 4. High financial leverage decreases investment**



Note: The left panel shows what would be the increase in the investment to fixed assets ratios under the hypothetical increase in the debt over total asset ratios shown in Figure 2 (left panel) for the median firm. Estimates on the correlation between debt and investment ratios are based on column (7) of Table A.2, i.e. the model including all the controls in the panel regression. The right panel shows the predicted percentage growth in the change in the investment to fixed assets ratio following a one standard deviation increase in the (post- minus pre-GFC) change in financial leverage, at different pre-crisis indebtedness levels. Estimates are based on specification 2 in Table A.3. To interpret the size of the effect, we scale the y-axis by the absolute value of the mean of the change in the investment ratio, hence obtaining the effect of a one standard deviation increase in the explanatory variable of interest on the average value of the dependent variable.

Source: OECD calculations based on Orbis® data.

#### 4. Policy discussion

The empirical analysis stresses that the rise of corporate debt could threaten the recovery, suggesting that governments should be careful when designing support packages. In the initial phase of the COVID-19 crisis, temporary deferral or repayments of loans either by private agents (e.g. banks in Netherlands) or public sources (e.g. loans by the Ministry of Tourism in Spain) played a key role to relieve financially distressed businesses and prevent early insolvency. Loan guarantees also help distressed firms to meet their immediate financial commitments, avoiding widespread defaults (e.g. the Überbrückungskredite –

loan guarantees for short-term credits - offered by the Austrian Economic Chamber). However, such support may not address the issue of their long-term viability due to the associated rise in indebtedness. The rest of the policy brief sheds light on various policy options to support distressed firms while not compromising their ability to invest. First, it focuses explicitly on the design of crisis-related measures and on the necessity to favour equity-type of financing over debt to recapitalise distressed firms. Second, it investigates the potential role of debt resolution mechanisms in mitigating debt overhang and in sorting out viable and non-viable firms.

#### **4.1. Flattening the curve of insolvency while reducing the debt overhang risk**

Increasing equity capital provides a way to support viable businesses without raising corporate debt. Relative to increases in debt, additional equity improves leverage ratios and reduces interest coverage ratios, thereby reducing corporate refinancing costs and benefitting a potential recovery. In times of high uncertainty over future sales growth, equity financing may also be desirable from the viewpoint of entrepreneurs, given that equity acts like an automatic stabiliser. Governments have various policy options to leverage on equity financing to support viable businesses.

##### **4.1.1. Favouring equity and quasi-equity type of public financing**

Equity injections can help firms, which suffer from financial difficulties solely due to COVID-19 but are likely to return to profitability afterwards, to raise much-needed cash to finance their working capital while keeping assets free for raising debt in the future. Hybrid instruments like preferred equity appear particularly well-adapted as they provide a senior claim to dividends and assets in case of liquidation while they entail no voting rights and hence do not require governments to be involved in management. However, authorities need to ensure that losses for taxpayers are minimised, competition on markets is not overly distorted and that equity injections do not crowd out other investors (OECD, 2020b). It is hence important to ensure that such support is state-contingent and includes mechanisms to incentivise all parties to wind down support when economic conditions improve (OECD, 2020c; OECD, 2020d). Temporary forms of preferred equity, e.g. retractable preferred equity, would also help to formulate an exit strategy in advance.

Supporting SMEs and start-ups financing needs may require a different and more comprehensive approach, as equity markets for small and medium-sized, as well as young, firms are thinner and often lacking altogether.<sup>16</sup> This makes the valuation of equity capital and thus the design of the injection more difficult. Policymakers could revert to more indirect measures. For instance, loans repayment could be linked to businesses' returns: firms that recover most robustly would pay back more, in the form of future taxes, while those that struggle longer would pay back less. Such support would have several advantages. It could contribute to flatten the curve of bankruptcies while limiting the risk of costly defaults. In addition, agreements to pay higher taxes in the future against guaranteed credits would be easier to monitor for authorities, than a potentially large number of equity injections in a large number of single entities. Similarly, though subject to the existence of sufficient fiscal space, another useful measure to address SME funding needs without raising debt consists in converting government (crisis related) loans into grants.

##### **4.1.2. Stimulating the uptake and provision of equity capital**

One way for policymakers to leverage on the need for equity in the post-COVID-19 world would be to grant an allowance for corporate equity. Such an allowance would partially or totally offset the tax benefits of using debt financing common in many OECD countries and make equity financing more attractive. Their design should however ensure that multinationals do not exploit ACE for tax-planning and that their fiscal cost is acceptable, for instance by granting them to new equity capital only. In the OECD area, a few

<sup>16</sup> For a recent discussion on start-ups during the COVID-19 see OECD (2020g).

countries (such as Italy and Belgium) have already introduced ACE or experimented with it in the past and their experience can serve as example (Zangari et al., 2014; Hebous and Ruf, 2017). Moreover, deductions on income taxes and reliefs on the taxation of capital gains for eligible investments can foster the provision of private equity capital. Such tax incentives are often used to stimulate investments in high-risk, early-stage businesses, e.g. as in the UK's Enterprise Investment and Seed Enterprise Investment scheme, but could potentially also be extended to a wider set of firms, e.g. smaller companies facing tight financing frictions.

Debt-equity swaps constitute a further tool to address high leverage. They involve the conversion of outstanding debt that cannot be repaid into equity of an otherwise viable company. Debt-equity swaps may appear attractive in theory, but raise some implementation issues. A debt-equity conversion requires the estimation of the market value of debt and equity and an agreement between shareholders and the debtholder on an exchange ratio. The lack of equity markets for SMEs, in particular smaller ones, impedes a cost-efficient estimation of the market value of equity. Consequently, debt-equity swaps appear more appropriate to address elevated leverage in circumstances where agreements on underlying terms are more likely to be reached, e.g. subsidiaries of a larger firm, than as a more general policy tool.

Besides immediate short-term measures aimed at dealing with the economic consequences of COVID-19, there are options to ensure that equity markets continue to develop, including by widening access to equity markets for smaller firms, e.g. through reducing costs and streamlining listing requirements (Kaousar Nassr and Wehinger, 2016). For instance, COVID related equity programmes could speed up the implementation of the Capital Market Union in European countries, which in turn could help to address intra-European segmentation along national boundaries. Similarly, policy makers can improve the development and attractiveness of equity markets by using financial literacy as a tool to boost stock market participation and financial knowledge of entrepreneurs.

#### ***4.2. Ensuring the restructuring of viable firms in temporary distress and liquidation of unviable ones***

Equity and quasi-equity injections might prove insufficient to allow firms to operate normally if leverage ratios and risk of default remain high. For those firms, reducing the debt burden through debt restructuring can change both the timing of the potential default and their possibility to invest (Frantz and Instefjord, 2019). Most countries have already modified their insolvency framework to give insolvent firms a chance to survive in the short-run, for instance by relaxing the obligation for directors to file for bankruptcy once insolvent (e.g. France, Germany, Luxembourg, Portugal and Spain) or by relaxing creditors' right to initiate insolvency proceedings such as done in Italy, Spain, Switzerland and Turkey (OECD, 2020e; INSOL International-World Bank Group, 2020). However, more structural changes to features of insolvency regimes, which can be a barrier to successful restructuring, could help to coordinate creditors' claims in a manner that is consistent with preserving the viability of the firm. This crisis can provide an opportunity for such reforms.

##### ***4.2.1. Favouring new financing***

Continuity of firm operations during restructuring increases the chances of a successful restructuring but often requires firms to have access to bridge financing. However, access to new funds may be difficult when the debt levels are already high and the risk of default is significant, leading to debt overhang. Across the OECD, new financing can have either no priority at all over existing creditors or priority over only unsecured creditors or else priority over both secured and unsecured creditors. In normal times, insolvency regimes have to balance incentives for debtors to invest and take risks with incentives for creditors to supply funds. Therefore, new financing should be granted priority ahead of unsecured creditors but not over existing secured creditors since this would adversely affect the long-term availability of credit and legal certainty (Adalet McGowan and Andrews, 2018). Yet, several OECD countries currently do not offer

any priority to new financing, so granting it over unsecured creditors would be beneficial. Further, in the context of the current crisis and assuming that the extensive guarantees and liquidity injections reach the right firms, the blocking of the “credit channel” might not be the main concern. An alternative but more controversial option to improve access to new financing is to temporarily suspend also the priority enjoyed by secured creditors in favour of new investors when they invest in distressed firms.

#### 4.2.2. Promoting pre-insolvency frameworks

Efficient pre-insolvency frameworks and debt restructuring could help to address debt overhang by lowering the negative impact of deleveraging on GDP growth and quickening the resolution of non-performing loans (Carcea et al., 2015; Bricongne et al., 2017). While a majority of OECD countries has some type of pre-insolvency legislation, until recently they were generally missing in non-European OECD countries (Adalet McGowan and Andrews, 2018). A number of countries has strengthened out-of-court procedures in recent years. For example, in 2018, Belgium, granted the courts the ability to endorse a settlement between a debtor and two or more of its creditors to make it enforceable. Lithuania overhauled the insolvency regime in 2020, accelerating timely initiation and resolution of personal and corporate insolvency proceedings and increasing returns for creditors, bringing them among the countries with the most efficient insolvency regimes according to the OECD indicator (OECD, 2020f). In addition, several countries have encouraged lenders to reach out-of-court agreements with debtors materially affected by COVID-19, especially when these agreements just involve a deferral of loan repayments (Australia, China, India, Malaysia, and Singapore). More generally, introducing preventative restructuring or pre-insolvency frameworks, for instance as in the *EU Directive on Preventive Restructuring Frameworks and Second Chance*, could be accompanied by other incentives for private creditors to restructure debt, such as tax incentives (e.g. tax exemption for creditors who forgive part of debt). Effective design of such policies can be based on existing guidelines, such as the World Bank’s *Toolkit for Out-of-Court Restructuring* (World Bank, 2016).

#### 4.2.3. Establishing specific procedures for SMEs

Small and medium-sized enterprises (SMEs) may warrant different treatment from other firms in a debt restructuring strategy, as complex, lengthy and rigid procedures, required expertise and high costs of insolvency can be demanding for this category of firms. Indeed, SMEs are more likely to be liquidated than restructured, since they have to bear costs that are disproportionately higher than those faced by larger enterprises. In the current juncture with a high risk of insolvency among SMEs, the social cost of an inefficient debt restructuring for SMEs could be very large.

Against this background, formal procedures can be simplified for SMEs and informal procedures, which typically avoid the procedural complexities and timelines of court proceedings and are often associated with better outcomes for SMEs, can be adopted relatively quickly (World Bank, 2020). A number of countries have taken measures to simplify insolvency procedures for SMEs in response to the COVID-19 pandemic.<sup>17</sup> The introduction of simplified rules and flexibility with payment plans could increase the likelihood that non-viable SMEs exit and viable ones in temporary distress are restructured immediately.

<sup>17</sup> The new COVID-19 moratorium in Switzerland provides SMEs with a simple procedure to obtain a temporary stay of their payment obligations. Brazil has proposed to implement simplified insolvency rules for SMEs (during judicial restructuring plans, they can be allowed to pay debt in up to 60 monthly instalments instead of 36 months, as is currently the case). In the United States, the threshold required to access the simplified insolvency rules of the Small Business Reorganisation Act of 2019 has been increased to allow more companies access to simplified proceedings.



#### 4.2.4. *Dealing with systemic debt restructuring of large companies*

In-court debt restructuring for large firms appears broadly efficient in normal times, but during systemic crises case-by-case restructuring can become difficult, private capital is limited and co-ordination problems become more serious. In these conditions, court-supervised restructuring can be too time-consuming. Against this background, government agencies could prioritise out-of-court renegotiations whenever possible, a strategy that proved to be successful after the global financial crisis (Bernstein, et al., 2019; Hotchkiss et al., 2012). When out-of-court restructuring is difficult due to too many creditors, a centralised out-of-court approach might be desirable; such as the centralised out-of-court debt restructuring approach (the so-called “London approach”) developed by the Bank of England in the 1990s or the “super Chapter 11” developed in the United-States designed to deal with systemic crises.

#### 4.2.5. *Strengthening the efficiency of the liquidation framework to improve resource allocation*

Providing equity support for distressed firms and ensuring debt restructuring should reduce a build-up of undesirable bankruptcies, but some firms will still remain un-viable in the post-COVID world (e.g., due to their business model, their financial situation or their product specialisation). Against this risk, policy makers need to address several challenges to ensure that the liquidation process of those firms is efficient.

*Ensuring the highest possible recovery rate for creditors.* When the number of distressed firms is too large, the courts become overwhelmed, standard insolvency procedures work less effectively, and the recovery rates for creditors can be reduced, potentially at fire-sale prices. Any reforms that can simplify and speed up in-court processes would help in this respect. In the short term, increasing resources for the court system, for instance by adding new temporary judges on insolvency procedures or reallocating judges depending on the busiest jurisdictions, would contribute to increase the recovery rate of creditors.

*Ensuring that liquidation is established by an independent broker.* Public agencies such as public development banks in charge of loan guarantees may not be well placed to negotiate liquidation given their own balance sheets exposed (Bertay et al., 2015). Therefore, one challenge for policy makers is to establish an independent organisation to ensure that decisions with respect to liquidation and debt restructuring are not distorted (Hege, 2020).

*Reducing specific barriers to market exit for small firms.* The corporate vs personal distinction in assets and liabilities is often blurred for small firms. In that context, the type of personal insolvency regime matters to reduce the scars from the crisis, in particular by enabling a post-insolvency second chance for entrepreneurs and the availability of a “fresh start” – i.e. the exemption of future earnings from obligations to repay past debt due to liquidation bankruptcy. Many countries are already lowering time to discharge to 3 years to be in line with the EU Directive on Insolvency and Second Chance (e.g. Germany), but they could try to expedite this part of the reform, which can facilitate reallocation (e.g. Spain is considering this option).

## References

- Acharya, V., D. Gale, and T. Yorulmazer, (2011), “Rollover risk and market freezes,” *The Journal of Finance*, 66 (4): 1177-1209.
- Adalet McGowan, M., and D. Andrews, (2018), “Design of insolvency regimes across countries”, *OECD Economics Department Working Papers*, No. 1504, OECD Publishing, Paris.
- Adalet McGowan, M., D. Andrews and V. Millot, (2017), “The walking dead? Zombie firms and productivity performance in OECD countries”, *OECD Economics Department Working Papers*, No. 1372, OECD Publishing, Paris.

- Bajgar, M., Berlingieri, G., Calligaris, S., Criscuolo, C., and J. Timmis, (2020), "To use or not to use (and how to use): coverage and representativeness of Orbis data", *OECD Science, Technology and Industry Working Papers*, No. 2020/06, OECD Publishing, Paris.
- Barbiero, F., A. Popov and W. Marcin, (2020), "Debt overhang, global growth opportunities, and investment", *Journal of Banking and Finance*, Vol. 120, Article 105950.
- Becker, B., and V. Ivashina, (2014), "Cyclicality of credit supply: Firm level evidence", *Journal of Monetary Economics*, Vol. 62, pp. 76-93.
- Bernstein, S., J. Lerner, and F. Mezzanotti, (2019). "Private equity and financial fragility during the crisis", *Review of Financial Studies*, 32(4)
- Bertay, A., A. Demirguc-Kunt and H. Huizinga, (2015), "Bank ownership and credit over the business cycle: Is lending by state banks less procyclical?", *Journal of Banking and Finance*, Vol. 50(3): 326-339.
- Bricongne, J.C, M. Demertzis, P. Pontuch and A. Turrini, (2016). "[Macroeconomic relevance of insolvency frameworks in a high-debt context: An EU perspective](#)", *European Economy - Discussion Papers, No.2015-032*, Directorate General Economic and Financial Affairs, European Commission.
- Brunnermeier, M., and A. Krishnamurty, (2020), "COVID-19 SME evergreening proposal: Inverted economics", mimeo.
- Caballero, R., T. Hoshi and A. Kashyap, (2008), "Zombie Lending and Depressed Restructuring in Japan", *American Economic Review*, Vol. 98(5): 1943-1977.
- Carcea, M., D. Ciriaci, C. Cuerpo, D. Lorenzani and P. Pontuch, (2015), "The Economic Impact of Rescue and Recovery Frameworks in the EU", *EU Discussion Papers*, No. 004.
- Carletti, E., T. Oliviero, M. Pagano, L. Pelizzon and M. G. Subrahmanyam, (2020), "[The COVID-19 shock and equity shortfall: Firm-level evidence from Italy](#)", *CEPR Discussion Paper* No. 14831, also published [COVID Economics: Vetted and Real-Time Papers](#), issue 25.
- Chatterjee, S., (2013), "Debt overhang: Why recovery from a financial crisis can be slow", *Business Review*, Federal Reserve Bank of Philadelphia, issue Q2, p.p. 1-9.
- del Rio-Chanona, R. M., P. Mealy, A. Pichler, F. Lafond and J. D. Farmer, (2020), "Supply and demand shocks in the COVID-19 pandemic: An industry and occupation perspective", [COVID Economics: Vetted and Real-Time Papers](#), issue 6.
- Dell'Ariccia, G., D. Igan, L. Laeven and H. Tong, (2016). "Credit Booms and macrofinancial stability", *Economic Policy* 31(86): 299-355.
- Demmou L., G. Franco, S. Calligaris and D. Dlugosch, (2021), "Liquidity shortfalls during the COVID-19 outbreak: assessment of risks and policy responses", *OECD Economics Department Working Papers*, No 1647, OECD Publishing.
- Demmou, L., I. Stefanescu and A. Arquie, (2019), "Productivity growth and finance: the role of intangible assets - a sector level analysis", *OECD Economics Department Working Papers*, No 1547, OECD Publishing.
- Frantz, P., and N. Insteffjord, (2019), "Debt overhang and non-distressed debt restructuring", [Journal of Financial Intermediation](#), Vol. 37 (C): 75-88.
- Gourinchas, P.O., S. Kalemli-Özcan, V. Penciakova and N. Sander, (2020), "COVID-19 and SME failures," *NBER Working Papers No. 27877*, National Bureau of Economic Research.
- Guerini, M., L. Nesta, X. Ragot and S. Schiavo, (2020), "Firm liquidity and solvency under the COVID-19 lockdown in France", *OFCE policy brief*, No.76.
- Hanson, S., J. Stein, A. Sunderam and E. Zwick, (2020), "Business Continuity Insurance: Keeping America's lights on during the pandemic", *White Paper of Becker Friedman Institute*.
- Hebous, S., and M. Ruf, (2017),"Evaluating the effects of ACE systems on multinational debt financing



- and investment”, *Journal of Public Economics*, Vol. 156: 131-149.
- Hennessy, C. A., A. Levy and T. M. Whited, (2007) “Testing ‘Q’ Theory With Financing Frictions,” *Journal of Financial Economics*, Vol. 83 (3): 691–717.
- Hege, U., (2020), “Corporate debt threatens to derail recovery”, *TSE Mag #20*.
- Hotchkiss, E.S., P. Stromberg and D. Smith, (2012), “Private equity and the resolution of financial distress”, AFA 2012 Chicago Meetings Paper, *ECGI - Finance Working Paper*, No. 331.
- International Monetary Fund, (2020), “World Economic Outlook, October 2020: A Long and Difficult Ascent”, IMF Publications.
- Iverson, B., (2018), “Get in line: Chapter 11 restructuring in crowded bankruptcy courts”, *Management Science*, Vol. 64 (11): 5370-5394.
- INSOL International-World Bank Group, (2020), *Global Guide Corporate Insolvency: Responses in Times of Covid-19: Report*.
- Kalemli-Ozcan, S., L.A. Laeven, and D. Moreno, (2019) “Debt Overhang, (2019) Rollover Risk, and Corporate Investment: Evidence from the European Crisis”, *ECB Working Paper*, No. 2241.
- Kaousar Nassr, I., and G. Wehinger (2016), “Opportunities and limitations of public equity markets for SMEs”, *OECD Journal: Financial Market Trends*, vol. 2015/1
- Kent, P., (1993), “The London Approach”, *Bank of England Quarterly Bulletin*.
- Myers, S. C., (1977) “Determinants of Corporate Borrowing”, *Journal of Financial Economics*, Vol. 5 (2), 147–175.
- OECD, (2020a), Initial impact of COVID-19 pandemic on the non-financial corporate sector and corporate finance”, *Forthcoming Tackling Coronavirus Series*.
- OECD, (2020b), “COVID-19 Government Financing Support Programmes for Businesses”, OECD Paris.
- OECD, (2020c), “The COVID-19 crisis and state ownership in the economy: Issues and policy considerations”, *Tackling Coronavirus Series*.
- OECD, (2020d), “Supporting businesses in financial distress to avoid insolvency during the COVID-19 crisis”, *Tackling Coronavirus Series*.
- OECD, (2020e), “National corporate governance related initiatives during the COVID-19 crisis: A survey of 37 jurisdictions”, *Tackling Coronavirus Series*.
- OECD (2020f), “OECD Economic Surveys: Lithuania 2020”, OECD Publishing, Paris.
- OECD, (2020g), “Corporate bond market trends, emerging risks and monetary policy”, *OECD Capital Market Series*.
- Schivardi, F., and G. Romano, (2020), “A simple method to compute liquidity shortfalls during the COVID-19 crisis with an application to Italy”, mimeo.
- World Bank, (2016), “Principles for effective insolvency and creditor/debtor regimes”, *World Bank Group*.
- World Bank, (2020), “COVID-19 Outbreak: Implications on Corporate and Individual Insolvency”, *World Bank Group*.
- Zangari, E., (2014), “Addressing the debt bias: A comparison between the Belgian and the Italian ACE systems”, *Taxation Papers – Working Paper No. 44*, European Commission.

## Annex A. Additional tables and figures

Table A.1. Descriptive statistics

Variable	p5	p25	p50	mean	p75	p95
	<i>Simulation exercise (2018 data)</i>					
Number of employees	3	5	8	36	19	100
Gross revenues	105,230	365,610	942,714	10,000,000	2,962,000	24,600,000
Wage bill	22,999	81,090	197,778	831,422	540,683	3,452,000
Intermediates	39,060	194,487	568,505	7,750,000	1,989,000	18,100,000
Profits	4,621	21,628	62,818	365,920	204,780	1,522,000
Total assets	59,812	235,996	683,120	4,223,000	2,294,000	17,500,000
Equity (book value)	12,699	65,389	215,972	1,687,000	829,020	7,238,000
Total liabilities	20,270	113,742	369,761	2,369,000	1,291,000	9,774,000
Current liabilities	13,286	78,079	258,662	1,690,000	919,982	7,207,000
Equity to total assets ratio	0.0525	0.198	0.388	0.416	0.616	0.867
Total liabilities to total assets ratio	0.133	0.384	0.612	0.584	0.802	0.947
Interest coverage ratio	2.225	6.819	19.95	321.8	77.43	1123
	<i>Debt overhang empirical analysis, 1995-2018 panel data</i>					
Investment ratio	-0.040	0.023	0.109	0.244	0.309	1.021
Financial leverage ratio	0.009	0.073	0.191	0.232	0.354	0.598
Interest coverage ratio	-1.42	2.52	6.10	19.43	16.84	84.85
	<i>Debt overhang empirical analysis, cross-sectional analysis over GFC</i>					
Change in investment ratio	-0.551	-0.221	-0.0612	-0.0845	0.0539	0.331
Pre-crisis financial leverage ratio	0.018	0.085	0.184	0.222	0.327	0.550
Change in financial leverage ratio	-0.19	-0.0536	0.0131	0.0306	0.105	0.304
Change in interest coverage ratio	-41.57	-5.983	-0.945	1.034	3.715	56.21

Note: In the simulation exercise, the sample is restricted to firms with available financial data, non-negative equity buffers and positive profits in normal time; monetary values in EUR current (2018) prices. By contrast, the only constraint imposed on the sample for the empirical analysis is data availability for the variables of interest.

Source: OECD calculations based on Orbis® data.

**Table A.2. High leverage decreases investment**

	Dependent variable: Investment ratio						
	(1)	(2)	(3)	(4)	(5)	(6)	(7)
Debt to total assets( <i>i,t-1</i> )	-0.348*** (0.002)	-0.351*** (0.002)	-0.346*** (0.002)	-0.356*** (0.002)	-0.314*** (0.002)	-0.314*** (0.002)	-0.294*** (0.002)
Interest coverage ratio ( <i>i,t-1</i> )	0.053*** (0.001)	0.053*** (0.001)	0.054*** (0.001)	0.056*** (0.001)	0.039*** (0.001)	0.033*** (0.001)	0.025*** (0.001)
Controls	none	age	size	sales growth	cash holdings over total asset	ROA	age, size, sales growth, cash holdings over total assets, ROA
Observations	4,409,819	4,404,870	4,409,819	4,409,819	4,269,554	4,408,432	4,263,327
R-squared	0.298	0.299	0.299	0.304	0.307	0.301	0.317
Firm FE	YES	YES	YES	YES	YES	YES	YES
Country * Sector * Year FE	YES	YES	YES	YES	YES	YES	YES

Note: The dependent variable is the ratio between total investments a time *t* and total capital at *t-1*; "debt to total assets" is the ratio between total financial debts and total assets of firm *i* at *t-1*; "interest coverage ratio" is the ratio between profits and interest expenses of firm *i* at *t-1*. Controls: log age at *t*, log of size in *t-1*, cash holdings over total assets and ROA at *t-1*, and sales growth at time *t*. Firm fixed effects and country by sector by time dummies, as well as a constant, are included. Standard errors clustered at the firm level.

Source: OECD calculations based on Orbis® data.

**Table A.3. Firms experiencing an increase in leverage in the aftermath of the GFC decreased their investment, and especially so if highly indebted at the beginning of the crisis**

	Dependent Variable: Change in the investment ratio		
	(1)	(2)	(3)
Pre-crisis financial leverage levels		-0.1251*** (0.0080)	-0.2091*** (0.0080)
Change in financial leverage	-0.0490*** (0.0066)	0.0298*** (0.0105)	0.0648*** (0.0111)
Pre-crisis leverage levels * Change in leverage		-0.4663*** (0.0325)	-0.4882*** (0.0310)
Change in interest coverage ratio	0.0001*** (0.0000)	0.0001*** (0.0000)	0.0001*** (0.0000)
Observations	111,753	111,753	100,948
R-squared	0.0885	0.0944	0.1164
Control variables	YES	YES	YES
Country * Sector FE	YES	YES	YES

Note: The dependent variable is the difference between the average of the yearly post-crisis (2008-2013) and the average of the yearly pre-crisis (2002-2007) investment ratio; the investment ratio is defined as the ratio between total investments a time *t* and total capital at *t-1*. The main explanatory variables are the difference between the post- and the pre-crisis average financial leverage ratios, the difference between the post- and the pre-crisis average interest coverage ratios and the pre-crisis levels (the average in model 2 and the 2007 value in model 3) of financial leverage. "Financial leverage" is the ratio between total financial debts and total assets of firm; the "interest coverage ratio" is the ratio between profits and interest expenses. Controls included are: the pre-crisis age level, the change in size, the change in the holdings over total assets ratio and in the ROA, as well as the change in sales growth; all changes are computed as the difference between the post- and the pre-crisis yearly averages. Country by sector fixed effects, as well as a constant, are included. In parentheses, standard errors clustered at the country-sector level.

Source: OECD calculations based on Orbis® data.

## Annex B. Alternative accounting framework

As for the baseline framework outlined in the text, the model assumes that the last available data for each firm (end of 2018) represent its financial situation in normal times and obtains firms' profits during the COVID-19 outbreak according to Equation 1. At this point, rather than using Equation 2 to compute the hypothetical new value of equity based on the decline in profits, it attempts to model explicitly the evolution of both assets and liabilities. More specifically:

- *Assets side.* We assume that firms are forced to sell assets and/or use their cash buffers to cover losses induced by the pandemic when they experience negative profits, while “Covid Total Assets” are unchanged for firms still displaying positive profits. Analytically:

$$CovidAssets_i = NormalTimeAssets + CovidProfits_i \text{ if } CovidProfits_i < 0 \quad (6)$$

$$CovidAssets_i = NormalTimeAssets \text{ if } CovidProfits_i \geq 0$$

- *Liabilities side.* We assume that firms are able to only partially repay their current liabilities during confinement months and hence are modelled to raise new debt to cover a share of current liabilities proportional to the length of confinement measures and the size of the sectoral confinement shock. Analytically:

$$CovidLiabilities_i = NormalTimeLiabilities + \left[ \left( \frac{CurrentLiabilities}{N} \right) * Shock \right] \quad (7)$$

where N is equal to six (four) in the upside (downside) scenario. In other words, if the confinement lasted two (three) months as in the upside (downside) scenario, firms total liabilities are expected to increase by one sixth (one fourth) of their current liabilities, weighted by the size of the shock.

Table B.1 reports the main results obtained using the above alternative accounting framework and shows that findings are consistent with the baseline model.

Table B.1. Percentage of distressed firms, alternative model

Percentage of distressed firms, alternative model				Difference between baseline and alternative model in the percentage of distressed firms (p.p.)	
		Upside	Downside	Upside	Downside
<b>Overall</b>	Whole economy	6.7%	9.8%	0.6	-0.7
<b>By Sector</b>	Professional serv.	0.8%	1.2%	0.0	-0.3
	Info&Communication	0.8%	1.2%	0.0	-0.2
	Construction	3.1%	4.9%	-0.2	-1.1
	Real estate	5.0%	7.5%	-0.7	-2.1
	Wholesale&Retail Trade	5.9%	9.0%	0.4	-1.0
	Manufacturing	6.0%	9.0%	-0.6	-2.2
	Administrative serv.	7.0%	10.0%	0.3	-1.0
	Other services	9.4%	13.5%	2.2	0.8
	Transportation	14.0%	20.0%	2.2	0.3
	Arts&Entertainment	17.4%	23.3%	2.3	0.4
Accommodation&Food	20.4%	27.4%	6.0	4.1	
<b>By Size</b>	Micro	6.7%	9.8%	0.6	-0.7
	Small	7.0%	10.2%	0.7	-0.6
	Medium	5.6%	8.0%	0.4	-0.7
	Large	5.7%	8.6%	0.5	-0.8
<b>By Age</b>	Young	16.5%	22.1%	2.5	0.7
	Mature	9.0%	13.2%	1.1	-0.6
	Old	4.0%	6.2%	0.1	-1.0
<b>By Productivity</b>	Low	8.3%	11.7%	0.2	-1.3
	Med-Low	7.6%	11.1%	0.7	-0.8
	Med-High	6.6%	9.7%	0.7	-0.6
	High	4.5%	6.9%	0.9	0.0
<b>By Intangible Intensity</b>	Low	8.7%	12.4%	1.2	-0.2
	High	5.0%	7.6%	0.1	-1.1

Source: OECD calculations based on Orbis® data.

# On the measurement of disease prevalence<sup>1</sup>

Sotiris Georganas,<sup>2</sup> Alina Velias<sup>3</sup> and Sotiris Vadoros<sup>4</sup>

Date submitted: 12 February 2021; Date accepted: 13 February 2021

*For any infectious disease, including the Covid-19 pandemic, timely, accurate epidemic figures are necessary for informed policy. In the Covid-19 pandemic, mismeasurement can lead to tremendous waste, in health or economic output. "Random" testing is commonly used to estimate virus prevalence, reporting daily positivity rates. However, since testing is necessarily voluntary, all "random" tests done in the field suffer from selection bias. This bias, unlike standard polling biases, goes beyond demographical representativeness and cannot be corrected by oversampling (i.e. selecting people without symptoms to test). Using controlled, incentivized experiments on a sample of all ages, we show that people who feel symptoms are up to 42 times more likely to seek testing. The testing propensity bias leads to sizeable prevalence bias: even under costless testing, test positivity can inflate true prevalence fivefold. The inflation factor varies greatly across time and age groups, making intertemporal and between-nation comparisons misleading. We validate our results using the largest population surveillance studies of Covid-19 in England, and indeed find that the bias varies intertemporally from 4 to 23 times. We present calculations to debias positivity, but importantly, suggest a parsimonious approach to sampling the population that bypasses the bias altogether. Estimates are both real-time and consistently close to true values. Our results are relevant to any epidemic, besides Covid-19, where carriers have informative beliefs about their own status.*

1 We thank Andrew Atkeson, Rebecca Thornton, William Havage, Ichiro Kawachi, PJ Healy, and Roberto Weber for useful comments, Fay Angelidou for outstanding research support, and the Department of Economics, City University, for funding the experiments.

2 Associate Professor, City University.

3 Associate Professor, City University.

4 PhD candidate, City University.

Copyright: Sotiris Georganas, Alina Velias and Sotiris Vadoros

# 1 Introduction

How to measure prevalence for infectious diseases? In the Covid-19 pandemic, health agencies and lay citizens alike, closely watch two measures derived from daily testing, the absolute number of recorded cases and the percentage of positives in the tested population. These numbers influence individual decisions but also official measures against the pandemic, with a profound impact on public health and the economy.

In this paper we claim that such commonly used measures are fundamentally flawed, because they ignore the demand side for testing. In virtually all countries in the world, testing is voluntary, leading to *self-selection bias*. People are likelier to self-select into testing if they have reasons to believe they might be having Covid-19 (such as, e.g. if they have symptoms or if they are exposed to a high-risk environment). We experimentally show there is a substantial bias in testing, driven by self-selection and demonstrate how the testing bias translates into *biased prevalence estimates*. We then validate our results on how the accuracy of prevalence estimation is affected by the bias, using external data. Finally, we propose a novel, fast and relatively economical method to estimate prevalence in real time, using a combination of polling methods and characteristics of endogenously done virus testing.

Let us start with a simple illustration of the problem for both economic policy makers and health agencies, using a real example from a European country. During Christmas all shops and schools were closed. On January 18 2020 the government allowed elementary schools and the retail sector to open (for in-store buys). About a week later, recorded cases started to rise. On the 29th of January, 941 cases were recorded, almost double the cases a week before (506). Ignoring standard statistical questions of significance, two questions arise: is that rise in cases a clear sign of a worsening disease, and can we blame the retail sector or schools? Due to the selection bias, even the first question is hard to answer. At the same time as cases rose, testing rose too. The number of tests on 29 January was about double the amount of tests on the 22nd. Actually, *test positivity* is similar between these dates. But our self-selection argument implies that the number of tests is endogenous. Higher disease

prevalence leads to higher demand for testing. As we will demonstrate, the self-selection bias changes over time, making comparisons using test positivity data meaningless in many cases.

The self-selection bias is idiosyncratic and varies with age, which complicates answering the second question too, how to tell whether schools or shops are to blame. One would think to (and indeed, health agencies *do*) compare test positivity among school pupils and middle aged people who went shopping, to see what channel of infection was more important. But our experiments show that demand for testing differs strongly by age, and also, virus symptoms affect this demand differentially. This means we cannot compare positivity across age groups either.

The use of standard test positivity or the number of recorded cases, to compare prevalence over time or across age groups, is rarely advisable. In the paper we use incentivised controlled experiments to estimate the size of the testing bias and calculate the corresponding prevalence bias. Interestingly the bias is estimated to be drastically different by age groups (as mentioned above) and to also rely greatly on two important characteristics of the testing procedure: waiting times and cost.

Our testing bias estimates can be used to calculate the prevalence bias, and debias the current prevalence estimates in the field (as derived from test positivity). As long as the characteristics of the testing procedures are known by the health agencies and published (unfortunately, the former is rare and the latter is most often not the case), we sketch the parameter estimations necessary for debiasing. Given that we have estimates by age, simulations can be done for countries with different demographic structures too. Of course accurately estimating all necessary parameters presents challenges of its own.

To fix all the problems with measurement, we suggest a novel method to *bypass* the self-selection bias altogether, with an estimation procedure that is at the same time faster, more accurate and more feasible than current methods. The idea is to poll a representative sample about their symptoms, and get the symptoms-to-virus conversion parameters from



existing tests.<sup>1</sup>

To give an overview of the experimental results, we find that the commonly used “test positivity” measure may inflate actual prevalence by up to 5 times, even if testing is provided at zero cost. If Covid-19 tests are costly for the testee (as is common), this inflation factor or *prevalence bias* can be much higher. To make estimation harder, the prevalence bias is *not constant*, but rather depends strongly on actual prevalence. This means that we cannot apply a fixed adjustment to test positivity measures, and such measures cannot be used to compare prevalence across countries, as is commonly done. To validate our results, we compare prevalence estimates from the REACT and ONS studies in the UK, to test positivity ratios at the same dates (Riley et al., 2021). As predicted by our calculations, the prevalence bias is indeed positive, very large and time varying, ranging from 3.8 to 23.6 in the different waves of the study. To say it another way, our estimates of the testing bias and calculations of how this translates to a prevalence bias, explain why test positivity rates always seem to be too high.

To understand the relevance of these results, start by noting that suggested policy responses and their implementation (e.g. social distancing rules) will inevitably be inefficient if we are not aware of the real number of active cases, and in which areas and age groups these occur. Observing mortality rates or the number of hospitalisations and patients in ICU are not real time measurements; they only provide an estimate of how many people caught Covid-19 *weeks earlier* (and estimating the fatality rate is also challenging, Atkeson, 2020). This time lag is very important when trying to evaluate interventions. Without real time data, measuring the effect of a vaccine will take months, on top of the time the vaccine takes to have a medical effect. Understanding the full effect of other events on the disease, like the Christmas holidays (which led to more interaction and possibly higher transmission)

---

<sup>1</sup>Replacing mass testing with polling may sound unusual, but it is in line with suggestions of using statistical sampling to replace exhaustive counting, when the latter can be biased, as in a census. In the case of the pandemic, it has even been argued that symptoms-based diagnosis should be used instead of PCR testing (Cadejani et al., 2021), because it is more informative.

similarly takes months (see the influential cross country study on the effectiveness of pharmaceutical interventions (NPIs), which uses death counts, lagging by several weeks, Brauner et al., 2020). On the other hand, knowing the current number of actual cases, allows the design of optimal policy response, and also provides a forward-looking estimate of hospitalisations and mortality. Health systems get warning several weeks ahead, gaining invaluable time for necessary adjustments.

Community testing, often conducted in the high street and in neighbourhoods, is widely considered a useful tool to monitor incidence and trends. The ECDC, 2020 listed “[to] reliably monitor SARS-CoV-2 transmission rates and severity” among five objectives of testing. It also published weekly testing data and “positivity rates” by EU State (ECDC, 2021). However, as we have argued, such testing cannot provide accurate estimates of Covid-19 prevalence, and the main problem is not related to typical issues that arise in population sampling, such as sampling representative age groups (contrary to what some studies suggest (Pearce et al., 2020)). We find in our data that the self-selection bias increases non-linearly with waiting times and any other cost associated with testing. To make prevalence estimation harder, the bias is time-varying, and also depends non-linearly on time varying parameters. For example, when cases rise steeply, people might be more likely to want to test out of fear. This leads to longer queues for testing, longer waiting times and a disproportionately larger testing bias.

To summarise, using standard self-selection calculations and results from a large scale, incentivised and controlled experiment, we formulate three main hypotheses:

1. Test-positivity is always inflated due to self-selection
2. The inflation factor is time-varying
3. As virus prevalence in the population increases, so does the bias in its measurement (for reasonable prevalence ranges in the Covid-19 pandemic)

We validate our results comparing prevalence estimates from the REACT study in the UK, to official test positivity figures. Our two predictions are strongly confirmed and we

also find support for the hypothesis that the bias rises with prevalence.

Finally, we present an application of the testing bias to the much debated policy question of school openings. We show that the testing bias can explain why the young do not show up in simple case counts, while they are very likely getting infected (and possibly transmitting) more than older people.

The possibility that infection rates in the untested population can be different than in the tested subsample, has been raised (Manski and Molinari, 2021). The issue is treated as a purely econometric inference problem however, with no reference to self-selection. In a somewhat similar vein, (Greene et al., 2021) propose statistical nowcasting, but the accuracy of both these methods is not as high as polling and detection of trend reversals is not possible in real time.

Experimental methods with incentives have been used on virus testing before, in a seminal paper to measure demand for HIV testing (Thornton, 2008). However prevalence estimation was not the goal of that paper, and of course the diseases are different in several ways.

More generally, the existing literature does not offer much guidance on personal incentives to test on a large scale. Should people be averse to learning they are infected, as information avoidance models suggest (Golman et al., 2017), prevalence figures would be deflated due to symptomatic people testing less than non-symptomatic ones. If, however, people do not test unless they experience symptoms, as is a known case in medical literature (Oster et al., 2013), this would lead to inflated prevalence figures due to non-symptomatic people testing less frequently than symptomatic ones.

Why care about test positivity rates? These are currently widely used to evaluate the effect of the mass testing *within* a country (Mahase, 2020), to compare the effect of government policies *between* countries (Haug et al., 2020), to build arguments about which age or socio-demographic groups are most affected (Elimian et al., 2020), and generally as a “baseline against which the impact of subsequent relaxation of lockdown can be assessed” (p2, Riley et al., 2020). A biased prevalence estimate makes these comparisons at best uninformative

(Middelburg and Rosendaal, 2020) - a problem to which we offer a solution.

Our approach is also relevant for past research based on historical data. For example, major studies of policy measures to prevent spread of viral diseases rely on prevalence estimates affected by the same type of bias (Adda, 2016).

Some studies rely on death rates instead of test positivity to evaluate effect of the policies aimed to contain the pandemics (Dergiades et al., 2020). This measure does not circumvent the problem of incomparability. Deaths are affected by harvesting and specifics of the health system, so do not fit as a perfect proxy of prevalence for cross country comparisons. Likewise, the infection fatality rates (IFR) are also subject to the testing bias. Whilst researchers already raise concerns about methodological and econometric issues affecting IFR (Shen et al., 2021), the bias we find cannot be addressed by the measures they propose.

The rest of this paper is organised as follows. Section 2 presents calculations of the self-selection testing bias. Section 3 describes the experimental procedures to measure this bias. Section 4 presents the experimental results and their implications regarding the prevalence bias. Section 5 compares our debiasing solutions, partly with parameters derived from the experiments, to field data. Section 6 presents an application to a common policy problem, the evaluation of school openings, while Section 7 concludes.

## 2 Bias calculations

The aim of the calculations is to infer the percentage of sick people in the population from the “random” testing in the field figures, as released by Health Agencies worldwide. The problem is that testing is voluntary, which leads to selection bias. How large is this bias?

To start, some people believe they have symptoms, some do not: call them  $S(\text{ymptomatic})$  and  $H(\text{ealthy})$ . Note that the discussion below has to do with what people believe, not what they actually have. Also, we distinguish between people believing they have symptoms and those who do not, but the analysis readily extends to people having strong beliefs that they

might be carrying the virus and those who do not.

Let the frequency of people who believe they have symptoms be  $p_s$ , or just  $p$ , with  $(1-p)$  being the frequency of people who do not think they have symptoms.

Of each group, some percentage turns out having the virus. Let  $v_s$  be the virus prevalence for those who believe they have symptoms,  $v_h$  for those who do not.

Of each group, some percentage are willing to take the test (for a given waiting time to take the test). Assume this only depends on symptoms, but not on actually having the virus (this assumption is mostly innocuous, unless there is a very large number of people in hospital). Let then  $t_s$  be the percentage of people who believe they have symptoms who actually take the test, and  $t_h$  for those who do not.

True prevalence is then

$$\tau = p_s v_s + (1 - p_s) v_h \quad (1)$$

The sample prevalence, also called test positivity throughout the paper (i.e. the virus frequency in the sample population)  $\phi$ , however, is given by the positive rate in the sample (assuming that the test itself is perfect).

$$\pi = p_s t_s v_s + (1 - p_s) t_h v_h \quad (2)$$

Divided by the total sampling rate

$$m = p_s t_s + (1 - p_s) t_h \quad (3)$$

Note that if  $t_s = t_h = t$ , then  $\pi = t(p_s v_s + (1 - p_s) v_h)$  and  $\phi = t(p_s v_s + (1 - p_s) v_h) / t = p_s v_s + (1 - p_s) v_h = \tau$  which makes sense; if testing propensities are equal, there is no bias.

If on the other hand the testing propensities  $t$  are not the same, then the sample is selected leading to bias. Before we calculate the bias, express the propensities to test and be virus positive, for the people who believe they have symptoms, as a multiple of the propensities of those who do not:  $v_s = a v_h, t_s = b t_h$  vs  $v_s = a v_h, t_s = b t_h$ . Then, using these equations,

rewrite (1), (2) and (3).

$$\tau = p_s v_s + (1 - p_s) v_h = a p_s v_h + (1 - p_s) v_h = v_h (a p_s + 1 - p_s)$$

$$\pi = p_s t_s v_s + (1 - p_s) t_h v_h = a b p_s t_h v_h + (1 - p_s) t_h v_h = t_h v_h (a b p_s + 1 - p_s)$$

$$m = p_s t_s + (1 - p_s) t_h = b p_s t_h + (1 - p_s) t_h = t_h (b p_s + 1 - p_s)$$

Simplify the notation by writing  $p$  for  $p_s$  and calculate

$$\phi = \frac{\pi}{m} = \frac{t_h v_h (a b p + 1 - p)}{t_h (b p + 1 - p)} = \frac{v_h (a b p + 1 - p)}{(b p + 1 - p)}$$

Now, divide  $\frac{\phi}{\tau}$  which yields the bias in the estimates

$$\beta = \frac{a b p + 1 - p}{(a p + 1 - p)(b p + 1 - p)}$$

For example, suppose the true symptoms prevalence is 10%,  $p = 0.10$ . Then  $\beta = (0.1ab + 0.9)/(0.1a + 0.9)/(0.1b + 0.9)$ . Figure 1 illustrates the size of the prevalence bias for different values of  $a$  and  $b$ . For instance, if  $a = b = 20$ , street testing is overestimating the virus prevalence by about 5 times.

In order to debias the test positivity in the field, one simply has to deflate the field figures by the estimated  $\beta$ , as long as  $p$  is known. If it is not, calculations are available upon demand to get  $p$  from the data.

### 3 Experiment Design

To find the testing propensity parameters  $t_h$  and  $t_s$ , we design an incentivised experiment where we

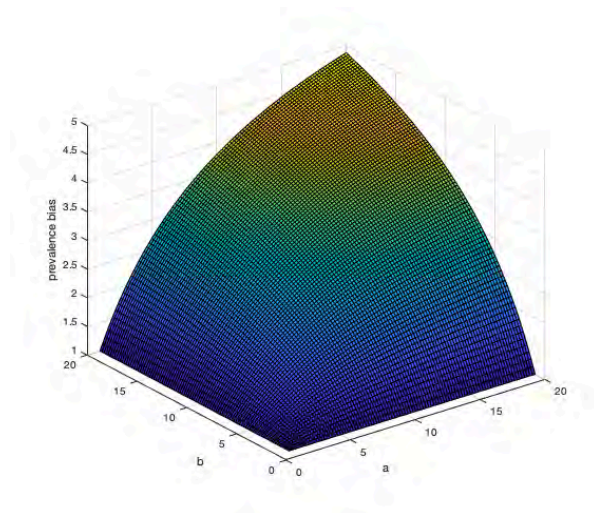


Figure 1: Bias in estimates for the true prevalence of 10%. (z-axis). X-axes:  $a$  (propensity-to-be virus positive ratio between those who have symptoms and not). Y-axis:  $b$  (propensity-to-test ratio between those who have symptoms and not).

1. Elicit hypothetical willingness to wait (WTW) to take a rapid test for Covid-19, conditional on (i) feeling healthy, (ii) having flu-like symptoms, (iii) having Covid-19 like symptoms.
2. Elicit real WTW to gain a voucher for a free rapid test for Covid-19.

### 3.1 Experiment data

Data collection took place over a week, from 11 till 18 December 2020. The majority of the responses were collected online, via the *QualtricsTX* platform. To enable greater representativeness of the sample, 94 responses (16%) from elder people (median age = 63) were collected using phone interviews. Out of 608 participants starting the online study, 24 (4.7%) dropped out mostly after the first few questions, 3 did not report age, resulting in the final sample of 575 observations. Median age for the sample was 39 years (median for Greece 45.6), and the age distribution is shown in the appendix.

Subjects were recruited from the database paignia.net and invited to participate in a study, answering a few question on behavior. Upon signing up for the experiment, they and signing a consent form, the participant was first asked about general and Covid-19-related health. We then elicited hypothetical willingness to wait (WTW) to take a rapid test for Covid-19, conditional on (i) feeling healthy, (ii) having flu-like symptoms, (iii) having Covid-19 like symptoms. For all three hypothetical scenarios, the test was being offered by the national health authority (EODY) while the participant was walking down the street (this is a procedure actually happening and discussed on popular media, so they should be well familiar with it). The hypothetical location of the participant was chosen to eliminate the (hypothetical) travel costs and reliability-related concerns. After eliciting the hypothetical WTW, we asked the subjects several control questions, including exposure to Covid-19 risky environments (e.g. taking public transport or working face-to-face with many people) and socio-demographics. After completing the compulsory part of the study, the participants were randomly allocated to one of the two treatments. In treatment *Test*, the participant would be offered a 1/30 chance lottery for a voucher for a home-administered Covid-19 test, worth €80 at the time of the study<sup>2</sup>. In the baseline treatment *Book*, the participant would be offered the same 1/30 chance lottery for a voucher for the local large-scale bookshop chain (“Public”), which we also set to €80 value, for comparability<sup>3</sup>. Crucially, the participant had to complete a real-effort task to enter the lottery, and we made it clear that the part was optional and would only need to do it if they wanted to enter the lottery for the prize. Participants were also reminded that they could stop the waiting task and leave at any moment.

All 575 participants completed the hypothetical elicitation and the control questions (left part of Figure 2).

As was partly expected, a substantial part of the sample (n=174) did not continue to the

---

<sup>2</sup>For both prizes, the delivery was guaranteed within next 36 hours.

<sup>3</sup>Evidence shows that people tend to value a high stakes lottery much higher than a certainty equivalent of its expected value (Kachelmeier and Shehata, 1992)



optional task. A major part of it ( $n=78$ ) was the elder people subsample. We are not very concerned that the inconvenience of the waiting task over the phone was the issue, since the participants came from the sample that had participated about a month ago in an unrelated study involving a real effort task over the phone. For  $n=38$  participants, a software glitch in Qualtrics, in the first five hours of the study resulted in missing recording of the treatment allocation, so we had to drop their data despite completion of the optional task.

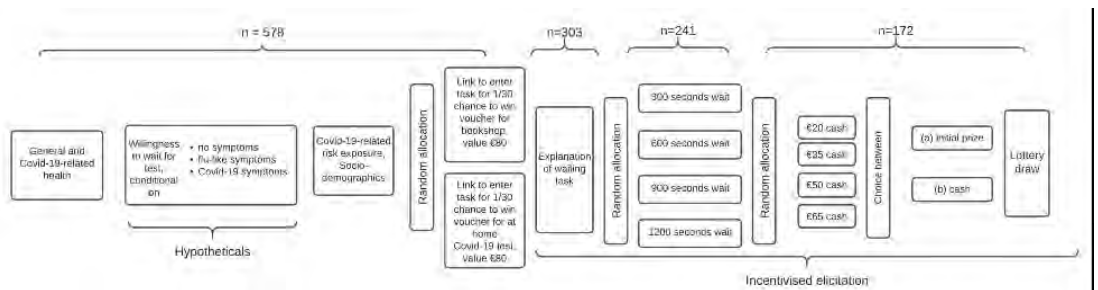


Figure 2: Experimental Flow.

The participants then read the description of the optional task. They learned that it involved waiting in front of their screen for some time (target) that would be revealed in the next screen, and the lottery draw for the prize would take place right after the wait. They also learned that to ensure that they are waiting, a button would appear at random times and they would need to press it within 4 seconds to avoid being disqualified. Among the 303 participants who read the description of the optional task, 241 continued to the next screen which revealed the waiting target. At this stage, they were randomly allocated to one of the four *Wait* target conditions {300, 600, 900, 1200} seconds. Upon learning the *Wait* time, further 59 participants dropped out instantly (median target time 900 seconds). Among the 241 waiting, 69 dropped out before completing the target (median *Wait* = 900 seconds). In total, 172 participants completed the waiting target (median *Wait* = 600 seconds).

Upon completing the waiting task, each participant was randomly allocated to one of the four *Cash* conditions, {€20, €35, €50, €65}. The participant was offered a choice to enter the lottery for: (a) the original prize (*Book, Test*), or (b) the displayed *Cash* amount. Out of the

172 participants, 112 chose to swap the original prize for the cash amount, whilst 60 chose to stay with the original prize (median cash value €35 for both). A total of 7 participants won the lottery.

## 4 Experiment Results and Prevalence Bias

### 4.1 Impact of self-selection on the bias in prevalence measurement

#### 4.1.1 Hypothetical

We find heterogeneity of waiting times between the age groups, driven by the self-assessed symptoms (Table 1). Younger people tend to behave similarly to elder people, while people between 30 and 50 are willing to wait the least time. This can be reconciled with the fact that this age group has the highest employments rates and possibly family obligations, leading most probably to the least available free time.

Age group	WTW— No Symptoms	WTW — Flu Symptoms	WTW — Covid-19 Symptoms	N
Under 30	0.156	0.391	0.641	192
30-50	0.094	0.279	0.558	222
50+	0.161	0.373	0.596	161

Table 1: Proportions of respondents reporting willingness to wait for a Covid-19 PCR test for over half an hour

Table 2 shows the testing bias, as calculated by the ratio of willingness to test between people with symptoms and those without. The figure ranges between 1.5 and 42, depending on the age group and waiting times. People under 30 with symptoms are 1.5 times more likely to test when there is no waiting time, compared to those without symptoms. This figure increases to 2.74 when there is a short wait of 5-15 minutes; 4.10 with a 15-30 minute wait; 11.67 with a 30-60 minute wait and 42 with a 1-2 hour wait. The ratio for 30-50 year-olds ranges between 1.50 for no wait and 17.33 for a 1-2 hour wait. For over 50-year-olds, the ratio ranges between 1.66 and 9.4. The symptom-conditional difference is significant at  $p < 0.01$ , see appendix for details.

Age group	No wait/ Immediate	5-15 min	15-30 min	30-60 min	1-2h	over 2h	N
Under 30	1.50	2.74	4.10	11.67	42.00	42+	192
30-50	1.50	3.29	5.91	9.57	17.33	17.333 +	222
50+	1.66	2.67	3.69	7.62	9.4	9.4 +	161
Total	1.54	2.91	4.46	9.43	15.67	15.67 +	575

Table 2: Bias (ratio of people with Covid-19 symptoms to people with no symptoms) by hypothetical waiting time for rapid test, N=575

The propensity to test bias, translates to a biased virus prevalence estimate  $\beta$ , according to the calculations in Section 2. The prevalence bias is also time varying, even with no changes in testing strategies. It depends, crucially, on symptom prevalence, which, given the exponential spread of Covid-19, can change drastically in a short period of time. This means that the estimate depends on symptom prevalence, but the bias itself also depends on it – so the bias is time variant.

#### 4.1.2 Incentivized Elicitation

Apart from waiting times, self-selecting into testing also depends on the cost associated with it (if applicable – costs can vary from time to monetary value, travel etc). We test whether the hypothetical willingness to wait to take a Covid-19 test correlates with the incentivized real waiting time for the 1/30 lottery and find a significant positive relationship between the two ( $p < 0.05$ ).

Also, we measure willingness to pay for the test (see Table 5 in the appendix). Of those who won a test voucher, 83.8% swapped it for cash, as opposed to 48.9% of those who won the book voucher, indicating that the majority of subjects would not be willing to pay to receive a test.

Note that there were too few people reporting no symptoms to be able to compare the willingness to pay of people with symptoms, to those without. The scope of this study is to measure and correct the bias for free tests subject to different waiting times, and further experiments are needed to explore the effect of other monetary and non-monetary costs.

## 4.2 Impact of the Bias on Prevalence Estimates - Calculations and Demographic Simulation

We have launched an online calculator that provides estimates on the testing bias (available at <http://georgana.net/sotiris/task/atten/covid.php>), as described in Section 2. The estimates on the testing bias depend on (a) the percentage of tests yielding positive results; (b) the percentage of the general population that reports symptoms; (c) the relative likelihood of having Covid-19 for those with symptoms compared to those without symptoms; and (d) how more likely are people with symptoms to self-select into testing than those without symptoms. According to our methodology, it is possible to calculate these figures and thus estimate the bias. Parameter (a) is provided by the results of community testing; (b) is provided by surveying; (c) can be obtained by asking people a simple question before testing them for Covid-19; and (d) is provided by surveying.

A simple example is the following: Assume community testing led to 10% positive results, and 5% of the population reported symptoms. Without waiting time, if those with symptoms are 5 times more likely to have the virus than those without symptoms, then the results of community testing exaggerate by 27.71%, and the true prevalence in the population is 7.83% (instead of the reported 10%). At a 30-60 minute waiting time, the bias increases to 106.95%, meaning that the true prevalence in the population is 4.83%.

To further illustrate our results, Figure 3 depicts our best estimate of the virus prevalence bias, i.e. the ratio between reported prevalence and actual, depending on symptoms prevalence and waiting time, for the three age groups.

Based on these estimates, we can simulate how different demographic structures would affect the prevalence bias. In Figure 4 we depict the results from 3 million draws from the plausible parameter space (we assume symptoms prevalence of 5%, and allow the testing bias parameter to vary uniformly within the 95% confidence interval gained from the experiments) applied to three countries, with different demographic structures: Nigeria (with one of the youngest populations globally), Italy (heavily ageing population) and the USA (between the

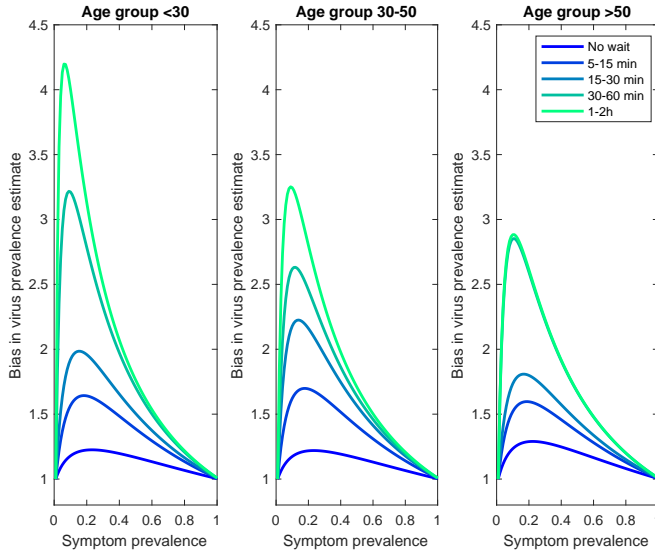


Figure 3: Best estimate of the virus prevalence bias: The ratio between reported prevalence and actual, depending on symptoms prevalence and waiting time, for the three age groups.

two extremes). The simulation shows that demography matters: a young country like Nigeria could have a substantially higher prevalence bias than Italy. However, it is also clear that the waiting times are more important than demographics. Lowering waiting times would result in a low bias for all countries.

## 5 Debiasing vs Polling for Prevalence Estimation: Validation using Existing Data

Debiasing the field prevalence numbers can be performed using our methodology, as long as there are good estimates for four parameters, namely (a) the percentage of tests in the field yielding positive results; (b) the percentage of the general population that reports symptoms;

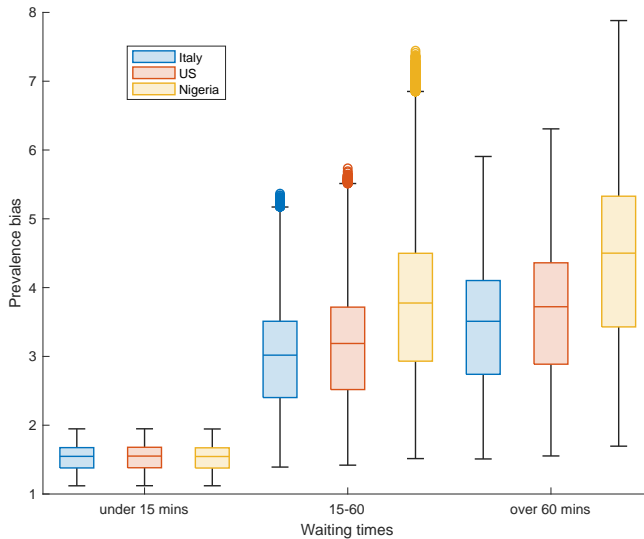


Figure 4: Simulation of the effect of different demographic structures on the prevalence bias.

(c) how more likely are people with symptoms to be carrying the virus than those without symptoms; and (d) how more likely are people with symptoms to self-select into testing than those without symptoms. Obtaining estimates for the above parameters is of varying difficulty: (a) is obtained in any country doing “random” street testing (it is important to keep track of important factors, such as waiting times though), (b) can be estimated with standard polling and (d) can be estimated with our experimental methodology. Estimating (c) would require asking subjects at testing stations to self-report their symptoms before testing.

We suggest however a novel, more economical and accurate alternative for prevalence estimation. The important parameter to estimate is the probability of having covid-19 conditional on having symptoms, and on not having symptoms, similar to parameter (c)

above. This can be done by asking a simple question at existing testing sites (indeed we have ongoing parallel work underway to obtain these estimates in cooperation with testing centres in the field). These parameters could be country-specific and time-variant, but we do not expect changes to be too fast. Obtaining a few estimates in each virus season could suffice, and this estimate could be used for many similar countries. The next step is unusual in the context of the pandemic: poll a representative sample regularly, *to obtain symptoms prevalence*. A common misunderstanding involves the argument that laymen cannot measure their symptoms properly. This is not a bug, but a feature of our procedure. Since the testing bias depends on self-reported symptoms, we need to condition on subjects *believing* they have symptoms, not on actually having them. Using both steps above can yield accurate prevalence estimates in real time at very low, comparatively, cost.

In the following we try simulate the novel polling method and compare to data that are as accurate as possible. That is, we need a benchmark figure to approximate true prevalence, derived by a study that does not suffer as much from the self selection bias. We use the REACT study in England (REACT, 2020) and the ONS Infection Survey, which are to our knowledge the two studies, that likely do not suffer from an inordinately high testing bias.<sup>4</sup> REACT is done on a large sample of all ages and locations, and importantly non response is relatively low<sup>5</sup>

REACT has been conducted in eight waves, to date. Two of the waves have been published in two sub-waves, yielding 10 different observations (we match the ONS data to these dates). The data consists of non-overlapping random samples of the population of England at lower-tier local authority level (LTLA, n=315) that were invited to take part in each

<sup>4</sup>Both studies are aiming to test large, representative samples at home. An important difference is that REACT sends testing kits to homes, and participants can choose to self-test and send back the results, while ONS sends health workers to test citizens at home. It is not clear without further research which method leads to a lower bias.

<sup>5</sup>The overall conversion rate from invitation letter to registration for a swab kit was 23.8% (1,474,824 registrations from 1,474,824 invitations sent), but this is not the main problem, because symptoms at this stage would not last for the duration of the study. Self-selection leading to bias can happen when people receive swabs and decide to test or not. The average proportion of swabs returned was 74.6% (1,100,270 swabs returned from 1,474,824 kits sent). There was some variation in response rates between rounds.

round of the study based on the National Health Service list of patients.

For those registering to take part, a swab kit was sent to a named individual with a request to provide a self-administered throat and nose swab (or for a parent/guardian to obtain the swab for children aged 12 years or younger). The participant was requested to refrigerate the sample and order a courier for same or next day pick-up and transporting to the laboratory for RT-PCR. There is no obligation to take the test at any stage of the process. Participants then completed an online questionnaire (or telephone interview) giving information on history of symptoms, health and lifestyle. The publicly available data includes the raw figures on tests and outcomes, as well as unweighted prevalence estimates and estimates weighted to be representative of the population of England as a whole.

Covid Economics 69, 18 February 2021: 109-139

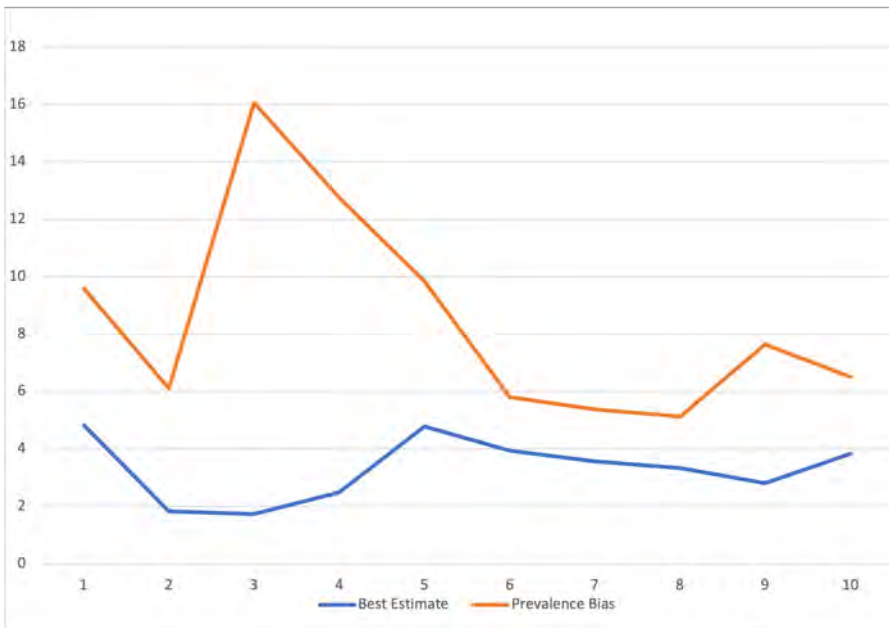


Figure 5: Estimate of the prevalence bias in field testing. Test positivity divided by the weighted prevalence from REACT.

We focus on the weighted prevalence figures, as the most accurate and take the simple average of the two surveys to get our best prevalence estimates. The number of daily tests is



publicly available, along with the number of tests being positive, yielding test positivity. We divide test positivity by the best prevalence estimate to obtain an estimate of the prevalence bias in field testing.

From our calculations and the experiment, three main hypotheses follow regarding the prevalence bias:

1. Test-positivity is always inflated due to self-selection, meaning the prevalence bias is large.
2. The prevalence bias is time-varying
3. As virus prevalence in the population increases, so does the bias in its measurement (for reasonable prevalence ranges in the covid-19 pandemic)

As presented in figure 5, in the 10 different subwaves of the study, the estimated prevalence bias indeed is positive, substantial, but also highly variable, ranging from 3.8 to 23.6, thus confirming our two main predictions. Apart from the first waves, during which the testing strategy was changing, complicating comparisons, it seems there is a weak effect for the bias to be rising in prevalence. A proper test of this hypothesis would require more waves and a constant testing strategy.

In the next graph we compare the best estimates of positivity with the two methods used currently to proxy prevalence, field positivity and case counts (as a percentage of the country's population), along with the our two new methods, the debiasing estimate and a simulation of the polling method.

We simulate the polling method by taking symptom conversion parameters, as published in REACT, but from the immediately preceding wave. The symptoms prevalence numbers we use are then from the current wave. As long as agencies can get a polling estimate that is similarly accurate to REACT, this simulation places a lower bound on the accuracy of the polling method.

We find that the polling method is consistently closest to “true prevalence”, while the debiasing estimate is further away and still inflates actual prevalence to some extent. As

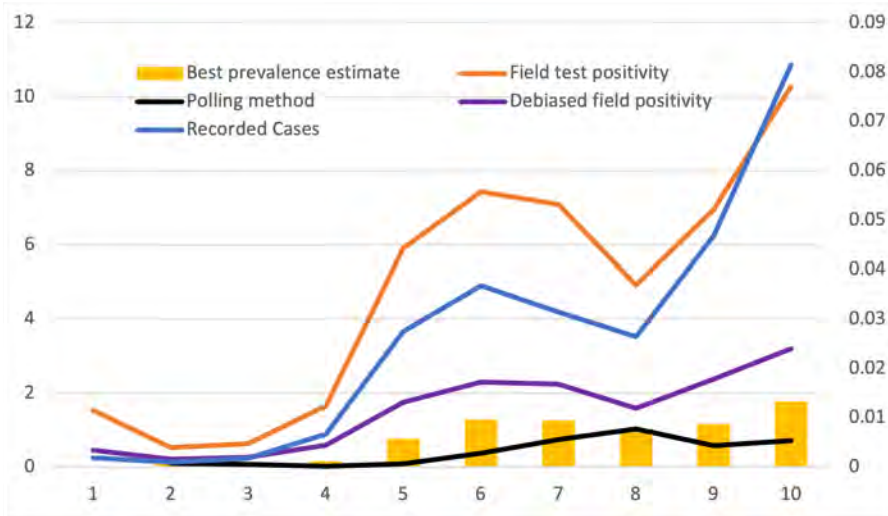


Figure 6: Comparison of the various prevalence estimates, in percentage of the UK population.

shown before, field positivity is an order of magnitude higher in most waves, while recorded cases are underestimating prevalence by at least an order of magnitude. Even assuming that cases sum up over several days to 10 times the daily rate, this estimate is still many times lower than estimated prevalence. Also note that all traditional methods are very variable, for example recorded cases increase almost fivefold when true prevalence doubles. Again, this is in line with our bias calculations.

A final note on the usefulness of the REACT and ONS methods: the marked difference between their prevalence estimates and common field test positivity, is driven by the fact that the monetary and non-monetary cost of testing happen are much lower in REACT and the ONS Infection Survey. Crucially, participants were able to administer the test and report symptoms without leaving the house. While this is a step in right direction, other significant non-monetary costs need to be mitigated in order to address self-selection bias. For example, for both studies, the physical unpleasantness of conducting the test may still make those not experiencing symptoms more likely to test. While it is possible to reduce other non-monetary costs of *testing*, we believe that making large-scale regular *self-reporting* of symptoms easy

would be a more effective step towards achieving accurate prevalence estimates.

## 6 Application: Do Open Schools Lead to Transmission?

Closed schools cause problems to working parents, besides hindering the education of young pupils who reportedly find it hard to follow remote teaching. Studies have not yet yielded a clear, conclusive answer regarding the epidemic cost of school opening though and the debate remains heated.

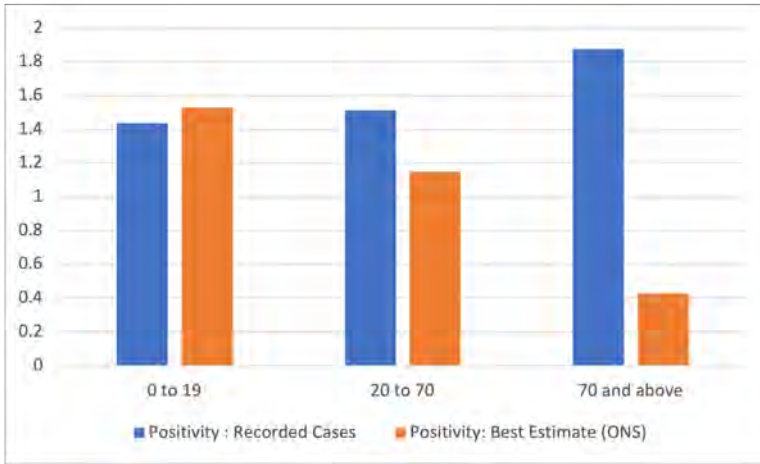


Figure 7: Recorded case positivity by age, vs best estimates.

Understanding the testing bias and how it varies by age group, allows us to reconcile the various pieces of evidence and solve existing puzzles. Looking at case counts, children and youngsters up to 19 years of age, seem not to be major carriers of the disease. Indeed, in a sample of 16 European countries for which data were available, children and teenagers up to 19 are always underrepresented among confirmed cases.<sup>6</sup> Authorities around the world have

<sup>6</sup>The sample includes Belgium, Czechia, Denmark, Estonia, Finland, France, Greece, Germany, Italy, Latvia, Netherlands, Norway, Portugal, Spain, Sweden, Ukraine. The largest percentage was found in Finland and Norway, above 15%, while the lowest were in France, Greece and Spain, at below 7%. For comparison,

used this as an argument that school opening is relatively harmless.

However, we know from our experiment that young people are much less likely to test. While absolute testing propensities are similar, they are very different between those with symptoms and those without. Combined with the fact that the young have a much lower symptoms prevalence (Qiu et al., 2020; Kelvin and Halperin, 2020), they test much less frequently.<sup>7</sup>

As a consequence of the testing bias, the young are underrepresented in testing, meaning their cases are underreported. Indeed, looking at the data from the ONS Infection Survey in the UK, high-school children seem to have the highest prevalence of all (see figure). This example illustrates the importance of the selection-bias: how it complicates comparisons of prevalence in different age groups and can lead to wrong, in this case missing, pandemic prevention interventions.

## 7 Discussion

Using an incentivised online experiment, we found that the probability of taking a Covid-19 test for those who have symptoms (or believe they are more likely to have caught the virus) is many times higher than those who do not. In our sample, this testing propensity bias ranged from 1.5 times (for people under 30 years with no waiting time) to 42 times (for people under 30 and a 2-hour waiting time). The bias becomes larger with longer waiting times, and any cost associated with taking the test. Testing stations cannot readily correct this by oversampling (i.e. selecting people without symptoms to test).

A person's age also influences the testing propensity bias, which means that different areas (or countries) will have different biases depending on the age composition. Furthermore, there have been reports of very long waiting times in some cases of community testing, which greatly exacerbates the bias and makes comparisons even within a country hard.

---

the population share of 0-19 year olds in a fairly typical country like Germany is 18.7%.

<sup>7</sup>Additionally, there seem to be reasons strictly related to the test itself that contribute to bias, due to the the under-detection of Covid-19 positivity in children, compared to that of adults (Dattner et al., 2020).

Lastly, even keeping everything else constant the bias depends strongly on the actual virus prevalence. All these effects combined mean the bias is very likely to be varying across space and time.

Our findings imply that virus positivity results from community testing sites are heavily biased. Contrary to conventional wisdom in the health policy community that suggested the bias would be, if anything, downward, our results suggest that prevalence is inflated by up to 5 times, even if tests are not costly.

We recognise the importance of giving people the opportunity to test, as this identifies positive cases, thus allowing them to self-isolate and stop spreading the disease. If the goal of street testing is just to allow random people to have a quick and free test, then this possibly meets its goal. Note, however, that random testing is not efficient, economically, or epidemiologically: subsidising tests specifically for populations with a high risk of getting infected and infecting others would probably save more lives at lower cost (say, tests for young people working in service industries and living with their parents). These questions remain open for future research.

What we have shown is that “random” voluntary testing is not really random. As such, it does not provide accurate information on disease prevalence, which is important to design and implement urgent policy responses to the pandemic, in terms of type, intensity and geographic area. Since voluntary testing is always biased, aggregate results on prevalence should be corrected. We have explained a method to do such debiasing. Note that debiasing can be useful to get better estimates of prevalence in real time, but also to correct the past time series that are used to estimate and calibrate many models related to the pandemic. The object of such studies ranges from the effectiveness of measures against the pandemic (Brauner et al., 2020; Hsiang et al., 2020), to health outcomes and economic effects. Furthermore, the probability to test is recognised as an important parameter in macroeconomic models evaluating economically optimal lockdown strategies (Alvarez et al., 2020),

Our methodology is not limited to correcting the results of community testing. We

showed that the number of confirmed cases reported daily is also biased, strongly downward in this case. People might not test because of costs, or the inconvenience of going to a testing site, or even due to being afraid of losing income. According to our results, more than 85% of the people who are not feeling any symptoms, would not wait more than 30 minutes (a likely time in many street testing procedures) to have a test, even if it is provided free of charge. For people feeling symptoms the estimated percentage of non-testers is still about 40%. These percentages rise even further when tests have a non-negligible cost to the citizen.

Using polling results from a representative sample can correct the error both in recorded cases and field test positivity. Our proposed method is more accurate than these traditional proxies. Moreover the polling method is not costly, and does not require an extraordinary testing capacity, which means it can be used daily, allowing real-time prevalence estimation in myriads of communities worldwide.

The REACT study in the UK (along with the ONS Survey) is an interesting special case of large-scale community testing on a nationally representative sample. The authors claim that this sample is truly random. While we use REACT data as the best estimate we have, our experimental results suggest the sample might still not be truly random. Even for people taking a free test at home (compare to the no waiting time condition in the experiment), a substantial testing bias exists. Importantly, REACT is also very expensive to run, while simultaneously less timely than our polling proposal. REACT has been done monthly or less often, while our procedure can be run daily.

This paper also contributes to the literature on testing regimens (Mina et al., 2020). Mass testing, extending to a very large part of the population, is useful as it can provide more accurate figures, and also identifies positive cases. It has been used, among others, in Liverpool, Slovakia and South Korea (Pavelka et al., 2020; BBC, 2020; Bloomberg, 2020; Brauner et al., 2020). However, mass testing is extremely expensive, and might be infeasible, especially at frequent intervals, due to capacity and technical constraints.

In the absence of mass testing, obtaining unbiased prevalence estimates is of paramount

importance for health and the economy. Underestimating disease prevalence can trigger inadequate measures and further spread of disease, while overestimating can be detrimental to economic activity. We thus urge policy makers to redesign “random” testing as a matter of priority in the effort to tackle the pandemic.

As a final note, our methodology is applicable to the prevalence measurement of any epidemic, when carriers have informative private information about their health status. Fighting disease is hard, even without the added complication of not knowing the location and magnitude of the fight. Our work offers tools to measure prevalence in real time. Further work is needed, to estimate specific selection-bias parameters for every disease, as they are necessarily related to the health burden and life expectancy reduction caused by the specific pathogen.

## References

- Adda, J. (2016). Economic activity and the spread of viral diseases: Evidence from high frequency data. *The Quarterly Journal of Economics*, 131(2):891–941.
- Alvarez, F. E., Argente, D., and Lippi, F. (2020). A simple planning problem for Covid-19 lockdown. *Covid Economics*, 4.
- Atkeson, A. (2020). How deadly is COVID-19? Understanding the difficulties with estimation of its fatality rate. Technical report, National Bureau of Economic Research.
- BBC (2020). Covid: Mass testing in Liverpool sees ‘remarkable decline’ in cases. Available at: <https://www.bbc.com/news/uk-england-merseyside-55044488> accessed 19 december 2020.
- Bloomberg (2020). Seoul’s full cafes, apple store lines and show mass testing success. Available at: <https://www.bloomberg.com/news/articles/2020-04-18/seoul-s-full-cafes-apple-store-lines-show-mass-testing-success> accessed 19 december 2020.
- Brauner, J. M., Mindermann, S., Sharma, M., Johnston, D., Salvatier, J., Gavenčiak, T., Stephenson, A. B., Leech, G., Altman, G., Mikulik, V., Norman, A. J., Monrad, J. T., Besiroglu, T., Ge, H., Hartwick, M. A., Teh, Y. W., Chindelevitch, L., Gal, Y., and Kulveit, J. (2020). Inferring the effectiveness of government interventions against COVID-19. *Science*.
- Cadegiani, F. A., McCoy, J. A., Wambier, C. G., and Goren, A. (2021). Clinical diagnosis of COVID-19: A prompt, feasible, and sensitive diagnostic tool for COVID-19 based on a 1,757-patient cohort (The AndroCoV Clinical Scoring for COVID-19 diagnosis). *medRxiv*, pages 2020–12.

- Dattner, I., Goldberg, Y., Katriel, G., Yaari, R., Gal, N., Miron, Y., Ziv, A., Hamo, Y., and Huppert, A. (2020). The role of children in the spread of COVID-19: Using household data from Bnei Brak, Israel, to estimate the relative susceptibility and infectivity of children. *medRxiv*.
- Dergiades, T., Milas, C., and Panagiotidis, T. (2020). Effectiveness of government policies in response to the COVID-19 outbreak. *Available at SSRN 3602004*.
- ECDC (2020). Covid-19 testing strategies and objectives. Technical report, Available at: <https://www.ecdc.europa.eu/sites/default/files/documents/TestingStrategy-Objective-Sept-2020.pdf>.
- ECDC (2021). Data on testing for Covid-19 by week and country. Technical report, Available at: <https://www.ecdc.europa.eu/en/publications-data/covid-19-testing>.
- Elimian, K. O., Ochu, C. L., Ebhodaghe, B., Myles, P., Crawford, E. E., Igumbor, E., Ukponu, W., Olayinka, A., Aruna, O., Dan-Nwafor, C., et al. (2020). Patient characteristics associated with COVID-19 positivity and fatality in Nigeria: Retrospective cohort study. *BMJ open*, 10(12):e044079.
- Golman, R., Hagmann, D., and Loewenstein, G. (2017). Information avoidance. *Journal of Economic Literature*, 55(1):96–135.
- Greene, S. K., McGough, S. F., Culp, G. M., Graf, L. E., Lipsitch, M., Menzies, N. A., and Kahn, R. (2021). Nowcasting for real-time COVID-19 tracking in New York City: An evaluation using reportable disease data from early in the pandemic. *JMIR Public Health and Surveillance*, 7(1):e25538.
- Haug, N., Geyrhofer, L., Londei, A., Dervic, E., Desvars-Larrive, A., Loreto, V., Pinior, B., Thurner, S., and Klimek, P. (2020). Ranking the effectiveness of worldwide COVID-19 government interventions. *Nature Human Behaviour*, 4(12):1303–1312.
- Hsiang, S., Allen, D., Annan-Phan, S., Bell, K., Bolliger, I., Chong, T., Druckenmiller, H., Huang, L. Y., Hultgren, A., Krasovich, E., et al. (2020). The effect of large-scale anti-contagion policies on the COVID-19 pandemic. *Nature*, 584(7820):262–267.
- Kachelmeier, S. J. and Shehata, M. (1992). Examining risk preferences under high monetary incentives: Experimental evidence from the People's Republic of China. *The American Economic Review*, pages 1120–1141.
- Kelvin, A. A. and Halperin, S. (2020). Covid-19 in children: the link in the transmission chain. *The Lancet Infectious Diseases*, 20(6):633–634.
- Mahase, E. (2020). Covid-19: Mass testing in Slovakia may have helped cut infections.
- Manski, C. F. and Molinari, F. (2021). Estimating the COVID-19 infection rate: Anatomy of an inference problem. *Journal of Econometrics*, 220(1):181–192.
- Middelburg, R. A. and Rosendaal, F. R. (2020). Covid-19: How to make between-country comparisons. *International Journal of Infectious Diseases*, 96:477–481.
- Mina, M. J., Parker, R., and Larremore, D. B. (2020). Rethinking Covid-19 test sensitivity — a strategy for containment. *New England Journal of Medicine*, 383(22):e120.



- Oster, E., Shoulson, I., and Dorsey, E. (2013). Optimal expectations and limited medical testing: Evidence from Huntington disease. *American Economic Review*, 103(2):804–30.
- Pavelka, M., van Zandvoort, K., Abbott, S., Sherratt, K., Majdan, M., Jarcuska, P., Krajci, M., Flasche, S., Funk, S., working group, C. C.-., et al. (2020). The effectiveness of population-wide, rapid antigen test based screening in reducing SARS-CoV-2 infection prevalence in Slovakia. *medRxiv*.
- Pearce, N., Vandenbroucke, J. P., VanderWeele, T. J., and Greenland, S. (2020). Accurate statistics on COVID-19 are essential for policy guidance and decisions.
- Qiu, H., Wu, J., Hong, L., Luo, Y., Song, Q., and Chen, D. (2020). Clinical and epidemiological features of 36 children with coronavirus disease 2019 (COVID-19) in Zhejiang, China: an observational cohort study. *The Lancet Infectious Diseases*, 20(6):689–696.
- REACT (2020). React-1: Summary of sample extraction and fieldwork dates, and response rates, by round. Technical report. Retrieved on 2021-01-30.
- Riley, S., Ainslie, K. E., Eales, O., Jeffrey, B., Walters, C. E., Atchison, C. J., Diggle, P. J., Ashby, D., Donnelly, C. A., Cooke, G., et al. (2020). Community prevalence of SARS-CoV-2 virus in England during may 2020: React study. *medRxiv*.
- Riley, S., Ainslie, K. E., Eales, O., Walters, C. E., Wang, H., Atchinson, C., Fronterre, C., Diggle, P. J., Ashby, D., Donnelly, C. A., et al. (2021). React-1 round 8 interim report: SARS-CoV-2 prevalence during the initial stages of the third national lockdown in England. *medRxiv*.
- Shen, C., VanGennep, D., Siegenfeld, A. F., and Bar-Yam, Y. (2021). Unraveling the flaws of estimates of the infection fatality rate for COVID-19. *Journal of Travel Medicine*.
- Thornton, R. L. (2008). The demand for, and impact of, learning HIV status. *American Economic Review*, 98(5):1829–63.

## Appendix A. Supplementary Figures

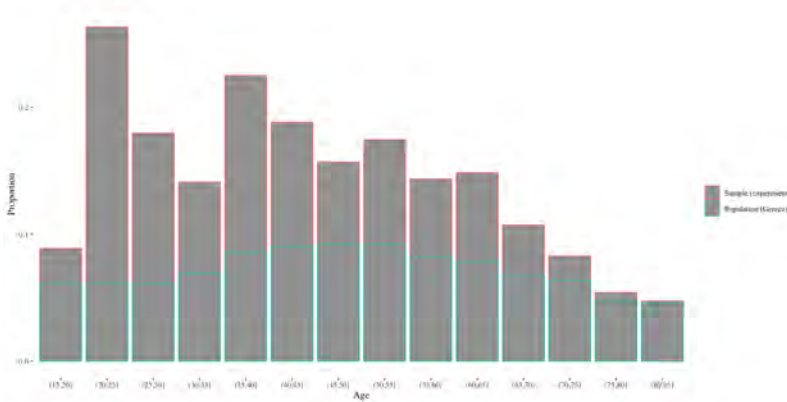


Figure 8: Age distribution in the experiment (n=578) and in population of Greece (source: populationpyramid.net).

## Appendix B. Descriptive Statistics and Hazard Models for the Experiment

	Mean	Std dev	min	max
Covid symptoms (0=no; 1=yes)	1.38	0.12	0	1
Age	40.404	15.302	18	84

Table 3: Summary statistics of sample demographics and symptoms.

Hypothetical willingness to test (N=575)		
	By symptoms	By waiting time
<b>No Symptoms</b>		
Mean (SD)	2.96 (1.48)	2.39 (2.04)
Median (Min, Max)	3.00 (1.00, 5.00)	2.00 (0, 8.00)
<b>Flu Symptoms</b>		
Mean (SD)	2.00 (1.20)	3.81 (2.26)
Median (Min, Max)	2.00 (1.00, 5.00)	4.00 (0, 8.00)
<b>Covid Symptoms</b>		
Mean (SD)	1.46 (0.951)	5.19 (2.35)
Median (Min, Max)	1.00 (1.00, 5.00)	5.00 (0, 8.00)

By-symptoms key: 1: certainly yes; 2: probably yes; 3: maybe; 4: probably no; 5: certainly no

By-wait-time key: : 0: would not wait at all; 1: would only take it if available immediately; 3: 5 - 15 minutes; 4: 15 - 30 minutes; 5: 30 - 45 minutes; 6: up to an hour; 7: 1 - 2 hours; 8 over 2 hours

Table 4: Summary statistics for hypothetical willingness to wait to take the test, by symptoms and waiting time.

Covid Economics 69, 18 February 2021: 109-139

Prize	Not entered	Dropped upon learning waiting time	Dropped after some wait	Swapped prize for cash	Kept prize	N
Book voucher	103	31	38	46	48	266
Test voucher	138	25	31	62	12	268
Bias	1,263	1,267	1,28	4,03	0,25	534

Table 5: Willingness to wait for a 1/30 chance of winning a prize. Number of subjects by level of task completion and incentive (rows 1-2), bias by incentive (row 3).

Table 6: Proportional hazard ratio for dropping out from (hypothetical) wait for a free Covid-19 test, by age group and symptoms.

<i>Dependent variable:</i>	
Odds of not waiting for Covid-19 test (Reference: Age 30-50  No symptoms)	
Under 30  No symptoms	-0.114 (0.099)
Under 30  Symptoms	-1.342*** (0.109)
30-50  Symptoms	-1.279*** (0.105)
50+  No symptoms	-0.107 (0.105)
50+  Symptoms	-1.403*** (0.119)
Observations	1,150
R <sup>2</sup>	0.264
Max. Possible R <sup>2</sup>	1.000
Log Likelihood	-6,177.707
Wald Test	351.360*** (df = 5)
LR Test	352.721*** (df = 5)
Score (Logrank) Test	388.121*** (df = 5)

*Note:*

\*p<0.1; \*\*p<0.05; \*\*\*p<0.01

# Social distancing policies and intersectoral spillovers: The case of Australia<sup>1</sup>

Mikhail Anufriev,<sup>2</sup> Andrea Giovannetti<sup>2</sup> and Valentyn Panchenko<sup>3</sup>

Date submitted: 11 February 2021; Date accepted: 12 February 2021

*The surge of the COVID-19 pandemic urged regulators all over the world to deploy measures aimed at rarefying social contacts to contain the spread of the pandemic, the so-called social distancing policies. Social distancing depresses employment and hinders economic activity. As shocks unevenly spill through the network of sectors, social distancing has unclear aggregate implications. We adopt a multi-sector model to explore the effect of social distancing in an economy characterized by sectoral spillovers. We focus on the Australian economy, due to the availability of granular data-sets on sectoral fluctuations and COVID-19 employment variations. We analyse two scenarios. First, we attribute the employment shock to a structural change in factor utilization and study the effect on GDP for varying temporal windows. We obtain a drop ranging between 6.6% (20-week lockdown) and 28% (1-year lockdown). Second, we evaluate the short-run effect of the observed employment shocks on sectoral value added growth. Several up-stream sectors are subject to larger losses in value added than predicated by the observed change in employment. In fact, for several of these sectors, employment change in the relevant period is actually positive. These results can be attributed to a compounded network effect.*

1 We thank Evgeniya Goryacheva for helping with this research and preliminary data work, and Jorge Miranda Pinto for providing his code. This research was supported by the Australian Research Council through Discovery Project DP170100429.

2 University of Technology Sydney, Business School, Department of Economics.

3 University of New South Wales, School of Economics.

Copyright: Mikhail Anufriev, Andrea Giovannetti and Valentyn Panchenko

# 1 Introduction

In response to the global surge of the COVID-19 pandemic governments around the world deployed a set of measures aimed at rarefying social contacts (i.e. “social distancing”) to prevent the spread of the pandemic within national borders<sup>1</sup>. The combination of the epidemic and associated policy responses triggered massive and sudden effects on employment in U.S. (Gupta *et al.*, 2020) as well as in Europe (Fana *et al.*, 2020). Sectors are inter-connected, and a result, sector-specific shocks can cluster and funnel through the wider economy generating sizeable aggregate effects (Acemoglu *et al.*, 2012). As such, the impact of localized shocks emerging from sector-specific social distancing regulations can spillover from that sector to other sectors through the economy’s production layer. In this paper we develop a model of an economy characterized by inter-connected sectors to answer the following question: what is the aggregate effect of social distancing policies in an economy characterized by sectoral spillovers? We use the Australian economy due to availability of detailed data-sets on sectoral fluctuations and COVID-related employment variations to study the economic implications of COVID-induced social distancing policies<sup>2</sup>

Sectors are interrelated through inputs from one sector to others (Barrot and Sauvagnat, 2016, Carvalho *et al.*, 2016). These are reflected in the input-output (IO) tables<sup>3</sup>. Figure 1 exemplifies this idea by representing the network constructed from the Australian IO table as compiled by the OECD for financial year 2015. In the picture, each node represents one of the  $n = 36$  sectors of the Australian economy. Each link points from the input-provider sector toward the input-receiver sector. Each node’s size is weighted by the relative size of the corresponding sector as supplier to other sectors, relative to the size of other sectors. A community-detection algorithm identifies five groups of densely inter-connected sectors<sup>4</sup>. Each group corresponds to a different color: energy sector, mining and oil extraction, together with construction and transportation (blue); agriculture and dairy product manufacturing; manufacturing industries and wholesale trade

<sup>1</sup>Brodeur *et al.* (2020) provides an excellent survey of the emerging literature on the economic consequences of COVID-19 and government response.

<sup>2</sup>In our analysis we don’t discuss the epidemiological merits of social distancing policies. However, it is important to remark that such measures have been proved very effective for containing the spread of the pandemic in Australia.

<sup>3</sup>Given an economy made of  $n$  sectors, an IO table gives, for each sector  $i$  and  $j$ , the amount of intermediate good produced by sector  $i$  that goes into the production of sector  $j$ . Any IO structure can be naturally represented as a network where sectors are the *nodes* connected by *links* representing the resource exchanges.

<sup>4</sup>Each community (i.e. a *partition*) is made of sectors that are densely connected with sectors belonging to the same community and sparsely connected with other communities, see Blondel *et al.* (2008) for details.

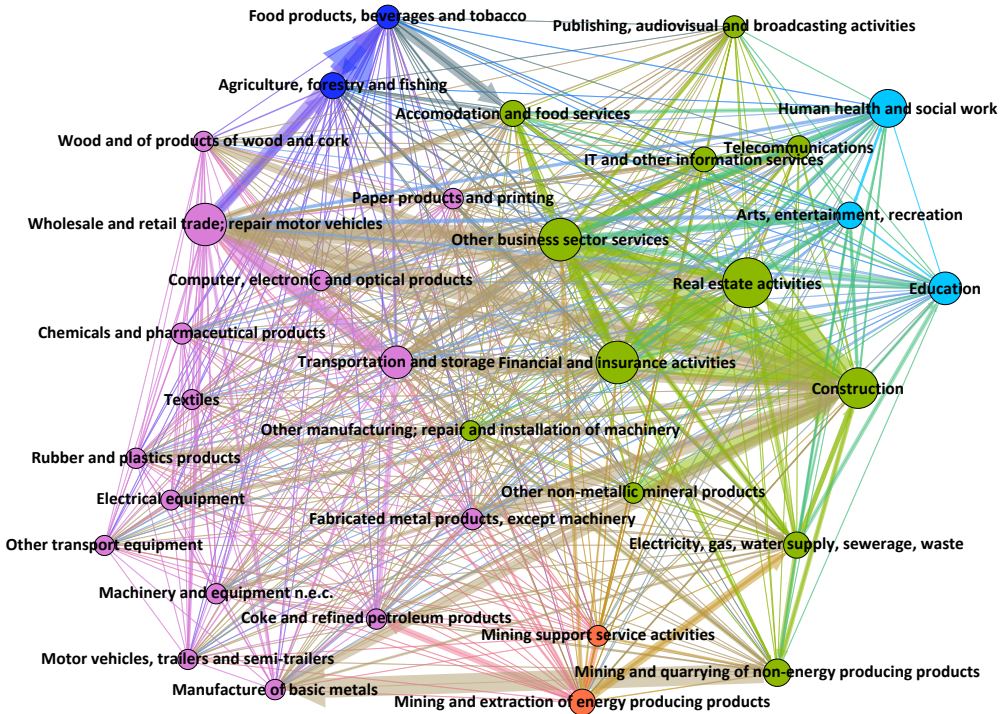


Figure 1: The Australian Production Network, flows in Australian Dollars (Source: Input by industry and final use category, OECD, fiscal year 2015).

(purple); finance (dark green) and services (light green). The highly interconnected nature of Australian economy offers a natural laboratory for empirically testing the relationship between production structure and sector-specific shocks.

We develop a static model of a multi-sectoral economy similar in many aspects to Acemoglu *et al.* (2012): sectors assemble one production factor, labor, and intermediate goods (materials). Intermediate goods can be either domestically consumed or used for the production of domestic intermediate goods. However, to better understand the effects of social distancing regulations, we relax the canonical assumption inherent to Cobb-Douglas technologies of production inputs being substitutes with degree one. This is crucial, as substitution of degree one represents a knife-edge case hardly observed in reality in which producers can perfectly deflect shocks by rearranging the input basket, thus mechanically moderating the potential extent of sectoral comovements (Carvalho *et al.*, 2016). As a major drawback, in the canonical Cobb-Douglas setting, intermediate input spending shares do not change in response to changes in input prices. In our set-up, we allow for broader profiles of elasticities of substitution by using a production technology

that features constant elasticity of substitution (Baqee and Farhi, 2020, Barrot and Sauvagnat, 2016, Carvalho *et al.*, 2016 and Miranda-Pinto, 2021), thus opening up an important amplification channel of sector-specific shocks due to social distancing regulations.

We make two contributions. First, we assess the relevance of the Australian inter-sectoral network on its domestic aggregate fluctuations for generic shocks. To do so, we calibrate the model's elasticity of substitution and the sectoral shock process to closely reproduce historical sectoral comovements<sup>5</sup>. This is made possible by the extensive data-set on output growth provided by Australian Bureau of Statistics (ABS) for  $n = 80$  sectors and the exceptional granularity of Australian input-output tables<sup>6</sup>, ranging between  $n = 110$  and  $n = 114$  sectors<sup>7</sup>.

We achieve the best match with an elasticity of substitution below 1, that is 0.9, indicating an input complementary that Cobb-Douglas formulation is not able to capture<sup>8</sup>. On these grounds, we design counter-factual experiments to quantify the role of network in determining aggregate GDP volatility along two dimensions: the degree of factors' substitution and the role of trade. Reassuringly, we find that our model performs the best in tracking observed volatility when a relatively high degree of substitution is interacted with the trade channel. Furthermore, the counter-factual analysis shows that the trade channel moderated the impact of sectoral shocks and therefore smoothed the economy's business cycle in at least two major downturns: in 2005 and between 2013-2014.

Geared with the calibration, we quantify the economic implications of the contemporaneous COVID-19 global pandemic. We feed our  $n = 114$  sectors model

<sup>5</sup>Following Foerster *et al.* (2011), we measure comovements in terms of the correlation structure of the sectoral output growth.

<sup>6</sup>The U.S Bureau of Economic Analysis Industry Account covers output growth only for  $n = 66$  domestic sectors. Outside U.S, the EU KLEMS database covers, for 30 European countries, the output growth of  $n = 28$  industries along 1970-2007.

<sup>7</sup>The finest level of disaggregation is given by the detailed benchmark input-output accounts, compiled every five years between 1972 and 2002 by the U.S Bureau of Economic Analysis ranging between  $n = 417$  and  $n = 529$  sectors, with most sectors (roughly) corresponding to four-digit SIC definitions. The second highest level, comparable to the U.S detailed IO, is given by the Canadian Input-Output tables. Most research on U.S economy uses the  $n = 66$  BEA tables (see, for example, Baqee and Farhi, 2020), whereas multi-country analyses rely on standardized data-sets such as the  $n = 54$  World Input-Output Database (see, for example, Barrot *et al.*, 2020), or the  $n = 36$  sectors OECD IO Tables ISIC Rev. 3 or 4 (see, for example, Miranda-Pinto, 2021).

<sup>8</sup>Some papers estimate a smaller elasticity of substitution. For example, Barrot *et al.* (2020) determine an elasticity of substitution between inputs of 0.5, whereas Atalay (2017) estimates an elasticity of substitution across intermediates and labor ranging between 0.4 and 0.8 and an elasticity of substitution across intermediates of 0.001. This can be in part attributed to the coarser structure of their IO tables relative to our own (respectively given by  $n = 30$  for Atalay (2017) and  $n = 56$  for Barrot *et al.* (2020), corresponding to sectors being less able to recombine input baskets and thus to deflect shocks.



with the exceptionally detailed administrative employment data released by ABS on monthly basis during the pandemic for  $n = 86$  sectors, and provide the first granular account of the early economic effects on the Australian economy of the social distancing regulations<sup>9</sup>. We perform two complementary exercises. In the first exercise, we attribute the employment shock to a long-run structural change in factor utilization and study the effect on GDP for varying temporal windows. We obtain a drop ranging between 6.6% (20 weeks of lockdown) and 28% (1 year of lockdown). When we set the window to 5 weeks of July level employment, on top of the 15 weeks of employment variation recorded since 15 of March, we obtain an overall yearly variation of real *GDP* equal to  $-7.4\%$ , very close to the  $-6.3\%$  variation recorded by ABS for the shorter span June 2019 - June 2020. Using a  $n = 33$  sectors economy from the OECD inter-country IO (ICIO) dataset, Bonadio *et al.* (2020) find an expected fall of Australia's GDP of 25%, which they further decompose in 13% domestic-induced shock and 12% foreign-induced shock. Our estimates are smaller relative to Bonadio *et al.* (2020), but may be more reliable since we are using actual employment rather than estimated effects on employment caused by social distancing measures. In the second exercise, similar to Barrot *et al.* (2020), we directly evaluate the short-run disaggregate effect of the employment shock on sectoral value added growth. Similar to Barrot *et al.* (2020), we find that a sizeable fraction of up-stream sectors are subject to larger losses in value added. This is particularly interesting as for several of these sectors, employment variation in the relevant period is actually positive. Therefore, the result can be attributed to a compounded network effect.

## 1.1 Literature Review

This paper relates to the literature on the propagation of shocks through the IO network, see Carvalho and Tahbaz-Salehi (2019) for a contemporary review. Most contributions exploit the Acemoglu *et al.* (2012) model, where the Cobb-Douglas characterization of both the production functions and preferences allows for a clear separation between the direction of supply-side (productivity) shocks and demand-side shocks (e.g., government expenditure). Acemoglu *et al.* (2016) showed that the supply-side shocks propagate downstream via price adjustments,

<sup>9</sup>Worldwide, sectoral employment data for the pandemic period is still scarce and aggregated (see Baqaee and Farhi, 2020 and Fana *et al.*, 2020), so that in absence of actual data, contributions rely on thought experiments. For example, Baqaee and Farhi (2020) apply a  $n = 66$  sector model with the May 2020 U.S BLS Economic News release, using demographic and survey data. An alternative approach (e.g., Barrot and Sauvagnat, 2016, Fana *et al.*, 2020, Bonadio *et al.*, 2020) is to estimate the reduction in workforce due to social distancing by interacting proxies on the flexibility to teleworking and administrative data on essential occupations.

whereas the demand-side shocks follow the opposite direction as affected industries adjust production levels. One of the consequences inherent to the use of Cobb-Douglas technologies is that an industry's expenditure on inputs as a fraction of its sales is invariant to the realization of the shock. Carvalho *et al.* (2016) and Miranda-Pinto (2021) addresses this limit by replacing the Cobb-Douglas with a more general CES technology. In this paper we also take the CES framework and show that the elasticity of substitution that better fit our data is smaller than 1. As a result, for productivity shocks the channel described above is paralleled by a further effect on production levels whose direction can be upstream.

There is now increasing interest on exploring the economic consequences of the COVID-19 pandemic. McKibbin and Fernando (2020) considers a global dynamic computational general equilibrium model with heterogeneous agents and heterogeneous elasticity for 6 macro-sectors and 24 countries including Australia. We look at more granular sectoral data and high frequency of contemporary unemployment data. Our paper is close to Barrot *et al.* (2020), who specifies a static IO model with  $n = 56$  sectors in the tradition of Long and Plosser (1983) and Carvalho *et al.* (2016), to decompose the impact of six weeks of social distancing regulations on French economy. They find that the combination of measures depresses GDP by 5.6%. Baqaee and Farhi (2020) take a general model with multiple sectors, factors, and IO linkages to study the effects of negative supply shocks and shocks to the composition of final demand on aggregate output. They show how nonlinearities associated with complementarities in consumption and production amplify the effect of negative supply shocks by creating supply bottlenecks and disrupting supply chain networks. Nonlinearities are strengthened when households switch the composition of their demand towards negatively shocked sectors directly and indirectly through their supply chains. They find that such nonlinearities may amplify the impact of the COVID-19 shock by between 10% – 100%.

Lastly, our paper is also linked to literature studying the effect of sectoral distortions from a IO perspective. For example, Bigio and Lao (2016) show that distortions manifest at the aggregate level via two channels: total factor productivity and the labor wedge. The strength of each channel jointly depends on the IO structure and the distribution of shocks. From a complementary angle, Liu (2018) studies economic effects of industrial policies targeting specific sectors, showing that economic interventions or wedges affecting upstream sectors (Liu, 2018) may bear disproportionate effects on the economy. While we do not explicitly consider wedges in this paper, in our break-down of the effect of social distancing rules we find abundant evidence that economic shocks – in our case, an exogenous and asymmetric fall in employment primarily hitting downstream

sectors – disproportionately affects the value added by upstream sectors.

The remainder of the paper is organized as follows. Section 2 presents the multi-sector economy. In Section 3 we operationalize in simulations the theoretical framework to quantify the effect of the network in propagating sector-specific shocks on the business cycle. Section 4 concludes.

## 2 Theoretical Framework

To investigate the network properties of the Australian economy we present a static multi-sector general equilibrium economy with constant elasticity of substitution (CES) production technologies. The model is similar to those developed in Carvalho *et al.* (2016) and Miranda-Pinto (2021).

The economy is populated by a representative consumer (i.e. a household) and  $n$  production sectors, indexed by  $j = 1, \dots, n$ , with  $j \in N$ . Goods are identical within a sector but differentiated across sectors.

**The Household.** A representative household owns all sectors of the economy. The household's preference for the goods produced by sectors are captured by a utility function  $U(\cdot)$  given by

$$U(c_1, \dots, c_n) = \prod_{i=1}^n c_i^{\beta_i}, \quad (1)$$

where  $c_i$  is the household's consumption of good  $i$ , and  $\beta_i \in (0, 1)$  weighs good  $i$ 's relevance in the household's utility. The household provides one unit of labor  $\ell$  inelastically. The budget constraint of the household is given by

$$\sum_{i=1}^n p_i c_i \leq w\ell + \pi. \quad (2)$$

In this formula, the left hand side is total expenditure, which we equivalently call  $C$  and it also corresponds to the nominal GDP of the economy. The right side is given by the wage income  $w\ell$  and total dividends from owning the firms,  $\pi$ . We assume there are no inter-sectoral frictions and as such wage is equalized across sectors. Labor is the only primary production factor of this economy.

**Firms.** Technology is symmetric across firms belonging to a sector, which is equivalent to assume the existence of a representative firm  $j$  for each sector  $j = 1, \dots, n$ . Any good  $j$  is produced by combining labor,  $\ell_j$ , and materials,  $M_j$ ,

by means of a constant elasticity of substitution (CES) technology with constant returns to scale. The output of sector  $j$  is given by

$$y_j = A_j \left[ (1 - \mu_j)^{\frac{1}{\sigma}} \ell_j^{\frac{\sigma-1}{\sigma}} + \mu_j^{\frac{1}{\sigma}} M_j^{\frac{\sigma-1}{\sigma}} \right]^{\frac{\sigma}{\sigma-1}}, \tag{3}$$

where  $A_j$  is the exogenous Hicks-neutral industry-specific productivity shock (i.e. the TFP),  $\mu_j$  is the share of materials used in the production and parameter  $\sigma$  denotes the degree of substitution between labor and the composite material. This is given by

$$M_j \equiv \left[ \sum_{i=1}^n \omega_{ij}^{\frac{1}{\eta}} x_{ij}^{\frac{\eta-1}{\eta}} \right]^{\frac{\eta}{\eta-1}}, \tag{4}$$

where  $x_{ij}$  is the amount of material produced by  $i$  and used by sector  $j$  for the production of material  $j$ ,  $\omega_{ij} \geq 0$  is a parameter reflecting the importance of output of sector  $i$  in the production of sector  $j$  and  $\eta$  is the elasticity of substitution between different intermediate goods. The CES formulation of the production technology is agnostic relative to the relationship between inputs' price and usage. It allows to consider the alternative cases in which production inputs are either substitutes (i.e. either  $\eta > 1$  or  $\sigma > 1$ , or both are larger than one) or complements (i.e. either  $\eta < 1$  or  $\sigma < 1$ , or both are smaller than one), as well as the knife-edge situation where  $\eta = \sigma = 1$ . In the latter case, (3) collapses into the Cobb-Douglas formulation commonly assumed in previous set-ups (see, for example, Acemoglu *et al.*, 2012, Acemoglu *et al.*, 2015, Bigio and Lao, 2016 or Foerster *et al.*, 2011).

**Input-output matrix.** We normalize the importance of various sectors in the production by setting  $\sum_{i=1}^n \omega_{ij} = 1$ . Let us define the  $n \times n$  matrix  $\mathbf{\Omega}$  that describes the *input-output structure* of the economy as<sup>10</sup>

$$\mathbf{\Omega} \equiv \begin{pmatrix} \omega_{11} & \dots & \omega_{1n} \\ \vdots & \ddots & \vdots \\ \omega_{n1} & \dots & \omega_{nn} \end{pmatrix}. \tag{5}$$

Each element  $\omega_{ij}$  represents the share of the total intermediate production of sector  $i$  that is used by sector  $j$ .  $\mathbf{\Omega}$  is the model's counter-part of Input-Output tables produced by statistical offices.

The output of industry  $j$  can be used either in the final consumption,  $c_j$ , or as an intermediate product for producer  $i \in N$ , defined as  $x_{ji}$ . Thus, for each firm

<sup>10</sup>Bold notation describes matrices and vectors;  $\mathbf{I}_n$  is the identity matrix of dimension  $n$ ,  $\mathbf{1}_n$  is the vector of  $n$  ones. For a generic vector  $\mathbf{x} \equiv \{x_i\}_{i=1}^n$ ,  $\mathbf{x}^a$  implies  $\{x_i^a\}_{i=1}^n$ , whereas  $\log \mathbf{x}$  is equivalent to  $\{\log x_i\}_{i=1}^n$ . The entry-wise multiplication is given by  $\circ$ .

$j \in N$  it holds that

$$y_j \geq c_j + \sum_{i=1}^n x_{ji}.$$

## 2.1 Equilibrium

Next, we define the competitive equilibrium of this economy.

**Definition 2.1** (Competitive Equilibrium). *A competitive equilibrium for the economy with  $n$  sectors is a vector of prices  $\mathbf{P} = [p_1, \dots, p_n]'$ , a wage  $w$ , a consumption vector  $\{c_i\}_{i=1}^n$  and a production bundle  $(\ell_j, \{x_{ij}\}_{i=1}^n, y_j)$ ,  $j = 1, \dots, n$  such that*

1. *The consumption vector  $\{c_i\}_{i=1}^n$  maximizes the representative consumer utility in (1) subject to*

$$\sum_{i=1}^n p_i c_i = w\ell + \pi, \tag{6}$$

where  $\pi = 0$ .

2. *For every producer  $j = 1, \dots, n$ , the bundle  $(\ell_j, \{x_{ij}\}_{i=1}^n, y_j)$  maximizes profits:*

$$\max_{\ell_j, \{x_{ij}\}_{i=1}^n} p_j y_j - \sum_{i=1}^n p_j x_{ij} - w\ell_j \tag{7}$$

where  $y_j$  is defined in (3).

3. *The wage  $w$  clears the labor markets*

$$\sum_{i=1}^n \ell_i = \ell, \tag{8}$$

4. *For every industry  $j$ , market clears*

$$y_j = c_j + \sum_{i=1}^n x_{ji}. \tag{9}$$

We can now introduce the core theoretical result of the paper, which we use to trace the relationship between sectoral shocks, prices, inputs usage and aggregate production<sup>11</sup>.

<sup>11</sup>For the proof, see the Online Appendix or, for a similar result, Jorgenson *et al.* (1987)

**Proposition 2.1** (GDP). *In the competitive equilibrium, under the assumption that  $\eta = \sigma \neq 1$ , the real gross domestic product (GDP) of the economy is given by*

$$\log GDP = \beta' \log \beta - \left( \frac{1}{1-\sigma} \right) \beta' \log [(\mathbb{I}_n - \mathbf{B}')^{-1} \mathbf{A}^{\sigma-1} \circ (\mathbf{1}_n - \boldsymbol{\mu})], \quad (10)$$

where

$$\mathbf{B} \equiv \mathbf{A}^{\sigma-1} \circ \boldsymbol{\mu} \circ \boldsymbol{\Omega}, \quad (11)$$

is the Allocation matrix of the economy.

The Allocation matrix  $\mathbf{B}$  in (11) is an  $n \times n$  matrix, endogenously dictating the allocation of inputs for each sector. The allocation is determined from the share of total intermediate production,  $\boldsymbol{\Omega}$ , as weighted for the share of intermediate usage  $\boldsymbol{\mu}$  and productivity shocks  $\mathbf{A}$ . We notice that the allocation matrix  $\mathbf{B}$  is fixed only in the knife-edge case of substitutability between inputs corresponding to  $\sigma = 1$ . In this case, producers are able to deflect shocks to the production structure by perfectly recombining the input bundle. We now introduce the second tool used in the empirical part of our paper.

**Lemma 2.1.** *Let the sales share of sector  $j$  be defined as  $s_j \equiv p_j y_j / C$ , it then holds that*

$$\mathbf{s} \equiv \mathbf{y} \circ \mathbf{P} = \beta' [\mathbf{I}_n - \boldsymbol{\phi}^{1-\sigma} \circ \mathbf{A}^{\sigma-1} \circ \boldsymbol{\Omega}' \circ \boldsymbol{\mu}]^{-1}, \quad (12)$$

where  $\boldsymbol{\phi}$  is the matrix of relative prices defined as

$$\boldsymbol{\Phi} \equiv \begin{pmatrix} 1 & \dots & \frac{p_1}{p_j} & \dots & \frac{p_1}{p_n} \\ \vdots & \dots & \dots & \dots & \vdots \\ \frac{p_n}{p_1} & \dots & \frac{p_n}{p_j} & \dots & 1 \end{pmatrix}. \quad (13)$$

in which any element  $p_i$  corresponds to the  $i$ -th element of vector  $\mathbf{P}$ , where

$$\mathbf{P} \equiv [\mathbb{I}_n - \mathbf{B}']^{-1} (\mathbf{A}^{\sigma-1} \circ (\mathbf{1}_n - \boldsymbol{\mu}))^{\frac{1}{1-\sigma}}. \quad (14)$$

From the definition of sale shares in (12), we notice that for any good  $i \in N$ , sales depends on relative prices for all goods in the economy  $j \in N$  as mediated by the elasticity of substitution  $\sigma$  and productivity shocks  $\mathbf{A}$ . Only in the knife-edge case of substitution corresponding to  $\sigma = 1$ , sale shares is fixed and equivalent to

$$\mathbf{s} = \beta' [\mathbb{I}_n - \boldsymbol{\Omega}' \circ \boldsymbol{\mu}]^{-1}, \quad (15)$$

which corresponds to the vector of equilibrium sales of Acemoglu *et al.* (2012) under the simplifying assumptions of uniform consumer preferences,  $\beta = \mathbf{1}_n \cdot 1/n$  and uniform shares of materials,  $\mu = \mathbf{1}_n \cdot \mu$ , with  $\mu > 0$ .

### 3 Quantitative Analysis

In this section we apply the model with the main goal of understanding the aggregate implications of sector-specific shocks. We will proceed in three directions. First, we will calibrate the model to match observed sectoral comovements and discuss the evolution of comovements relative to the change of the input-output structure. Secondly, we will look at the implications of input-output structure on translating sector-specific shocks into aggregate fluctuations. Third, we will use our model to understand the early economic implications of the contemporary COVID-19 pandemic.

#### 3.1 Calibration

We calibrate the parameters of the model to match our data.

**Preferences and production parameters.** We use the Input-Output tables issued by the Australian Bureau of Statistics to construct the counter-parts of the input-output structure  $\Omega_t$  as defined in (5), the vector of input weights  $\mu_t$  and preferences  $\beta_t$ , with the time period  $t$  coincident with fiscal year  $t$ . We focus on table “Use Table - Input by industry and final use category and imports by product group” as follows. The main item of the Use Table is given by a  $n \times n$  square table in which every entry  $(i, j)$  measures the dollar expenditure on the commodity  $i$  (both locally sourced and imported) of the corresponding row  $i$  by the industry  $j$  in the corresponding column  $j$ , that is  $p_i x_{ij} + imp_{ij}$ , where  $imp_{ij}$  is the value of the imported good  $i$  used in the production of industry  $j$ . Hence, in any given year  $t$  and for each commodity  $i, j \in N$ , the input-output structure element  $\omega_{ij}$  is given by the expenditure share<sup>12</sup>  $\omega_{ij} \equiv (p_i x_{ij} + imp_{ij}) / \sum_i (p_i x_{ij} + imp_{ij})$ .

**Treatment of Foreign Sector.** Our model is a closed economy, whereas input-output tables include a foreign sector. We will treat exports similarly to Bigio

<sup>12</sup>Models with Cobb-Douglas technology (see Acemoglu *et al.*, 2012 or Bigio and Lao, 2016) use dollar expenditures to calibrate elasticities of output. Given any good  $i$  and  $j$ , in equilibrium, the elasticity of input  $i$  for the production of output  $j$  is given by  $(p_i x_{ij} + imp_{ij}) / p_j y_j$  in Cobb-Douglas environments, where  $p_j y_j$  is provided in the Table under the label “Australian Production”.

and Lao (2016) and assume that domestic households consume intermediate exported and competing imported goods along with domestically produced goods. In other words, for each sector  $j \in N$ , we assume that  $\beta_j \equiv (p_j c_j + imp_j + exp_j)/(C + imp + exp)$ , where  $exp_j$  is the value of export of good  $j$ ,  $imp_j$  is the dollar value of competing imports,  $exp$  corresponds to  $\sum_{i=1}^n exp_i$  and  $imp$  corresponds to  $imp \equiv \sum_{i=1}^n imp_i$ . Lastly, we impose that for any sector  $j \in N$ , the incidence of materials in production corresponds to  $\mu_j \equiv \sum_{i=1}^n (p_i x_{ij} + imp_{ij})/(p_j y_j)$ . Whenever requested, we deflate consumption and production values for relevant years by using the consumer price index and producer price indexes, respectively<sup>13</sup>.

**Elasticity of Substitution.** In the following we follow the structure of Proposition 2.1 and assume that the elasticity of substitution  $\sigma$  regulates the degree of substitution between intermediate goods and labor and across intermediate goods (i.e.  $\sigma = \eta$ ). As such plays a critical role in simulations. Given the CES nature of the production structure,  $\sigma$  determines the degree to which producers in each sector can deflect shocks by rearranging input basket. In Section 3.2, we calibrate  $\sigma$  to minimize the mean square residual between observed and artificial sectoral growth.

**Shocks.** Our treatment of shocks is in the tradition of Horvath (2000) and aims at understanding whether the combined effect of sector-specific and common shocks can reproduce observed aggregate fluctuations through sectoral comovements. We will calibrate the productivity process to match the shock comovements of Horvath (2000). We assume that productivity follows a simple  $AR(1)$  innovation process given by

$$A_{j,T} = A_{j,T-1} e^{k_{j,T} + \kappa_T} . \quad (16)$$

for period  $T = 1, 2, \dots$  and sector  $j$ . In the baseline model, we impose that  $k$  is an identically and independently distributed random variable across time and sectors following a normal distribution with mean 0 and standard deviation  $s_{k,j}$ , whereas  $\kappa_T$ , has mean 0 and standard deviation  $s_\kappa$ . Following Horvath (2000), we assume a simple structure for shock variance. Namely, we impose that sector-specific volatility  $s_{k,j} \equiv s_k^s = 0.02$  for all service sectors and to  $s_{k,j} \equiv s_k^{ns} = 0.04$  for non-service sectors (Miranda-Pinto, 2021). As in Horvath (2000), we then add a small common-shock component with  $s_\kappa = 0.004$ .

<sup>13</sup>The final consumption component of the following sectors is available only for years 2014-2016: “Water, Pipeline and Other Transport” and “Postal and Courier Pick-up and Delivery Service”. We construct the missing observations by linear interpolation.



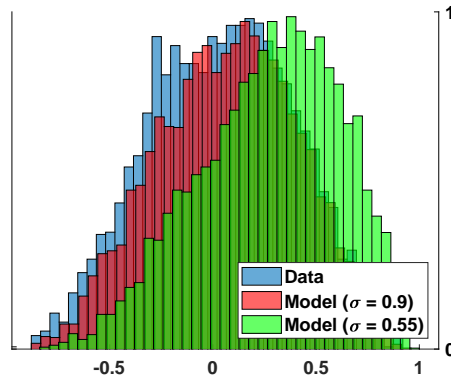


Figure 2: Correlation output growth across sectors. The blue histogram corresponds to Australian economy industry output growth correlations in chain volume measures. The red histogram corresponds to output growth correlations as generated by the simulated model with optimally calibrated elasticity of substitution  $\sigma = 0.9$ . The green histogram corresponds to output growth correlations of a discretionary elasticity of substitution  $\sigma = 0.55$ . Data source: Economic Activity Survey, ABS.

### 3.2 Matching Elasticity of Substitution and Comovements

We carry out two analyses relative to sectoral comovements. First, we fix the production structure  $\Omega_t$  to the most recent available structure,  $t = 2017$ , and calibrate the coefficient of substitution  $\sigma$  to maximize the model's capability to replicate observed sectoral comovements. This provides a first-pass measure of the shock conductivity of the Australian economy (Baqae and Farhi, 2020). Secondly, we let  $\Omega_t$  vary across the available years of observation  $t$  and use the calibrated model to measure the effect of the evolving production structure on sectoral comovements.

We measure sectoral comovements by means of pairwise correlations of sectoral output growth (Foerster *et al.*, 2011, Miranda-Pinto, 2021). We use the  $n = 80$  sectors data-set included in the Economic Activity Survey released by ABS on yearly basis along fiscal years 2007-2017. Formally, let the observed output growth rate of sector  $i$  be  $dy_{i,t} \equiv \log dy_{i,t} - \log dy_{i,t-1}$ . The pairwise correlation matrix  $\mathbf{R}$  with elements  $\rho_{ij} \equiv \text{corr}(dy_i, dy_j)$ , is constructed from series  $dy_{i,t}, dy_{j,t}$  for all available sectors  $i, j \in N$  across years  $t = 1998, \dots, 2017$ .

Given the set of time-varying parameters  $\{\Omega_t, \mu_t, \beta_t\}$  and given  $\sigma$ , we use 100 simulations, and for each  $t$  we simulate  $T = 1, \dots, 12$  periods of observations, with productivity shocks following (16). The equilibrium output growth rates are

defined as  $dy_{t,T} \equiv \log \mathbf{y}_{t,T} - \log \mathbf{y}_{t,T-1}$ , where

$$\mathbf{y}_{t,T} = \mathbf{s}_{t,T} - \mathbf{P}_{t,T},$$

in which  $\mathbf{P}_{t,T}$  and  $\mathbf{s}_{t,T}$  are defined in (12) and (14), respectively. Then, the pairwise correlation matrix  $\hat{\mathbf{R}}_t$  with generic element  $\hat{\rho}_{ij,t} = \text{corr}(dy_{i,t}, dy_{j,t})$ , is constructed from the time series  $dy_{i,t,T}, dy_{j,t,T}$  for all available sectors  $i, j \in N$  across simulation years  $T = 1, \dots, 11$  for a given configuration  $t$  and averaged across all  $m$  simulations. The optimal coefficient of substitution  $\sigma = \sigma^*$  is calibrated to match

$$\sigma^* \equiv \operatorname{argmin}_{\sigma} \left\{ \text{mse} \left( \mathbf{R}, \hat{\mathbf{R}}_t \right) \right\}, \quad (17)$$

where  $\text{mse}$  is the mean square error and  $t$  is set to  $t = 2017$ .

**Elasticity of Substitution.** We find that the optimal elasticity corresponds to  $\sigma^* = 0.9$ , smaller than the Cobb-Douglas case ( $\sigma = 1$ ). Barrot *et al.* (2020) determine an elasticity of substitution between inputs of 0.5, whereas Atalay (2017) estimates an elasticity of substitution across intermediates and labor ranging between 0.4 and 0.8. The difference with these papers can be in part attributed to the coarser structure of their IO tables relative to our own (respectively given by  $n = 30$  for Atalay (2017) and  $n = 56$  for Barrot *et al.*, 2020), corresponding to sectors being less able to recombine input baskets and thus to deflect shocks. Apart from the granularity of data, two reasons can drive elasticities of substitution below 1, thus signaling input complementarity. First, the above estimates assume homogeneous elasticities. By allowing for heterogeneous elasticities across sectors, Miranda-Pinto and Young (2020) obtain an average elasticity of substitution between intermediate and labor of 2.14. The motivation is that a common elasticity estimation weights sectors equally, but several large sectors appear to have large elasticities. The second driver is the short-term temporal horizon of elasticity estimation. In fact, the previous papers estimate elasticities with an horizon within one year. By using a 7-years horizon, Peter and Ruane (2018) find, for the Indian economy, an elasticity of substitution between materials in the range of 2.9 – 6.5. In their paper, there does not seem to be significant heterogeneity in elasticities of substitution between industries.

**Comovements.** We do the following exercises. First, we test the model's capability to replicate observed comovements and relate our calibration to extant result in the literature. In Figure 2 we plot historical sectoral comovements (blue histograms) measured across time span 2007-2017 against artificial comovements

	Data	1998	2001	2004	2005	2006	2007	2008
median	0.05	0.1361	0.1520	0.1498	0.1527	0.1463	0.1440	0.1576
$\sigma_{\text{corr}}$	0.35	0.3271	0.3242	0.3258	0.3253	0.3257	0.3257	0.3235
kurtosis	2.38	2.5338	2.5512	2.5509	2.5560	2.5522	2.5478	2.5596
		2009	2012	2013	2014	2015	2016	2017
median	-	0.1366	0.1380	0.1395	0.1380	0.1372	0.1423	0.1333
$\sigma_{\text{corr}}$	-	0.3260	0.3264	0.3275	0.3266	0.3267	0.3267	0.3283
kurtosis	-	2.5414	2.5329	2.5353	2.5409	2.5399	2.5368	2.5360

Table 1: Statistics of artificial versus observed output correlations.

generated from two alternative set-ups. In the first set-up (red histograms) we use the optimal coefficient of substitution  $\sigma = \sigma^* = 0.9$ . In the second one (green histograms) we use a value close to the calibration of Barrot *et al.* (2020) for an economy of  $n = 56$  sectors, with  $\sigma = 0.55$ . We can thus observe the qualitative effects of complementarity. From the figure, first, we notice that the optimally calibrated model is able to generate sectoral comovements in close fit with the observed ones. Second, by comparing the comovements obtained under optimal elasticity  $\sigma^*$  against the alternative level  $\sigma = 0.55$ , we see that higher substitution is key for generating the result. It is also interesting to notice that lower substitution between sectors induces a more prominent positive correlation between sectoral outputs, as we expect from economies where producers are less able to deflect volatility by substituting intermediate in the input basket. This observation is consistent with works studying the role of substitution relative to output comovements (see, for example, Horvath, 2000 and Miranda-Pinto, 2021), and shock propagation (Baqae and Farhi, 2020).

Next, we measure the implications of the evolving production network over sectoral comovements. We use the model characterized by  $\sigma = 0.9$  and compute artificial sectoral comovements for each of the input-output table produced by ABS. Results are collected in Table 1. While median correlations are stationary around 0.145, we notice that kurtosis and standard deviation of simulated comovements moved in opposite directions<sup>14</sup>, with a strong correlation of  $-0.84$ .

<sup>14</sup>We report a negative correlation of  $-0.30$  between standard deviation and the shape parameter  $\hat{\gamma}$  and a positive correlation of 0.19 between kurtosis and the shape parameter  $\hat{\gamma}$ . This shows that the growing pervasiveness of the largest input suppliers is associated to an increased sectoral output volatility and higher likelihood of extremal correlations.

### 3.3 Assessing the Impact of COVID-19

We can now use the model to understand how localized shocks compound into GDP fluctuations through the input-output structure. In response to the COVID-19 pandemic, the Australian government deployed a set of social distancing measures. The measures contributed to a strong exogenous shock to the employed workforce. In this section we apply our multi-sectoral model to measure the economic consequences of the shock. We design two exercises. In the first exercise, we attribute the employment shock to a long-run structural change in factor utilization. In other words, we assume that the shock induced by social distancing translates into a technological shift recombining the share of labor and capital in the production function. In the second exercise, we assume that the social distancing shock is fully captured by employment variation, as we would expect in short-run type of scenario. In this second exercise, we directly evaluate the disaggregated effects of the employment shock on sectoral value added growth.

A number of papers have explored various extrapolation methods to establish a bound on unemployment resulting from social distancing measures in multi-factor models<sup>15</sup>. For example, adopting the French economy as benchmark, Barrot *et al.* (2020) decompose the employment effects of social distancing in three components: law-enforced closings, closures of schools and confinement. The share of the total workforce affected by law-enforced closings stands at 10.9% and is concentrated in directly affected sectors: hotel and restaurants, arts and leisure, wholesale and retail, social work. The share of the total workforce affected by childcare caused by the closings of nurseries and schools stands at 13.2%. Lastly, they attribute an average of potential temporary job losses due to confinement equal to 32%, motivated by the heterogeneous degree of teleworking availability. The aggregate effects generates a 52% drop in the employed French workforce. Bonadio *et al.* (2020) compute the expected job losses using the classification of occupations and country-specific lockdown intensity.

In our paper, we take advantage of the high-frequency “Weekly Payroll Jobs and Wages in Australia report” issued by ABS starting in the awakening of COVID-19 crisis, where change in employment at  $n = 83$  ANZSIC industry subdivision level is updated on monthly basis. This supplies us with five months of employment data (from 15th of March, corresponding to the 100th case of COVID-19 recorded in Australia).

**Regulatory background.** Four classes of regulations have been adopted across

<sup>15</sup>Adolph *et al.* (2020) propose a comprehensive data-set on social distancing measures enforced in U.S at state level.

Australian states for varying extension of time<sup>16</sup>: sectoral shut downs, remote working, travel ban and school closure. Critical for our analysis, sectoral shut-downs aim to artificially freeze or drastically reduce sectoral activities by inhibiting face-to-face interaction<sup>17</sup>. For example, under shutdown, restaurants can operate only at reduced capacity or delivery. Indeed, sectoral shutdown has a drastic effect on employed workforce. Work from home regulations subdivided Australian businesses into “essential” and “non-essential” categories. Businesses and workforce belonging to “non-essential” categories have been incentivized to work from home whenever possible<sup>18</sup>. The set of social distancing measures exogenously depressed the workforce mass across the Australian economy. The reduction combines two effects: higher unemployment due to sectoral shutdown, and reduced worked hours affecting workers employed in non-essential businesses.

### 3.3.1 Calibration: Long-run effects on real GDP

To assess the long-run implications of social distancing regulations on real GDP, we consider ABS data for the last available IO structure, corresponding to a  $n = 114$  economy, and calibrate shock  $\mathbf{A}_t$  to  $\mathbf{A}_t^*$ , in order to match observed GDP and sectoral outputs. In other words,

$$\mathbf{A}_t^* \in \operatorname{argmin}_{\mathbf{A}} \left\{ \operatorname{mse} \left( \boldsymbol{\Theta}_t, \hat{\boldsymbol{\Theta}} \right) \right\}, \quad (18)$$

where  $t = 2017$ ,  $\boldsymbol{\Theta}_t \equiv \left[ \{p_{i,t}y_{i,t}\}_{i=1}^N, GDP_t \right]$  and  $\hat{\boldsymbol{\Theta}}$  is given by its artificial counterpart. More precisely, we let the model iterate for  $T = 1, 2, \dots$  periods. In every iteration, we compute equilibrium sectoral output (12) and GDP (10) and adjust the shock vector toward the direction which minimizes (18).<sup>19</sup>

We observe that the model calibrated on configuration for the last available fiscal year and  $\mathbf{A} = \mathbf{A}_t^*$  is able to endogenously generate expenditure on labor  $\ell_i$  that

<sup>16</sup>Australian borders were closed to all non-residents on 20 March 2020. Social distancing rules were imposed on 21 March, and state governments started to close ‘non-essential’ services. As of 27 October 2020, Australia has reported 27,541 cases, 25,055 recoveries, and 905 deaths.

<sup>17</sup>On 29th March 2020, public gatherings of more than two people have been banned. Sectoral shutdown was imposed to virtually all types of public establishments.

<sup>18</sup>A recent ABS survey found that during the acute phase of the pandemic, 46% of Australian workers are in work from home arrangements, whereas only 59.7% of persons aged 18 or above left home in the previous week for work (ABS, Household Impacts of COVID-19 Survey, 29 April - 4 May 2020). School closures forced the implementation of distance learning in universities as well as in schools for all parents working in “non-essential” job categories.

<sup>19</sup>Resulting gap between artificial  $GDP$  for  $t = 2017$  and observed  $GDP_{2017}$  is equal to 0.005. In terms of sectoral output, the chosen calibration is such that gap between artificial and observed data is under 80% for at least 50% of the  $n = 114$  sectors and no sector experiences a gap above 100%.

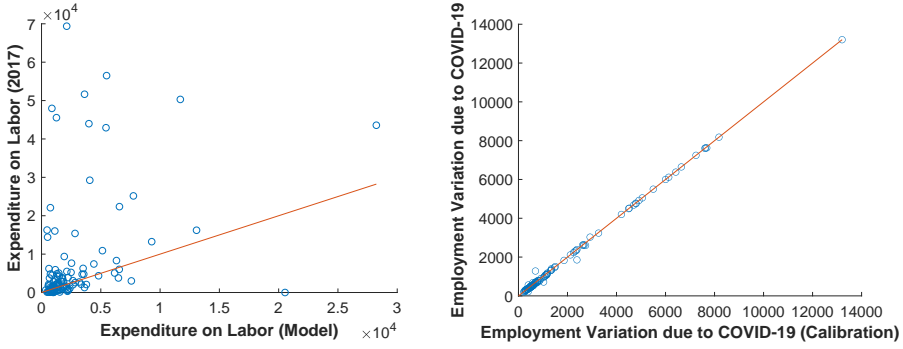


Figure 3: (Left) Equilibrium expenditure on labor against empirical expenditure on labor as observed in  $t = 2017$  for the  $n = 114$  sectors. Data source: ABS. (Right) Calibration of equilibrium employment variations on measured changes (March-Jul 2020). In both figures, the red line is the 45° line.

replicates empirical one quite well (see left pane of Figure 3). Therefore, given the adopted empirical characterization of the incidence vector  $\mu_t$  (see Section 3.1), we explore the possible long-run effects of lock-down by attributing employment variations to incidence variations of  $\mu_t$ , and let equilibrium share  $\ell$  free to float. Let  $\mathbf{u}_{\tau,t}$  be the vector of changes in payroll jobs in month  $\tau$  of year  $t$  and let  $\mathbf{l}_t \equiv 1 - \mu_t$ . We construct the incidence vector  $\mu_C(z)$  during COVID-19 restrictions with  $z \in [0, 1]$  as

$$\begin{aligned} \mu_C(z) \equiv & 1 - \left( \frac{11}{52} \times \mathbf{l}_t + \frac{5}{52} \times \mathbf{l}_t \times \mathbf{u}_{Apr20} + \frac{5}{52} \times \mathbf{l}_t \times \mathbf{u}_{Apr20} \times \mathbf{u}_{May20} \right. \\ & + \frac{5}{52} \times \mathbf{l}_t \times \mathbf{u}_{Apr20} \times \mathbf{u}_{May20} \times \mathbf{u}_{Jun20} \\ & \left. + \frac{26}{52} (z \times \mathbf{l}_t \times \mathbf{u}_{Apr20} \times \mathbf{u}_{May20} \times \mathbf{u}_{Jun20} \times \mathbf{u}_{Jul20} + (1 - z) \times \mathbf{l}_t) \right). \end{aligned}$$

In other words, the incidence vector  $\mu_C$  captures the yearly employment variations as observed along 2020, where we assume that the economy input utilization stays at July 2020 levels for a window corresponding to  $z \times 26$  weeks and goes back to levels of year  $t$  after  $(1 - z) \times 26$  weeks, where  $t$  corresponds to the most recent available IO configuration.

### 3.3.2 Calibration: Short-run effects on Value Added

In the second set of simulations we explore the short-run implications of COVID-19 shock on sectoral gross value added (GVA). To do so, we consider the shock vector as obtained in the previous exercise,  $\mathbf{A} = \mathbf{A}_t^*$  and calibrate it to  $\mathbf{A} = \mathbf{A}_t^{**}$ , where

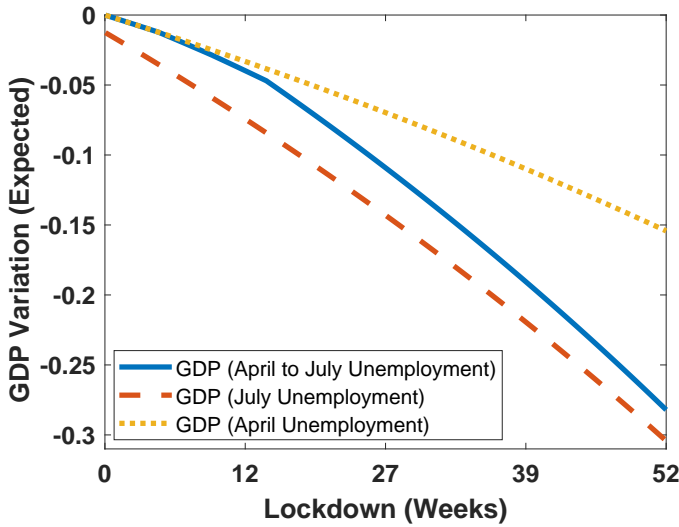


Figure 4: The blue line corresponds to the change in Australian GDP under an employment variation corresponding to the April-July 2020 levels.

$A_t^{**}$  minimizes the mean square error between the model’s equilibrium expenditure on labor  $\ell_t^{**}$  and the expenditure of labor as observed in the most recent IO configuration  $t$ ,  $\ell_t$ . Then, let  $\mathbf{u}_{mar/jul,2020}$  be the change in payroll jobs as measured by ABS from the 15th of March to 25th of July 2020 and let  $\ell_C(z)$  be the vector of employment due to COVID-19 restrictions defined as

$$\begin{aligned} \ell_C(z) \equiv & \frac{11}{52} \times \ell_t^{**} + \frac{20}{52} \times \mathbf{u}_{Mar/Jul20} \times \ell_t^{**} \\ & + \frac{21}{52} (z \times \mathbf{u}_{Mar/Jul20} \times \ell_t^{**} + (1 - z) \times \ell_t^{**}). \end{aligned}$$

In the above, we assume that employment stays at July 2020 levels for a window corresponding to  $z \times 21$  weeks and goes back to the level of year  $t$  after  $(1 - z) \times 21$  weeks. Subsequently, we calibrate  $\mathbf{A} = \mathbf{A}_t^{**}$  to  $\mathbf{A} = \mathbf{A}_C$ , where  $\mathbf{A}_C$  minimizes the mean squared error between the resulting equilibrium employment shares and  $\ell_C(z)$  (see also Figure 3).

### 3.3.3 The effect of the pandemic on Australian Economy

**Long-term Implications.** First, we assess the overall effect of COVID-19 restriction measures on GDP. We follow the calibration strategy outlined in Section 3.3.1 to obtain a base point-estimate, we set the window parameter  $z$  to give 5

weeks of July level employment in addition to the 15-week employment variation recorded since 15 of March. This gives us an overall yearly variation of real *GDP* equal to  $-7.4\%$ , similar to the  $-6.3\%$  variation recorded by ABS for the shorter span June 2019 - June 2020.

McKibbin and Fernando (2020) consider several scenarios with the highest predicted drop of the Australia's *GDP* of  $7.9\%$ , which is similar to what we find. Using the  $n = 33$  OECD inter-country input-output (ICIO) data-set, Bonadio *et al.* (2020) find that the Australia's *GDP* is expected to fall by  $25\%$ , and they further decomposed this drop in  $13\%$  domestic-induced shock and  $12\%$  foreign-induced shock. Our estimates are smaller relative to Bonadio *et al.* (2020) since we are tracking actual employment rather than estimated effects on employment caused by social distancing measures. For the French economy with  $n = 56$  IO sectors, Barrot *et al.* (2020) estimates that six weeks of social distancing depress *GDP* by  $5.6\%$ . Imputing a six-week homogeneous employment drop of  $52\%$  followed by the immediate recovery to the full pre-Covid employment into the model for Australia that makes it comparable to the cumulative effect considered by Barrot *et al.* (2020), generates a  $8.71\%$  contraction in real *GDP*.

Second, we replicate the calibration strategy of Section 3.3.1, to measure the potential effect of lockdown rules on *GDP* for a varying window under three alternative scenarios. Each scenario corresponds to a specific labor usage vector. Specifically, we will use April employment (corresponding to the first month of Covid response), July employment and April-July net employment. This gives us an upper bound represented by April employment and a lower bound represented by July employment. We measure effects on a varying lockdown window ranging between 0 and 52 weeks. The result is reported in Figure 4. As we see from the figure, we estimate a maximum of  $31\%$  of real *GDP* drop corresponding to applying the July employment levels in a one-year scenario, and a *GDP* drop ranging between  $4.9\%$  and  $10.1\%$  for an overall lockdown period corresponding to 20 weeks. Using the April-July employment data, the *GDP* drop ranges between  $6.6\%$  and  $28\%$  for for 20- and 52-week lockdown, respectively.

**Short-term Implications.** Third, we leverage the granular view of our model to make a sector-level assessment of the effect of COVID-19 induced unemployment. We make the assessment by measuring the variation of sectoral value added following the calibration procedure outlined in Section 3.3.2 under two alternative scenarios, respectively corresponding to  $z = 0$ , *observed lockdown* (OL) and  $z = 0.5$ , *extended lockdown* (EL). Notice that in our model nominal value added to sector  $j \in N$  corresponds to labor cost,  $V_j \equiv wl_j$ . Then, the change in value



added is defined as

$$\Delta V_{j,t} \equiv V_{j,t} - V_{j,t-1},$$

We report simulation results on the effect of employment on added value in Table 2 and 3 for the most negatively and least negatively (or positively) affected sectors respectively. Complete results for all  $n = 114$  sectors are reported in an online Appendix. We compare our simulation with the most granular measurements of gross added value growth produced by ABS<sup>20</sup>, corresponding to  $n = 30$  sectors. To make the comparison possible, we compute the observed value added growth using quarterly data from September 2018 to June 2020 (corresponding to eight quarters), where we removed taxes and subsidies from the last available quarter (June 2020). From observation of data, it appears that the most affected

INDUSTRY	EMP. VAR. (14/04-25/07)	EFFECT ON GVA (OL)	EFFECT ON GVA (EL)
Iron Ore Mining	-0.30%	-31.86%	-34.91%
Coal mining	1.20%	-30.57%	-33.45%
Meat and Meat product Manufacturing	-3.40%	-29.64%	-33.73%
Heritage, Creative and Performing Arts	-26.00%	-19.22%	-23.65%
Forestry and Logging	-6.90%	-18.97%	-21.50%
Poultry and Other Livestock	-10.40%	-15.98%	-19.27%
Rental and Hiring Services (except Real Estate)	-5.70%	-14.36%	-18.12%
Oil and gas extraction	-1.50%	-13.40%	-14.50%
Road Transport	-5.60%	-13.22%	-17.29%
Internet Service Providers	-1.40%	-13.10%	-16.12%
Sports and Recreation	-17.10%	-12.24%	-16.76%
Motion Picture and Sound Recording	-20.80%	-12.17%	-17.07%
Accommodation	-21.30%	-12.12%	-15.51%
Food and Beverage Services	-17.40%	-12.03%	-16.28%
Water Supply, Sewerage and Drainage Services	0.90%	-11.31%	-14.22%
Arts, Sports, Adult and Other Education Services	-16.50%	-10.11%	-14.55%
Broadcasting (except Internet)	-9.80%	-9.70%	-14.23%
Forged Iron and Steel Product Manufacturing	-1.20%	-9.69%	-14.23%
Tanned Leather, Dressed Fur and Leather Product Manufacturing	-11.30%	-9.60%	-12.74%
Glass and Glass Product Manufacturing	-5.50%	-9.19%	-13.43%
Other Agriculture	-10.40%	-9.03%	-14.50%
Water, Pipeline and Other Transport	-8.40%	-8.39%	-12.30%
Sheep, Grains, Beef and Dairy Cattle	-10.40%	-8.18%	-11.73%
Textile Manufacturing	-11.30%	-7.09%	-10.81%
Oils and Fats Manufacturing	-3.40%	-7.07%	-11.42%
Beer Manufacturing	-10.80%	-7.00%	-10.65%
Plaster and Concrete Product Manufacturing	-5.50%	-6.95%	-11.75%
Other Fabricated Metal Product manufacturing	-2.60%	-6.85%	-11.36%
Metal Containers and Other Sheet Metal Product manufacturing	-2.60%	-6.63%	-11.26%
Other Repair and Maintenance	-4.60%	-6.59%	-11.18%

Table 2: Effect of Employment variation on Added Value (30 most negatively affected sectors).

sectors are those that are either directly impacted by COVID-19 social distancing rules (e.g. *Accommodation and food services* and *Arts and recreation services*, experiencing a drop in GVA of 17.32% and 11.67% respectively) or upstream in the production chain, such as *Agriculture, forestry and fishing, Construction*

<sup>20</sup>Corresponding to Australian National Accounts: *National Income, Expenditure and Product, Jun 2020*, Table 45.

*Transport, postal and warehousing* and *Electricity, gas water and waste services*, respectively characterized by a fall of 12.54%, 5.44%, 2.70% and 1.60%. The least affected sectors are *Mining, Public administration and safety, Ownership of dwellings* and *Financial and insurance services*, characterized by a growth of gross value added<sup>21</sup> between 2.80% and 8.91%. Service sectors with limited ties with the heavily affected sectors above, such as *Information media and telecommunications, Health care and social assistance, Education and training* and *Professional, scientific and technical services* report either neutral or moderate growth, ranging between -0.14% and 1.33%.

INDUSTRY	EMP. VAR. (14/04-25/07)	EFFECT ON GVA (OL)	EFFECT ON GVA (EL)
Construction Services	-5.70%	1.07%	-4.56%
Technical, Vocational and Tertiary Education Services	-6.10%	1.08%	-5.94%
Primary and Secondary Education Services	-3.40%	1.48%	-4.29%
Structural Metal Product Manufacturing	-2.60%	1.91%	-3.41%
Defence	-0.30%	2.39%	-1.61%
Agriculture, Forestry and Fishing Support Services	-9.90%	2.67%	-2.18%
Health Care Services	-2.80%	3.23%	-2.89%
Retail Trade	-2.70%	3.88%	-2.29%
Non Ferrous Metal Ore Mining	-0.30%	4.05%	-2.09%
Rail Transport	2.40%	4.15%	-0.81%
Electricity Generation	0.60%	4.57%	4.98%
Auxiliary Finance and Insurance Services	2.60%	5.21%	1.70%
Waste Collection, Treatment and Disposal Services	-0.10%	5.52%	0.47%
Polymer Product Manufacturing	-0.60%	5.86%	-8.25%
Cleaning Compounds and Toiletry Preparation Manufacturing	7.40%	7.83%	3.69%
Residential Building Construction	-2.60%	8.34%	2.95%
Human Pharmaceutical and Medicinal Product Manufacturing	7.40%	8.76%	3.64%
Public Administration and Regulatory Services	2.50%	9.06%	6.40%
Specialised and other Machinery and Equipment Manufacturing	-2.50%	9.26%	3.31%
Iron and Steel Manufacturing	-1.20%	10.16%	1.89%
Insurance and Superannuation Funds	0.70%	12.30%	8.74%
Public Order and Safety	-0.30%	12.50%	7.81%
Exploration and Mining Support Services	1.60%	12.65%	6.80%
Basic Chemical Manufacturing	7.40%	12.80%	8.02%
Prof., Scien., Comp. and Elect. Equip. Manufacturing	-2.50%	14.41%	-0.23%
Veterinary Pharm. and Medicinal Product Manufacturing	7.40%	16.17%	11.07%
Basic Non-Ferrous Metal Manufacturing	-1.20%	19.48%	15.86%
Computer Systems Design and Related Services	-1.20%	21.21%	17.86%
Gas Supply	12.50%	21.93%	16.35%
Building Cleaning, Pest Control and Other Support Services	-6.00%	30.69%	21.20%

Table 3: Effect of Employment variation on Added Value (30 least negatively affected or most positively affected sectors).

Our results agree with contemporary literature suggesting that economic shocks disproportionately affect upstream sectors (Liu, 2018). Using a  $n = 56$  sectors representation of the French economy, Barrot *et al.*, 2020 observe that a similar mechanism can be triggered by constructed employment variations due to social distancing rules. Leveraging on actual employment variation data and a very gran-

<sup>21</sup>The growth in *Mining* gross value added (8.91%) is motivated by ABS by a rise in Iron Ore Mining driven by increased global demand and a rise in Other Mining due to strong production volumes in gold and copper, which offset the drop in the exports of coal (-8.3%) and other mineral fuels (-1.7%) on quarterly basis.

ular input-output framework, we find evidence a positive relationship between sectoral upstreamness and the impact of economic shocks on sector's growth of gross value added. In both scenarios considered in our simulations, Observed Lockdown and Extended Lockdown, respectively characterized by 20 and 41 weeks of social distancing induced unemployment, the most affected macro-sectors coincide with up-stream sectors (particularly, *Agriculture, Mining*), sectors which have been directly hit by the COVID-19 social distancing regulations, such as industries in the broad area of Arts, Recreation, Food and Accommodation services and their primary suppliers, as it is the case for *Meat and Meat product Manufacturing*. Furthermore, the overall reduction of exchanges and the general slowdown is reflected into a drop of added value of *Utilities* and *Transport* sectors which is particular evident in the Extended Lockdown scenario, in which, for example *Road transport* gross value added is expected to drop by 13.22%.

INDUSTRY	GROWTH OF GROSS VALUE ADDED (From Sep. 2018 to Sep. 2020)
Other services	-20.49%
Accommodation and food services	-17.32%
Agriculture, forestry and fishing	-12.54%
Arts and recreation services	-11.67%
Rental, hiring and real estate services	-5.61%
Construction	-5.44%
Administrative and support services	-4.51%
Transport, postal and warehousing	-2.70%
Retail trade	-2.31%
Electricity, gas, water and waste services	-1.60%
Information media and telecommunications	-0.14%
Manufacturing	0.31%
Health care and social assistance	0.58%
Education and training	0.62%
Professional, scientific and technical services	1.33%
Wholesale trade	1.42%
Financial and insurance services	2.80%
Ownership of dwellings	4.45%
Public administration and safety	5.42%
Mining	8.91%

Table 4: Observed growth of Gross Value added from fiscal year 2018/19 to fiscal year 2019/20, where last available quarter (September 2020) is net of subsidies and taxes. Source: ABS.

## 4 Conclusion

Governments all over the world are presently adopting social distancing policies as institutional reaction to the contemporary surge of the so called COVID-19 pandemic. In this paper we investigated the short-term economic implications of social distancing in an economy characterized by sectoral spillovers. To do so, we developed a multi-sectoral model in which sectors are endowed with technologies characterized by constant elasticity of substitution. As such, sectors are allowed to recombine the input bundle in response to economic shocks. Leveraging on the availability of very granular data-sets, we applied our model to Australia. We provided two contributions. First, we assessed the relevance of the Australian inter-sectoral network on its domestic aggregate fluctuations for generic economic shocks. Second, and more important, we provided the first granular account of the early economic effects on the Australian economy of the social distancing regulations. We performed two complementary exercises. In the first exercise, we attributed the employment shock to a long-run structural change in factor utilization and studied the effect on GDP for varying temporal windows. We obtained a drop ranging between 6.6% (20 weeks of lockdown) and 28% (1 year of lockdown). In the second exercise, we directly evaluated the short-run disaggregate effect of the employment shock on sectoral value added growth. We found that a sizeable fraction of up-stream sectors are subject to larger losses in value added. This is interesting as for several of these sectors, employment variation in the relevant period is actually positive, showing the presence of a compounded network effect.

## References

- Acemoglu, D., Akcigit, U., and Kerr, W., 2016. Networks and the macroeconomy: an empirical exploration, *NBER Macroeconomics Annual*, 30 (1), 273–335.
- Acemoglu, D., Carvalho, V.M., Ozdaglar, A., and Tahbaz-Salehi, A., 2012. The network origins of aggregate fluctuations, *Econometrica*, 80 (5), 1977–2016.
- Acemoglu, D., Ozdaglar, A., and Tahbaz-Salehi, A., 2015. Systemic risk and stability in financial networks, *American Economic Review*, 105 (2), 564–608.
- Adolph, C., Amano, K., Bang-Jensen, B., Fullman, N., and Wilkerson, J., 2020. Pandemic politics: Timing state-level social distancing responses to COVID-19, *medRxiv*.
- Atalay, E., 2017. How important are sectoral shocks?, *American Economic Journal: Macroeconomics*, 9 (4), 254–80.
- Baqae, D. and Farhi, E., 2020. Nonlinear production networks with an application to the COVID-19 crisis, Working paper, National Bureau of Economic Research.
- Barrot, J.N., Grassi, B., and Sauvagnat, J., 2020. Sectoral effects of social distancing, Working paper, Available at SSRN.
- Barrot, J.N. and Sauvagnat, J., 2016. Input specificity and the propagation of idiosyncratic shocks in production networks, *The Quarterly Journal of Economics*, 131 (3), 1543–1592.
- Bigio, S. and Lao, J., 2016. Financial frictions in production networks, Working paper, National Bureau of Economic Research.
- Blondel, V.D., Guillaume, J.L., Lambiotte, R., and Lefebvre, E., 2008. Fast unfolding of communities in large networks, *Journal of Statistical Mechanics: Theory and Experiment*, 2008 (10), P10008.
- Bonadio, B., Huo, Z., Levchenko, A.A., and Pandalai-Nayar, N., 2020. Global supply chains in the pandemic, Working paper, National Bureau of Economic Research.
- Brodeur, A., Gray, D.M., Islam, A., and Bhuiyan, S., 2020. A literature review of the economics of COVID-19, IZA discussion paper.
- Carvalho, V.M., Nirei, M., Saito, Y., and Tahbaz-Salehi, A., 2016. Supply chain disruptions: Evidence from the great east Japan earthquake, Research paper 17-5, Columbia Business School.

- Carvalho, V.M. and Tahbaz-Salehi, A., 2019. Production networks: A primer, *Annual Review of Economics*, 11, 635–663.
- Fana, M., Tolan, S., Torrejón, S., Urzi Brancati, C., and Fernández-Macías, E., 2020. The COVID confinement measures and EU labour markets, Working paper, Joint Research Centre, EU.
- Foerster, A.T., Sarte, P.D.G., and Watson, M.W., 2011. Sectoral versus aggregate shocks: A structural factor analysis of industrial production, *Journal of Political Economy*, 119 (1), 1–38.
- Gupta, S., Montenegro, L., Nguyen, T.D., Rojas, F.L., Schmutte, I.M., Simon, K.I., Weinberg, B.A., and Wing, C., 2020. Effects of social distancing policy on labor market outcomes, Working paper, National Bureau of Economic Research.
- Horvath, M., 2000. Sectoral shocks and aggregate fluctuations, *Journal of Monetary Economics*, 45 (1), 69–106.
- Jorgenson, D., Gollop, F.M., and Fraumeni, B., 1987. *Productivity and US economic growth*, Elsevier.
- Liu, E., 2018. Industrial policies in production networks, *Available at SSRN*.
- Long, J.B. and Plosser, C.I., 1983. Real business cycles, *The Journal of Political Economy*, 91 (1), 39–69.
- McKibbin, W. and Fernando, R., 2020. The global macroeconomic impacts of COVID-19: seven scenarios, *Covid Economics*, 10, 116–156.
- Miranda-Pinto, J., 2021. Production network structure, service share, and aggregate volatility, *Review of Economic Dynamics*, 39, 146–173.
- Miranda-Pinto, J. and Young, E.R., 2020. Flexibility and frictions in multisector models, CAMA working paper.
- Peter, A. and Ruane, C., 2018. The aggregate importance of intermediate input substitutability, Working paper.

# School-closure is counterproductive and self-defeating<sup>1</sup>

Coen N. Teulings<sup>2</sup>

Date submitted: 12 February 2021; Date accepted: 17 February 2021

*The Netherlands has recently closed down primary and secondary education in response to the covid-19 pandemic. Using a SIR (Susceptibles-Infected-Recovered) model for the Netherlands, this closure is shown to be counter-productive (as it increases future vulnerability to infection) and hard to reverse (since the increased vulnerability demands continuation). Though the rise of B117 (“the British version”) has been used to argue for school-closure, B117 increases the negative effects of school-closure. School-closure has been based on a misunderstanding of the dynamics in a multi-group SIR model. Furthermore, immunity by prior infection is shown to provide a larger contribution to ending the pandemic than vaccination. Finally, a cost-benefit analysis shows school-closure to be extremely costly. Behavioural economics explains why decision making and the public debate are so distorted, to the detriment of youngsters.*

- 1 The author thanks Robin Fransman, Bas Jacobs and Thijs van Rens for useful suggestion. The data used for this paper are available at [www.coenteulings.com/multigroup-sir-model-covid-19/](http://www.coenteulings.com/multigroup-sir-model-covid-19/).
- 2 Utrecht University and CEPR.

Copyright: Coen N. Teulings

## 1 Introduction

In response to the ongoing covid-19 pandemic, the Dutch government has closed down primary and secondary school from December 16, 2020 onwards. The fear for B117 (“the British version”) with a 30% higher infection rate has played a major role. Empirical evidence suggests indeed that school-closure has strongly reduced infections among youngsters in the short run, but the beneficial effects on health outcomes in the long run are less clear.

Solid evaluations of the corona-policies will appear in the years to come. However, these evaluations are to no avail for policy makers who have to decide here and now. Early provisional analyses on the effectiveness of various policies are therefore useful. This is exactly my aim in this article. I use a standard multi-group SIR (Susceptibles-Infected-Recovered) model calibrated on the pandemic’s evolution in the Netherlands since September 2020. The wisdom of school closure turns out to be doubtful.

My analysis starts in Section 2 and 3 with the case if there were no vaccination. That is most helpful for understanding the mechanisms at play. Section 4 accounts for upcoming vaccination. This really changes the nature of the game, in favour of school-closure. A cost-benefit-analysis shows, however, that even with vaccination school-closure is a prohibitively costly. Section 5 then addresses the issue why society has nevertheless embarked on this policy.

## 2 Four conclusions

The defining feature of covid-19 is its highly differentiated impact between age-groups. Nearly all casualties occur among elderly. My SIR model has therefore three age-groups: youngsters (aged 10-39), middle aged (40-64) and elderly (65+). Table 1 list some critical dates since September 2020, the starting date of my model simulations. The table relates these dates to week numbers in the simulations. The number of infections has risen steeply from early September until late October, as I shall discuss below. The lockdown policies of October 24 brought down the growth of the number of infections.<sup>1</sup> My analysis focusses on the effect of school-closure on December 16. This analysis yields four conclusions.

**Table 1 Crucial dates**

Event	Date	Simulation week
<b>Start simulation</b>	Sept 7	1
<b>Start lockdown</b>	Oct 24	7
<b>School closure</b>	Dec 16	15
<b>New year</b>	Jan 1	17
<b>End simulation</b>	June 30	42

### Conclusion 1: School-closure trades casualties today for casualties in May/June

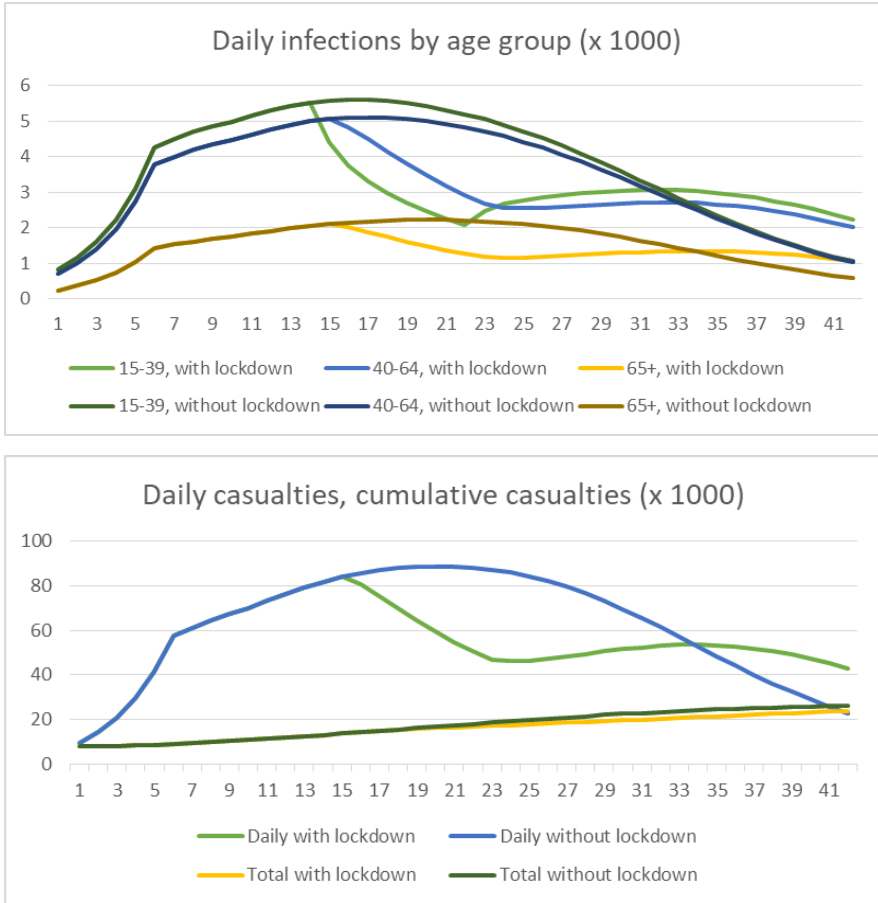
Figure 1 shows the effect of school-closure for 8 weeks (week 15-22). The number of infections among youngsters falls sharply in the short run. However, starting from mid-April, after reopening schools, the number of infections is predicted to be higher with rather than without school-closure in week 15-22. The same holds for the other age-groups, but the effect is obviously smaller. Since the number of casualties is proportional to the infections among the elderly, both series follow the same

<sup>1</sup> This explains the kink in the number of infections at week 7,



pattern: school-closure reduces them initially, but increase them in May and June.<sup>2</sup> The effect on the cumulative number of casualties by end of June is therefore limited: the initial reduction is offset by the subsequent increase.<sup>3</sup> This is the first conclusion: school-closure merely trades casualties today for casualties in a couple of months.

Figure 1 The effect of school-closure in week 15 (December 16) to 22 (February 8)



Conclusion 2: School-closure is hard to end

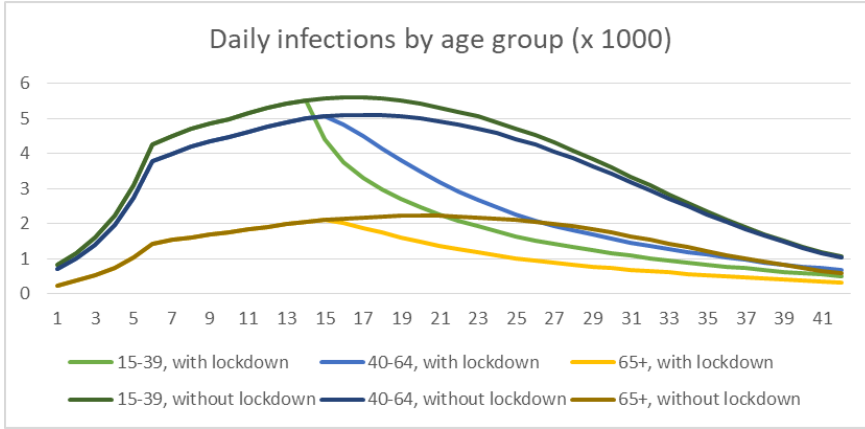
The second conclusion follows from the first. If reopening schools drives up daily infections above the level that would have been attained without school-closure, the temptation for policy makers is to keep schools closed until the end of the simulation, see Figure 2. Only a permanent school-closure can keep the number of infections with school closure below the number without until the end of the simulation period, as shown in Figure 1. However, a permanent school closure is extremely costly, as will be shown in Section 4.

<sup>2</sup> 23,800 casualties with closure versus 26,200 without.

<sup>3</sup> This holds also for Figure 2 and 3. Since the number of casualties is proportional to the number of infections among elderly, we don't report the number of casualties in these panels.

Covid Economics 69, 18 February 2021: 166-175

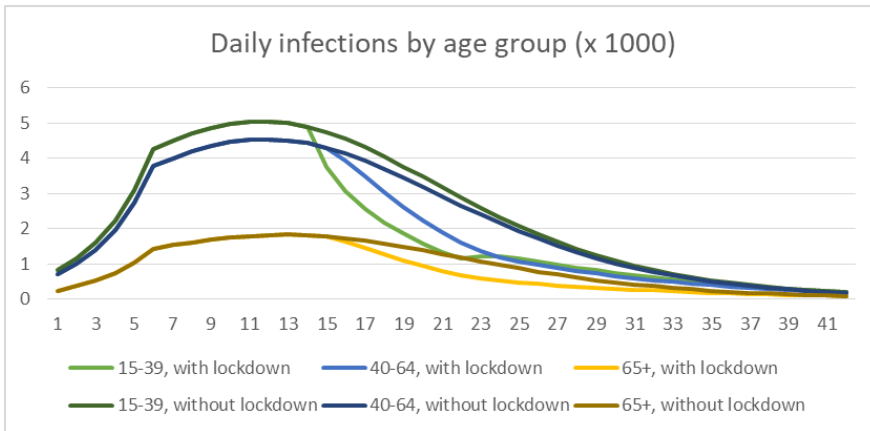
Figure 2 The effect of school-closure in week 15 (December 16) to 42 (June 30)



Conclusion 3: B117 only reinforces the arguments against school closure

The public motivation for advocating school-closure has been the arrival of B117 with a 30% higher infection rate. The simulations in Figure 1 and 2 include this version. As a thought experiment, Figure 3 presents a simulation of school-closure in week 15-22 without B117. Clearly, the number of infections and casualties would be substantially lower in that case. The surprise is in the effect of school-closure under this alternative scenario: it would be highly effective, without negative long run effects. The third conclusion is therefore exactly opposite to the public legitimization of school-closure: without B117, school-closure might have been effective; with B117, school-closure merely delays casualties and prolongs the pandemic.

Figure 3 The effect of school-closure in week 15 to 22 in the absence of B117



Covid Economics 69, 18 February 2021: 166-175

Conclusion 4: Immunity by previous infection offers a substantial contribution

In his first speech on covid-19,<sup>4</sup> prime-minister Mark Rutte stated as the main policy objective to avoid overburdening the health care system by smoothing the number of infections over time. In this way, we would gradually achieve immunity by previous infection. This notion quickly vanished from the debate, since this process was generally presumed to be too slow. Figure 1 and 3 show this presumption to be incorrect: without B117, the reproduction rate  $R$  would have got below unity by immunity due to previous infection in the beginning of December; with B117, one might expect this have to happen in course of February, even without school-closure.

What drives these counterintuitive conclusions? For this, one has to dig deeper into the surprising dynamics of a multi-group SIR model.

3 The unavoidable logic of the SIR model

For the simulations above, I use a standard SIR model with multiple age-groups analogous to Acemoglu et al. (2020). In its simplest form, this model consists of two difference equations for each age-group:<sup>5</sup>

$$\Delta I_i = \beta \alpha_i S_i [\sum_j I_j + (\theta - 1) I_i] - \gamma I_i \tag{1}$$

$$\Delta S_i = - I_i \tag{2}$$

Equation (1) describes the change in the number of infections as the difference between new infections (the first term on right hand side) and people who recover (the second term  $\gamma I_i$ ,  $\gamma$  is the recovery rate). Since the disease is spread by infected people to others who are still susceptible, new infections in age-group  $i$  are proportional to two factors: (i) the number of people in age-group  $i$  still susceptibles  $S_i$ , and (ii) the weighed sum of infected people in all age-groups,  $\sum_j I_j$ .  $\beta$  is the general infection rate; B117 raises this parameter by 30%.<sup>6</sup> The infection rate varies by age-group, which is captured by the parameter  $\alpha$ . Since infected people disproportionately infect their own age-group, this group overweighed in the sum of infected people by a factor  $\theta$  greater than one.

The second equation describes the evolution of the number susceptibles: people who recover from an infection are immune afterwards and hence leave the pool of susceptibles. New infections therefore have a negative short run effect on the number of infections, as infected people spread the virus, but a positive long run effect, as they reduce the number susceptibles. The latter effect is key understanding the dynamics of the pandemic.

Table 2 Daily infections (by age-group) and casualties

Date	10-19		10-39		40-64		65+		Casualties
	Data	Data	Model	Data	model	data	model	Data	
Sept 7	100	500	900	400	700	100	200	5	
Oct 26	1000	4500	4300	4000	3800	1500	1400	75	
Dec 21	1800	5000	5200	4500	5400	1700	2200	90	
Jan 18	500	2000	2600	2000	3700	1000	1600	50	

<sup>4</sup> On March 16, 2020.

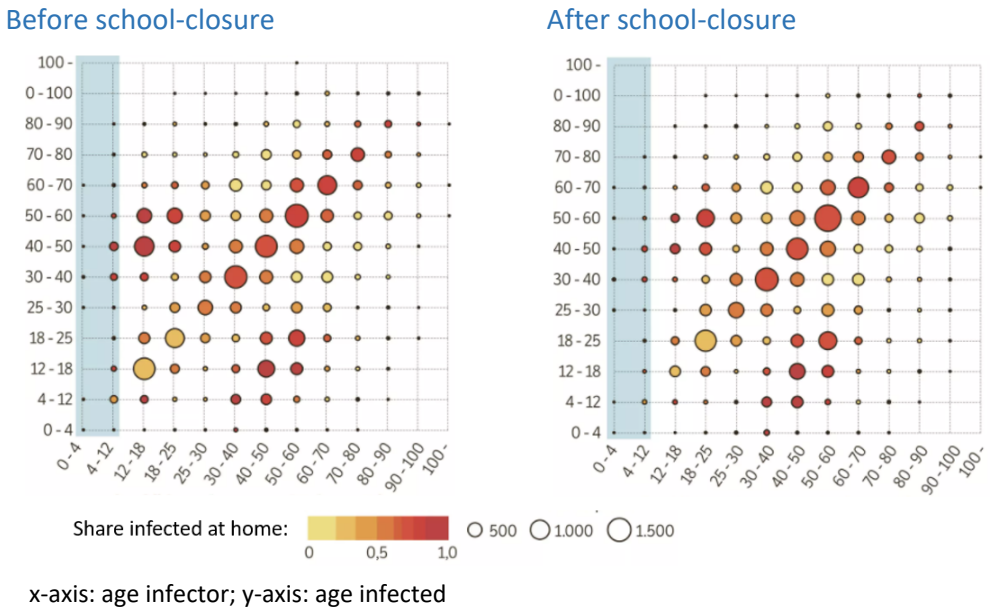
<sup>5</sup> This representation of the SIR model is more parsimonious than the usual version. Technically, infections  $I$  are treated as a flow rather than a stock variable. It simplifies the exposition without affecting the analysis.

<sup>6</sup> The starting values are such that new infections are distributed 50-50 among the standard version and B117 on February 1, 2021.

Source: RIVM <https://www.rivm.nl/coronavirus-covid-19/actueel/wekelijkse-update-epidemiologische-situatie-covid-19-in-nederland>

The parameters are set as to match the number of daily infections in each age-groups, see Table 2. There is direct evidence on the number of people who have antibodies against the virus.<sup>7</sup> This evidence shows that the registered number of infections is roughly half of the actual number of infections. A more recent quote by chief-epidemiologist Jaap van Dissel confirms this ratio.<sup>8</sup> The simulations use this number. Almost all fatalities are among elderly. The number of casualties has indeed moved parallel to the number of infections among the elderly. Figure 4 provides evidence on the parameter  $\theta$ : the overweighing of the own age-group when infecting other people is visible from the relative sizes of the circles on- and off- the main diagonal. A comparison of the panels before and after school-closure documents the effectiveness in reducing the number of infections among youngsters. The model matches the data reasonably well.<sup>9</sup>

Figure 4 Who infects who?



<sup>7</sup> <https://www.rivm.nl/pienter-corona-studie/resultaten>

<sup>8</sup> See <https://www.nu.nl/coronavirus/6095609/van-dissel-momenteel-twee-miljoen-nederlanders-beschermde-gegen-corona.html>. In my simulations, 2.1 million people are immune by previous infections by December 2020.

<sup>9</sup> The parameters used in the simulation are:  $\beta = 0.032$ ,  $\alpha_1 = 2.4$ ,  $\alpha_2 = 2.2$ ,  $\alpha_3 = 1$ ,  $\theta = 2$ ,  $\gamma = 0.75$ . The lockdown policies of October 24 reduce  $\beta$  by a factor 0.72, while school-closure reduces  $\alpha_1$  by a factor 0.72. The starting value of  $S_i = 4.7$  million for each age-group. Excel-file is available for people who want to run their own experiments. These values imply  $R_0$  before the lockdown policies of October 24 to be:

$$\beta (\alpha_1 + \alpha_2 + 1) [(2 + \theta)/3] 5 \text{ mln} / \gamma = 1.34,$$

assuming the infection-rates to be equal subgroup. In fact, youngsters have a higher infection-rate, pushing  $R_0$  up.

Source: RIVM

[https://www.tweedekamer.nl/sites/default/files/atoms/files/20210204\\_tech\\_nische\\_briefing\\_vws\\_presentation\\_jaap\\_v\\_dissel.pdf](https://www.tweedekamer.nl/sites/default/files/atoms/files/20210204_tech_nische_briefing_vws_presentation_jaap_v_dissel.pdf)

The analysis of Acemoglu et al. (2020)<sup>10</sup> is particularly helpful to understand the counterintuitive conclusions in Section 2. The mechanism is most easy to understand for the simple case  $\alpha_1 = \alpha_2 = \alpha_3 = \theta = 1$ . For this simple case, the reproduction-factor  $R_i$  for age-group  $i$  is defined as<sup>11</sup>

$$R_i = (\beta / \gamma) S_i \Sigma_j (I_j / I_i) \quad (3)$$

As soon as  $R_i$  gets below unity for all age-groups, the number of infections starts declining and the pandemic dies out. For a single age-group SIR model, this is the case when the total number of susceptibles  $S$  gets below  $\gamma/\beta$ . The same relations applies for multi age-group model

$$S_1 + S_2 + S_3 < \gamma/\beta \quad (4)$$

The pandemic dies out when the sum of the number of susceptibles in all age-groups gets below  $\gamma/\beta$ . Equation (4) shows that there is some freedom how to satisfy condition (4): fewer susceptibles  $S_1$  among youngsters imply that more elderly can remain susceptible, while the pandemic nevertheless dies out. As long as there is no vaccine, previous infection is the only road out of susceptibility towards immunity. However, unlike youngsters, that road is fraught with the risk of a deadly fatality for elderly. Hence, policy makers should try to let few elderly travel that road as possible. Hence, youngsters should get infected to safeguard elderly from infection. This is the positive long run effect of infections of youngsters for elderly. This explains why school closure is counter-productive: it merely reduces infections among youngsters, while these infections have a positive long run effect.<sup>12</sup>

This mechanism helps understanding the difference between Figure 1 and 3. In Panel 3 (without B117),  $R$  would have fallen below unity in December (week 17) anyway. After that, a forced reduction of infections speeds up the process of dying out of the pandemic. In Panel 1 (with B117),  $R$  is expected to remain above unity until February in the case of school-closure.<sup>13</sup> School-closure in December limits the number infections among youngsters, keeping the number of susceptibles high and delaying the moment at which  $R$  gets below unity. In the public discussion, the rise of B117 has been the legitimation for school-closure. This analysis shows that it is exactly the other way around: B117 is reason not to close schools, since it slows down the speed at which youngsters become immune and it prolongs the period during which elderly are at risk.

For the same reason, the regular public pleas for a short sharp lockdown are ill-conceived. As long as  $R$  is above unity, a short sharp lockdown is useless. It will bring down infections, but as soon as the

<sup>10</sup> See their Section 3, in particular Figure 3.1.

<sup>11</sup> In this case, the infection rate is the same for all age-groups and infected do not disproportionately infect their own age-group. For the general case, a more complicated, but similar relation holds. Equation (4) can be derived by realizing that for each age-group,  $R_j < 1$ . Hence:  $\beta S_i \Sigma_j I_j < \gamma I_i$ .

Dividing by  $I_3$  and elimination of the ratios  $I_1/I_3$  and  $I_2/I_3$  yields equation (4)

<sup>12</sup> Following the logic of the model, middle aged can bear this burden equally well. The main argument against infecting the middle age group is that though they rarely die from corona, they need hospitalisation, see Baarsma et al. (2020, table 3). Since the pressure on the health care system is an important constraint, infections can better occur among youngsters than middle aged.

<sup>13</sup> There is considerable uncertainty regarding these dates, in particular on the peak of the B117-wave. There is a paradox in the communication of the government's medical advisors. On the hand, they warn for a high upcoming peak, on the other hand they claim that B117 already accounts for the half of the infections. If the latter is true, the peak of  $R$  under B117 cannot be much higher than today's value, which is close to unity.

lockdown is relaxed, the inescapable logic of an  $R$  above one will resume, undoing all acclaimed benefits of the short sharp lockdown. Only after  $R$  has fallen below one, a sharp lockdown has lasting effects.

The main policy mistake made by RIVM and OMT (the medical advisors of the Dutch government) has been to target on total infections rather than infections among elderly (since they run the risk of dying) or the middle age-group (since they might end up in hospital, thereby putting stress on the health care system). Infections among youngsters do not impose any cost, except that they might infect other age-groups. However, the latter cost is offset by the benefit an infection a youngsters provides to future immunity. This article has shown that the latter benefit is substantial and outweighs the cost after just a couple of months, see Conclusion 4 in Section 2.

#### 4 Upcoming vaccination and the costs and benefits of school-closure

The simulations in Figure 1-3 ignore the upcoming vaccination. Vaccination strengthens the case for school-closure in Figure 1. Postponing of infections among elderly for just a couple of months might be sufficient to safeguard them for ever, by their vaccination. Figure 1 allows us to estimate the maximum effect of school-closure in week 15-22 on the number of casualties. In the absence of vaccination, school-closure reduces casualties until week 33 (May 1) and increases them afterwards. Suppose that everybody gets vaccinated exactly at May 1. Then, all lives saved in our simulation are also actual lives saved, since nobody is vaccinated before that date, while all additional casualties after May 1 do not count, since people are vaccinated by that time and therefore do not die from covid-19 anymore. The cumulative reduction in the number of casualties at May 1 is therefore the maximum benefit in terms lower casualties that can be attributed to school-closure. Using this reasoning, school-closure saves at most 3,000 lives.

Is this gain worth the effort of an 8 week school-closure? In general, it is hard to make a credible cost-benefit-analyses of lock-down policies. There are so many moving parts that it is difficult to construct a solid counterfactual. However, for this particularly narrowly defined policy, one can give a sensible first shot. Let's assume that online education is about half as effective. A wide body of research shows that the return to a year of education can be bracketed between 5 and 10%. To be on the safe side, I use the lower bound. I ignore other (private or social) benefits of education: higher life expectancy and life satisfaction, lower criminality and agglomeration externalities. These are potentially large, but they tend to be more disputed among economists. Using these numbers as lower bound of the cost of school-closure, we obtain a cost of 30 billion for a gain of 15,000 life-years, hence at least 2 million for each life-year saved.<sup>14</sup> Other researchers reached similar conclusions for other countries, e.g. Van Rens and Oswald (2020) for the UK.<sup>15</sup> The conclusion is inevitable: the closure of primary and secondary education has been a major policy mistake.

<sup>14</sup> The remaining life expectancy of avoided casualties is about 5 years, see Baarsma et al. (2020), leading to  $5 \times 3,000 = 15,000$  life-years. 2 months closure is 20% of a year education  $\times$  50% loss in effectiveness  $\times$  5% return to education = 0.5% loss of human capital for all affected cohorts; 10 cohorts aged between 5 and 15 are affected. The length of a labour market career is 40 years. During these 40 years, 10 out of 40 cohorts = 25% of the workforce is affected. Due to the low interest rate, we ignore discounting. The labour share in GDP is 2/3. Hence:  $0.5\% \text{ loss} \times 40 \text{ years} \times 25\% \text{ of the workforce} \times 2/3 \text{ labour share} = 3.3\% \text{ of annual GDP} = 30 \text{ billion}$

<sup>15</sup> See Van Rens' FT article for a short summary: <https://www.ft.com/content/32b5a894-c0b1-49e7-9378-90b23774ed93>

## 5 Why is the public discussion so one sided?

Why are the policy advices, the actual policy, and the corresponding public debate so one-sided? Remarkably, two emeriti professors in ethics, Heleen Dupuis and Marli Huijjer, were among the few people who were most vocal in their opposition.<sup>16</sup> Many economists have been reluctant to contribute to the discussion.

This hasn't been a typical Dutch phenomenon: strict lockdown policies have been advocated worldwide. The director-general of the World Health Organisation (WHO) Tedros Adhanom Ghebreyesus has qualified policies that aim for immunity by previous infection as unethical.<sup>17</sup> This statement lets normative judgement precede positive analysis. From an economist's point of view this position is untenable. Trade-offs are part of our life, also in public health. One cannot impose policies by *a priori* ruling out all alternatives on acclaimed moral grounds, in particular for diseases where the risks are so asymmetrically distributed among age-groups, so that it is sensible to let one group with almost no fatality risk get infected to contribute to the group immunity, while other groups are protected. One cannot justify these policies with the dictum "*better to be safe than sorry*" either: indeed, the large cost inflicted on youngsters are "*safe*", it is hard to see how one can say "*sorry*" for that.

Economic theory, in particular behavioural economics provides two clues as to why the public discussion has been so one-sided. First, Kahneman and Tversky (1980) have shown that humans tend to overestimate small probabilities. That is our motivation for buying lottery tickets: we really think we can win. The same applies to covid-19: for people aged below 65, the probabilities of dying from covid-19 is comparable to dying by a traffic accident. Making this observation tends to invoke just outrage among the audience, not contemplation. This overestimation of small probabilities is reinforced by the daily attention on the television news and talkshows, which have spent half of their time budget on the pandemic in past four months.

Second, mankind does not satisfy the standard economic model of the *homo economicus*, who cares about himself only. Mankind isn't a *homo kantiansis* either, who cares only about the group, not about himself. Real-life humans are a mixture of both types, a *homo moralis*, see Alger and Weibull (2019). Our moral stance helps us as a group to provide public without strict government enforcement. We rally behind the flag. There is a danger, however. The "war" against covid-19 has got defined as a public cause, which we can win only by a joint effort, as the billboards along the highway tell: *Samen tegen corona* (together we beat corona). The danger of this moral definition of the effort to contain the pandemic is that it may invoke tunnel vision: serious weighing of cost and benefits is disqualified, almost as form of high treason.

## Literature

Acemoglu, D., Chernozhukov, V., Werning, I., & Whinston, M. D. (2020). *A multi-risk SIR model with optimally targeted lockdown* (No. w27102). National Bureau of Economic Research.

Alger, I., Weibull, J. W., (2019). *Morality: evolutionary foundations and economic implications* in: Basu, K., Rosenblatt, D., & Sepulveda, C. *The state of Economics, the State of the World*, MIT Press.

<sup>16</sup> See <https://www.nrc.nl/nieuws/2020/12/04/medisch-ethicus-heleen-dupuis-solidariteit-moet-ie-niet-eindeloos-oprekken-a4022594> and <https://www.nrc.nl/nieuws/2021/01/15/arts-en-filosooft-marli-huijjer-niemand-heeft-recht-op-een-zo-lang-mogelijk-leven-a4027683>

<sup>17</sup> <https://www.nbcnews.com/health/health-news/who-says-herd-immunity-strategy-simple-unethical-n1243009>

Baarsma, B., van den Broek-Altenburg, E., Fransman, R., Jacobs, B., Koopmans, C., & Teulings, C. Is the current COVID-19 strategy effective?

Kahneman, D., & Tversky, A. (1980). Prospect theory. *Econometrica*, 12.

Van Rens, T., & Oswald, A. J. (2020). *Age-Based Policy in the Context of the Covid-19 Pandemic: How Common are MultiGenerational Households?* (No. 522). Competitive Advantage in the Global Economy (CAGE).